Heterogeneous Deployment Analysis for Cost-Effective Mobile Network Evolution

- An LTE Operator Case Study

Coletti, Claudio

Publication date:
2013

Document Version
Accepted author manuscript, peer reviewed version

Heterogeneous Deployment Analysis for Cost-Effective Mobile Network Evolution

- An LTE Operator Case Study -

PhD Thesis
by
Claudio Coletti

A dissertation submitted to
Department of Electronic Systems,
the Faculty of Engineering and Science, Aalborg University
in partial fulfillment for the degree of
PhD Degree,
Aalborg, Denmark
September 2012.

Supervisors:
Preben E. Mogensen, PhD,
Professor, Aalborg University, Denmark.
Principal Engineer, Nokia Siemens Networks, Aalborg, Denmark.
István Z. Kovács, PhD,
Wireless Networks Specialist, Nokia Siemens Networks, Aalborg, Denmark.

Opponents:
Jens Zander, PhD
Professor, Royal Institute of Technology (KTH), Sweden.
Trevor Gill, Eng.
Distinguished Engineer, Vodafone Group R&D, United Kingdom
Knud Erik Skouby, Prof.
Professor, Aalborg University, Denmark.

"Se siete attirati dal mare aperto del mondo, andate. Partite. Scappate. Ma ricordate che una nazione, una regione, una città, un quartiere, una scuola, un'associazione, un gruppo di amici e una famiglia sono il porto da cui siete partiti; e dove, magari, tornerete. Anche nomadi e marinai hanno una patria."

Beppe Severgnini, *"Italiani di domani"*

Abstract

The plethora of connected devices, such as attractive smartphones, data dongles and 3G/4G built-in tablet computers, has brought mobile operators to face increasing demand in mobile broadband traffic and services. In addition to the roll-out of Long Term Evolution (LTE), the deployment of small low-powered base stations is a promising, cost-effective solution to considerably enhance user experience. In such a network topology, which is denoted as heterogeneous deployment, the macro layer is expected to provide wider coverage but lower average data speeds whereas small cells are targeted at extending network coverage and boosting network capacity in traffic hot-spot areas. The thesis deals with the deployment of both outdoor small cells and indoor femto cells. Amongst the outdoor solution, particular emphasis is put on relay base stations as backhaul costs can be reduced by utilizing LTE spectrum available at the macro layer for wireless backhaul.

The main goal is to investigate the LTE downlink performance of different deployment configurations, focusing on spectrum allocation schemes and deployment strategies that are needed to maximize network coverage. The coverage performance is expressed as the percentage of satisfied users achieving a data rate above a required minimum, with targets in the range of 90-95% coverage. Differently from most studies using statistical models of deployment areas, the performance analysis is carried out in the form of operator case studies for large-scale deployment scenarios, including realistic macro network layouts and inhomogeneous spatial traffic distributions. Deployment of small cells is performed by means of proposed heuristic deployment algorithms, which combine network coverage and spatial user density information. As a secondary aspect, deployment solutions achieving the same coverage performance are compared in terms of Total Cost of Ownership (TCO), in order to investigate the viability of different deployment combinations from both a performance and economic perspective.

The first part of the thesis is dedicated to the potential of deploying relays in both suburban and dense urban scenarios. In the suburban or noise-limited case, the coverage performance of in-band relays, i.e. backhaul transmission on the same spectrum as used at the macro layer, is strongly dependent on the signal quality of the backhaul link, which limits the relay performance. Therefore, high-gain antennas at the backhaul side or the use of a dedicated carrier for backhaul transmission (out-band configuration) are needed to reach the coverage target. A similar performance can be achieved through a macro-only upgrade to lower frequency spectrum (e.g. 800 MHz), and this solution turns out to be, together with in-band relays, the most cost-effective as compared to macro densification and out-band relays. In the dense urban scenario in-band relays are not able to deliver substantial performance gains as the dissatisfied users are located in high traffic areas rather than in poorly covered locations. Without large availability of spectrum, a co-channel deployment of micro cells is the optimal small cell solution to considerably improve coverage and yield average throughput gains of up to 5 times.

In the second part of the thesis, micro and femto cell deployments are investigated in a high traffic urban scenario, including three-dimensional distribution of indoor users across the building floors. By assuming a 50-fold traffic growth relative to today's levels, significant performance benefits are obtained with highly dense small cell deployment. In order to mitigate severe inter-cell interference, small cells shall be deployed on dedicated frequency channels that are not interfering with the macro layer. Micro-only deployment with 3 micros per macro sector, or alternatively an open access femto-only deployment with a density of 400 femtos/km^2, is sufficient to offload half the users and fulfill the coverage target. As for the TCO analysis, the cost trends are strictly correlated with the small cell backhaul cost assumptions. In general, a dense deployment of femto cells is preferable due to reduced backhaul costs compared to micro cells. Yet, if low installation costs can be guaranteed for the outdoor small cells, a hybrid deployment of indoor femtos and outdoor micros - with each layer transmitting on dedicated frequency resources - is capable of achieving a trade-off between network costs, outdoor coverage and capacity enhancement.

Dansk Resumé[1]

Den store mængde enheder forbundet til Internettet, såsom attraktive smartphones, USB 3G/4G modemmer og bærbare computere og tablets med indbygget 3G/4G modem har forårsaget, at mobil-operatører oplever stigende krav til mobilt bredbånd og den tilhørende service. Udover udrulning af Long Term Evolution (LTE) teknologien, er udrulning af små basestationer med lavt strømforbrug en omkostningseffektiv løsning til at forbedre brugeroplevelsen betragteligt. I et netværk bestående af makro basestationer og små basestationer, kaldet et heterogent netværk, forventes det, at makro-laget dækker et stort område, men med lavere gennemsnitlige datahastigheder, mens de små celler er ment som en udvidelse af netværksdækningen og skal øge netværkets kapacitet i områder med øget mobiltrafik. Denne afhandling omhandler udrulning af udendørs små celler og indendørs femto-celler. Blandt de udendørs løsninger lægges der særlig vægt på relay-basestationerne, da backhaul-omkostningerne kan reduceres væsentligt ved at udnytte det tilgængelige makro-lags LTE spektrum som trådløs backhaul.

Det altoverskyggende mål er at undersøge LTE downlink udførelsen af forskellige udrulnings-konfigurationer, med fokus på spektrum-allokeringplanerne og de udviklingsstrategier, som er nødvendige for at maksimere netværksdækningen. Dækningesgraden formuleres som fordelen af mobilbrugere, hvis datahastighed er højere end den lovede, med kraver i størrelsen af 90/95%-dækning. Hovedparten af de eksisterende studier bruger statistiske modeller for udrulningsområder , hvorimod denne afhandling adskiller sig ved at være en operatør case-study, hvilket inkluderer et realistisk makro-netværk og en realistisk uhomogen geografisk datatrafik-fordeling. Placeringen af små celler er bestemt ved hjælp af foreslåede heuristiske placerings-algoritmer, som inkluderer både aktuel netværksdækning og den geografiske datatrafik-fordeling. Derudover sammenlignes udrulnings-

[1]The author is extremely thankful to Niels Terp Kjeldgaard Jørgensen and Jytte Larsen for their support in translating and proofreading this abstract.

løsninger, som opnår den samme dækning, med hensyn til Total Cost of Ownership (TCO), således at det er muligt at fastslå mulighederne for de forskellige udrulnings-kombinationer fra både et ydeevne- og økonomisk perspektiv.

Første del af afhandlingen omhandler potentialet ved udbredelsen af relay- basestationer i både forstadsområder og tæt bebyggede områder. I scenariet med forstadsområder, hvor netværket er dækningsbegrænset, er ydeevnen af in-band relay-basestationer betydeligt afhængig af signalkvaliteten af den trådløse backhaul forbindelse, hvilket begrænser relay-ydeevnen. In-band er defineret ved, at backhaul transmissionen foregår i det samme frekvensområde, som bruges af makro netværket. Derfor er det nødvendigt at anvende antenner med høj forstærkning i backhaul transmissionen eller dedikere et frekvensområde til backhaul transmission (out-band konfiguration), hvis man skal opfylde dækningskravet. En tilsvarende ydeevne kan også opnås kun ved brug af makro basestationer. Dette kræver dog, at makro basestationerne benytter et ekstra frekvensområde (f.eks. 800 MHz). Denne løsning er sammen med in-band relay-basestationer den mest omkostnings-effektive, når man sammenligner med out-band konfigurationen og makro netværk med øget tæthed. I scenariet med tæt bebyggelse er in-band relay-basestation løsning ikke attraktiv, da problemet i dette tilfælde ikke er netværksdækning, men derimod netværkskapacitet. Medmindre mobiloperatøren har store frekvensområder til rådighed, er den optimale løsning i tæt bebyggede områder at udrulle mikro-basestationer, der benytter samme frekvensbånd som det oprindelige netværk. Denne løsning reducerer antallet af mobilbrugere, der oplever netværksudfald, samtidig med, at den gennemsnitlige downlink datahastighed femdobles.

I anden del af afhandlingen undersøges mikro- og femtocelle udrulning i tæt bebyggede områder, hvor der er stort behov for datatrafik. Dette inkluderer en 3D fordeling af indendørs mobilbrugere på forskellige etager i bygninger. Hvis man antager en datatrafikvækst på 50 gange i forhold til datatrafikmængden i dag, øges netværkets ydeevne betragteligt ved en høj tæthed af små celler. For at minimere interferensen fra små celler til makro celler, og omvendt, skal de små celler anvende et eller flere dedikerede frekvensbånd. 3 mikro-celler per makro sektor eller en femto-celle-tæthed på 400 femto-celler per kvadratkilometer er tilstrækkeligt til at servicere halvdelen af mobilbrugerne samt overholde dækningskravet. For TCO analysen gælder det, at omkostningerne for de små celler afhænger af prisen for backhaul forbindelsen. Generelt gælder det, at femto-celler er at foretrække, da backhaul udgiften for disse er mindre end backhaul udgiften til mikro-celler. Hvis det er muligt at garantere en lav udgift til udendørs små celler, er en hybrid udrulning af indendørs femto-celler og udendørs mikro-celler det bedste kompromis med hensyn til netværksudgifter, udendørs dækning og netværkskapacitet. Dette forudsætter dog, at femto-cellerne og mikro-cellerne anvender hver sit dedikerede frekvensbånd.

Preface and Acknowledgments

This thesis is the result of a three-year research project carried out at the Radio Access Technology (RATE), Department of Electronic Systems, Aalborg University (Denmark), under the supervision and guidance of Prof. Preben E. Mogensen (Aalborg University, Nokia Siemens Networks) and Wireless Networks Specialist Dr. István Z. Kovács (Nokia Siemens Networks). The work was carried out in parallel with the mandatory courses and teaching obligations required to obtain the Ph.D. degree. The project has been co-financed by the Faculty of Engineering, Science and Medicine, Aalborg University (AAU) and Nokia Siemens Networks (NSN), Aalborg, Denmark.

The thesis revolves around a performance evaluation and cost analysis of different deployment solutions featuring small cells, such as LTE-Advanced relays and indoor femto cells. Hence, basic knowledge of LTE mobile networks and network deployment is preferable when reading the content of this thesis. Based on realistic network scenarios, the overall work is aimed at providing mobile operators with techno-economic guidelines as to how the existing network infrastructure should evolve to meet ever increasing mobile broadband traffic volumes.

Despite the challenging task, to complete this PhD project has been an immensely rewarding and enriching experience. First of all, I am sincerely grateful to my supervisors for their constant support and dedication to my project. Their technical knowledge, excellent feedback, thorough reviews, energy, and generosity have simply made this journey easier. But more than that has been their trust in my skills and their endless encouragement what I will cherish the most. Being proud of myself has never been one of my fortes, but today I surely feel more confident about what I did.

The RATE section and the NSN site have been a truly vibrant environment, full

of talented researchers and helpful people. It has been an honor for me to be part of these groups, and I thank all of them for sharing this period and all our social activities. In particular, I am very grateful to Lauri Kuru, ZhuYan Zhao, Ekkehard Lang from NSN, Liang, Yu, Huan, Nacho and Viviane from AAU, and Ralf Irmer from Vodafone, for their valuable feedback and support during my studies. To Lisbeth and Jytte goes my deepest gratitude for their help in administrative issues and proofreading of this manuscript. In addition to that, a special "thanks" goes to my office mate, Italian speaking and dear friend Gilbert Micallef, with whom I had the pleasure of sharing this "ride towards the PhD", with its joys, pains and doubts about the future.

Moving to Denmark has given me the opportunity to expand my horizons and join an international, cheerful and multi-language community. For this reason, I would like to thank all my international friends, who made my life in Aalborg richer, funnier and unforgettable. From the "kollegium", my humble abode during the last years, a special thanks goes to Carmen, a truly amazing friend and travel mate. And lately to Marta, whose glaring smile has been a ray of light through this difficult last period.

Living abroad allows you to better understand the nuances of your own culture and look at your own country from different perspectives. For this reason, I would like to say to Luca M., Luigi, Luca D.G., Giuliano and Deboruccia that I have never felt so "Italian" before, and this is thanks to all the wonderful time we spent together here in Denmark. From the Alps down to Mount Vesuvius, we made it, we unified Italy again!

Last but absolutely not the least, I do extend my deeply heartfelt gratitude to my parents and sister, to whom this thesis is truly dedicated. In these times of economic uncertainties, despite the physical distance separating us, you made me feel every single day the proudest son and the luckiest brother on earth. As suggested in the dedication page of this thesis, being curious about the world has never dimmed the passion for my roots, the love for my family and the friendship I shared with my dearest "high-school" friends from Pescara.

Claudio Coletti,

Aalborg, November 2012

Contents

Chapter 1

Thesis Introduction

1.1 The Mobile Traffic Growth Challenge

As a result of the undeniable success of mobile broadband, the demand for higher data rates in cellular networks has been constantly increasing over the last years. Mobile broadband has become a vital part of our everyday life with a strong need for "everywhere and seamless" connectivity [1]. The initial cellular networks were designed to provide only voice traffic and fulfill wide area voice coverage, whilst nowadays the extremely higher number of subscribers, more appealing data applications, and the widespread adoption of smartphones and tablets have pushed the operators to boost the performance of the existing network.

The mobile data explosion has undoubtedly been sparked by the exceptional success of the Third Generation Partnership Project (3GPP) standard of families. In the last years, Third Generation (3G) deployments based on High Speed Packet Access (HSPA) and its enhanced version HSPA+ [2, 3] have established themselves as the dominant mobile broadband solution, leading to tremendous uptake of mobile broadband and causing mobile data to surpass voice traffic consumption [4]. To sustain the mobile broadband growth, the new Orthogonal Frequency Division Multiplexing (OFDM)-based LTE technology [5, 6] is now seeing rapid deployment thanks to the release of new spectral band licenses and attractive downlink peak data rates. In addition to this, an enhanced version of LTE, also known as LTE-Advanced (LTE-A) or LTE Release 10 [7, 8], is in the

pipeline. Advanced features, such as the use of aggregated spectrum and improved support for small cell deployment, enable the network to deliver donwlink peak data rates of 1 Gbps and meet the requirements set for International Mobile Telecommunications-Advanced (IMT-A) Fourth Generation (4G) systems, as defined by the International Telecommunications Union (ITU) [9].

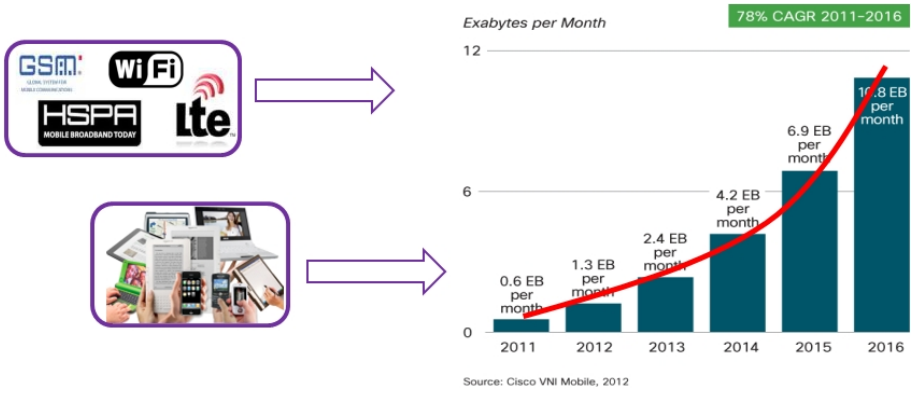

Fig. 1.1: Mobile broadband traffic growth predicted in [10] and the main factors unleashing the mobile data explosion, that is to say mobile broadband technology evolution together with advanced mobile devices.

Along with more efficient technologies delivering faster data connections, the proliferation of attractive mobile-connected devices, such as smartphones, data dongles, tablets and netbooks, is another crucial factor driving the increasing traffic demand [11]. Due to improved processing capabilities, these devices can offer consumer content and applications that were not supported by the previous generation of mobile phones. As shown in Fig. 1.1, all these factors add up to create an exponential traffic increase. As evidenced by Cisco's mobile traffic forecast [10], global mobile broadband traffic had been more than doubling every year since 2008, and such a trend is expected to maintain its course with a Compound Annual Growth Rate (CAGR) of 78% from 2011 to 2016, i.e. a 18-fold increase over the forecast period. In addition to this, the traffic content seems to shift towards high-definition and streamed video applications, which are predicted to account for 70% of the overall mobile traffic in 2016.

To deal with surging traffic demand – which comes as a combination of a growing number of subscriptions and increasing data usage per user –, mobile operators are offered a variety of solutions for expanding network capacity. Amongst the traditional methods, acquiring additional spectrum, introducing a higher number of sectors per macro site or deploying brand new macro sites generally incur high deployment costs as well as facing limitations due to licensed spectrum scarcity, site location availability and achieved performance enhancement [12]. Therefore, to meet future capacity and coverage demands within a wider time frame, the de-

ployment of small low-power cells is gaining momentum as a cost effective solution complementing the macro overlay and delivering high-quality user experience. In essence, small cells are strategically deployed in targeted high traffic areas, also denoted as traffic "hotspots" or "hot zones", with the purpose of efficiently offloading data traffic from the macro layer to the small cells.

This thesis focuses on various small cell deployment strategies, which are evaluated from both a radio performance and infrastructure cost perspective. The analysis is carried out in the form of different LTE case studies that are based on realistic network scenarios. This requires a holistic performance evaluation methodology, which includes different aspects of network deployment such as realistic network layouts and traffic distributions, detailed propagation modeling and infrastructure cost models. Based on a joint techno-economic performance evaluation, the main target is to give deployment guidelines and recommendations on optimal network evolution to meet the expected traffic demand.

In the remainder of the chapter, the investigated small solutions, namely micro, relay and femto cells, are presented in Section 1.2; thesis scope and objectives assuming a realistic case study are discussed in Section 1.3 before addressing the key points of the research methodology in Section 1.4; ultimately, Section 1.5 deals with thesis structure and its main contributions.

1.2 Being "Heterogeneous" to Meet Demand

In order to support rising traffic demands, mobile operators can resort to a variety of technology and deployment options that can be jointly considered when boosting network performance in different scenarios and traffic conditions. From the operators' perspective, the main targets to be fulfilled when upgrading the existing network can be summarized in the following:

- Provide blanket service coverage and high average data rates to all connected users making an efficient use of the available spectral resources. This is to be achieved by also considering how the traffic is distributed in the network and prioritizing the areas where larger network capacity is required.
- Select future-proof and scalable solutions that can rapidly adapt and evolve to sustain traffic demand in the mid and long term. In this concern, network architecture and backhaul availability play an important role in accommodating larger traffic volumes.
- Ensure cost efficiency or, in other words, keep the Total Cost of Ownership (TCO) for network infrastructure [13] to a minimum. Lowering the overall

cost per delivered bit is a necessity for operators to render the mobile broadband sustainable and avoid the well-known and dreaded "scissor effect" [14]– network expenses overcoming flat revenues at high market penetration.

- Last but not least, be "green"-minded when deploying network radio equipment to safeguard energy efficiency and reduce CO_2 emissions [15].

To put this into practice, operators can start improving the macro cell network. The evolution towards LTE and HSPA future releases provides a platform for enhanced mobile broadband experience, with the advantage of reusing existing macro sites. Spectral efficiency can be boosted through greater baseband processing capacity, transmission schemes with higher-order modulation and especially advanced multi-antenna solutions, pushing the link level capacity closer to the Shannon Bound [16]. However, the theoretical gains related to multi-antenna transition can hardly be achieved in practice due to constraints in the number of antennas to be deployed or operational points that are far from the signal quality usually perceived in real communication systems [17]. Another option for expanding capacity is the acquisition of additional spectrum so that each site can transmit on multiple carriers and potentially aggregate the available spectrum [18]. But licensed spectrum is de facto a scarce and extremely expensive resource, the availability of which strictly depends on country regulations and the operators' strategic decisions. Thus, spectral efficiency enhancements and acquisition of new spectral resources do not seem to resolve the mobile data explosion challenge on their own.

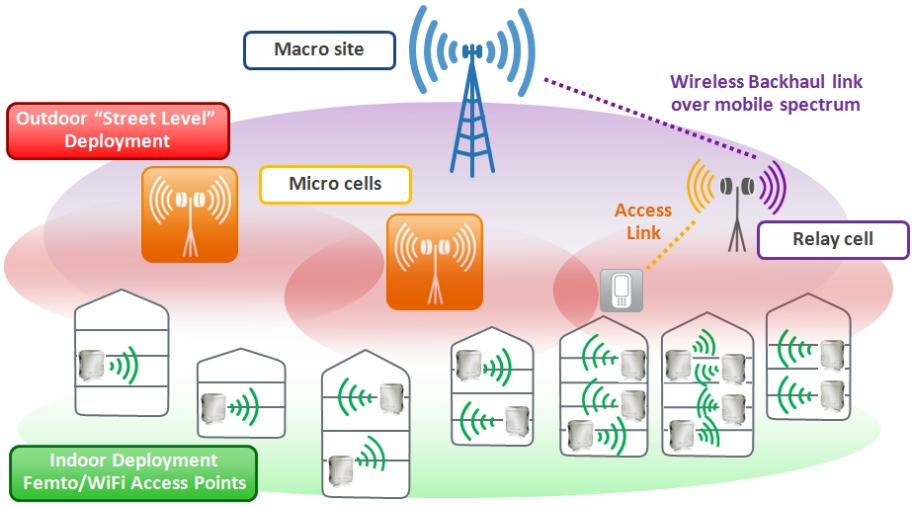

Fig. 1.2: Overview of a heterogeneous deployment scenario built upon multiple deployment layers. Together with high power macro sites, outdoor small cells such as micro and relay cells are deployed along with low power and high density femto deployment across the city buildings.

In face of spectrum scarcity and limitations of advanced features, the next big leap in network performance improvement consists of rethinking the topology of traditional networks and bringing serving base stations closer to the users. To densify the existing macro layout with only newly deployed macro sites is usually impractical and cost prohibitive due to site acquisition and cell tower deployment restrictions. Hence, a promising and cost-effective deployment paradigm aimed at increasing the spectral efficiency per unit of area is denoted as *heterogeneous deployment*, or "HetNet" [19]. As illustrated in Fig. 1.2, HetNets present a diversified set of transmitting base stations having different size, transmission power and ensuing cell areas. Such a hierarchical approach utilizes macro cells with high transmit power (20-40 W) and high antenna mast to mainly provide coverage, whereas extended coverage and capacity are achieved through the small cell underlay. Amongst those, micro and relay base stations are deployed outdoors for transmission power levels of around 1-5 W, whereas dedicated indoor solutions employing even lower power levels are pico and femto cells, Distributed Antenna Systems (DASs) or non-cellular local area technology such as WiFi [20].

With regard to the evolution of the mobile network, the deployment of heterogeneous network is envisaged to fulfill most of the following;

- Enhance user performance throughout the network area by tailoring small deployment to high-traffic areas [21], considering that mobile broadband traffic is mainly generated in indoor locations (e.g. 70% according to [22]). Covering high-traffic areas with small cells also means to decrease the traffic load on the overlaying macro cell and improve macro user experience.
- Small form factor for equipment and ease of installation at street level and indoor locations.
- Backhaul towards the mobile core network with various options, including both wireless and wired solutions [23].
- Low installation, equipment and operational costs as compared to macro-related network upgrades.

Operating complex heterogeneous networks poses key challenges in terms of traffic balancing amongst the different deployment layers [24, 25], user mobility, interference management for extremely dense cell deployments [26, 27], and self configuration and healing features [28]. Moreover, backhaul is another factor that will be instrumental to the success of deploying small cells in hotspots [29]. High-performance backhaul at reasonable costs is fundamental for supporting the data rates experienced on the radio access network and guaranteeing scalability when an increasing amount of small cells has to be added to satisfy traffic demand.

Before addressing the scope and goals of this dissertation, the following subsections provide further insight into the considered small cell solutions, focusing on deploy-

ment aspects and related work present in the literature for both radio performance evaluation and cost assessment.

1.2.1 Outdoor Deployments: Micros and Relays

As previously explained, outdoor small cells deployed below the rooftop on lamp-posts or walls are expected to boost user performance in urban areas where it is prohibitive to further increase the existing macro network density. Such a deployment paradigm has already been utilized in the past for Second Generation (2G) and 3G deployments, mainly to enhance macro network coverage in isolated, poorly covered areas or locations with intensive phone usage, such as train stations and stadiums. Typically, small cells rely on traditional means of backhaul such as leased lines, microwave point-to-point links, and fiber connections [30]. Under these backhaul assumptions, such cells are usually denoted as micro or pico cells[1], and the available backhaul capacity does not act as a bottleneck for the connected users.

The impact of deploying the micro or pico layer on network performance has been mainly investigated in regular scenarios – with hexagonal macro layout –, showing network performance improvements together with cost and energy implications [31–33]. In [27, 34, 35] the authors deal with co-channel pico deployment, focusing on enhanced Inter-Cell Interference Cancellation (ICIC) schemes that are needed to mitigate interference between macro and pico cells. Instead, the research study in [36] proposes a network evolution study for an HSPA realistic scenario, illustrating different modalities for using the available spectrum and estimating micro deployment business profitability in comparison with macro layer upgrades.

However, it is also well known that the costs related to the backhaul connection – e.g. leasing fees, trenching costs, microwave link maintenance, and planning permissions – can certainly be a limiting factor for deploying micro and pico cells. For this reason, the licensed frequency bands used for radio access are very attractive also for backhaul transmission, and the small cell operated with wireless backhaul is denoted as relay. Indeed, the radio access and backhaul link depicted in Fig. 1.2 could use the same radio technology and share the resources used to serve ordinary users. The relaying concept has been extensively discussed in academia and industry [37–39], and has ultimately found its way through the LTE standardization, becoming an LTE-A standardized feature [40].

[1] The distinction between the two types of base station is quite blurry in the literature. In this dissertation micro cells are considered as compact base stations deployed outdoors, with transmission power in the range 1-5 W using omni-directional antennas and without access restriction policies. Although not covered in this study, pico cells can transmit at lower power levels as well as being deployed indoors to cover large building areas.

The end-to-end link between the macro base station and the user is split into two hops, the first one being the backhaul link connecting the macro *donor* cell, and the second one the access link from the relay cell towards the relay user. As LTE spectrum is mainly available at high frequency carriers (e.g. 1.8 and 2.6 GHz), it is more challenging to improve coverage, due to higher propagation losses, also considering that the majority of traffic is generated indoors. The main target for relays is to improve the network performance at the cell-edge and specifically in the areas affected by poor coverage. Relays can act as traditional repeaters when they simply amplify and forward the received analog signals, at the cost of noise and interference enhancement. Decode-and-Forward (DF) relays, which decode and re-encode the signal before forwarding it, have proven to perform better than Amplify-and-Forward (AF), especially in environments affected by poor signal quality conditions, as shown in [41].

In case of *in-band* relays, backhaul and access transmissions take place on the same carrier, sharing the same radio resources. Such a relay configuration is the most challenging as it is crucial to strike a balance between overall cell capacity and resources "sacrificed" for the backhaul link. In addition, backhaul reception and access transmission (and vice versa for the uplink) are split into two different time intervals (half duplex) to avoid loop interference. Therefore, ensuring excellent backhaul signal quality is of fundamental importance to achieve optimal performance through the dual-hop connection. This can be obtained through the use of directional antennas at the relay backhaul side and planned site positioning to avoid shadowed areas [42]. Moreover, the use of LTE spectrum for backhaul transmission below 3 GHz offers inherent propagation advantages as compared to dedicated microwave backhaul at higher frequencies. In fact, in the potential LTE frequency bands the backhaul transmission can be supported also in Non-Line of Sight (NLOS) conditions, which can be a typical scenario for relays deployed below the rooftop in dense urban areas.

Besides the mere theoretical analyses related to capacity estimation and optimal scheduling algorithms, a certain number of research papers adopted a more practical approach to investigate the potential of deploying LTE relays in future network deployment. For instance, coverage and capacity evaluation has been carried out in regular scenarios, highlighting the combination between relay deployment and macro densification to deliver the same performance for the downlink [43–46]. This approach has paved the way to further analyses addressing the economic viability of deploying relays, according to different radio configurations [47] and traffic demand assumptions [48] in regular layout networks. Relaying performance assessment based on realistic dense urban scenarios is addressed, for example, in [49, 50] mainly through a coverage study and relay position optimization. However, real traffic distributions and multi-user system simulations were not considered. Lastly, the authors in [51] propose a performance comparison between relays and picos in both coverage and interference-limited regular scenarios.

In brief, deploying a cluster of outdoor low-power cells is an interesting solution to enhance network performance and meet customer expectations. In particular, relay base stations seem to be extremely attractive to relieve backhaul costs, but coverage and capacity improvements need to be investigated under more realistic assumptions with regard to network scenarios, traffic growth, achieved backhaul performance, and spectrum availability – e.g. *out-band* relays can be deployed by allocating a different band with respect to the access link. In this dissertation, emphasis is mainly put on the viability of deploying relays when addressing outdoor deployment solutions, and a comprehensive comparison between micro and relay deployment is provided to get an insight into whether or not relays can effectively boost network performance in high-traffic scenarios.

1.2.2 Femto Cells as an Indoor Offloading Solution

As mentioned earlier, the mobile broadband traffic is expected to be generated in a vast variety of indoor locations, ranging from shopping malls, train stations, business offices to residential apartments. Due to spatial characteristics of network traffic, the deployment of low-power cells directly inside the indoor areas is no doubt a step forward with regard to increasing the network density. The LTE small cells specifically engineered for indoor application are defined as femto cells, or LTE Home enhanced eNodeBs (HeNBs) in the 3GPP nomenclature [52, 53]. These are envisaged to offer great benefits in terms of coverage extension in indoor areas and capacity offload from the macro layer. For instance, 3G femto cell deployments have recently been rolled out to offer voice coverage at enterprise premises or poorly covered rural areas [54].

From a technical point of view, the transmission power does not exceed 100 mW, femtos are normally equipped with omni antennas, and their size is extremely compact. Being essentially a cellular node, femto cells are able to support the same level of mobility and coverage of cellular networks, thus differing from WiFi network performance. In general, femtos are mostly user-deployed, and they leverage the customer's existing broadband internet connection as backhaul. For this reason, femto deployment can be regarded as cost-efficient due to no additional expenditure for backhaul connection, energy supply and site rental – they are all provided by the user [55, 56]. Furthermore, femto cells can be configured to operate in Closed Subscriber Group (CSG) mode, when user admission is limited to a selected set of subscribers, or Open Subscriber Group (OSG) mode, with no admission restriction for the nearby subscribers within the femto covered area, or a hybrid version [57].

Based on the spectrum allocation and the admission configuration, dense femto cell deployment is challenging with regard to interference management and offloading potential. Deployment aspects of femtos together with macro layer have been

investigated in the literature, mostly considering statistical 3GPP scenarios with regular building complexes within the macro cell area [58–61]. The bottom line is that OSG deployments are less critical than CSG from an interference perspective, also when sharing the same carrier with the macro. This configuration is certainly advantageous to mobile operators as they can optimize the number of offloaded users to the femto layer while leveraging the user owned backhaul connection. With CSG, instead, macro users in proximity of a femto and not registered in the femto access list suffer from heavy interference in a co-channel deployment. In this scenario the use of an additional femto-free ("escape") carrier at the macro layer is beneficial for heavily interfered macro users. If no escape carrier is available, interference can be mitigated by tuning the femto coverage with a downlink power calibration or partially muting femto transmission to improve nearby macro users' received signal quality.

1.3 Thesis Scope and Objectives

After presenting the state-of-the-art and reviewing published material on small cell deployment studies, it is clear that a major part of the studies presented so far was carried out in statistical scenarios with regular macro layout – e.g. the scenario described in [62]. Obviously, the main target was to estimate the potential of deploying small cells in such a type of scenarios, or investigating the performance of specific features, such as interference management schemes . While still selecting regular network scenarios, the authors took one step forward in [31, 48], trying to look at the overall problem from a broader perspective that included sensitivity studies to propagation models, traffic spatial distributions and cost input. As for realistic scenarios, most research contributions propose coverage-based studies without considering real traffic distributions, or deal with trial results verifying performance predictions on the single link with small cell prototypes.

The starting point of this dissertation is to remove the assumption that the deployment study is carried out in regular scenarios that are not fully representative of real network scenarios. The main target is that of presenting the overall deployment aspects in such a way that mobile operators can more easily draw general conclusions about the investigated deployment configurations. This is achieved by means of a series of case studies in which massive efforts are put, not only on the radio performance evaluation, but also on the modeling of realistic network scenarios. The latter includes information about existing macro layout, spectrum availability, inhomogeneous traffic distribution amongst the existing macro cells and network areas, and accurate propagation predictions. Such assumptions substantially influence the way small cells must be deployed in a network scenario and to what extent they can be useful to sustain the traffic demand in the coming years.

From a high-level perspective, the main research questions to be addressed in the thesis are formulated as follows:

1. *What type of small cells can keep up with the traffic growth?*
2. *How shall small cells be deployed in realistic scenarios?*
3. *Which small cell deployment configuration is the most cost-effective?*

The scope of the dissertation is the study of different LTE deployment solutions based on small cells deployment, as illustrated in Fig. 1.3. Downlink performance evaluation is the main focus of the thesis, and a deployment cost analysis for different options is added to support the network evolution guidelines. To better present the conclusions and recommendations from the case studies, two main areas have been explored, which also reflect the structure and the chronology of the PhD study.

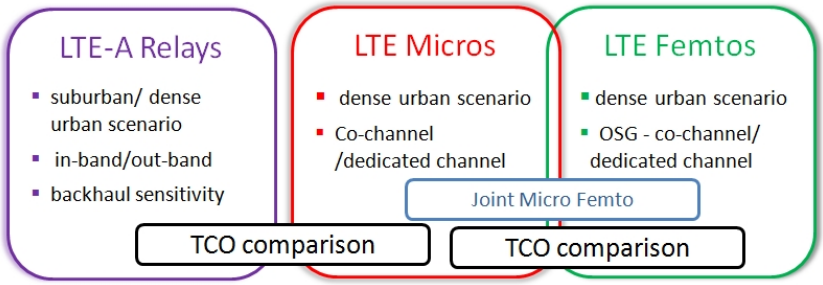

Fig. 1.3: Scope of the PhD study subdivided into the investigated small cell deployment options. Each of them is analyzed through different network scenarios, spectrum configurations, and cost comparisons.

Part I deals with outdoor small cell deployment, with particular emphasis on relay deployment performance and its comparison with micro cell deployment. The main purpose of the analysis is to evaluate the viability of wireless backhaul in large-scale heterogeneous networks. In particular, the following targets can be outlined:

- Investigate the potential of relay deployment from a coverage and capacity perspective in coverage and interference-limited scenarios.
- When possible, identify the optimal use of spectrum and other deployment aspects, e.g. backhaul related parameters, to meet traffic demand.
- Quantify the performance gap between relays and micro cells in a dense urban scenario in terms of coverage and capacity.

- Evaluate the cost-efficiency of deploying relays in comparison with other deployment architectures, based on macro upgrades and micro deployment, delivering similar network performance.

Following the outcome of the outdoor deployment study, Part II shifts the attention from outdoor to indoor deployment, narrowing down the analysis to a high-traffic dense urban scenario. OSG femto cells are considered as the deployment solution for indoor traffic offloading. Relying on a full multi-layer heterogeneous deployment, which includes outdoor micro and indoor femto cells, the specific objectives of the second research area can be stated as:

- Investigate the performance of micro and OSG femto deployment solutions, both as stand-alone options or jointly deployed, for high traffic scenarios.
- Determine the best spectrum allocation for dense and multi-layer heterogeneous deployment, as a trade-off between coverage and capacity performance.
- Identify the most cost-effective combination of the investigated network architectures, given the same coverage performance.

To sum up, the thesis is aimed at providing mobile operators with deployment guidelines about heterogeneous deployment strategies from a techno-economic perspective. The next section is dedicated to the description of the scientific method, employed to investigate network performance and cost analysis.

1.4 Research Methodology

The section addresses the scientific methodology underlying the investigations conducted in the PhD study. As previously stated, the research project is targeted at providing network operators with tangible deployment guidelines for cost efficient network evolution. In order to better fulfill this purpose, the previously described deployment options are evaluated by setting up case studies based on real life network scenarios. The network scenarios are carefully selected as being representative of typical network deployments that are situated in a main European country and owned by an incumbent operator, i.e. having a strong market position and owning the network infrastructure.

To properly build a case study and obtain valuable conclusions, a holistic approach is used when evaluating the network performance, as depicted in Fig. 1.4. Firstly, the realistic scenario modeling involves the selection of the network area, existing macro site information, spatial traffic distributions and propagation models tuned

on the specific investigated scenario. Then, once the scenario is built, the network performance is estimated for different network deployment configurations by means of a static simulator. Finally, the simulation results are used to select, amongst the investigated network options, the iso-performance scenarios that are compared in terms of costs. The main Key Performance Indicator (KPI) used to set the performance target is network coverage, which is expressed in terms of *user outage*, i.e. the percentage of users which are not served with a minimum downlink data rate, e.g. 5 or 10 %.

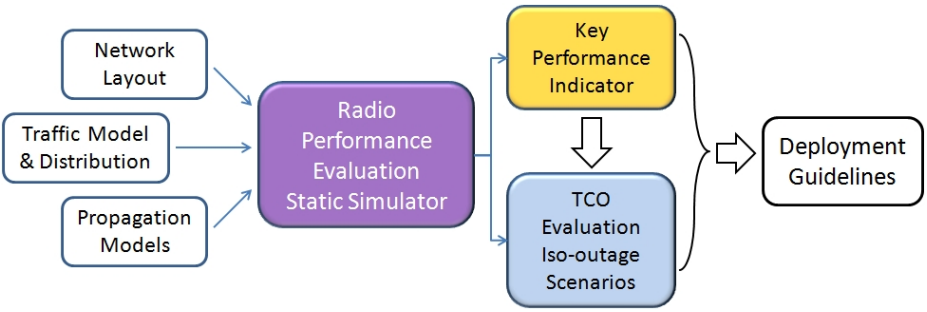

Fig. 1.4: Overview of the holistic methods utilized to evaluate the techno-economic performance of various small cell deployment solutions. All different input data to the simulator are needed to build the realistic network scenarios whereas the simulated performance results are combined with TCO cost analysis to provide the final deployment recommendations.

1.4.1 Network Scenario Modeling

In order to differentiate the presented research work from previous studies, a large effort is devoted to model the realistic reference network scenario underpinning the overall case study. Live 3G network deployments owned by a European incumbent operator have been used as a reference macro LTE network scenarios on top of which small cell deployment solutions have been investigated. The validity of utilized data input and scenario assumptions has been examined through discussions with industry experts (from Nokia Siemens Networks and a major mobile operator) involved in this research project. In order to map the case study outcome into more general deployment guidelines, the selected scenarios present the following characteristics:

- The initial macro deployment densities for urban and suburban scenarios are aligned with typical European deployments involving major mobile operators. In particular, this can be seen in the investigated dense urban high-traffic zones where the average macro inter-site distance and building density are similar to the ones encountered in the main European capital cities.

- Analogously to the initial macro layout, the assumed traffic spatial distributions can be considered as typical for European deployments. This applies to how mobile traffic is distributed amongst the macro cells (e.g. 30% of cells carry half of the network traffic) and within the investigated area (e.g. half the traffic concentrated in 10-20% of the area).

Regarding the network layout, site coordinates and site configuration information are utilized to build the reference macro scenario and estimate the downlink performance baseline according to an assumed traffic load. Parameters related to site configuration include the sector orientation, transmission power, antenna pattern and feeder losses, which are all used when calculating the macro link budget. To accurately predict macro coverage, path loss predictions based on ray-tracing are utilized in most cases. Moreover, 3D building maps are utilized to better model the propagation at street level, including the indoor penetration. To increase the simulation speed, statistical propagation models are used for small cells in most cases, and they are tuned on the basis of the specific investigated scenario.

Along with the above modeling blocks, the traffic spatial distribution is of crucial importance to properly evaluate the impact of small cell deployment. Traffic and related user density maps are obtained in the form of geo-location traffic data, or by directly processing cell-based weekly traffic data. Given the average daily traffic volume, the employed spatial user densities represent the traffic spatial distribution during "busy hour", i.e. the hour of the day with highest data consumption. To simulate network performance, only a fraction of the subscribers is considered, and they represent the simultaneously active broadband users. As explained in the following chapter, the number of active users, i.e. the network load, is estimated based on the coverage performance of the reference network (Part I) or a more detailed traffic growth model (Part II).

Within the dissertation the network scenario modeling varies from one case study to the other. This is mainly due to the fact that additional data input is available or lacking for each specific network scenario – e.g. the available spatial user density. As for the propagation models, the use of a ray-tracing tool has been constantly improved during the course of the PhD study, and used more extensively in the second part of the thesis. Network scenario and propagation models are presented in detail in each of the investigated cases.

1.4.2 Network Performance Evaluation: Simulations and KPIs

In the various heterogeneous deployment scenarios the radio network performance has been estimated by means of Monte-Carlo based simulations. In general, closed

form analytical expressions characterizing system performance can hardly be found when realistic large-scale irregular deployments introduce a vast number of parameters. In these scenarios simplified assumptions about interference and user distributions may not accurately hold in practice [63]. Moreover, heuristics methods finding sub-optimal solutions are used in the search of optimal locations for small cell deployment. Such methods have been selected instead of numerical optimization algorithms in order to reduce execution time and focus on the performance trends for a wider set of heterogeneous deployment configurations.

During the course of the PhD, a significant amount of time has been spent on developing and calibrating a network planning tool including a static network simulator, in co-operation with Nokia Siemens Networks colleagues and other PhD students (a more comprehensive description of the simulator is given in Appendix A). Major contributions have been made to the network data input processing, small cell deployment and resource sharing algorithms, and the indoor deployment modeling framework.

User outage is used to set the deployment target to be fulfilled (e.g. below 5%) when deploying small cells. *Average User Throughput* is utilized as a secondary indicator to evaluate the capacity improvements. User traffic model is assumed to be full buffer, meaning that the active user is always seeking to download data from the network and utilize all the available resources. This implies that the network performance is evaluated under full load conditions, which is more challenging in terms of interference compared to the fractional load case.

User LTE downlink data rates achievable at the radio access network are estimated through a Signal to Interference plus Noise Ratio (SINR)-to-throughput mapping curve, with interference and radio resource sharing explicitly modeled. With the simulator being static, the estimated data rates are to be considered as average values, based on average propagation losses and under full load conditions. Yet, the achieved user data rates presented hereinafter must be considered as representative of relative trends, useful for performance comparison amongst different scenarios and not indicative of realistic values. For the sake of simplicity, the effect of higher level protocols and user mobility are out of the scope of this dissertation.

1.4.3 TCO Comparison for Iso-Performance Scenarios

The employed holistic approach for evaluating the most viable heterogeneous deployment solution also includes a financial estimate of the investigated network configurations. Hence, a TCO analysis is carried out with the purpose of complementing the performance evaluation results and identifying the deployment configuration striking the optimal balance between network performance and infrastructure costs.

Following the cost structure proposed in [13], the utilized cost model includes upfront costs needed to acquire assets and install the network, and running costs that are spread over time, such as maintenance and rental expenditures. Specific cost figures are used for each type of deployed base stations. To fairly compare different heterogeneous deployment options, iso-performance, or more precisely iso-"outage", scenarios are selected. This means that a predefined user outage level within a predefined error margin is the target to be fulfilled prior to assessing the cost effectiveness of one deployment solution.

It is worth saying that the cost analysis has not been the main focus of this dissertation, meaning that detailed and extensive studies about cost sensitivity or multi-year deployment studies have not been performed. Regarding the validity of the cost analysis, it can be stated that:

- The proposed cost numbers must not be associated with any existing commercial product. Those are used for research purposes, mainly to estimate the cost ratio between different base station types rather than providing absolute numbers.
- The cost models are only related to the radio access network, excluding transport and core networks, and administrative costs.
- Cost inputs have been thoroughly examined and agreed with experts representing both Nokia Siemens Networks and a leading mobile operator involved in this PhD study.
- The empiric cost figures can be considered valid for the specific European case studies carried out in the thesis, but it must be stressed that the cost assumptions can significantly change due to different market conditions, the country or the availability of network infrastructure.

1.5 Thesis Outline and Contributions

This sections describes the structure of the thesis and points out the main contributions for each of the presented case studies. As mentioned earlier, the outline of the thesis is aligned with the chronological order of the thesis. This implies that network scenario and performance models have been constantly improved and become more complex when proposing a new case study.

From a general point of view, the main contribution of the PhD study is in the method and framework used to evaluate heterogeneous deployment performance. The novel aspect is the attempt to perform a techno-economic analysis of varied

heterogeneous deployment options based on case studies that are built on realistic network scenarios. Such an approach allows operators to draw more practical conclusions and recommendations about how to efficiently evolve the existing network.

Chapter 2 – Mobile Network Evolution: the Road to Meet Traffic Demand

This chapter reviews in a tutorial-like style the main deployment options for network operators to increase network capacity and meet future traffic demand. These include the deployment of additional spectrum and also macro site upgrades, such as high-order sectorization and optimized antenna tilting. Then insights into relay and femto cells from a standardization perspective are presented. The final part is dedicated to cost infrastructure modeling for radio access networks.

Part I, Chapter 3 – Network Deployment Modeling Framework

The modeling framework supporting the performance evaluation and cost analysis of various network scenarios is presented in this chapter. The utilized models and tools lay the foundation not only for the case studies presented in Part I, but also, in part, the indoor deployment scenarios presented in Part II. The realistic scenario modeling is described through its main three parts: reference macro layout, spatial traffic distribution data input, and propagation models. Furthermore, radio resource sharing algorithms and physical layer capacity estimation models are illustrated, including the more complex case with deployed in-band relays. Finally, the proposed heuristic deployment algorithms for outdoor small cell deployment and the cost figures for the TCO analysis are presented.

Part I, Chapter 4 – Relay Deployment in a Suburban Scenario

The first case study investigates the viability of deploying relay cells in a realistic coverage-limited scenario, which is inherently expected to favor relay deployment. After describing the scenario assumptions, network performance results are shown for in-band and out-band relay configurations according to realistic LTE spectrum availability. The study also addresses the performance sensitivity to the backhaul signal quality and the required assumptions to meet the outage target. As an alternative option, macro upgrades introducing an additional low frequency carrier or a plain macro densification are studied to build the iso-outage scenarios. The additional TCO analysis gives the final deployment guidelines. As an outcome of this study, the following conference paper was published:

- Claudio Coletti, Preben Mogensen, Ralf Irmer, "Performance Analysis of Relays in LTE for a Realistic Suburban Deployment Scenario", *VTC-Spring 2011. IEEE 73rd.*, Budapest, May 2011.

Part I, Chapter 5 – Relay and Micro Deployment in a High-Traffic Metropolitan Scenario

This chapter presents the second case study involving both relay and micro cells in a dense urban interference-limited scenario. The network area is denoted as "hot-zone" as the mobile data consumption is considerably higher than in the surrounding areas. The focus is on in-band relaying and co-channel micro deployment, evaluating coverage and capacity performance of both deployment options. Detailed sensitivity studies on transmission power and relay backhaul performance enhancement, such as additional spectrum for out-band relays or the potential of interference cancellation at the relay side, are also included. The final section presents a cost comparative study about iso-outage scenarios presenting relay or micro cells, and final deployment guidelines are provided based on the overall techno-economic analysis. The overall study led to the publication of the following conference paper:

- Claudio Coletti, Preben Mogensen, Ralf Irmer, "Deployment of LTE In-Band Relay and Micro Base Stations in a Realistic Metropolitan Scenario", *VTC-Fall 2011. IEEE 74th.*, San Francisco, September 2011.

Part II, Chapter 6 – Building the Indoor Deployment Framework: Models, Assumptions and Reference Scenario

The second part of the thesis begins with a description of the modeling framework and the reference network scenario that are utilized in the next chapter to investigate the potential of indoor femto cell deployment. Although based on the framework presented in Chapter 3, the network scenario models require more accuracy in spotting the presence of the building to evaluate the impact of those on propagation and traffic distribution assumptions. The deployment algorithms for selecting the positions of micro cells and OSG femtos are also described. It is also shown that the offered traffic load is chosen based on a traffic forecast model. The chapter ends with a performance evaluation study from the large-scale deployment scenario, which leads to the selection of the "hot-zone" reference scenario for femto cell deployment.

Part II, Chapter 7 – Multi-Layer Heterogeneous Deployment in a Hot-Zone Urban Scenario

The third and last case study intends to carry out a techno-economic analysis of a variety of deployment options, from outdoor micro deployment to OSG indoor femtos and their combination. Particular attention is given to the performance of different deployment schemes – namely co-channel or dedicated band deployment with respect to the macro overlay – in terms of both coverage and capacity improvements. The multi-layer heterogeneous deployment solutions are aimed at

fulfilling the network coverage requirement, assuming a 50-fold traffic increase from today's traffic levels. A set of deployment options are selected when analyzing the network costs, showing also some sensitivity study as to the cost of the small cells. The final recommendations were summarized in the following publication:

- Claudio Coletti, Liang Hu, Huan Nguyen, István Kovács, Benny Vejlgaard, Ralf Irmer, Neil Scully, "Heterogeneous Deployment to Meet Traffic Demand in a Realistic LTE Urban Scenario", *VTC-Fall 2012. IEEE 76th.*, Quebec City, September 2012.

Chapter 8 – Conclusions and Future Work

Having in mind the previously mentioned goals of the thesis, the final chapter gives a summary of the lessons learned from the case studies and the main deployment recommendations for mobile operators facing deployment challenges similar to the ones presented in this dissertation. Finally, suggestions for future work are also provided.

In order to support and complement the case studies presented in the following chapters of the thesis, three appendixes are included. Appendix A provides a description of the network simulator structure and features; Appendix B offers insights into the calibration of the heuristic deployment algorithms and indoor femto performance; lastly, Appendix C lists all the different cost components and related cost estimations that are assumed for the TCO analysis in the case studies.

Furthermore, although not included in the main part of this dissertation, a measurement campaign from a live network has been conducted as part of a master thesis project supervision. The goal was to evaluate the performance of the relay backhaul link for different potential relay locations and antenna configurations in a real urban macro-cell scenario. The following article has been co-authored and included in Appendix D:

- Ignacio Rodriguez, Claudio Coletti, Troels Sørensen, "Evaluation of Potential Relay Locations in an Urban Macro-Cell Scenario with applicability to LTE-A", *VTC-Spring 2012. IEEE 75th.*, Yokohama, May 2012.

As for the indoor deployment study, a parallel study on WiFi deployment has been supported. The work is based on simple models for WiFi (802.11g) capacity estimation and interference calculation. As a result, the two following conference papers have been co-authored:

- Liang Hu, Claudio Coletti, Huan Nguyen, Preben Mogensen, Jan Elling, "How much can Wi-Fi offload? – A Large-scale dense-urban Indoor deployment study", *VTC-Spring 2012. IEEE 75th.*, Yokohama, May 2012.

- Liang Hu, Claudio Coletti, Huan Nguyen, István. Kovács, Benny Vejlgaard, Ralf Irmer, Neil Scully, "Realistic Indoor Wi-Fi and Femto deployment Study as the Offloading Solutions to LTE Macro Network", *VTC-Fall 2012. IEEE 76th.*, Quebec City, September 2012 (reprinted in Appendix E).

Chapter 2

Mobile Network Evolution: the Road to Meet Traffic Demand

2.1 Introduction

The growing demand for affordable mobile broadband connectivity is pushing mobile operators to redesign the radio access network. Obviously, the main target is to strike a balance between enhanced network capacity and the cost per delivered bit. To keep up with the ever increasing traffic volumes, a variety of deployment solutions can be envisaged, ranging from the enhancement of the macro layer to the deployment of indoor access points.

As a first step, mobile operators can boost the existing macro performance in terms of coverage and capacity by upgrading the existing macro base stations. Multi-Radio Access Technology (RAT) deployments displaying 2G, HSPA and LTE will co-exist to ensure wide-area coverage and increase network capacity for voice and data services. Additional spectrum, macro densification and advanced antenna technologies represent other evolution paths to improve the macro performance.

However, once the benefits of macro upgrades reach a saturation point, a massive deployment of small cells – or alternatively heterogeneous deployment– is expected to achieve substantial performance gains in network performance. As macro networks are generally characterized by a considerably uneven distribution of traffic amongst sectors, small cells are targeted at serving traffic hot-spots or improving

coverage when the macro overlay does not provide adequate performance.

This short chapter provides a tutorial-like description about deployment solutions for optimal network expansion roadmap, ranging from macro layer enhancements to user-deployed indoor small cells. The purpose is to give background information about the deployment options considered in the dissertation, and references to deployment solutions not addressed in this thesis are also provided. An overview on the current radio access technologies and spectrum availability is provided in the next section; macro layer evolution and outdoor small cell deployment are addressed in Section 2.3 and 2.4, respectively; indoor offloading solutions are addressed in Section 2.5, whereas Section 2.6 provides insight as to radio access infrastructure costs.

2.2 Multi-RAT and Spectrum Availability Overview

Through constant innovation and improvement, the 3GPP cellular technologies have contributed to the astounding success of mobile broadband. In the next years it can easily be foreseen that 2G, HSPA/HSPA+ and LTE/LTE-A technologies will co-exist and evolve together to provide mobile data coverage. As for LTE deployment, the widespread adoption of such a technology and its advanced releases is strictly dependent on the availability of LTE spectrum and LTE capable devices, which differs from country to country [64].

The reasons for having a Multi-RAT deployment can be manifold. Certainly, 2G deployments represent the most widely deployed cellular technology, providing the best wide area coverage for voice services; in addition to this, the low-rate data connections can be used to enable mobile communication between electronic devices, generally known as "Machine-to-Machine" communications [65]. With regard to 3G networks, HSPA and its evolution will be the dominant mobile broadband solution in the mid-term. Moreover, long-term spectrum licenses tied to 2G/3G technologies and the large number of legacy terminals will keep these air interfaces running in the following years. Massive LTE and LTE-A take-up is expected to take place in more than 3-5 years, although initial LTE roll-outs are already in place for both dongles and smartphones to boost network performance in urban hotspots and rural areas lacking high-speed fixed network connection.

To facilitate the co-existence of different radio access technologies and drive down deployment costs, the base station design shifts from traditional cabinet-based installation to modular and compact site architectures [66, 67]. The modular base station design provides a flexible platform that supports concurrently all the previously mentioned radio access technologies, thanks to advanced baseband and radio capabilities based on software-defined radio. Such an integrated approach

allows for the multiple RATs to share Radio Frequency (RF) units and antennas according to the utilized spectral bands, and to optimize the traffic load amongst the deployed radio access interfaces. Moreover, the more recent Remote Radio Head (RRH) design reduces feeder losses by bringing the RF module closer to the antenna connectors.

However, the mobile broadband industry is strictly dependent on the availability of spectrum in which mobile operators can operate their service. Albeit not sufficient to accommodate the expected traffic growth alone, radio spectrum is a limited and precious resource that needs to be used in the most efficient way when deploying various radio technologies. Fig. 2.1 shows the licensed frequency bands available for a typical European network deployment together with the related cellular technology. An interesting option for operators is the possibility of refarming part of the spectrum used for 2G deployment to more spectral efficient air interfaces. For instance, due to the more efficient use of spectrum resource in Global System for Mobile communication (GSM) networks [68], part of or the entire spectrum at 900 MHz can be reallocated to HSPA (or LTE) while guaranteeing better coverage than in the higher frequency bands.

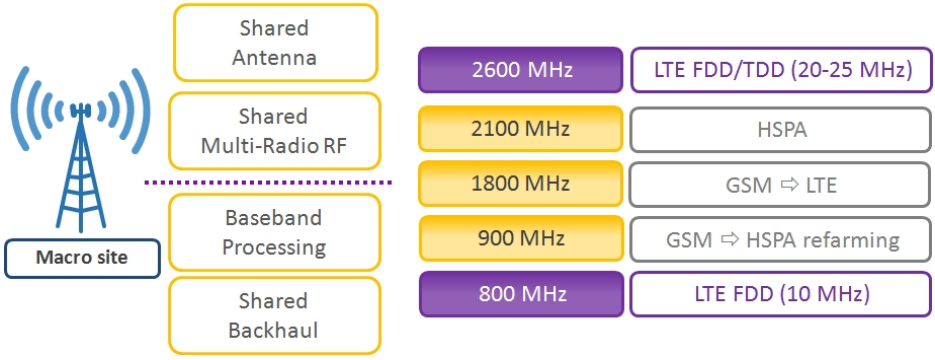

Fig. 2.1: Overview of evolved macro architecture (left) and spectrum allocation with different cellular technologies (right) in a potential European network scenario.

As the focus of the dissertation is on LTE downlink performance in realistic European scenarios, it can be seen that LTE spectrum is available in the 2.6 GHz band and the lower frequency spectrum at 800 MHz. The latter has been obtained after replacing the analog TV transmitters with newer digital TV technology [69]. Refarming GSM spectrum to LTE in the 900 and 1800 MHz spectra has not been considered in the case studies although this could be seen as an alternative option to further increase network capacity for mobile broadband services. Yet, spectrum refarming strategies depend on the operator's spectrum availability and the time frame needed to entirely decommission legacy networks.

LTE supports two operational modes that are denoted as Frequency Division

Duplexing (FDD) and Time Division Duplexing (TDD). The former is suited for paired spectrum where separate bands having the same size are allocated to uplink (user to base station) and downlink (base station to user), respectively; the latter is applied to unpaired spectrum, which is the case when uplink and downlink signals are separated in the time domain, requiring time synchronization of both base stations and user devices. In Europe, paired spectrum is released at both 800 MHz and 2.6 GHz with different band sizes, and it is known that lower frequency spectrum is generally purchased at extremely higher prices due to better coverage performance. In the 2.6 GHz band, TDD spectrum has been released in adjacent channels with respect to the FDD bands, placing severe requirements on filtering performance and adjacent channel masks to reduce interference [70].

2.3 Upgrading the Macro Layer

The deployment of more spectral efficient technologies on different frequency bands are certainly the basic measures to increase network capacity. Along with them, advanced features can be applied to the macro sites to further boost macro performance in a more cost-efficient way than densifying the existing network with brand new macro sites.

For each of the existing technologies, deploying additional spectrum generally provides a simple and cost-efficient solution for upgrading the network when spectrum is available [36]. Aligned with the same concept implemented in HSPA [70], one of the key features for LTE-A is "Carrier Aggregation"(refer, for details, to [18, 71] and references therein). Such a feature enables mobile operators to provide higher peak data rates and capacity by extending the overall transmission bandwidth beyond the 20 MHz upper limit set in first releases of LTE. In essence, spectrum resources within the same band (intra-carrier) or across different bands (inter-carrier, e.g. the 800 MHz and 2.6 GHz bands) can be pooled together up to a total bandwidth of 100 MHz. Besides extending the transmission bandwidth and avoiding spectrum fragmentation, the support of "cross-carrier" scheduling can dynamically improve network efficiency according to the signal quality perceived on the different carriers. This facilitates interference mitigation in dense heterogeneous network scenarios when some of the carriers are utilized for small cell co-channel deployment, and users move across the cell edges.

Another solution to boost macro capacity is higher order sectorization, which consists in deploying a higher number of antennas/sectors with respect to traditional macro sites. As shown in Fig. 2.2(a), the most typical configuration is to double the number of sectors from 3 to 6 on the horizontal plane by installing narrow beam antennas. This approach allows mobile operators to fully leverage the existing sites and almost double network capacity [72, 73], despite practical limitations

due to interference between adjacent antennas and increased user hand-overs. Yet, a major drawback is that high-order sectorization deployments perform best for uniform traffic distribution across the covered area, and the sector split gain considerably decreases in dense urban scenarios where high traffic areas are extremely localized.

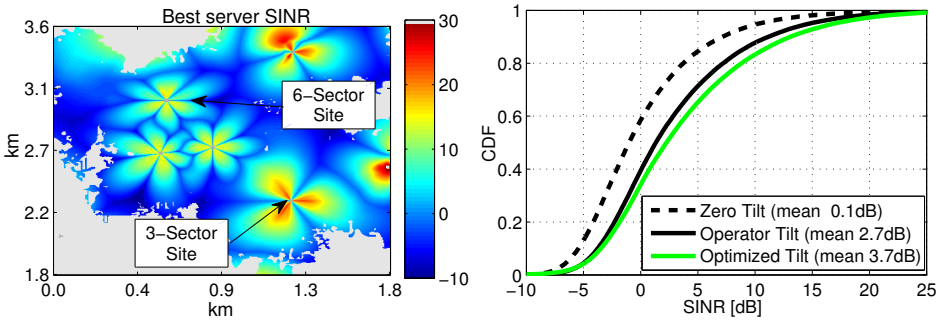

(a) High-order sectorization (b) Tilting SINR gains

Fig. 2.2: Macro layer upgrades to enhance network capacity by doubling the number of sectors per site (left) or the antenna tilting (right). Based on a large-scale network scenario, the optimization of electrical tilting improves the average SINR by 1 dB with respect to the current tilting setup utilized by the operator.

Furthermore, antenna down-tilting optimization provides a cost-efficient deployment solution to improve user performance at the cell-edge [74]. By optimizing the antenna vertical tilting angle it is possible to reduce inter-site interference and enhance the perceived signal quality. An example is given in Fig. 2.2(b) for a large-scale network deployment in a urban scenario. The tilt settings can be tuned by either mechanical tilting, applied on-site, or by electrical tilting with remote modifications [75]. Besides the single sector case, antenna down-tilting is also fundamental for the deployment of vertical sectorization, or alternatively vertical beamforming [76]. With advanced antenna configurations, known as "Active Antennas" [77], the conventional antenna beam can be vertically split into two main lobes, thereby increasing the spatial reuse of the spectrum. The vertical beams can be dynamically steered in order to not only reduce interference between the vertical lobes, but also to better serve the non-uniform capacity demand across the sector area.

As concerns advanced antenna techniques, LTE-A includes advanced multi-antenna schemes that go beyond the basic 2x2 Multiple Input Multiple Output (MIMO) antenna schemes. Although not addressed in this thesis, spectral efficiency can be raised in the donwlink by increasing the MIMO spatial multiplexing layers up to 8, i.e. 8 transmitting and receiving antennas. Besides the conventional single user link, beamforming techniques can be combined with spatial multiplexing to

serve multiple users simultaneously on the same frequency resource, relying mainly on spatial separation. This feature, denoted as Multi User (MU)-MIMO [78], is expected to substantially increase network capacity, but practical antenna deployment limitations on the devices and non-ideal channel feedback may limit their potential [79]. Further, future network deployment will tend to be based on Coordinated multipoint (CoMP) transmission and reception techniques that utilize multiple transmission and receive antennas from multiple antenna site locations [80]. The purpose is to enhance the signal quality at the cell edge by suppressing interference or combining the received signals. From a practical point of view, CoMP schemes will rely on high-speed and low-latency fiber interconnection between transmission points so that a centralized, or "cloud", processing unit will optimally combine the signals and jointly schedule the radio resources. Besides improved radio performance, the centralized baseband architecture can bring benefits in terms of reduced network operational costs and energy consumption.

2.4 Outdoor Deployment Solutions

Differently from traditional network topologies mainly based on macro base stations, a dense deployment of small cells is envisaged to cover high-traffic or poorly covered areas, and to boost user performance in such critical areas. Outdoor small cells seem to be a promising solution to meet traffic demand at reasonable costs [81]. In this section two different types of outdoor base stations, micro and relay base stations, will be described, pointing out the impact of various backhaul solutions on the viability of outdoor small cell deployment.

2.4.1 Micro Base Stations

When the macro layer enhancements do not suffice to provide the coverage and capacity requirements, additional capacity can be provided by micro base stations below the rooftop in dense urban environments. In such scenarios the deployment of additional macro sites is rarely a viable solution due to economic and practical constraints. Thus, outdoor micro cells are intended to facilitate the deployment of additional cells in the network, and this is achieved according to the following:

- Micro cells are mainly deployed in high-traffic areas with the purpose of serving both outdoor and indoor users. With the advent of mobile broadband, typical hotspots are not only public spaces (stadiums, airports, shopping malls,etc.), but also residential areas.
- Micro cells feature compact and lightweight base stations equipment to guarantee ease of installation. In general, micro cells can be seen as fully inte-

grated base stations including baseband and RF unit in one physical module. Transmission power can range from 1 to 5 W, depending on the deployment scenario. Omni-directional antennas are generally utilized although sectorial antennas can be deployed for specific cases. Micros mainly operate in open mode, admitting all the potential subscribers without any restriction.

- Micro base stations are deployed below rooftop at street level, leveraging innovative site locations such as traffic lights, utility poles (see Fig. 2.3(a)), building walls, and even power lines or cables. Such an approach reduces the site-related costs as compared to traditional macro towers.

- The support from self-optimized network features help in simplifying and reducing the cost of operational and maintenance procedure [82].

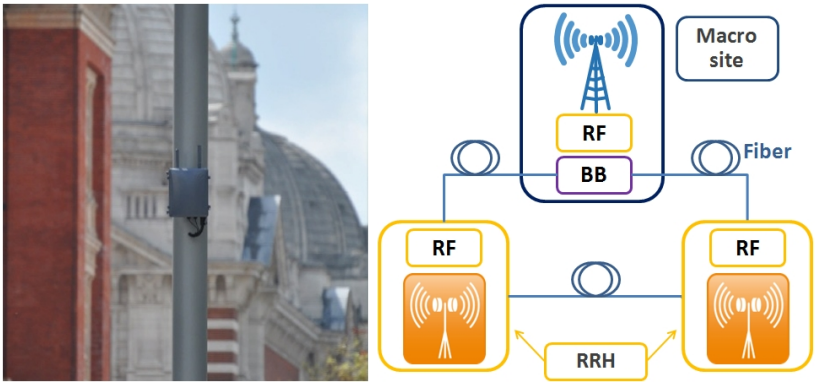

(a) Lamp-post deployment (b) Centralized baseband architecture

Fig. 2.3: Examples of site location for outdoor 3G micro deployment (left figure), as can be seen at http://www.awtg.co.uk. The right figure shows the principle of the centralized baseband architecture which features micro cells deployed as RRHs and baseband (BB) pooling at the macro site.

On a deployment level, initial planning may be involved when placing micro cells, in order to cover the expected high-traffic area and also mitigate interference. The latter is more challenging when micro and high-power macro cells share the same carrier. Hence, with increased small cell density, interference management becomes more complex with regard to striking the balance within the number of users offloaded to micros and the perceived signal quality. To find such a trade-off, micro cells can be deployed in the form of RRHs, which hosts only the RF unit at the micro location and is remotely connected via fiber to the macro baseband pool, as shown in Fig. 2.3(b). This architecture enables all the cells sharing the baseband processing to coordinate transmission and optimize traffic load amongst the different layers. In particular, interference between macro and co-channel

micro or pico cells can be reduced by means of enhanced ICIC schemes [27], which allow the small cells to extend their covered area while silencing macro transmission in specific time subframes to reduce interference.

Advanced techniques for handling interference, exploiting carrier aggregation across the different deployment layers, and performing coordinated transmission from multiple cells are beyond the scope of this dissertation. These features depend also on the micro backhaul connection and how fast signaling information can be exchanged between cells. In the next subsection, an overview of the main backhaul solutions for small cell deployment is provided.

2.4.2 The Backhaul Challenge

A critical aspect related to small cell deployment is the backhaul connection, and it is extremely arduous to find a single solution working in every network scenario. To provide optimal service experience to the users, mobile operators aim to build backhaul links with high performance, but on the other hand the adopted backhaul solutions can severely affect the overall network TCO when self-built backhaul is not available and backhaul lines are to be leased.

Due to the huge success of multimedia broadband services, the legacy "last mile" backhaul infrastructure optimized for circuit-switched voice traffic are being migrated to IP-based backhaul in order to cope with the increased data rates experienced at the radio access [83,84]. Based on the type of backhaul connection [85,86], the mobile backhaul solutions can be divided into two main groups, wireline and wireless. The most common solutions for mobile backhaul are the following:

Fiber: It basically guarantees no throughput limitations with respect to small cell radio access requirements. Fiber is commonly available in urban areas although not always owned by mobile operators. When not available, high trenching and installation costs drive the cost of fiber up as compared to alternative wireless solutions.

Copper: Digital Subscriber Line (DSL)-based technologies can be a cost effective solution for mobile backhaul [87]. They are mainly operated on copper pairs, which can also be bonded to increase the link capacity (e.g. Very-high-speed DSL, VDSL) up to 200 Mbps [88]. Carrier over Ethernet [84] operated on cables CAT 5/6 is another copper-based solution that is able to exceed the 1 Gbit/s threshold. The main setback of backhaul connections over copper is that high band is supported only for limited distances, and this could be a limiting factor with regard to the peak data rates guaranteed by the latest releases of LTE.

Microwave: Microwave backhaul includes point-to-point and point-to-multi point

wireless connections operated in licensed frequencies between 6 and 43 GHz [89]. Considering the large bandwidths and high order modulation schemes, microwave backhaul solutions can guarantee gross bit rates in the order of 1 Gbit/s. The main drawback is that the propagation conditions at the utilized frequencies impose strict Line of Sight (LOS) requirements on the wireless link. This enforces some limitation when selecting the position of the small cells, and in addition to this, high maintenance costs are needed to ensure high performance on the point-to-point link. The use of even higher frequencies – the E-band (MMW) at 70-80 GHz – is also an interesting solution thanks to larger available bands, but the more challenging propagation conditions and more complex RF components have a negative impact on backhaul related costs.

Mesh WiFi: WiFi multi-hop networks [90] can be deployed for backhaul and operated on unlicensed spectrum in the 2.4 GHz and 5 GHz bands. From a propagation perspective such bands allow for NLOS propagation, which is typically experienced at street level in dense urban scenarios. Although very competitive from a TCO perspective, the WiFi mesh network could prove insufficient for 4G technologies due to low throughput and large delay variations.

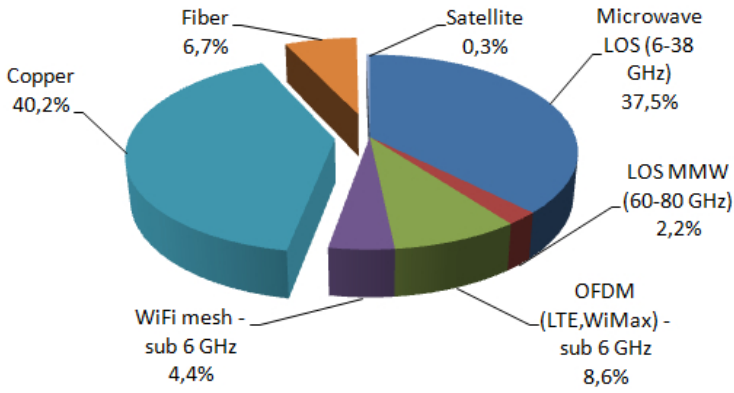

Fig. 2.4: Market share of current small cell backhaul solutions on a global scale, based on the data provided in [85].

The market share of the different backhaul solutions for small cell deployment is shown in Fig. 2.4 [85]. The analysis is conducted on a global scale, and it can be found that current small cell backhaul is dominated by copper and microwave solutions. The same source [85] predicts that in a span of 5 years from today's status, the fiber share will triple, gradually replacing backhaul over copper, whilst NLOS wireless solutions will tend to replace part of the microwave backhaul deployments. Obviously, the market share of backhaul solutions varies on a country and operator basis, depending on the availability of wired backhaul infrastructure.

Amid the wireless backhaul solutions, the use of mobile spectrum for backhaul, also known as in-band backhaul, is yet another option to reduce backhaul installation costs as well as having advantageous NLOS propagation conditions in the sub 6 GHz band. However, using the spectrum that can potentially be used to serve users poses challenges in resource sharing between backhaul and user connections.

2.4.3 The Wireless Backhaul solution: LTE-A Relays

Relay cells have been extensively studied and ultimately standardized amongst the various LTE-A features [40]. To decrease deployment costs, the possibility of deploying small cells not relying on wired backhaul solution is an attractive solution. The main target is to provide extended LTE coverage in targeted areas where macro users are poorly covered, especially in rural areas with sparse macro deployment. The peculiarity of relaying is that the wireless backhaul transmission and reception take place in the LTE spectrum where NLOS coverage gives more flexibility as to selecting the small cell position. Yet, such bands are more susceptible to interference than LOS microwave solutions, and backhaul spectral resources are to be shared amongst potentially multiple relays. Whether or not relays can be used also in suburban/urban scenarios to boost network performance in high-traffic scenario is among the objectives of this dissertation.

With the help of relay cells, the radio link between the macro cell and user is divided into two hops, as depicted in Fig. 2.5. The first hop is denoted as *backhaul link* since it is dedicated to backhaul transmission and reception between the relay and the serving macro cell, which is defined as macro *donor* cell. The connection between the relay cell and relay users is referred to as *relay link*, whereas the macro transmission towards macro users takes place on the macro *direct* link. Although different types of relays can be found in [40], the most promising relay configuration is the one featuring the relay cell as a stand-alone base station, such as the macro, rather than an amplify-and-forward repeaters. The considered relays are denoted as Type 1, and the main features are:

- Relay cells possess their own cell physical identity and transmit all the necessary physical channels. In this way, relays are non-transparent as they appear as a regular macro cell to all the users.
- Type 1 relays decodes the received signal prior to forwarding it to the transmitter, thereby increasing the processing delay; such a configuration improves the performance of the two-hop connection in low-SINR regions as compared to plain amplify-and-forward relays. Furthermore, separate rate adaptation and scheduling on backhaul and access links can be performed.
- With respect to the usage of spectrum amid the different links, the relay is further classified into two categories: *in-band* or Type 1b relays, which

operate backhaul and access link transmissions on the same frequency carrier, and *out-band* or Type 1a relays, in which case the two hops are separated in the frequency domain on different bands, as can be seen in Fig. 2.5.

- As for the conventional separation between uplink and downlink data transmission, relays can be operated in FDD or TDD mode.

As the relay transmitter causes interference to its own receiver, simultaneous backhaul and access link transmissions can be achieved only if the ingoing and outgoing signals are sufficiently isolated and separated. In case of in-band relays, access and backhaul subframes are multiplexed in the time domain (half-duplex), as shown in Fig. 2.5, thus isolating backhaul and access links. Thanks to the inherent separation in the frequency domain between backhaul and access links, out-band relays can be operated in full-duplex mode. However, an efficient spatial separation of the relay antennas is needed if the two backhaul and access transmission bands are contiguous.

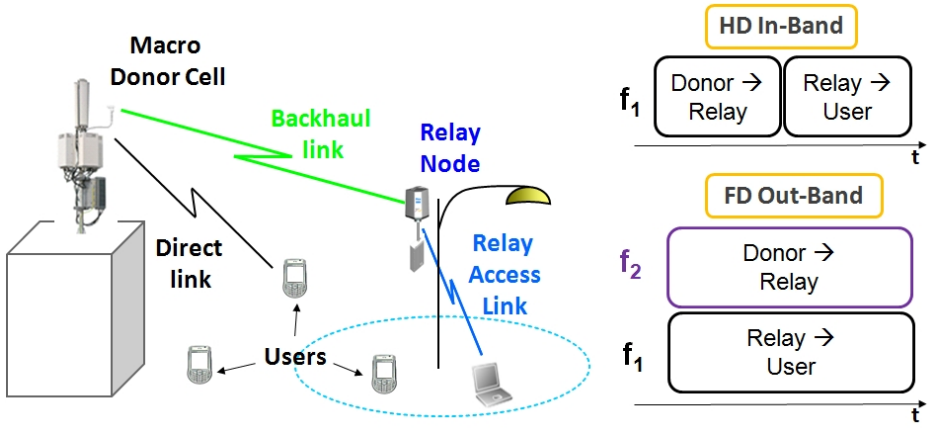

Fig. 2.5: Transmission links involved in a relay-enhanced network together with resource allocation for half duplex in-band and full duplex out-band relays.

Differently from the out-band configuration, in-band relays are more challenging in terms of optimal resource sharing. Due to the temporal separation, the relay receives data on the backhaul link in certain downlink subframes and transmits on the access link in the remaining ones, whereas the opposite occurs in the uplink. Backhaul subframes can be semi-statically or dynamically allocated so as to optimize the performance of not only relay users, but also the macro users connected to the donor cell. At the physical layer, the design of the backhaul channel requires the use of a specific control channel by means of which the donor cell schedules backhaul resources to the connected relays (refer to [91] for details). Moreover, relay cells ensure backward compatibility with terminals supporting previous re-

leases of LTE, whereas channel feedback transmission and retransmissions for error recovery are performed on both the backhaul and access link.

Other challenges and requirements related to in-band relaying are related to physical layer transmission while keeping the equipment costs low. For instance, in order to not waste physical resources, it is important to reduce the processing delays due to signal decoding and forwarding, and the period needed to switch the RF circuitry between backhaul and access link operations. But the most crucial challenge lies in operating the backhaul link at high spectral efficiency. As part of the spectrum is used for a redundant link, the least resources have to be allocated to the backhaul link while providing sufficient backhaul capacity to serve the relay users. Hence, the positioning and choice of backhaul antennas are fundamental to ensure high signal quality on the backhaul link, but it is also important to understand to what extent and under which traffic conditions the backhaul acts as a bottleneck for the overall network performance.

In this dissertation the focus is on fixed relays deployed outdoors similarly to micro cells. Only a two-hop connection is considered when transmitting from the donor to the relay user, but further studies are also oriented towards the deployment of LTE multi-hop networks and mobile relays.

2.5 Indoor Area Solutions

With mobile network being squeezed in terms of capacity, heterogeneous deployments can push themselves to serve indoor traffic hotspots by installing indoor access points. It is known that more than half the mobile broadband traffic is concentrated in indoor areas, ranging from business to residential areas. For this reason, femto cells are regarded as a cost effective deployment solution to guarantee a high quality of service for indoor users.

Offloading indoor users from the overlay macro towards indoor base stations brings several benefits. First of all, indoor users served by indoor cells experience high data rates thanks to a higher signal quality and a lower number of connected users in comparison with macro cells. Then, the lower traffic load at the macro layer improves the service experience of macro users, especially when the offloaded users are the indoor ones poorly covered by the macro cells. On top of this, indoor cells are supposed to leverage the existing broadband fixed line connection (Ethernet cable, DSL, etc.) as backhaul solution on a customer's premises, which lays the foundation for the convergence between fixed and cellular networks. Along with the broadband connection, no additional costs related to power supply and site rental are incurred as they are provided by the user.

Amid the different options, this dissertation focuses its attention on LTE femto cells, or HeNBs, as an offloading solution to boost network capacity and meet future traffic demand [92]. This deployment solution has already been utilized in 3G networks, mostly as a tool to solve macro coverage holes for voice services and avoid subscriber churn [93]. With regard to access restrictions, femto cells can be classified as [57]:

- Closed Subscriber Group: Only a subset of users, which is defined by the femto owner, can get access to the femto access point. In case of co-channel deployment with the macro, this scenario is extremely critical in terms of interference for those users placed within the femto footprint but forced to connect to the macro layer. To mitigate interference towards the macro users, several solutions are available: to inhibit femto transmission according to a predefined muting pattern [94], to control femto transmission power, or to deploy an additional femto-free ("escape") carrier at the macro layer [58].
- Open Subscriber Group: No access restriction is imposed on the subscribers camping onto the femto access points. From an operator's perspective, this configuration strengthens the offloading potential as more users can be moved towards the indoor layer. The drawbacks are given by a potentially higher number of handovers and the need for stricter security measures.

A hybrid version of the above can also be considered by introducing priorities for user access. The main issue is that femto cells rely on the broadband backhaul connection owned by the user, and sharing backhaul capacity with neighbors or passer-bys may not be an effective marketing strategy. Moreover, femto access strategies can also depend on the targeted indoor environment to be covered with femto cells. Based on the deployment scenario, it is possible to distinguish between the following femto solutions:

- **Residential**: home femtos are deployed at home or in small offices in an uncoordinated way, typically in CSG mode. The transmission power varies between 5 mW and 20 mW with the purpose of limiting the covered area within the apartment. In addition, these femto cells have self-configuring capabilities, and they can serve up to 4-8 simultaneously active users.
- **Enterprise**: enterprise femtos are engineered to operate at higher transmission power (100 mW), deliver higher capacity, and guarantee a certain predefined quality of service. From 8 up to 30 users can be supported by such femtos (small-medium enterprise). Due to the higher transmission power and massive deployment throughout the premises, enterprise femtos may require initial operator-assisted installation and management rather than having self-installation capabilities. In this scenario femtos can also be deployed in OSG mode.

This dissertation investigates the performance of indoor enterprise OSG femtos, which can be deployed on a dedicated or shared carrier with the macro layer. Although the use of open femtos is not extremely critical in terms of interference with respect to CSG, enterprise deployment poses additional challenges. As multiple femtos can be spread over a floor and also across different floors, inter-femto interaction is needed to support user mobility, which is higher than in residential scenarios. Then, the larger number of connected users put more emphasis on coverage and quality of service requirements, enhanced security, and backhaul line quality. The last one can use a dedicated connection or a shared one with the existing enterprise broadband connection at the cost of backhaul capacity limitations [53].

Fig. 2.6 shows the LTE femto architecture valid for LTE release 10 [95]. It can be seen that femto nodes can directly connect to the core network through the interface S1, or pass through an intermediate gateway denoted as HeNB-Gateway (HeNB GW) that is deployed at the operator's premises. The gateway solution, which is currently used for 3G femtos, has been devised to address the issue of supporting a large number of S1 interfaces towards the core network. The aggregation point guarantees scalability for dense femto deployment at the cost of increased latency. Moreover, as an additional feature of LTE-Advanced (Release 10), femtos can also support the X2 interface directly connecting the conventional LTE cells (eNodeBs). This makes it possible to have a faster and more robust handover between open femtos located in the same building.

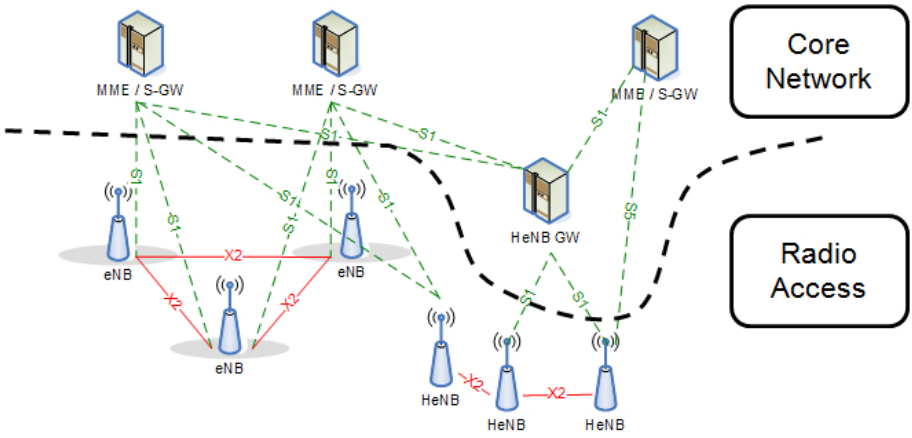

Fig. 2.6: Overall LTE architecture with deployed femto cells (HeNBs), as shown in [95]. Femtos can be directly connected to the core network via the interface S1 or through an intermediate gateway (HeNB GW). The macro cells, and optionally femtos, are interconnected via interface X2.

Besides femto cells, other indoor deployment options are available, although not

within the scope of this thesis. The most popular ones are briefly described below:

- **Distributed Antenna system (DAS)** [96]: This system is an in-building solution on multiple remote (or active) antennas which are spatially spread over the building areas. All the antenna units are connected to a central unit, and they simultaneously broadcast the same copy of the signal over the covered area using the same transmission band. Essentially, the antennas belong to the same cell, and no frequency reuse is achieved. For this reason, a single cell DAS provides good indoor signal coverage in large-sized buildings, but its capacity performance is significantly lower than deploying plain femto cells instead of the DAS antenna units [97]. Moreover, the DAS deployment costs can be higher than femtos due to installation works needed to lay fiber or heavy coaxial cables between antennas and central unit.
- **WiFi deployment**: WiFi is another important deployment technology for heterogeneous networks, which can be exploited for both indoor local area and outdoor deployment. Although seen as a competing solution for cellular technologies in previous years, WiFi has been integrated into the mobile network as a capacity relief to the congested macro overlay [98]. WiFi access points transmit and receive on unlicensed spectrum bands at 2.4 and 5 GHz, relying on a distributed medium access scheme. Mobile broadband users can switch from cellular to WiFi thanks to auto-login and authentication procedures [99]. In accordance with the latest IEEE 802.11ac standard [100], an increased number of antennas and the possibility of channel binding can push WiFi delivered throughput over the 1 Gbit/s barrier. Despite the large availability of spectrum, it is still an open issue to evaluate to what extent interference on unlicensed bands can affect realistic dense deployment of WiFi nodes as compared to the femto deployment on licensed spectrum. However, the large adoption and low deployment costs make WiFi an attractive offloading solution complementing the cellular network.

2.6 Radio Access Infrastructure Costs

From an operator's perspective, the choice of the best deployment strategy involves not only the fulfillment of technical requirements, but also at what cost the traffic demand can be met. Based on the approach outlined in previous works [31, 48], this dissertation proposes a cost analysis of the investigated deployment solutions, limiting the scope of the cost estimated to the radio access network.[1]

[1] As already stated in the introductory chapter, costs related to core network deployment and operation, spectrum licensing, customer support, service provisioning, etc. are excluded from the cost analysis. In general, the overall mobile network costs are dominated by the radio access part (the "last-mile") [101], whereas future spectrum license costs are difficult to predict due to country regulations and competition in the market.

A financial estimate of the radio access infrastructure is denoted as TCO. The overall expenditure can be divided into the following three cost components:

- **Capital Expenditures (CAPEX)**: It refers to the one-time investments a mobile operators makes when acquiring fixed assets to deploy or upgrade the initial network. These include bast station software and hardware equipment, antennas and auxiliaries (mast, power supply, battery), and backhaul connection.
- **Implementation Expenditures (IMPEX)**: It stands for the expenses needed to physically build and roll out the network. Typical IMPEX drivers are site acquisition, civil works for site construction and preparation, equipment (base station/backhaul) installation, and network planning and initial optimization.
- **Operational Expenditures (OPEX)**: It is related to the cost the mobile operator periodically incurs to run the network. These on-going expenses are mainly due to site rental, electricity costs, operation and maintenance (towers, base stations and backhaul), software licenses, backhaul rent or leasing fees, off-site support.

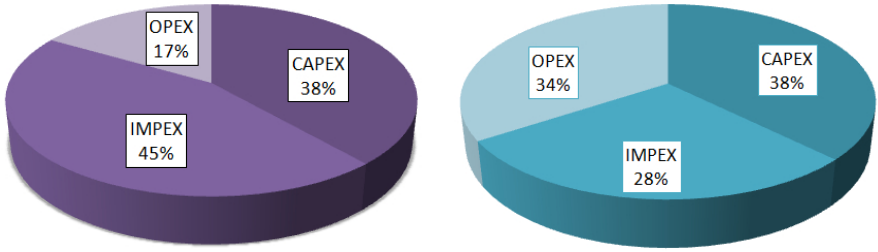

(a) Macro site (total cost:120 k€) (b) Micro site (total cost:23 k€)

Fig. 2.7: Breakdown of the overall infrastructure cost (CAPEX,IMPEX, and OPEX) for a newly deployed macro LTE site (left) and outdoor micro cell (right) in a European urban scenario. The OPEX is only considered for the initial year, whereas high-cost backhaul connection is assumed for micros

Typically, network investments are valuated over a multi-year period, considering different time instants at which the existing network is upgraded and enhanced. Deployment techno-economic studies [31,48] resort to a simplified Discounted Cash Flow model to estimate the TCO over a period of time. Such a tool accounts for inflation and time value of money by applying a risk-adjusted discount rate to future expenditures as compared to the present values. On top of this, price erosion can also be modeled when the price of certain assets –such as base station hardware equipment and software – decreases over time.

An example of cost structures utilized in this dissertation is illustrated in Fig. 2.7. For a newly deployed macro site, the costs are considerably dominated by CAPEX and IMPEX as upfront investments must be made for site acquisition and buildout, the purchase of radio and backhaul equipment, and the installation process. Hence, it is considerably cost effective to reuse 3G sites when rolling out the LTE network; in fact, the costs related to the site acquisition, backhaul connection and part of the radio equipment can promptly be saved. With regard to outdoor micro cells, the overall TCO, which is lower than the macro one, is almost equally split between the three cost components. This implies that, once the small cell is installed, the running costs (OPEX) determine whether or not micro cell deployment is a viable solution as compared to other deployment configurations. In particular, site rental and backhaul expenditures may vary greatly between markets and specific deployment scenarios. Thus, keeping site rental and backhaul costs to a minimum plays an important role in the commercial success of small cell deployment, such as outdoor micro cells.

Besides the performance evaluation of different heterogeneous deployment solutions, this thesis also presents a TCO analysis for each of the addressed case studies. The targets are to insert an additional measure to compare deployment solutions that are capable of fulfilling predefined service requirements, and point out under which cost assumptions certain deployment solutions are more profitable than others.

Part I

Analysis of Outdoor Small Cells Deployment

Chapter 3

Network Deployment Modeling Framework

3.1 Introduction

This chapter describes the modeling framework supporting the performance evaluation and cost analysis of various network scenarios. The proposed models are applied to the deployment case studies presented in Chapter 4 and 5, where the potential of deploying outdoor small cells, namely relay and micro base stations, has been investigated. Furthermore, most of the models, methods and algorithms described hereafter serve as the fundamental modeling block for the deployment studies presented in Part II. In those studies, the network scenario modeling is further improved with the purpose of capturing the nuances of indoor spatial traffic distribution and indoor small cell deployment.

In order to estimate the LTE radio performance for different deployment configurations, a snapshot based approach has been adopted for all the investigated case studies. As emphasis is put on large-scale deployments involving a large number of cells and users, network performance is estimated by means of static Monte-Carlo simulations [102] in which static users are generated on each snapshot according to a predefined spatial traffic distribution. Differently from a simple link-budget analysis, interference and radio resource sharing are explicitly modeled although the estimated data rates are to be considered as average values, based on average propagation losses. In fact, the static modeling framework falls short of capturing

dynamic aspects such as small scale channel variations, the time-variant behavior of resource scheduling, and user mobility. However, static simulations are widely used during the network planning and optimization phases in order to find the right tradeoff between computational complexity and performance evaluation accuracy [103, Chapter 3]. As the goal of this dissertation is to investigate the potential of different deployment solutions from a higher abstraction level, the static Monte Carlo-based method has been selected.

The chapter is organized as follows: Section 3.2 describes the main performance measures and targets associated with the network performance evaluation and dimensioning process. Section 3.3 presents the main assumptions and inputs needed to model realistic network layouts, propagation losses and spatial traffic density related to the investigated areas. Section 3.4 is dedicated to the description of the radio resource sharing modeling, which takes into account the wireless backhaul when relays are deployed in the network; Section 3.5 concerns the link budget calculations and the SINR estimations that are utilized to directly estimate the user experienced data rate at the physical layer. The deployment strategies for outdoor small cells is treated in Section 3.6 with the intent of illustrating the rationale behind the deployment algorithms employed in the following case studies. Finally, in Section 3.6 an overview of the main cost assumptions and figures for the investigated network configurations is presented.

3.2 Key Performance Indicators

When dimensioning their own networks, mobile operators are expected to satisfy the increasing traffic demand and guarantee a minimum performance level to most users. In order to evaluate the radio performance of different deployment solutions, it is important to define what sort of KPI must be considered, and to specify the performance targets to be accomplished when upgrading the existing network infrastructure. In this study, the considered performance measures are both *coverage* and *capacity*, as the former gives an indication of the guaranteed level of service achieved with a certain site density and spectrum availability, whilst the latter is a measure of the aggregate data rate delivered within the investigated area. Although the two KPIs are strictly correlated, the main network requirement is expressed in terms of coverage, or alternatively *user outage*, which is defined as the fraction of users that cannot be served with a predefined minimum data-rate. Network capacity, instead, is considered as a secondary performance measure that is used to further differentiate deployment alternatives giving similar coverage performance.

For the sake of simplicity, only the downlink transmission will be addressed in this study. By denoting n_{tot} as the total number of users simultaneously downloading

data packets, i.e. the network traffic load, we define the *user outage* , $\psi_{network}$, as follows:

$$\psi_{network} = \frac{1}{n_{tot}} \sum_{l=1}^{n_{tot}} \mathbf{1}\{R_l < r^*_{min}\} \tag{3.1}$$

where R_l stands for the downlink average data rate experienced by the *l-th* active user, and r^*_{min} is a predefined minimum required data rate. In this study the data rates are estimated at the radio access layer, i.e. the media access layer, and not at the application layer. This also means that the overhead related to the transmission of control channel information [104] for an LTE system is taken into account and then excluded when calculating the achieved data rate. $\psi_{network}$ represents the percentage of users whose average data rate is below the minimum required one. A typical outage target, ψ_{target}, for a large-scale deployment is in the order of 5-10% – or alternatively 95-90% coverage.

On condition that $\psi_{network} \leq \psi_{target}$, the network deployment alternatives can be further compared in terms of capacity for a fixed network traffic load. As a measure of network capacity, the arithmetic mean of average user throughput values is selected and defined as:

$$\bar{R}_{cap} = \frac{1}{n_{tot}} \sum_{l=1}^{n_{tot}} R_l \tag{3.2}$$

It is also assumed that for a given network traffic load, the user downloads data according to a full buffer traffic model, implying that all users have infinite data (or extremely large data packets) to download. Under this assumption, the overall average user throughput can outperform the minimum required data rate and for this reason, such a measure is utilized to quantify the cellular network capacity. Even though the full buffer assumption may not be considered practical [105] as compared to realistic traffic patterns, it has been widely used as a baseline traffic model for technology comparison in system-level simulations. From a deployment point of view, it can also be seen as a worst case scenario in terms of radio channel conditions, as full interference is generated by the surrounding cells transmitting on the same band. In such a scenario, network dimensioning is more challenging, and the proposed solutions are more conservative with regard to provision of the targeted network coverage.

3.3 Network Scenario Model

The modeling of real network deployment scenarios is an important aspect of network dimensioning and planning. In order to have adequate models, several input data are needed, and they can be grouped into three main areas: network

layout information, path loss predictions and propagation models, and spatial traffic distribution. The different types of input are described in the following subsections.

3.3.1 Realistic Network Layout

When evaluating the performance of LTE networks, it is reasonable to assume that an operator may wish to reuse as much as possible the existing 3G sites to decrease the deployment costs. At the time this study was started, European operators began planning extensive LTE roll-out for the following years, but no commercial LTE deployment was yet in place or reached mass market. Therefore, the existing 3G network is assumed to be the reference scenario for the LTE deployment, and this means that the existing 3G site locations are considered as LTE site locations to simulate the LTE macro cellular performance. The needed input data related to the base stations are listed below:

Site coordinates: the geographical position of the sites is given in Universal Transverse Mercator (UTM) or World Geodetic System-84 (WGS-84) coordinate systems specifying the easting and northing coordinate pairs in the investigated area. To avoid border effects, base stations located outside the investigated area are also included. By considering at least one tier of interfering cells, a more accurate performance evaluation can be guaranteed, especially for those users who are located at the edges of the selected area.

Site configuration: Sector and Cell IDs are to be specified to properly model the different sectors and possible multi-carrier configurations. Regarding the radio equipment, it is typically possible to have, for each of the considered cells, antenna mast height, feeder loss,transmitter and receiver antenna ports, receiver noise and polarization. An example of the utilized imported input data is illustrated in Fig. 3.1.

Antenna pattern: azimuth and vertical radiation patterns obtained from real antenna products can be utilized instead of theoretical models. Vertical tilting angles for the different 3G cells are also provided, and they are utilized as input for the LTE reference network. If the realistic antenna patterns are missing, 3GPP radiation patterns are assumed [62].

To better model the propagation characteristics in the investigated areas, digital maps are provided in the form of raster maps, where the raster unit stands for the map resolution or *pixel*. Typically, digital maps contain topographic data (terrain height), morphographic data (terrain and clutter type for path loss corrections) and building location data to spot the indoor areas. In the investigated deployments, resolution bin of 25 m x 25 m is utilized in the sub-urban scenario

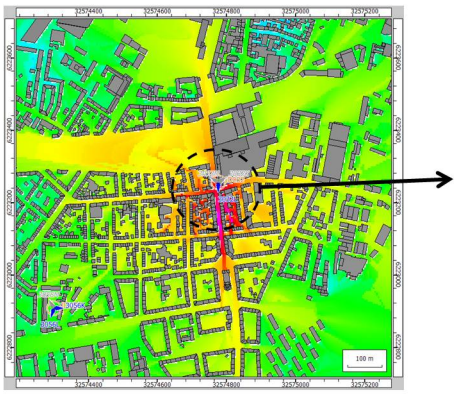

Parameter	Sector 1	Sector 2	Sector 3
Sector ID	3G-JD02-1	3G-JD02-2	3G-JDD02-3
Antenna Height	24.5 m	24.5 m	24.5 m
UTM WE_coord.	32574775 m	32574775 m	32574775 m
UTM NE_coord.	62223224 m	62223224 m	62223224 m
Bearing Angle	64°	177°	312°
Vertical Tilting	6°	4°	4°
Cable Loss	3 dB	3 dB	3 dB

Fig. 3.1: Site-related information concerning site position, sector IDs, antenna configurations and feeder losses. The map on the left provides an illustration of the real site locations and the realistic building maps that are imported to set up the reference scenario.

whereas a better resolution of 10 m x 10 m has been used in the metropolitan areas to increase the accuracy of ray-traced path loss calculations and indoor building areas.

3.3.2 Propagation Models

In the downlink performance analysis, it is of utmost importance to have an accurate estimation of the link loss between a base station and the mobile user. Two different approaches –*statistical* or *ray-traced* path loss models– are followed to calculate the propagation losses, and they are strictly related to the propagation characteristics of the investigated scenarios, simulation complexity and also the type of considered base station.

As concerns macro cell transmission towards users and also relays for the backhaul link, the propagation environment is generally characterized by a transmitter located over the rooftop, and the following assumptions have been made when modeling the macro link path gains:

- In the suburban deployment scenario presented in Chapter 4, the macro propagation losses have been modeled by means of the well-known Okumura-Hata model [106,107], which is well suited for macro cell transmission having the transmitting antenna located well above the surrounding rooftop level. The covered frequency range for LTE deployment and the possibility of accounting for the antenna height gain are also important factors that favored

the selection of such a propagation model. A fixed building penetration loss of 20 dB is also applied to indoor users.

- For the investigated dense urban scenario (see Chapter 5), ray-tracing [108] is used to evaluate path loss and antenna pattern effects on both macro and backhaul link budgets. A 3D ray-tracing modeling tool has been utilized, which provides radio propagation predictions at street level by considering realistic positions and heights of the buildings, similarly to the study presented in [49]. To properly set the ray-tracing model parameters, field measurements data have been used to calibrate the path loss predictions. Statistical indoor penetration models calculating the attenuation of the macro signal through the building areas are also available for this study.

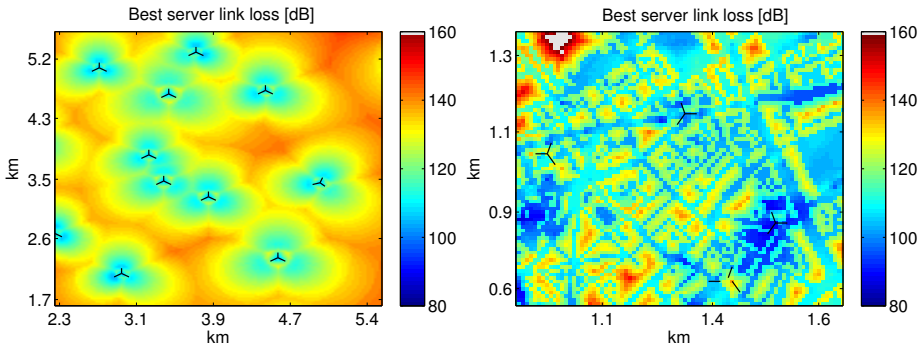

(a) Statistical Model (b) Raytracing Model

Fig. 3.2: Propagation loss maps from the serving base stations, for both statistical and ray-traced propagation models. The former is obtained for a suburban scenario where each pixel is considered indoor; the latter corresponds to a metropolitan area with available 3D building data and indoor penetration loss models.

In Part I, the path loss related to the access link between the relay/micro cell and mobile user is modeled by using the statistical 3GPP models described in [62]. Those are formulated for both urban and suburban 3GPP scenarios; the LOS condition is modeled through a probability function that depends on the distance between the small cell and the terminal. The use of a statistical model instead of ray-tracing is due to the need of speeding up the simulation time and reducing complexity when a large number of small cells is deployed in the network. This also facilitates sensitivity studies addressing different relay/micro deployment strategies and transmission configurations. All the previously mentioned propagation models will be described in detail in the chapters addressing the case studies.

3.3.3 Spatial Traffic Distribution

The spatial distribution of the network traffic plays a key role in efficiently upgrading the existing network to meet increased capacity demands [109]. Based on voice traffic measurements over GSM networks [110, 111], a typical approach is that of assuming a log-normally distributed traffic [112,113] over the investigated area, and a spatial exponential correlation is generally introduced to model the traffic hot-spot locations. However, the analysis of real deployment scenarios cannot be completely based on statistical traffic distribution: the mapping between the measured cell traffic and the estimated cell area is the first step to take when modeling inhomogeneous traffic densities. This is needed for spotting the areas and the cells of the network that experience higher user outage and need to be upgraded. In this subsection, the user density definition is provided together with the description of the methods employed for deriving the user density maps of the analyzed scenarios.

To generate the position of the users, the spatial traffic information is translated into a user density map whose resolution is denoted as pixel. Assuming that for a given pixel i, j (with i and j being the location coordinates) the amount of generated data traffic is T_{ij} [Mbps/km^2], the user density spatial distribution s_{ij} for the pixel ij is defined as follows:

$$s_{ij} = \frac{T_{ij}}{\sum\limits_{i,j} T_{ij}} \Rightarrow p^l_{\mathcal{L}} = \sum_{i,j \in \mathcal{L}} s_{ij} \tag{3.3}$$

where $p^l_{\mathcal{L}}$ denotes the probability for a generic user to be located in an area $\mathcal{L}$, which covers a set of pixels[1]. A random set of user locations is generated in each snapshot according to the user density distribution map. A sufficient number of snapshots is set in order to explore the spatial variations in traffic density and guarantee statistical confidence in the performed simulation experiments, as described in Appendix A.

To estimate the traffic volume T_{ij} in a specific pixel or set of pixels, different methods can be employed, depending on the availability of input traffic data. In this dissertation, traffic volume maps are extracted according to the following methods:

1. **Geo-location based**: the spatial traffic volume map is already available and estimated on the basis of extensive measurement campaigns. The position of 3G data users can be obtained by means of triangulation techniques [114],

[1] With the described approach, the spatial distribution of traffic volumes is directly mapped into user spatial distribution. In general, such an assumption may not be true as the amount of downlink data is strictly dependent on not only the number of connections, but also the type of application service/application the users are provided with.

Global Positioning System (GPS)-assisted, or location-based services [115] whereas the traffic data can be averaged over weeks, months or daily time frames. The accuracy of the estimated positions depends on different factors, such as user mobility and the number of available measurements, but a spatial resolution in the range of 50 m x 50 m can be achieved in urban scenarios. The traffic map is then converted into a user density distribution through Eq. 3.3. Moreover, population density distribution and building location data can be used, if available, to further tune the user density map within the traffic resolution bin, according to indoor locations and expected traffic hot-spot areas, as can be seen in Fig. 3.3(a).

2. **Cell-level based**: if spatial information is not available in advance, the cell traffic volumes extracted during, for example, the busy hour can be utilized to estimate the traffic volume density. We assume that the carried traffic of the k-th cell is T_k and $k = 0, 1...N_{cell}$, where N_{cell} is the total number of cells. Let $\mathcal{L}_k$ be the set of pixels covered by the k-th cell, then the traffic density for the pixel i, j is formulated as follows:

$$T_{ij} = \frac{T_k}{\sum_{l=1}^{N_{cell}} T_l} \cdot \frac{1}{\|\mathcal{L}_k\|} \tag{3.4}$$

where $\|\cdot\|$ denotes the cardinality of a set. Generally, downlink data cell traffic is provided on a hourly basis covering the time span of a week. By averaging out the aggregate network traffic over the different days, it is possible to obtain the average daily traffic trend for the overall network. Then, the busy hour is defined as the hour associated with the traffic peak in the average network daily traffic. In this dissertation, T_k is selected as busy hour cell traffic, and the cell coverage is estimated by means of the propagation models previously described, at a given transmission frequency. An example of the obtained user density maps is depicted in Fig. 3.3(b).

3.4 Radio Resource Sharing Model

This section presents the radio resource allocation algorithms that are used when sharing the radio resources amongst the users connected to the same cell. Due to the snapshot based approach, the proposed algorithms are aimed at modeling the average performance of a real packet scheduler in an LTE system. As the gains deriving from channel-aware scheduling [116, 117], as well as multi-user diversity [118], cannot be explicitly modeled, these will be taken into account by applying performance gains when mapping the estimated user wideband SINR to the experienced data rate. In the following subsections, the resource sharing models are described in the following order: first, the resource allocation scheme for the set of users connected to a cell; secondly, the backhaul link resource split to be

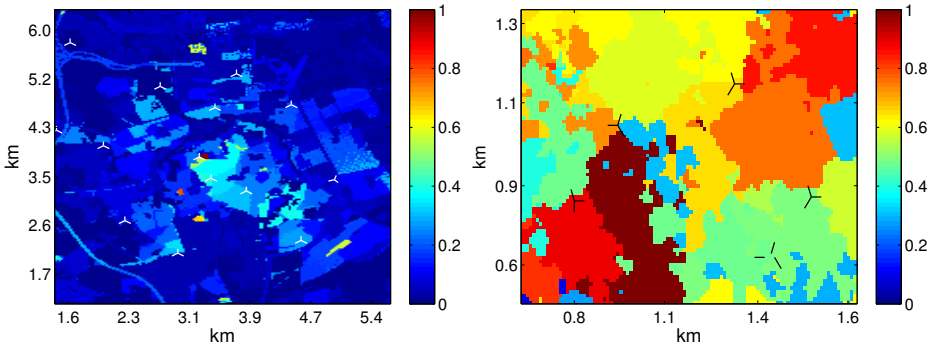

(a) Measured geo-location traffic (b) Cell-level traffic

Fig. 3.3: Examples of user density maps presented according to different traffic information sources. The user density is normalized with reference to the user density peak value.

allocated in relay-enhanced networks, and finally, the user load balancing among macro cells belonging to a multi-carrier sector.

3.4.1 User Resource Allocation Algorithm

Given a set of users connected to cell, they need to share the downlink resources so that predefined KPIs are met. In this dissertation, the radio resource sharing is aimed at serving as many users as possible with the minimum data rate r^*_{min}, thus minimizing the number of users in outage within the cells. As depicted in Fig. 3.4, each cell performs a resource allocation algorithm which is composed of two phases. In the first phase, the available resources are allocated in such a way that each user is assigned the resource share needed to achieve the predefined minimum data rate. The resources are first allocated to the users with higher SINR as they require the least amount of resources to get the required data rate. If additional resources are available, the second phase begins: the remaining resources are assigned to each user in a resource round-robin fashion so that the best SINR users are served with higher data rates. In case the network load increases or user SINR is extremely low, resources may not be sufficient to meet the minimum data rate for all served users. In such a situation, the resource allocation algorithm does not enter the second phase, and the worst SINR users are likely to be in outage.

Algorithm 1 summarizes the steps of the implemented method. In order to guarantee the minimum data rate in the downlink, a resource share equal to $\rho_l = r^*_{min}/\hat{R}_{wb,l}$ has to be assigned to user l, where $\hat{R}_{wb,l}$ is the wideband data rate that the user would experience if all the cell resources were assigned directly

to the single user. In case of relay deployment, the half-duplex transmission between backhaul and access subframes implies that the amount of available radio resources at the donor and relay cell access link is reduced by a percentage equal to the resource share dedicated to the backhaul link, as explained in the next subsection. Moreover, as for relay cells, the radio resource algorithm takes into account the backhaul link capacity, which sets a limit to the maximum achievable relay cell throughput. In this dissertation, the backhaul limitation R_{BH}^k for the $k-th$ cell is only applied to relays, whereas macro and micro cells are assumed to be provided with a backhaul connection that is able to support the aggregate throughput achieved over the radio interface, i.e. $R_{BH}^k = \infty$.

Algorithm 1 Downlink radio resource allocation algorithm for the k-th cell

Sort all the users served by cell k in descending order of $\{SINR_l\}_{l=1,2..,n_{tot}}$
Calculate for each user l the wideband throughput $\{\hat{R}_{wb,l}\}_{l=1,2,..,n_{tot}}$
Assign to cell k, the fraction of available radio resources P_k and backhaul throughput limitation R_{BH}^k
Initialize aggregated cell throughput $R_{cell}^k = 0$
for $l = 0$ to n_{tot} **do** ▷ Phase I: assign minimum data rate
    resource share for minimum data rate $\rightarrow \rho_l = \frac{r_{min}^*}{\hat{R}_{wb,l}}$
    if $P_k - \rho_l > 0$ **and** $R_{cell}^k + r_{min}^* < R_{BH}^k$
        assign user throughput $\rightarrow R_l = r_{min}^*$
        update cell throughput $\rightarrow R_{cell}^k = R_{cell}^k + R_l$
        update available resource share $\rightarrow P_k = P_k - \rho_l$
    else
        outage user throughput $\rightarrow R_l = min(P_k \cdot \hat{R}_{wb,l}, R_{BH}^k - R_{cell}^k)$
        update available resource share $\rightarrow P_k = max(0, P_k - \rho_l)$
        update cell throughput $\rightarrow R_{cell}^k = R_{cell}^k + R_l$ **then**
    end if
end for
if $P_k > 0$ **and** $R_{cell}^k < R_{BH}^k$ **then** ▷ Phase II: resource round robin
    Additional Throughput $\rightarrow \Delta_l = \frac{P_k}{n_{tot}} \hat{R}_{wb,l} \quad l = 1, 2, .., n_{tot}$
    if $R_{cell}^k + \sum_l(\Delta_l) < R_{BH}^k$ **then**
        Final data rate $\rightarrow R_l = R_l + \Delta_l \quad l = 1, 2, .., n_{tot}$
    else
        Final data rate $\rightarrow R_l = R_l + \frac{\Delta_l}{\sum_l \Delta_l}(R_{BH}^k - R_{cell}^k) \quad l = 1, .., n_{tot}$
    end if
    Final cell throughput$\rightarrow R_{cell}^k = \sum_l R_l$
end if

3.4.2 Resource Sharing in Relay-enhanced Networks

The most challenging aspect of radio resource sharing in relay networks is to optimally allocate resources to the backhaul link in such a way that the throughput performance of users connected to donor and relay cells is maximized. This is

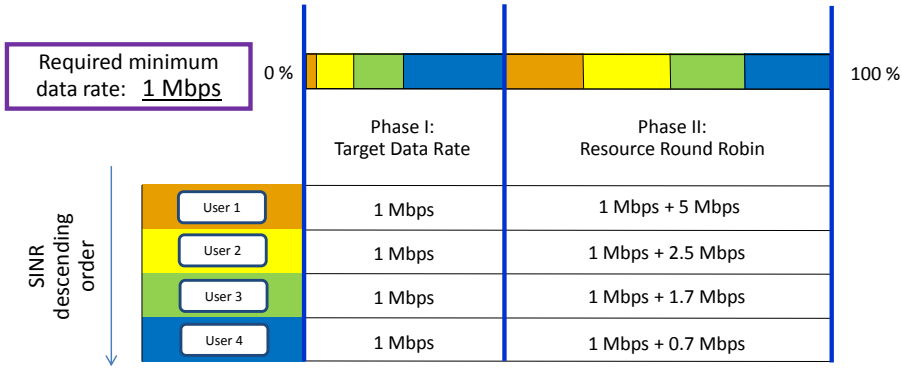

Fig. 3.4: Radio resource allocation divided into two stages and based on a predefined minimum data rate. Users with high SINR require a smaller resource share to achieve the target data rate and they experience higher data rates when radio resources are available for the second phase. As an example, minimum data rate is set at 1 Mbps and the achieved data rate numbers are only illustrative.

extremely important for in-band relay deployment as direct, backhaul and relay access link must share the same spectrum resources. Considering the in-band relay deployment scenario, the following assumptions are made: a macro donor cell k is serving N_{RN} relays and also n_{direct} users, the total number of users served by the N_{RN} relays is equal to n_{relay}, and therefore the total number of users served in the cell is $n_{tot} = n_{direct} + n_{relay}$. Assuming Decode-and-Forward relays with time domain split between backhaul and access transmission, the aggregated throughput achieved over a two-hop connection can be modeled, for a single relay i serving $n_{rn,i}$ users, as follows:

$$TP^{i}_{multihop} = min(\overbrace{\alpha_i \cdot \vartheta^{k}_{def} \cdot \hat{R}^{RN}_{wb,i}}^{R^{i}_{BH}},\ R^{RN,i}_{cell}(\vartheta^{k}_{def}, n_{rn,i})) \tag{3.5}$$

where ϑ^{k}_{def} is the resource share allocated at the $k-th$ donor cell for backhaul transmission towards all the connected relays, $\hat{R}^{RN}_{wb,i}$ is the wideband throughput the $i-th$ relay experiences on the backhaul link, and $R^{RN,i}_{cell}$ is the aggregate relay cell throughput estimated through Algorithm I. As the donor cell shares the allocated backhaul link resources amongst the N_{RN} connected relays, the factor α_i stands for the resource share allocated to the $i-th$ relay: this is calculated as $\alpha_i = n_{rn,i}/n_{relay}$, i.e. the proportion of the relay users served by the relay i as compared to the total number of relay users. The resulting backhaul link capacity R^{i}_{BH} is used in Algorithm I as potential backhaul limitation for the $i-th$ relay cell when calculating the relay users' data rates.

The throughput performance of the two-hop connection expressed in Eq. 3.5 depends on the assigned backhaul link ratio ϑ^{k}_{def}. The backhaul resource share

for in-band relays is assigned before running the user resource allocation scheme explained in subsection 3.4, and it is based on a preliminary estimation of the aggregated cell throughput for a donor cell k, which is defined as follows:

$$TP^{rr}_{donor,k}(\vartheta) = \sum_{i=1}^{n_{tot}} \tilde{R}^{rr}_i(\vartheta) = \sum_{s=1}^{n_{direct}} \tilde{R}^{rr}_s(\vartheta) + \sum_{t=1}^{n_{relay}} \tilde{R}^{rr}_t(\vartheta)$$
$$= \underbrace{\frac{(1-\vartheta)}{n_{direct}} \sum_{s=1}^{n_{direct}} \hat{R}_{wb,s}}_{direct\ users} + \underbrace{\sum_{t=1}^{N_{RN}} min(\alpha_t \vartheta \hat{R}^{RN}_{wb,t}\ ,\ \frac{(1-\vartheta)}{n_{rn,t}} \sum_{l=1}^{n_{rn,t}} \hat{R}_{wb,l})}_{relay\ users} \tag{3.6}$$

where $TP^{rr}_{donor,k}(\vartheta)$ is obtained by assuming a plain round robin resource scheme for both direct and relay users, whose experienced data rate is denoted as $\tilde{R}^{rr}_i(\vartheta)$. The user performance depends on the backhaul link ratio ϑ, and such a value can be selected on a donor cell basis to optimize different network performance indicators. As previously stated, coverage is the main deployment target rather than maximizing the donor cell throughput. Therefore, it is possible to extract the lowest user throughput from Eq. 3.6 and it becomes:

$$TP^k_{min}(\vartheta) = \min_i \{R^{rr}_i(\vartheta)\} \quad with \quad R^{rr}_i \neq 0 \tag{3.7}$$

where the inequality excludes the users whose measured SINR is so low that a connection to the serving cell cannot be established. Following a coverage-oriented approach, the backhaul link ratio for the donor cell k is chosen such that the maximum $TP^k_{min}$is guaranteed:

$$\vartheta^k_{def} = \arg\max_{\vartheta} \{TP^k_{min}(\vartheta)\} \quad with \quad 0.1 \leq \vartheta \leq 0.8 \tag{3.8}$$

where a discrete set of values for ϑ are considered within the specified range, with a step interval of 0.05.

In this fashion, the resources allocated on the different links are balanced so that also the users perceiving worse SINR values are likely to be served with sufficient radio resources to meet the minimum data rate KPI. The final backhaul link ratio ϑ^k_{def} is calculated and assigned to the $k-th$ donor cell prior to performing the definitive radio resource allocation explained in Algorithm I. As a consequence, ϑk limits the available resources at the macro and relay layers when users are served on the direct and relay link, respectively. In particular, the share of available resources, namely P_k in Algorithm 1, becomes equal to $1 - \vartheta^k_{def}$ for the donor cell k and all the connected relays.

When out-band relays are deployed in the network, it is assumed that the backhaul transmission occurs on a separate band that is orthogonal to the spectrum utilized on the relay access link. In the forthcoming cases studies, the carrier used

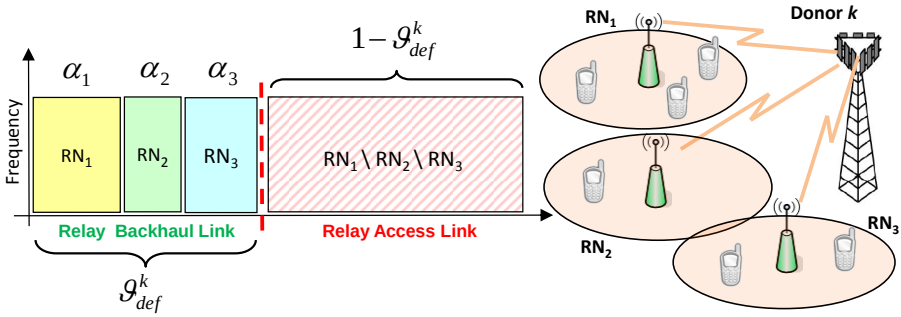

Fig. 3.5: Resource allocation including wireless backhaul in a relay-enhanced network. A deployment example with one donor and 3 relays is considered.

for backhaul is assumed to be entirely dedicated to backhauling data between the donor and connected relays. This implies that regular users do not establish any connection with the donor cell on the band dedicated to out-band wireless backhaul. In addition, we consider a Full-Duplex (FD) relay transmission, implying that the transmission on the relay access link can take place simultaneously with backhaul data transmission. Differently from in-band relaying, no time subframe is pre-allocated to receive backhaul data, and relay cells are allowed to continuously transmit over the time domain on the access link.

3.4.3 Load Balancing in Multi-Band Macro Cells

If macro sectors are deployed with multiple carriers – e.g. 800 MHz and 2.6 GHz for a typical European deployment scenario –, network performance can be improved by pooling the radio resources of multiple carriers in the same base station and enabling a collaborative scheduling operation between the two carriers. Although the carrier aggregation feature [119–121] allows the users to select both carriers and dynamically be scheduled on both of them, we assume that users can only connect to one carrier at a time, due to the simplified performance modeling framework. However, a smart distribution of the user load amongst the multiple carriers is performed based on Algorithm 2. Considering the users that have selected one of the carriers belonging to the multi-band sector, the main idea is that of distributing the users by prioritizing the carrier on which users experience better signal quality and a larger availability of radio resources.

The proposed algorithm distributes iteratively the macro users amongst the available carriers after calculating the wideband throughput performance of the macro users. When the user connects to one of the carriers, the load metric associated with that carrier is increased by a factor that is inversely proportional to the user

wideband throughput, as fewer resources are needed to guarantee the minimum data rate. The wideband throughput takes into account the carrier bandwidth, and this has impact on the user load balancing when the different carriers operate on different bandwidths. Moreover, when one of the carriers is used to serve relays and also direct users, the resource share allocated to backhaul transmission augments the load metric as fewer direct users can potentially be supported.

Algorithm 2 Multi-band load balancing algorithm for the k-th sector equipped with m carriers

Consider n_{tot} users connected to sector k
Calculate,for each user l, the wideband throughput related to each of the m available carriers $\rightarrow \{\hat{R}^t_{wb,l}\}_{t=1,2,..,m}$
Initialize the carrier load metric $L_i = 0$ with $i = 1, ...m$
for $l = 0$ to n_{tot} **do**
    Select the least loaded carrier $\rightarrow r = \arg\min_i\{L_i\}$
    Assign user l to carrier r
    if r is a donor cell **then**
        Update load in cell $r \rightarrow L_r = L_r + \frac{1}{(\hat{R}^r_{wb,l}\cdot(1-\vartheta^r_{def}))}$
    else
        Update load in cell $r \rightarrow L_r = L_r + \frac{1}{\hat{R}^r_{wb,l}}$
    end if
end for

3.5 Physical Layer

This section describes the models and the assumptions related to the physical layer of LTE system. First of all, the impact of propagation losses and interference power are shown through the link budget calculation and the resulting SINR formulation. Then, the last subsection proposes the end-to-end data rate approximation based on SINR-to-Throughput mapping curves, which are needed to calculate the wideband user wideband throughput to be used when allocating the radio resources.

3.5.1 Link Budget Considerations

The overall link loss L_{lk} between cell k and user l is expressed in the logarithmic domain as follows:

$$L^{dB}_{lk} = G^{Tx}_{lk} - CableLoss_k - PL_{lk} - IndL_{lk} + G^{Rx}_{lk} - BodyLoss_l \ \ [dB] \qquad (3.9)$$

where G^{Tx}_{lk} and G^{Rx}_{lk} denote the antenna gains at the transmitter and receiver side respectively, which generally depend on azimuth and elevation angles; $CableLoss_k$

stands for the base station feeder loss measured between the antenna port and the RF module; $BodyLoss_l$ represents the shadowing effect due to the physical presence of the user, and such attenuation is fixed at 2 dB [122]; PL_{lk} is the distance-dependent outdoor propagation loss between the transmitting cell and the receiver based on the methods described in Subsection 3.3.2, whereas the outdoor-to-indoor propagation losses are accounted for with the attenuation term $IndL_{lk}$. In this dissertation, shadow fading modeled in the form of a spatially correlated log-normal stochastic variable [107] has not been introduced for not increasing simulation complexity.

The link loss is then utilized to calculate the user received signal power from each of the transmitting nodes. By means of that, the average downlink SINR for the $l-th$ user with respect to cell k is calculated as follows:

$$SINR_{lk} = \frac{P_k L_{lk}}{\sum\limits_{s \in \mathcal{S}_k} \mu_s P_s L_{ls} \; + \; N} \tag{3.10}$$

where P_k is the full transmission power at the data channel for cell k; $\mathcal{S}_k$ is a set of cells transmitting at full power P_s and interfering with cell k due to co-channel transmission; N is the receiver noise power[2]. Furthermore, the interference power is scaled by the factor μ_s, which denotes the fraction of time during which the cell transmits downlink data. As full buffer traffic is assumed, the linear scaling factor[3] is only applied to in-band relay cells, which are silenced while receiving backhaul data. With regard to the backhaul SINR calculation, it is assumed that in-band relays are interfered only by the surrounding macro cells and not from relays connected to other donor cells and transmitting on the access link[4].

Furthermore, the cell selection is performed on a best-SINR basis, and this means that a generic user l selects the server cell S^* as follows:

$$S^* = \arg\max_k \{SINR_{lk}^{dB} + \Delta_{Offset,k}\} \tag{3.11}$$

where the offset $\Delta_{Offset,k}$, expressed in dB, can be used to extend or reduce the range of the cell k. The offset is generally associated with a specific layer of the

[2]It is calculated through the linear product of the noise power density (equal to 174 dBm/Hz), the transmission bandwidth and the receiver noise figure.

[3]The full buffer traffic model implies that the users utilize all the available resources of the serving cell. As a consequence, full load transmission is considered when calculating the interference power. Although fractional load may be a more realistic assumption due to user behavior and traffic characteristics, the full load assumption represents a worst case scenario in terms of interference. If relays are not deployed, the calculated SINR corresponds to the G-factor, i.e. the user geometry, due to full interference from surrounding cells and filtered small scale channel variations.

[4]According to the resource scheme presented in subsection 3.4.2, the backhaul transmission cannot be interfered by relays connected to the same donor due to time synchronization between backhaul and access link transmission. For relays connected to different donors, it is reasonable to assume that the use of directional antennas and a guaranteed minimum distance when deploying relays in the same area mitigate the effects of relay-to-relay interference.

heterogeneous deployment, especially when small cells are deployed on dedicated channels. In fact, the offset is a means for smartly distributing the traffic on the different deployment layers and decreasing network outage. In this dissertation, the offsets are statically set for each deployment layer.

3.5.2 User Data Rate Estimation

The estimation of the user wideband throughput for a given user SINR is performed by means of an SINR-to-throughput mapping curve, which is shown in Fig 3.6 in the form of spectral efficiency versus user average SINR. The mapping curve is obtained from extensive system and link level simulations [123, 124], in which the radio performance of a single LTE transceiver chain is accurately emulated in accordance with the 3GPP specifications. These include:

- Fast link adaptation with Adaptive Modulation and Coding (AMC) together with Hybrid Automatic Repeat Request (HARQ) retransmission schemes.
- MIMO schemes up to 2x2 spatial multiplexing.
- Implementation imperfections and RF impairments related to real equipment.
- Channel-aware scheduling gains obtained in multi-user scenarios through system level simulation.

By multiplying the estimated spectral efficiency by the spectrum bandwidth, it is possible to obtain the wideband data rate for the generic user l, $\hat{R}_{wb,l}$, which is used as input for the radio resource allocation algorithms. In Fig. 3.6 it can be seen that minimum allowed SINR for establishing a connection with the serving cell is fixed at -9 dB whereas the efficiency curve saturates for SINR values larger than 24 dB due to the best available MCS (64-Quadrature Amplitude Modulation (QAM) with coding rate 4/5). The gap from the Shannon limit [125] is also worsened by the fact that control channel overhead is accounted for, thereby limiting the system spectrum efficiency. Moreover, the utilized mapping curve gives similar performance when compared to a modified version [126] of the Shannon formula presented below:

$$\eta_{mod} = BW_{eff} log_2(1 + \frac{SINR}{SINR_{eff}}) \quad [bit/s/Hz] \tag{3.12}$$

where the system bandwidth and SINR efficiency are set to 0.65 and 1.67, respectively, to take into account protocol overhead, implementation imperfections and scheduling gains. The modified Shannon formula gives a valid approximation of the mapping curve based on link level simulations especially in the higher SINR region.

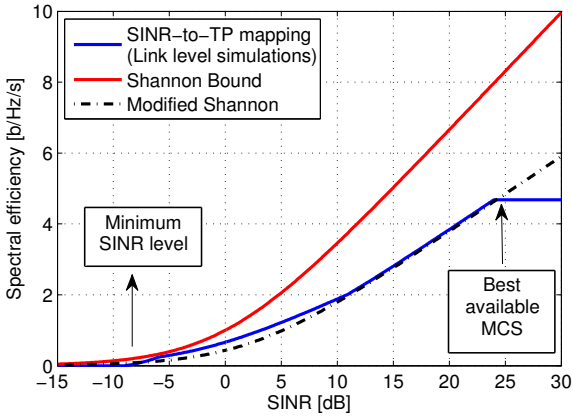

Fig. 3.6: Spectral efficiency vs. SINR obtained from system and link-level simulations (*blue curve*) is showed in comparison with the ideal Shannon bound [125] and a spectral efficiency curve based on modified Shannon formula [126].

3.6 Deployment Strategy for Small Cells

Planning the positions of small cells plays a key role in improving network performance and coverage in specific areas of the network. Generally, with a large number of new cells to be deployed, the search for the optimal solution [127, 128] would require higher simulation complexity and longer simulation sessions. Hence, similarly to [128, 129], a heuristic deployment algorithm is utilized, and the rationale behind that is next described.

As previously explained, the main performance target is to fulfill a predefined network outage level, thus the deployment of new cells aims at serving those users who are experiencing poor signal quality and therefore consuming more resources. Moreover, if macro cells are serving high-traffic areas without having sufficient capacity to satisfy the traffic demand, small cells can help decrease user outage by offloading part of the users connected to the overlay macro cell. For this reason, the proposed deployment strategy is based on the following objectives, which are strongly correlated:

- Deploy small cells in those areas of the network, where the existing infrastructure is not giving good coverage. In practice, the signal quality "coverage holes" are tracked with the purpose of improving the average user SINR all over the investigated area.
- Prioritize the locations close to or within the traffic hot-spots in order to decrease the traffic load of the macro cell covering the high-traffic area.

- Select locations around which the users served by the existing macro cells are in outage. This means that areas served by macro cells experiencing high outage levels have to be targeted when deploying relays or micros.
- With regard to relay deployment, the backhaul link quality is crucial for in-band multi-hop communication. Thus, the relay deployment strategy considers, amongst the other targets, also the necessity of selecting locations in which acceptable backhaul link SINR is guaranteed.

Considering an existing macro network deployment with a certain percentage of users in outage, the proposed coverage-oriented deployment approach is achieved by designing a specific metric for each potential small cell location. The set of candidate positions is obtained by subdividing the entire map into small identical square regions so that a regular grid pattern is formed over the full investigated area. The resolution of the grid gives the total number of candidate locations, and the finest achievable resolution coincides with pixel itself, i.e. the map resolution. Furthermore, the set of candidate locations can additionally be narrowed down if the initial candidate locations do not fulfill the deployment strategies (e.g. indoor or outdoor-only deployment) or constraints (regulation, site availability, limitation on wired backhaul connection).

Fig. 3.7 illustrates the algorithms steps leading to the selection of the best candidate locations. Each candidate location is associated with a deployment metric which is calculated over the pixels of a squared area, A_i, surrounding each location i. Based on the previously listed deployment objectives, the deployment metric carries, for each pixel lying in A_i, information about: macro layer coverage expressed in the form of wideband throughput $\hat{R}_{wb}$, normalized per-pixel user density $\bar{s}_{r,l}$, cell outage level $Outage_{r,l}$ related to the macro cell covering the pixel (r, l), and backhaul link wideband throughput referred to the specific candidate location. Then, The deployment metric, DM_i, is formulated as follows:

$$DM_i = \sum_{r,l \in A_i} \frac{\bar{s}_{r,l}}{(\hat{R}_{wb}(SINR_{r,l}))^{wCov}} \cdot e^{wOut \cdot (1+Outage_{r,l})} \cdot (\hat{R}_{wb}(SINR^i_{BH}))^{wBH} \tag{3.13}$$

The throughput terms depend on the SINR values calculated in those specific pixels, for both direct and backhaul links. In order to prioritize or reduce the impact of the specific terms, three exponential weights have been introduced in Eq. 3.13: $wCov$ biases the weight of macro coverage which depends on the experienced SINR, $wOut$ gives stress to the number of outage users served by the overlaying macro cells, and finally wBH weighs the impact of the backhaul link quality for the i-th candidate location. Such weights have been optimized heuristically to achieve the best performance for both relay and micro deployment, depending on the specific network scenario and small cell type. In general, more emphasis is put on coverage and outage measures to reduce network outage, although high backhaul link

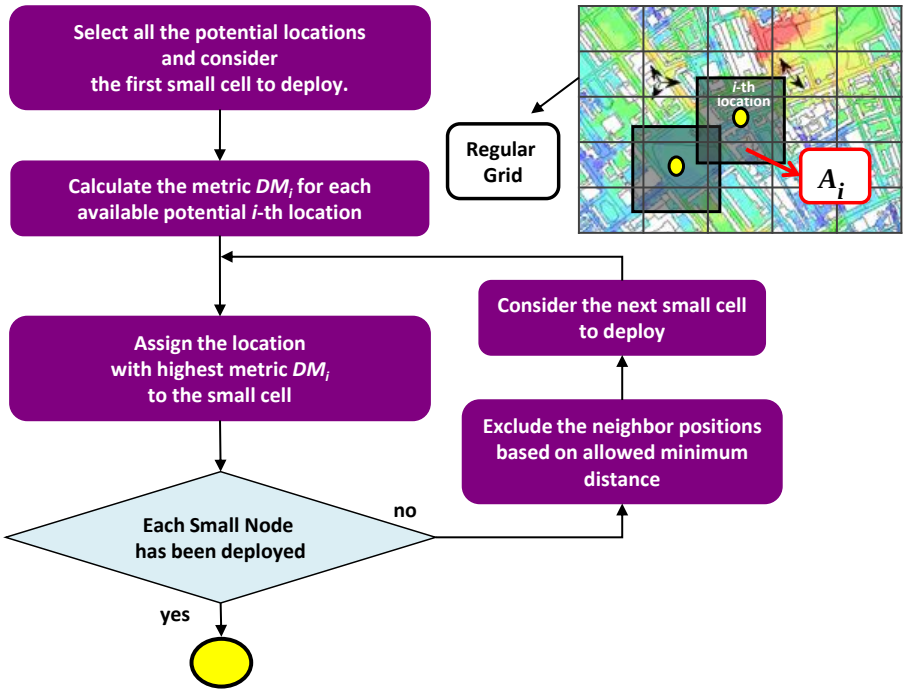

Fig. 3.7: Flowchart describing the iterative algorithm steps that are carried out when deploying new cells in the network. After selecting one location, the minimum ISD constraint is applied, thereby limiting the set of potential locations.

quality has to be guaranteed to achieve good performance with relay deployment.

The algorithm operates in an iterative fashion, assigning sequentially the best available location to the new small cell, based on the highest deployment metric. The potential locations in proximity of the assigned ones are removed from the set of candidate locations if those are below a pre-defined minimum distance, which is specified for neighbor small cells and also existing macro sites. The minimum ISD between small cells or between an existing macro and a new small node is set on the basis of relay/micro transmission power and expected cell size. This enables the algorithm to effectively spread the small cells in the targeted areas and keep at bay the interference level generated by the other small cells.

In dense urban scenarios it is proper to define the set of candidate locations with a high-resolution regular grid, which is close to the resolution of the map itself. This enables the deployment algorithm to take into account the presence of buildings, the narrow size of the streets (for outdoor deployment) and received power variations in a more efficient way. As illustrated in the deployment example of

Fig. 3.7, the size of the deployment metric area A_i can be extended beyond the square region of the regular grid, which surrounds the $i-th$ candidate location. This can be useful when adapting the size of the metric area to that of the traffic hot-spots and coverage holes. The parameter setting of the deployment formula is thoroughly addressed in each of the proposed case studies.

3.7 Cost Assessment Methodology

Besides evaluating the radio performance of the different deployment configurations, a financial estimate of the radio access network costs gives a broader picture of the potential of specific deployment solutions when comparing different network evolution strategies. As anticipated in Chapter 2, the TCO model includes three main components, namely CAPEX, IMPEX, and OPEX. The cost input figures are associated with the base station type, macro cell upgrade and also the deployment scenario assumptions. The objective of the cost analysis is to complement the network performance analysis and give a final techno-economic recommendation with regard to the analyzed deployment alternatives.

Fig. 3.8 shows the different phases of the cost analysis process: firstly, the cost figures have to be set for the different network upgrades together with the time span over which the running costs are estimated; secondly, the cost analysis is carried out on iso-performance, or more precisely iso-"outage" scenarios, i.e. deployment configurations providing the same outage level with a predefined error margin; last, the cost outputs are compared and general recommendations are given in terms of performance and economic impact for the different deployment combinations. Obviously, the iso-outage scenarios are obtained under the same network assumptions, which basically refer to the same network load and the same minimum data rate as main KPI.

The focus of the case studies presented in the following two chapters is on relay and micro deployment, along with LTE macro upgrades. The estimated cost figures are listed in Table 3.1, showing the different cost components and calculating the total TCO, which assumes a 4-year period of running costs. As the baseline scenario is provided by the existing 3G network fully upgraded to LTE, the cost of the LTE reference network is calculated by considering only the LTE upgrade expenses. If a new LTE site is to be deployed, the highest TCO is incurred due to the higher site acquisition and buildout related costs.

Two types of relay base stations are considered, depending on whether or not additive site planning costs are included. As can be seen from the overall TCO calculations, a relay node is approximately 9-10 and 19-20 times cheaper than an existing site upgraded toLTE and a brand new LTE site, respectively. With

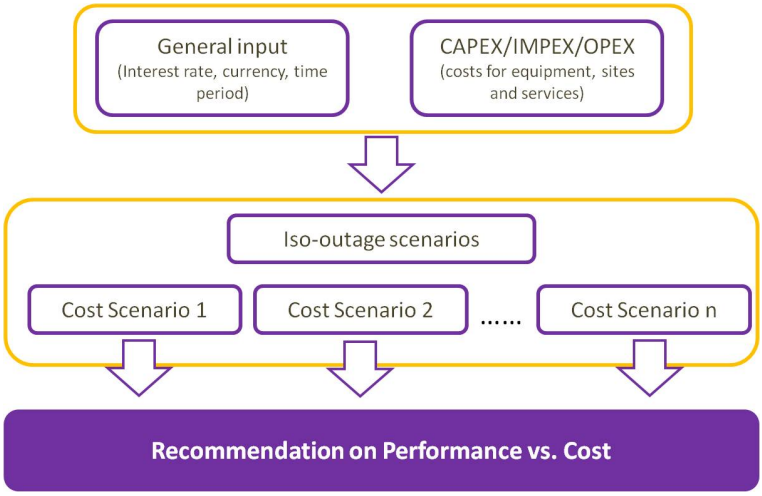

Fig. 3.8: Process for cost evaluation of iso-performance deployment scenarios, spanning from cost input definitions to final recommendations.

respect to a macro site second-carrier upgrade, the relay cost is, instead, 4.5-4.7 times lower. Further, two micro cell structures are proposed, based on different assumptions related to the backhaul costs. For high-cost micros, the TCO ratio between micro and relay cells is in the order of 5, whilst it reduces to around 2 when low-cost micros are considered. Rather than estimating the precise cost of different backhaul solutions – which is extremely variable –, the idea behind the proposed micro cost structures is to provide an expected cost range for micro deployment and run a cost sensitivity study based on the lowest and highest cost figures.

Table 3.1: TCO estimates for the different deployment layers, showing the split of the different cost components. The final TCO is calculated assuming 4 years of running costs, and the far right column shows the TCO values normalized to the cost of the cheapest solution.

Deployment Options	**CAPEX** in k€	**IMPEX** in k€	**OPEX** in k€	**TCO** in k€	**Normalized** TCO
LTE new site	46	53.5	19.8	178.8	20.4
LTE upgraded site	35	9	10.9	87.7	10
LTE second carrier	26.5	5.8	2.3	41.5	4.6
High-cost Relay	3.1	1.4	1.2	9.3	1.07
Low-cost Relay	3.1	0.8	1.2	8.7	1
Low-cost Micro	7.5	2.5	2	17.9	2
High-cost Micro	8.5	6.5	7.8	45.9	5.3

As previously stated, it is worth noting that the cost numbers presented herein

are to be considered as a mere approximation that is used for research purposes, without having any link to existing commercial products. The main idea is to provide an approximation of the radio access deployment costs for typical European scenarios, and highlight the cost ratios amongst the different base station types and upgrades. The cost structure assumptions have been discussed and verified together with representatives from the telecommunication vendor and mobile operator involved in the PhD study. Further information about the breakdown of the assumed costs can be found in Appendix C.

Chapter 4

Relay Deployment in a Suburban Scenario

4.1 Introduction

This chapter presents a deployment case study that is aimed at evaluating the viability of relay deployment in a realistic LTE network scenario, including inhomogeneous spatial traffic distributions and real LTE spectrum availability. As illustrated in Chapter 2, relay base stations have been conceived as an appealing solution to extend network coverage and provide excellent user experience along with contained deployment costs. As a first attempt to estimate the potential of relay deployment, the investigated network area has been selected with the purpose of reproducing a real suburban scenario where the existing network infrastructure is expected to cover the downtown and surrounding outskirts of a medium-size European city. Considering that part of the LTE spectrum is available on the 2.6 GHz band, such a scenario is definitely challenging in terms of network coverage due to high propagation losses. By deploying relays in the coverage-limited areas, user data rates at the cell edge can be efficiently boosted, but it is well known that relay performance is extremely sensitive to the signal quality experienced on the wireless backhaul link, and to how the available spectrum is shared between backhaul and access links. Moreover, differently from previous studies on regular networks, the non-uniform traffic distribution is of fundamental importance to understand the impact of coverage holes on the overall network outage, and quantify the number of relay cells or macro upgrades that are needed to meet a predefined

outage target.

This case study addresses the following key problems related to the performance assessment and cost effectiveness of relay deployment:

- To evaluate the radio performance of in-band and out-band relays for a given network load and spectrum availability. The main objective is to quantify to what extent the allocation of dedicated resources to the wireless backhaul, i.e. the out-band configuration, outperforms in-band relaying in terms of coverage and capacity. With regards to a predefined outage requirement, the performance analysis can be used to identify the break-even point in terms of relay densities between in-band and out-band relays when fulfilling the same overall outage requirement.
- To investigate the sensitivity of relay performance to the signal quality perceived on the wireless backhaul link, and determine optimal antenna configurations or site planning procedures that are needed to boost the backhaul link spectral efficiency.
- To take into account the possibility of deploying additional spectrum located in the 800 MHz band at the macro layer, and compare the corresponding dual-band macro performance with the one obtained by deploying relays with single-band macros on the 2.6 GHz band.
- To assess the TCO of different deployment configurations delivering the same outage performance, and to determine the most cost-efficient deployment scenario considering in-band and out-band relay deployment, macro carrier upgrades and macro densification.

The chapter is outlined as follows: Section 4.2 concerns the description of the scenario and the main simulation assumptions regarding propagation, traffic distributions, spectrum allocation and relay configurations; in Sections 4.3 and 4.4 simulation results are presented for both in-band and out-band relays considering single-band and dual-band macros, respectively; a cost analysis of iso-performance scenarios is provided in Section 4.5 before summing up the overall findings in Section 4.6.

4.2 Network Scenario Description and Assumptions

This section presents the investigated suburban network scenario and the main simulation assumptions of the case study. Firstly, details about the reference

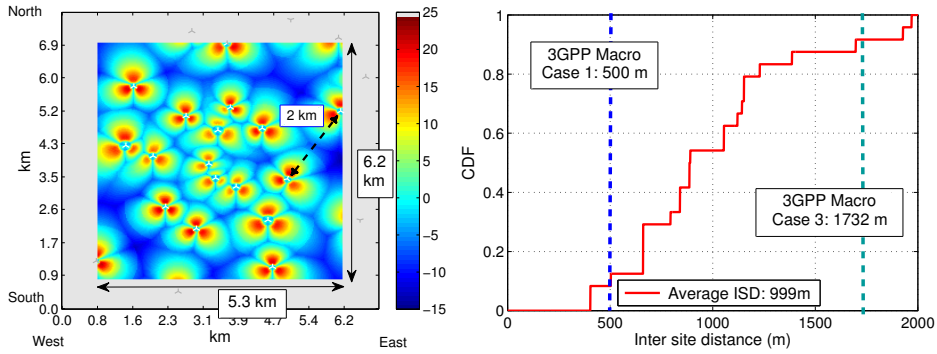

(a) Network Layout (b) ISD Cumulative Distribution Function

Fig. 4.1: Network Layout of the investigated area (left) is shown through a best server SINR map obtained at 2.6 GHz and expressed in dB (refer to subsection 4.2.3 for propagation assumptions). The ISD distribution (right) referred to the first closest site is shown and compared with the fixed ISDs employed in regular 3GPP scenarios.

macro deployment, employed propagation models, and spatial traffic distribution are provided. Then, relay base station setup and site planning propagation gains are explained before introducing the simulation scenarios based on different spectrum allocation alternatives and relaying operation modes. Finally, the outage performance of the reference macro-only scenario is presented for different values of network load, and this analysis is used to select the assumed network load when investigating the network performance with relay deployment.

4.2.1 Macro Cellular Network Layout

This study has been carried out for a suburban network scenario, which corresponds to an operational 3G macro deployment in a European city of less than 300,000 people. Part of the network layout has been used in previous studies [130, 131] with regards to self-optimized network features. As illustrated in Fig. 4.1(a), the investigated area has a rectangular shape. Its size is 5.3 km x 6.2 km with a spatial resolution of 25 m x 25 m. With regard to the macro infrastructure, 17 3-sector macro sites are deployed within the selected area, and each of those is considered upgraded to LTE with optimized antenna down-tilt angles. In order to avoid border-effects, multiple tiers of interfering base stations located outside the examined area are taken into account so that a total number of 44 sites is considered when estimating the radio performance. Users are generated only within the rectangular area, and radio performance statistics are extracted from the cells that are serving users. The main radio parameters are listed in Table 4.1.

Table 4.1: Macro Base Station Simulation parameters

Parameter	Value
LTE System	Downlink FDD LTE, 2x2 MIMO
Supported Carrier frequencies	2.6 GHz, 800 MHz
Macro eNodeB Power	46 dBm per carrier
Network Layout	44 sites in total 24 sites covering the investigated area 17 sites inside the investigated area
Antenna Pattern	3GPP 3D Antenna Pattern [62] Half-power beamwidth: $\theta_{3dB} = 70°$ Front-back ratio: $A_m = 25\ dB$ Vertical tilt: network input data
Antenna Gain	14 dBi including cable loss
Antenna Height	Network input data

Fig. 4.1(b) shows the cumulative distribution function of the ISD between the macro sites lying in the selected area. By considering only the closest site, the average ISD is approximately 1 km, although the sites are not homogeneously distributed over the area. The ISD ranges between 400 m and up to 2 km. When compared to the fixed ISD assumed in 3GPP regular networks, the base station density of the investigated scenario lies between the 3GPP interference-limited (Case I) and coverage-limited (Case 3) scenarios. By looking at the best server SINR map presented in Fig. 4.1(a), it can be noticed that at 2.6 GHz the "coverage holes", i.e. the worst SINR regions, are mainly located in the city outskirts where the macro deployment becomes less dense and gives worse coverage. Conversely, in the downtown zone the cell edge areas with low SINR are due to severe interference rather than poor signal coverage.

4.2.2 Traffic Density

Traffic data [130] is available directly in the form of a spatial traffic map with a 25 m resolution, and the normalized user density map is shown in Fig. 4.3. This has been derived from real 2G and 3G traffic, for both voice and data, provided by the operator owning the macro network. In addition, population density information and clutter data (e.g. streets, buildings or natural areas) have been used together with cell traffic volume to further distinguish high and low-traffic areas. It can be noted that most of the traffic is located within the downtown area, which is also served with higher base station density, whereas the user density becomes significantly lower as the distance from the city center increases.

Fig. 4.3 gives further insights as to how the the traffic is distributed across the serving cells and over the investigated area. By estimating the cell coverage areas at 2.6 GHz according to the propagation model presented in subsection 4.2.3, it can

be seen that the traffic is not equally distributed between cells. Half of the overall network traffic is carried by one third of the sectors covering the selected area. This result is aligned with the distributions shown in [36]. Furthermore, as for the traffic spatial characteristics, 50% of the network load is localized within 20% of the considered area, and such a skew distribution significantly narrows down the set of locations to be selected for effective relay deployment, or the macro cells that need to be upgraded to meet the outage requirement.

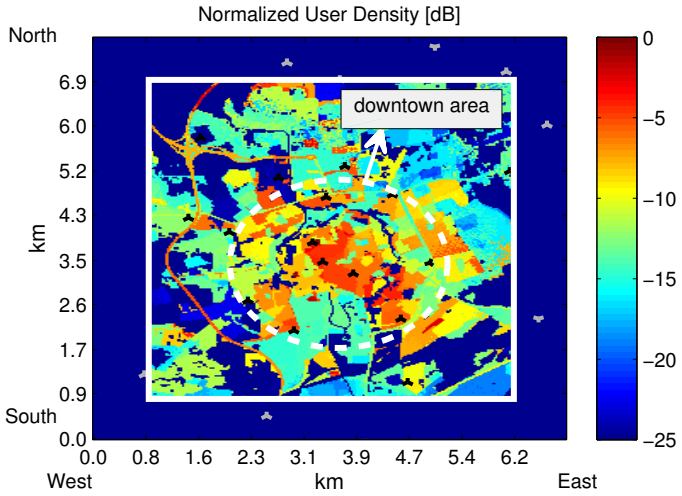

Fig. 4.2: Normalized user density map for the investigated suburban scenario, showing the non-uniform traffic distribution between the city center (in the circle) and the surrounding areas.

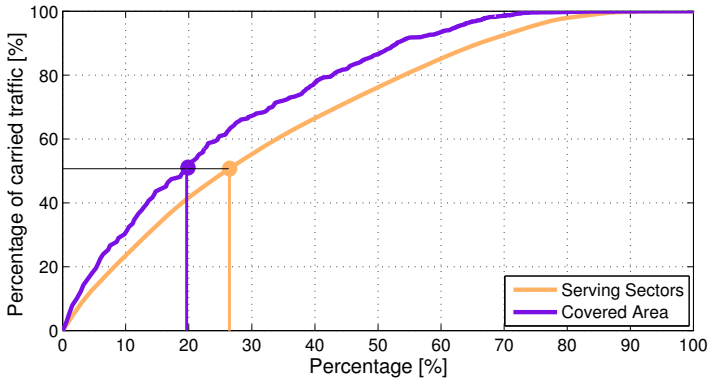

Fig. 4.3: Cumulative distribution function of the carried traffic share over the percentage of sectors, ordered in descending order of traffic, and the percentage of the covered area.

4.2.3 Propagation Models

In this case study statistical path loss models have been used to estimate the downlink path loss due to the lack of ray-traced path loss maps and detailed building information. To begin with, the COST-231 Hata model [132] has been used to calculate the macro link signal attenuation, taking into account a correction factor for suburban scenario [106] as presented below:

$$L_{macro}^{dB} = L_{Cost231}(d, H_l, h_k, f_c) - \underbrace{2[log(f_c/28)]^2 - 5.4}_{Suburban\ correction} \quad [dB] \tag{4.1}$$

where The COST-231 urban path loss model, $L_{Cost231}$, depends on the distance d expressed in km, the height in m of the $l-th$ base station, H_l, the height of the $k-th$ receiver, h_k, and the frequency carrier, f_c. The suburban correction is also a function of frequency and it has been introduced due to the suburban nature of the analyzed scenario. The selection of such a model can be explained by the following:

- The above statistical model has been developed for a typical over-the-rooftop propagation in both built-up and suburban deployments. Therefore, such a propagation scenario matches the characteristics of the investigated area as all the macro base stations are located above the rooftop level. Moreover, the model is used to estimate the propagation losses related to both macro users and relay backhaul link.
- The path loss depends on the height of the transmitter and the receiver. Considering that the base station heights are available as input data, it is also possible to capture the difference in received signal strength between the user (e.g. a 1.5 m height) and the relay backhaul receiver (e.g. at 5 m).
- The path loss model covers a wide frequency range, extending from 150 MHz to 2 GHz (the extended version). As the considered LTE spectrum is located in the 800 MHz and 2.6 GHz bands, the model only includes the lower frequency band. However, as illustrated in [133], the Hata model seems to fit measurement data also for frequencies beyond the validity range, and the frequency gap between 2.6 GHz and 2 GHz is not significantly large with an average path loss difference of approximately 3 dB.

The impact of macro link path loss model on the perceived user SINR is illustrated in Fig. 4.4 for both 800 MHz and 2.6 GHz carriers. The user SINR Cumulative Distribution Function (CDF) is shown by assuming that each receiver is at 1.5 meters and located indoor. Therefore, a wall penetration loss of 20 dB (the term

$IndL_{lk}$ in Eq. 3.9) is considered for calculating the link budget. When a uniform traffic distribution is assumed, i.e. each pixel of the area is equally weighted, the lower carrier spectrum gives better geometry especially at the cell-edge (the lower tail of the CDF) with an SINR improvement of ca. 3 dB as compared to the 2.6 GHz carrier. The coverage improvement is mostly achieved in the outskirts of the city where the higher attenuation at 2.6 GHz is the cause of the macro coverage holes. By weighting the SINR distributions with the real user density map described in 4.2.2, the SINR gain at the lower frequency over the 2.6 GHz band reduces, and this is mainly due to the fact that a major percentage of the traffic demand is located in the city area. In this area of the network, the base station density is higher, and user performance is mainly limited by interference, thereby diminishing the benefit of higher received signal strength on perceived SINR.

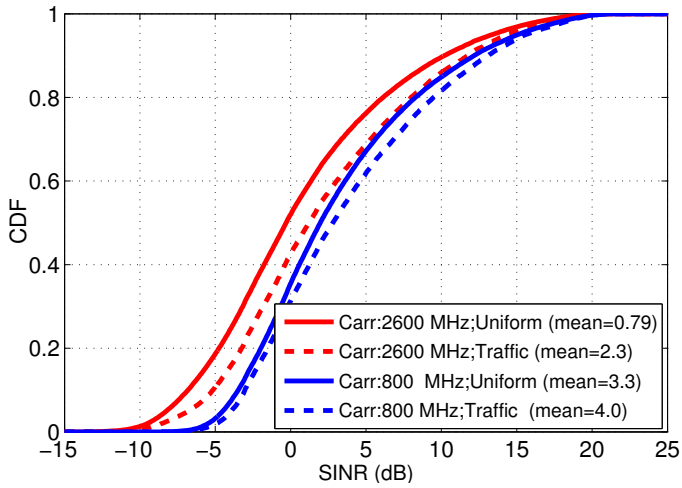

Fig. 4.4: SINR distributions at 2.6 GHz and 800 MHz for uniform traffic distribution and realistic traffic distribution.

The path loss between relay and user is estimated by means of a statistical path loss model that is utilized in 3GPP suburban scenarios [62]. The model makes distinction between LOS and NLOS propagation scenario, and the probability of being in one of those is a function of the distance between transmitter and receiver. The path loss model is intended to estimate the signal attenuation for base stations placed below the roof top, and it is formulated as follows:

$$L_{relay}^{dB} = \begin{cases} 103.8 + 20.9\log(d) + \Delta_{2.6GHz} & \text{in LOS (d in Km)} \\ 145.4 + 37.5\log(d) + \Delta_{2.6GHz} & \text{in NLOS (d in Km)} \end{cases} \tag{4.2}$$

$$\text{with } Pr_{LOS}(d) = 0.5 - \min(0.5, 3\exp(-0.3/d)) + \min(0.5, 5\exp(-d/0.095)) \quad (4.3)$$

The model is originally conceived for a carrier frequency of 2 GHz. As relays are assumed to be deployed at 2.6 GHz, a correction factor, $\Delta_{2.6GHz}$, is applied to the path loss with a penalty of 3.5 dB. The additional attenuation has been chosen by following a frequency decay of f^{-3}, which was also used in [134] and is closer to a propagation scenario involving base stations deployed at the street level. The probability of the LOS conditions decreases for larger distances, having only NLOS scenarios when the distance exceeds 500 m. The assumed height for the relay node is 5 m and since all the users are considered to be indoor, an additional wall penetration loss of 20 dB is added to the overall link budget.

4.2.4 Relay Deployment Assumptions

In this case study both in-band and out-band relaying operations are considered, according to the configurations illustrated in Fig. 4.5. In-band relays operate in half-duplex mode to separate backhaul and access transmission, and the backhaul link time ratio is calculated by following the algorithm described in Section 3.4.2. Regarding out-band relays, backhaul and access links operate on different frequency bands in a full-duplex mode. By assuming ideal separation between the antennas that receive and forward the signals, concurrent operation of backhaul and access link is not impaired by loop interference at the relay node and adjacent channel leakages between the two carriers. Moreover, TDD spectrum is available for out-band backhaul transmission, and this implies that half of the frames are allocated to the downlink (and the other half to uplink).

The main transmission related parameters are outlined in Table 4.2. Owing to suburban characteristics of the scenario, high-power (37 dBm) relays are used to maximize the cell coverage. At the backhaul side relays are equipped with a 7 dBi sectorial antenna, which is pointed at the best-SINR macro cell, i.e. the donor. As for the deployment strategy, the deployment metric input parameters presented in Section 3.6 have been chosen with the purpose of deploying relays in the coverage holes and reducing network outage. For this reason, particular emphasis is put on those macro cells where most of the users are not provided with the minimum data rate. A minimum distance between two neighbor relays is considered to effectively spread the relays in the targeted areas based on relay transmission power and covered area. In addition, the minimum ISD between relay and macro cells has been set based on the macro cell ISD of Fig. 4.1(b) in order to push relay cells towards the edges of high-outage cell areas. The detailed calibration of the deployment algorithm parameters to optimize network performance can be found in Appendix B.1.

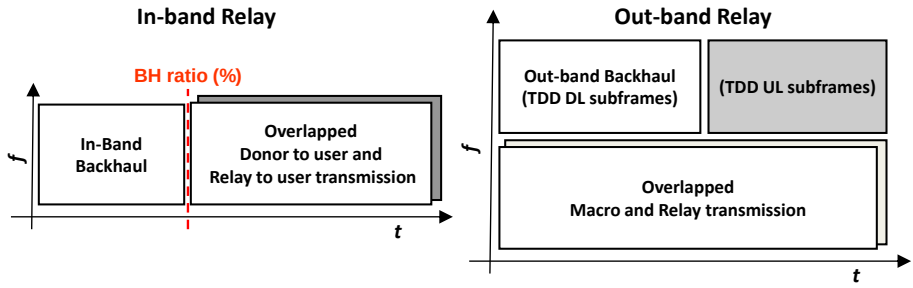

Fig. 4.5: Half-duplex in-band and full-duplex out-band relaying configurations.

In this specific study, such a coverage-oriented setting of the deployment metric does not include the usage of the backhaul link metric. In order to evaluate the relay performance sensitivity to the backhaul link quality, a site planning gain is introduced similarly to the approach presented in [62] and verified in [42]. Given a donor cell k belonging to the site K and a connected relay l, a gain equal to SP is applied to the link budget as follows:

$$L_{lk}^{dB,SP} = L_{lk}^{dB} + SP \quad [dB] \quad with\ k \in \{K\} \tag{4.4}$$

The augmented link budget $L^{dB,SP}$ relates to all the cells of the site hosting the donor cell, and the impact of site planning gain is herein evaluated when investigating the performance of in-band relaying. Such a correction can be interpreted as the result of relay site planning procedures for enhancing the backhaul link signal quality. In practice, optimal positioning of relays within available spatial resolution can reduce the impact of shadowing towards the donor whereas deploying more directive antennas gives the opportunity to mitigate interference from surrounding macro cells. In addition to the use of directional antennas, relays are assumed to be deployed only outdoor, thus preventing the relay link from being coverage-limited. A minimum distance of 250 m between two neighbor relays is considered to effectively spread the relays in the targeted areas based on relay transmission power and covered area.

4.2.5 Spectrum Allocation and Simulation Cases

The investigated network deployment alternatives are strictly correlated with the available spectrum and the assignment of the different frequency carriers. Based on the LTE spectrum auction outcome to be found in [135], three different frequency bands are considered, as shown in Table 4.3. Such a spectrum availability is a representative case for a major mobile broadband operator being able to con-

Table 4.2: Relay Base Station Simulation parameter

Parameter	Value
Relay Tx power	37 dBm
Carrier frequency	2.6 GHz
Antenna Pattern (Access Link)	Omni Antenna Pattern 5 dBi antenna gain
Antenna Pattern (Backhaul link)	Directional Antenna [62] Half-power beamwidth: $\theta_{3dB} = 70°$ Front-back ratio: $A_m = 20\ dB$ 7 dBi antenna gain
Antenna Height	5 m
Site Planning (SP) gain	varied
Relay Deployment Metric Setting	$wCov = 0.5$ $wOut = 3$ wBH disabled A_i = 100m x 100m ISD_{relay} = 250 m ISD_{macro} = 500 m Outdoor locations only

Table 4.3: Spectrum allocation and deployment cases

Network Deployment	**800 MHz** (FDD, 10 MHz)	**2.6 GHz (1)** (FDD, 20 MHz)	**2.6 GHz (2)** (TDD, 20 MHz)
Single-Band Macro & In-Band Relay	–	Direct Link Access Link Backhaul Link	–
Single-Band Macro & Out-Band Relay	–	Direct Link Access Link –	DL/UL split: 50/50 Backhaul Link
Dual-Band Macro & In-Band Relay	Direct Link –	Direct Link Access Link Backhaul Link	
Dual-Band Macro & Out-Band Relay	Direct Link –	Direct Link Access Link –	DL/UL split: 50/50 Backhaul Link

spicuously invest in additional spectrum for LTE deployment. The macro carrier for the reference single-band macro scenario is at 2.6 GHz with 20 MHz available for the downlink transmission on the direct link (FDD spectrum). Likewise, relay access link operates at 2.6 GHz on FDD spectrum in full frequency reuse with macro transmission. As for the backhaul link, two configurations are available: the in-band wireless backhaul operates on the FDD spectrum at 2.6 GHz, and radio resources have to be shared amongst direct, backhaul and access links; the out-band case assigns a fully dedicated TDD band of 20 MHz to backhaul transmission, without sharing resources with any direct or relay user. Moreover, allocating the lower carrier spectrum at 800 MHz to the macro cells determines the dual-band macro configuration, which gives another deployment alternative

to extend network coverage together with relay deployment on the 2.6 GHz band. Users are assigned to the two macro carriers by following the carrier load balancing algorithm described in Section 3.4. In conclusion, the combination of the two macro carrier configurations (single and double-band) with the two relay configurations (in-band and out-band) gives a total of 4 deployment scenarios that will be analyzed to assess the performance of relay deployment.

4.2.6 Macro-Only Reference Scenario Performance

This subsection focuses on the downlink network performance delivered by the single-band macro-only deployment transmitting at 2.6 GHz, over a 20 MHz band. This analysis is carried out for different values of active users, i.e. the network load, with the purpose of setting the initial network load prior to the deployment of relay nodes. Additionally, the single-band macro deployment is considered as the reference scenario, or LTE deployment at an initial stage, to which all outage improvements and capacity gains are to be referred to. Radio resources are shared according to the algorithm outlined in the previous chapter (subsection 3.4), and the required outage level is fixed at 5% for a minimum data rate of 500 kbps. All the users are considered to be indoor.

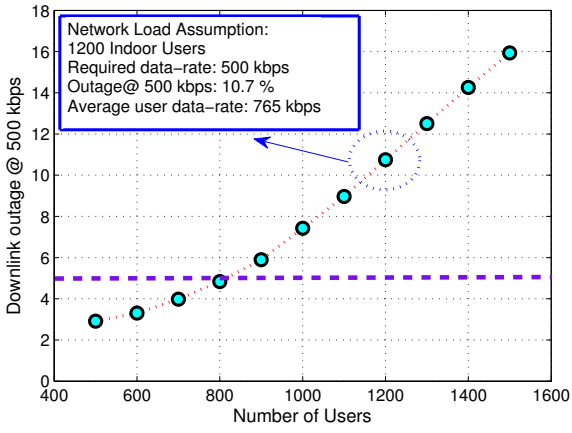

Fig. 4.6: User outage over different values of offered network load for a single-band macro deployment transmitting on a 20 MHz carrier at 2.6 GHz (*reference scenario*). Henceforth, the utilized reference network load for evaluating relay performance is fixed at 1200 users, giving a 10 % outage in the reference scenario.

Fig. 4.6 illustrates the network outage behavior over a different number of simultaneously active users. As an overall trend, it is clear that network outage at 500 kbps increases with network load. Obviously, this is due to the fact that, by

increasing the network load, radio resources are to be shared amongst a higher number of users, thereby penalizing the low SINR users who are unable to get sufficient resources for achieving the minimum data rate in the first phase of the resource sharing algorithm. When the number of users is kept below 800, with approximately 12 users/cell, the single-band LTE deployment is able to deliver the required outage performance, but as the network load is increased, user outage rises to 16% – 3 times the required level – after doubling the network load to 1500 users.

The outage level is twice the target when 1200 users are generated in the network, which corresponds to an average load of 18 users/cell. Such a network offered load is selected as the starting point with regard to evaluating the impact of relay deployment, which is needed to reduce the outage level below the target. To further visualize how the traffic load is spread across the cells, Fig. 4.7 depicts the average number of users (left) and outage users (right) that are highlighted over the cell coverage area; it can be clearly seen that the most loaded cells are located not only in the city center where the traffic demand is significantly higher, but also in the city outskirts where the cell coverage areas are larger due to sparser macro deployment. In the latter case, the increased ISD between neighbor macro cells determines the presence of coverage holes in the cell-edge locations (see SINR map in Fig 4.1(a)), and as a result, outage users are mostly situated in the south-east region of the area. Relays are expected to enhance network performance especially in these coverage-limited areas. The impact of relay deployment on user outage is addressed in the next section.

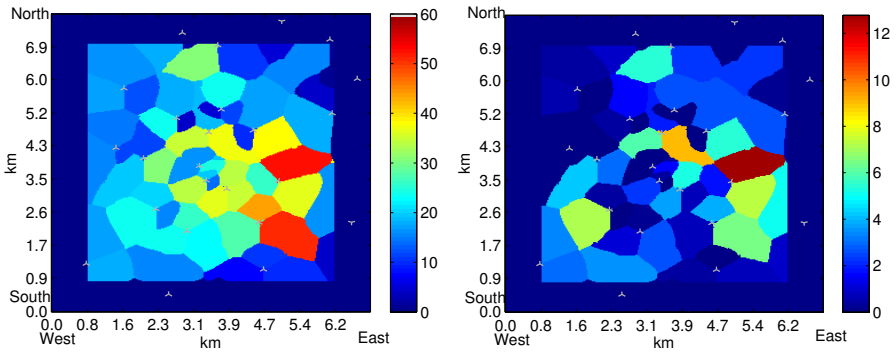

(a) Number of users

(b) Outage Users

Fig. 4.7: Average number of served users per cell (left) and outage users per cell (right) displayed over the cell coverage area.

4.3 Relay Performance Results with Single Band Macro Layer

In-band and out-band relay deployments are investigated by following the spectrum allocation schemes described in Table 4.3. All the involved transmission links operate on the 2.6 GHz band. Relay performance is evaluated by highlighting the two essential aspects: the sensitivity to relay density, i.e. the number of deployed relays, and the dependency on the backhaul link capacity, which is strictly related to the SINR perceived on the backhaul link or the possibility of using dedicated TDD spectrum. In the last subsection, a brief macro-only densification study at 2.6 GHz is carried out.

4.3.1 Relay Geometry and Backhaul Considerations

This subsection provides insight as to the experienced user geometry and backhaul link limitations with 50 deployed in-band relays. This amount of relays has been chosen since, under certain conditions (see next subsections), such a deployment configuration can fulfill the outage target. The small base stations enable the network to reduce the final outage from 11% (macro-only) to 7% without applying any site planning gain to enhance the backhaul link quality. User SINR distributions for both macro-only and in-band relay deployments, with regard to the different link involved in the relay framework, are illustrated in Fig. 4.8 together with a snapshot of the relay locations in the investigated area.

By deploying 50 relays, the average user SINR is improved by 3.4 dB compared to the initial macro network without relays, thereby extending network coverage. The relay users experience significantly high SINR values as relays are mainly deployed in coverage-limited zones, and the selected minimum ISD amongst relays guarantees low inter-relay interference. In addition to this, direct users also experience better SINR because the users that were initially located at the cell-edge in the macro-only scenario are now served by relays, thus decreasing the distance between macro users and serving cells. The backhaul link outperforms the other links in the lower tail of the SINR distribution as a directive antenna at the relay side (7 dBi gain) enables the relay to partially mitigate interference from the surrounding macro cells in the cell-edge areas. Yet, by looking at the average SINR performance, backhaul geometry is dramatically lower than the one experienced, for instance, by relay users: relays are deployed in coverage-limited areas that, albeit served by macro donor cells deployed within the city center, are located in the peripheral regions of the area, with distances from the donors that are larger than 1 km; under these conditions, the backhaul antenna directivity is not sufficiently high to significantly reduce interference originating from the high-density deployment area, at which most relay backhaul antennas are pointed. Hence, a

higher backhaul antenna gain, or alternatively a more directional antenna pattern, is needed to enhance the overall backhaul signal quality.

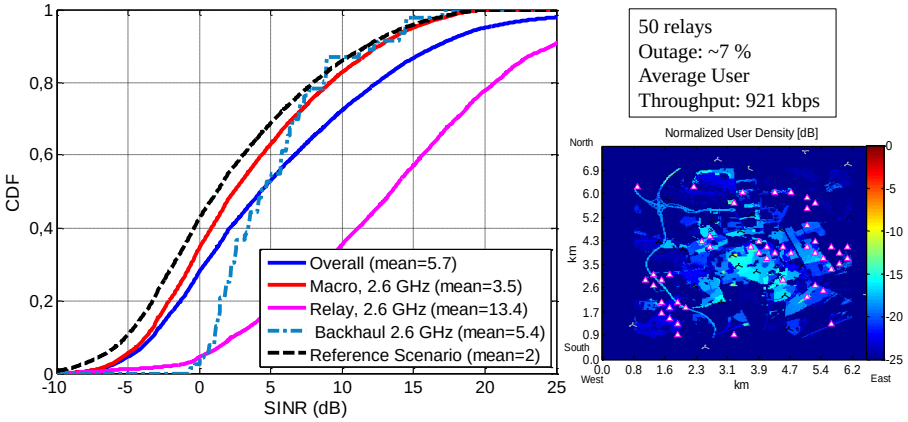

Fig. 4.8: SINR CDFs (left) for single-band macro-only reference scenario and in-band relay deployment with 50 relays, for all the different transmission links. A snapshot (right) of the selected relay positions is also provided.

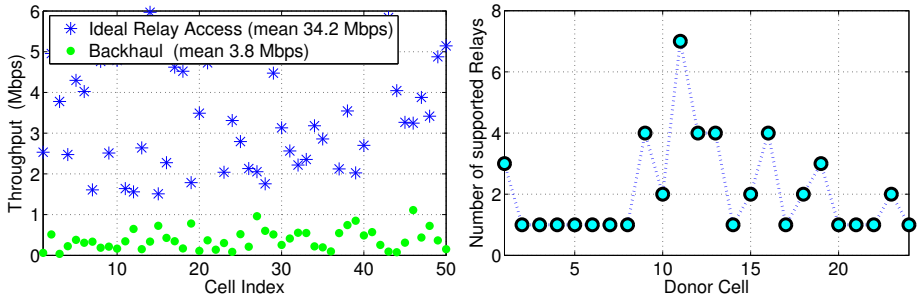

(a) Backhaul bottleneck (b) Relay connections per donor cell

Fig. 4.9: Overview of backhaul-related statistics showing the comparison between relay access aggregated throughput and the corresponding backhaul data rate (left), and also the donor cell load in terms of connected relays (right). The number of deployed relays is 50.

Another important aspect of in-band relay deployment is the relation between the aggregated relay access throughput and the supported backhaul link data rate, i.e. the two links of the two-hop transmission, as illustrated in Fig. 4.9(a) for each of the 50 in-band relays. It can be seen that the ideal aggregated throughput, i.e. the aggregated relay cell throughput without any backhaul link limitation, is on average 10 times larger the data rate achieved on the backhaul link. The two main reasons are: first, relay users perceive extremely good SINR as compared to relay backhaul (an average SINR improvement of ca.8 dB), thus increasing the

spectral efficiency gap between the two links; secondly, backhaul link resources are to be shared amongst a certain number of relays if donor cells have multiple relays connected. An overview of backhaul link connections over the different donor cells (24 in total) is depicted in Fig.4.9(b), with a maximum of 7 in-band relays served by one donor cell. The donor serving the highest number of relays is the one affected by higher outage in the macro-only scenario, and as a consequence, the deployment algorithm prioritizes the coverage-limited locations covered by that macro cell. Moreover, it is also clear that relays are not uniformly spread across the macro donor cells, having half of the relays connected to only 6 out of 24 donor cells.

4.3.2 Sensitivity to In-Band Relay Density

After analyzing the user geometry and giving insights about the backhaul bottleneck for a fixed number of relays, network outage performance and achieved averaged user throughput are evaluated with respect to different densities of deployed in-band relays. Fig.4.10 shows both network outage and average throughput gains over relay density: the former is illustrated by considering the split between users connected to relays and those connected to the macro cells, whereas the capacity gains are calculated with reference to the macro-only scenario. In this sensitivity study, no site planning gain is assumed to boost the backhaul link capacity.

By increasing the number of relay cells, user outage turns out to be significantly sensitive to the number of new small cells if less than 50 relays are deployed in the network. In fact, the first candidate locations are the ones lying in low-SINR regions served by high-outage macro cells, and for this reason the outage improvement is significant. Nonetheless, as the number of deployed relays increases, the user outage saturates, reaching a minimum of 6 % outage with 100 deployed relays, and most of the user outage is caused by the relay cells. According to the current assumptions, the deployment of a large number of relays is unable to reduce the user outage to 5 %, and this can be explained as follows:

- The average in-band backhaul link SINR is not sufficiently high, and thus the achieved backhaul link data rate limits the relay outage performance when a higher number of users are connected to the relay layer. With increased relay density, a larger amount of resources are allocated to the backhaul and shared amongst multiple relays, which do not experience homogeneous SINR conditions on the backhaul. In order to keep the network outage low for both relay and direct users, resources cannot be entirely dedicated to the backhaul link, but the achieved backhaul link capacity does not allow each of the relays to deliver the minimum data rate to all their connected users.
- To limit intra-tier interference, ISD between relays is kept at 250 m, thereby

spreading the small cells in different areas of the network. When the number of relays gets higher, not every relay can be deployed in those macro cells that are affected by the highest outage levels. Therefore, relays tend to be deployed also in locations that are not critical in terms of user outage as the overlay macro cells are already providing good coverage.

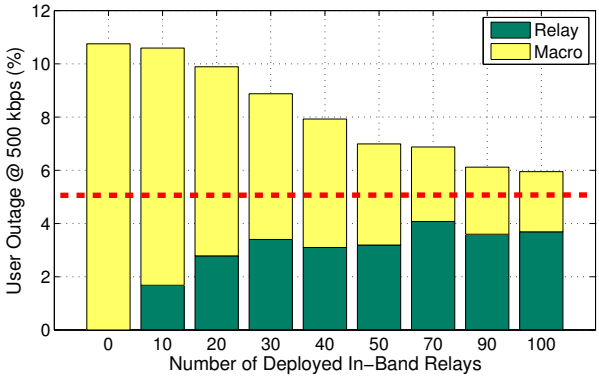

(a) User Outage

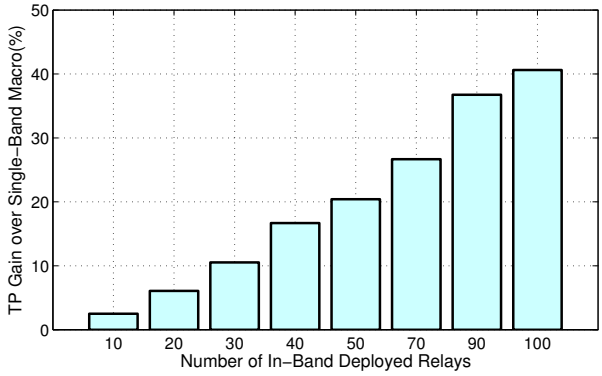

(b) User Throughput

Fig. 4.10: User Outage and Average Throughput (TP) over different numbers of in-band deployed relays. The former is shown by splitting the contribution from macro and relay layers to the overall outage level.

As concerns user average throughput, relays yield throughput gains over the macro-only scenario, which increase linearly with the number of deployed relays. As previously shown in Fig. 4.8, relay deployment boosts the overall user SINR, and despite the resource consumption on the backhaul link, relay and macro users experience better average throughput than in the macro-only case. However, with 100 relays deployed, the capacity improvements do not exceed 40% due to the

backhaul-limited nature of the two-hop connection, which does not allow relay users to unleash the potential the data rate experienced on the access link. Further details related to relay user load and number of relays served by donor cells are illustrated in Fig. 4.11(a) and 4.11(b). It is clear that macro cells cover the majority of the area in all the investigated deployment configurations, and 50 relays have to be deployed to offload approximately one fourth of the users to relay cells. The low user intake is also related to the employed deployment strategy, which is mostly aimed at covering cell-edge areas rather than the high-traffic zones. Moreover, with highly dense relay deployment, the percentage of donor cells serving more than 2 relays becomes larger, peaking at around 40% with 90 in-band relays. As previously explained, overloading the donor cells with an increased number of relays does not give significant outage improvements as the backhaul link data rates do not suffice to satisfy the relay users.

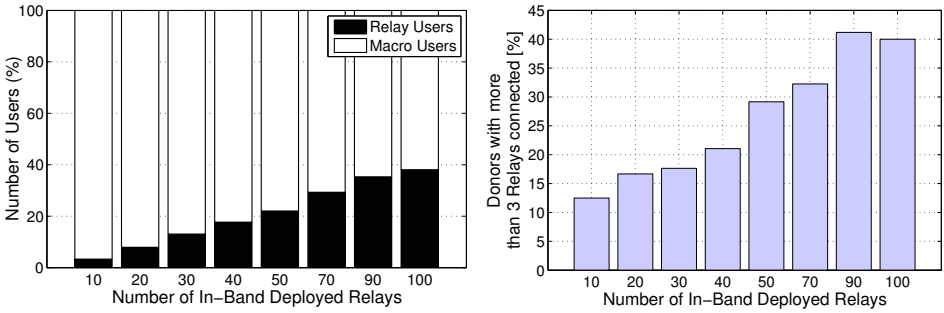

(a) User split (b) Donor relay load

Fig. 4.11: User split amongst the different deployment layers (left) and donor cell load (right) for different numbers of in-band relays. The donor load is expressed as the percentage of donors having more than 2 relays connected.

4.3.3 Sensitivity to In-Band Relay Site Planning

In order to evaluate to what extent relay performance is sensitive to the backhaul signal quality, different values of site planning gains (see Eq. 4.4 for details) are applied to the backhaul link for a number of 50 relays deployed in the network. As for the backhaul link SINR, Fig. 4.12(a) shows the improvements on the backhaul signal quality upon applying the site planning gains: it can be noted that the average SINR does not increase proportionally to the applied site planning gains; the site planning bias is applied to the links between the relays and all the cells belonging to the donor cell site, and this means that the resulting SINR gain is lower than the applied gain if the main interferers are the co-sited cells. The improved backhaul link geometry leads to reduced user outage, as shown in Fig. 4.12(b).

Obviously, having better backhaul link SINR has a double effect: relay users can be supported with higher backhaul data rate, relaxing the bottleneck problem on the first hop, and potentially fewer resources need to be allocated to the backhaul link so that more resources are available for direct users. To fulfill the 5% outage target with a tolerance error of 0.5%, a site planning gain of 7 dB is needed, as relay outage constantly reduces while increasing the site gain.

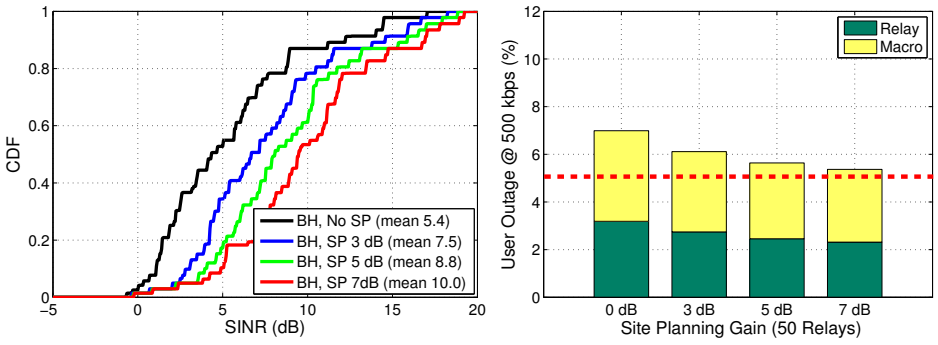

(a) Backhaul geometry

(b) User Outage

Fig. 4.12: Sensitivity to backhaul site planning gains over perceived backhaul SINR (left) and resulting user outage (right)

From a practical point of view, the site planning gain modeled in this study can be realized as follows:

- According to the study assumptions, the main limitation for the backhaul link SINR is interference from the surrounding cells. To improve the signal quality, backhaul antennas with gains that are higher than 7 dBi shall be utilized. By having a radiation pattern narrower than 70°, it is possible to filter and mitigate interference, thus boosting the backhaul SINR. However, this comes at a higher cost in terms of equipment quality and installation.
- In case the donor cell is severely shadowed, accurate positioning of the relay base station can be carried out in proximity of the originally selected locations so as to circumvent shadowing. This can be achieved not only on the horizontal plane, but also by deploying the relay on a higher antenna mast. Obviously, such a procedure requires higher implementation costs.

4.3.4 Out-band Relay Deployment

Similarly to the in-band case, the main performance indicators for out-band relay deployment are evaluated for different numbers of deployed relays, as can be seen

from Fig. 4.13. The wireless backhaul operates on a TDD dedicated frequency band at 2.6 GHz whereas the relay access link is operated similarly to a full co-channel deployment with the macro layer. Moreover, all macro sites are deployed with the TDD frequency carrier, even though no relay backhaul has to be fed: this assumption sets a sort of pessimistic scenario in terms of interference generated on the backhaul link, thus obtaining a conservative estimation of out-band relay performance. Essentially, propagation and interference conditions are the same experienced in the in-band relay scenario. Furthermore, no site planning gain is considered for this specific relay configuration.

With reference to user outage, out-band relays can significantly reduce outage as the number of small cells is increased. Differently from the in-band case, relays can rely on a larger yet fixed amount of radio resources to be shared amongst the connected relays, and this reduces the number of relay users in outage. 30 out-band relays suffice to decrease the outage to the 5% target, and the trend is similar until 50 out-band relays are deployed. After that, user outage saturates at around 3% for larger numbers of relays , and it is evident that most of outage users are the ones connected to relays: being the TDD spectrum shared by a larger amount of relays, backhaul resources are not sufficient to deliver the minimum data rate to all relay users. Moreover, the average relay backhaul data rates for in-band and out-band relays are compared in Table 4.4: the throughput gain is higher for small numbers of deployed relays as fewer resources are allocated, on average, to the in-band backhaul link. When the number of relays per donor increases, the in-band backhaul link ratio becomes larger, and the gap with the out-band case shrinks. However, the in-band wireless backhaul detracts resources from the direct users, and the overall outage is due to both relay and macro users. In the out-band case, macro resources are, on the other hand, fully utilized to serve direct users, and macro outage dramatically declines when an increased number of users is offloaded to relays.

Table 4.4: Average relay backhaul capacity comparison between in-band and out-band relays.

Relay number	In-band backhaul data rate [Mbps]	Out-band backhaul data rate [Mbps]	Gain over In-band case
10	1.7	9.9	+ 404%
50	3.8	7.3	+ 92%
100	4.4	6.5	+ 48%

Based on the foregoing observations, the use of a dedicated TDD spectrum for backhaul brings also benefits in terms of average user throughput with respect to in-band relay deployment. In Fig. 4.13(b), it can be seen that the capacity gains over the macro-only scenario increase linearly with the number of deployed relays, without flattening out for higher relay densities. The throughput gains over the reference scenario are approximately twice the ones experienced with in-band relay

deployment.

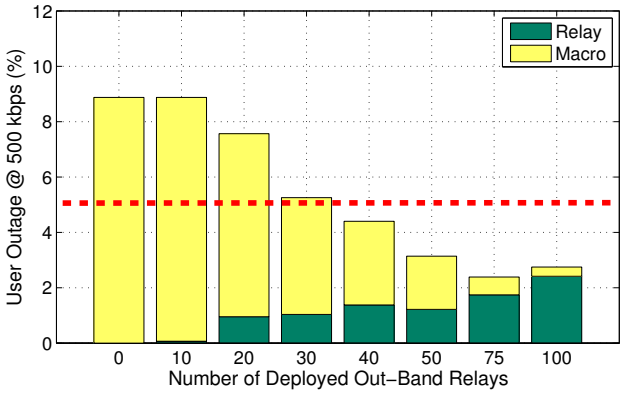

(a) User Outage

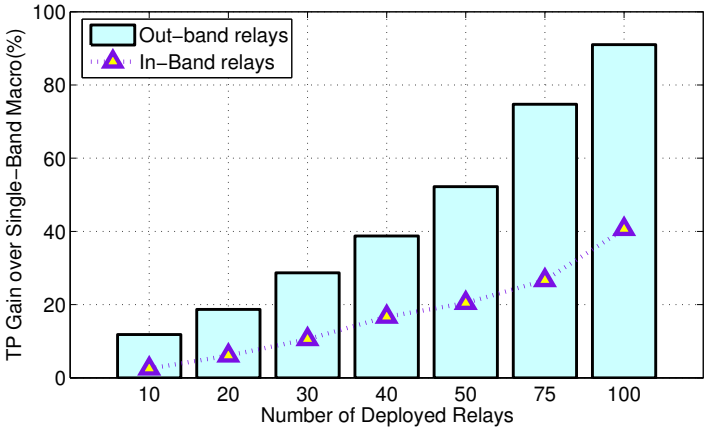

(b) User Throughput

Fig. 4.13: User Outage and Average Throughput (TP) over different numbers of out-band deployed relays. The former is shown by splitting the contribution from macro and relay layers to the overall outage level. Out-band relay throughput performance is compared with corresponding in-band relay deployment.

4.3.5 Single-Band Macro Densification

A simple yet costly deployment solution to meet the outage requirement is given by macro site densification at 2.6 GHz over the existing single-band macro deployment. In particular, 9 new macro sites are to be deployed to reach the outage target. The deployment algorithm setting is similar to the relay one even

though different minimum ISD requirements are set so as to take into account the higher transmission power and extended radio coverage (A_i = 300m x 300m and ISD_{macro} = 500 m). The selected positions are highlighted in Fig.4.14, and it can be seen that the high-outage cell areas are prioritized as with relay deployment. Moreover, the new sites are deployed assuming an antenna height of 27 m (average value for the existing macro deployment), whereas sector bearing and tilting angles are not optimized – a fixed downtilt angle of 6° is utilized based on the average value related to the reference macro configuration. Furthermore, macro densification achieves an average throughput gain of around 20% as compared to in-band relay deployment delivering the same outage level. This macro densification scenario is considered when comparing the infrastructure costs of different deployment solutions.

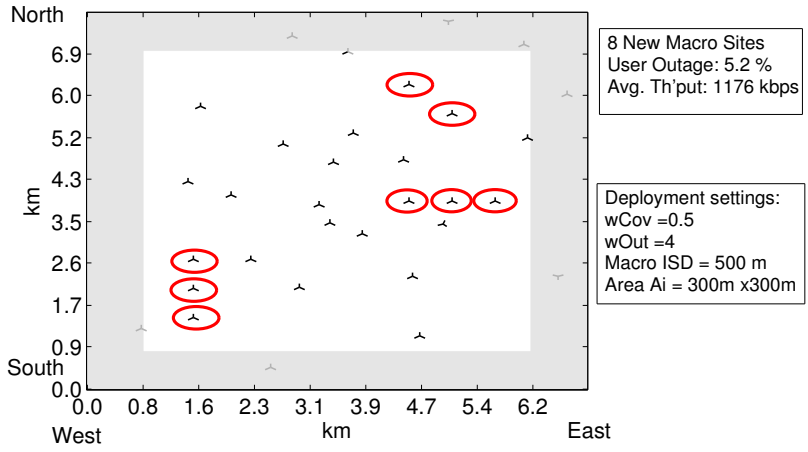

Fig. 4.14: Macro site densification over existing macro layout. The newly deployed macro sites are highlighted with the circles.

4.4 Relay Performance results with Dual-Band Macro deployment

The focus of this section is on evaluating the network performance when the lower frequency carrier at 800 MHz is available at the macro layer. The KPIs will be presented for the macro-only dual-band scenario, in which all the macro cells are deployed with both carriers at 2.6 GHz and 800 MHz, and also relay deployment on top of the macro dual-band overlay. The network load is kept at 1200 users, as in the previous analysis with single-band macros.

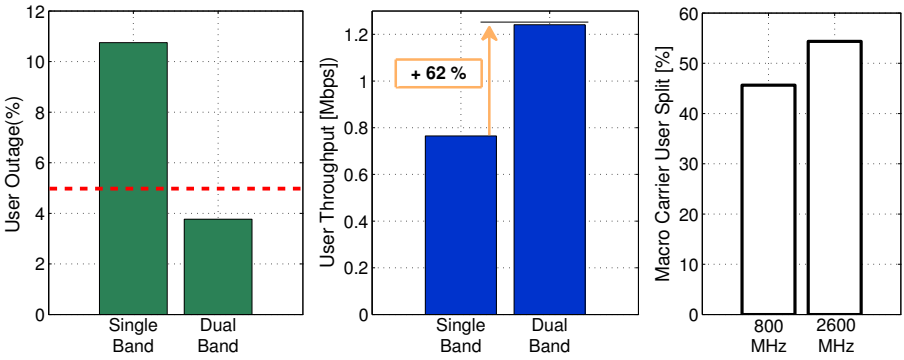

Fig. 4.15: Dual-Band Macro performance in terms of outage(left) and average user throughput (center), which are compared with the single-band macro scenario, and user split (right) between low carrier and high carrier bands.

4.4.1 Macro-only Deployment with Dual-Band Sectors

To begin with, the impact of the second carrier upgrade on macro-only network performance is investigated and the main KPIs are depicted in Fig. 4.15. As compared to the macro deployment with one carrier at 2.6 GHz, the dual-band configurations outperform the reference scenario with regard to both user outage and average throughput. By upgrading each cell of the reference scenario with the 10 MHz bandwidth at 800 MHz, user outage goes below the outage requirement, reaching around 4%. Such an improvement can certainly be explained with the better SINR conditions (refer to Fig. 4.4) experienced by those users located in the macro coverage holes at 2.6 GHz. Also the average user throughput benefits from the deployment of the lower carrier, and the overall performance is in the same order as the one obtained with approximately 40-50 out-band relays with single-band macro overlay. Moreover, it can be seen that users are almost uniformly distributed between the two carriers, as a result of the load balancing algorithm. Although user SINR is better at 800 MHz, the available bandwidth is half the one at 2.6 GHz, and the smaller band is taken into account when distributing the users so that the the lower carrier does not become overloaded.

Since the full dual-band upgrade brings the user outage well below the target, it can safely be stated that some of the macro cells can be spared when performing the upgrade to the second carrier to hit precisely the 5% target within a +/- 0.5% error. Fig. 4.16 shows the cell areas of the sectors that need to be upgraded to 800 MHz to achieve the outage target. To select the candidate sectors to be upgraded, the macro cells are ordered in descending order of the corresponding outage level in the single-band macro scenario; then, the second carrier is deployed starting from the cells delivering the worst outage performance until the network outage

level lies in proximity of the 5%-target. As a result, 13 sectors belonging to 9 different sites are upgrade and throughput performance is in the same order as the one achieved with in-band relaying.

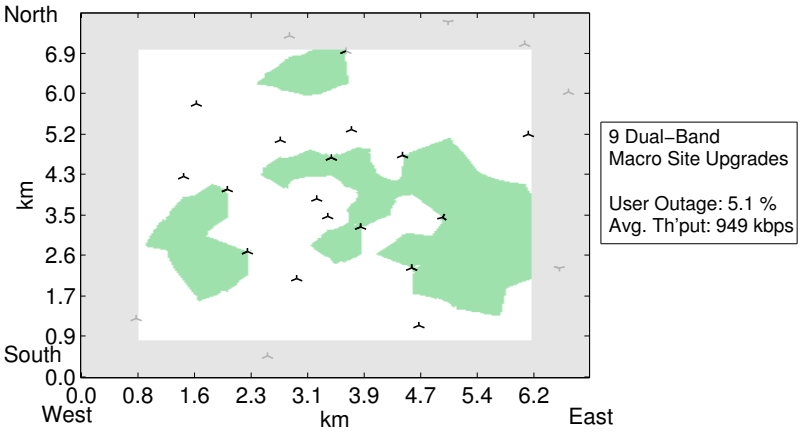

Fig. 4.16: Optimized dual-band macro upgrade delivering an outage level between 4.5 and 5.5%.The cell area of the sector upgraded to 800 MHz is shown in green.

4.4.2 Relay Deployment Performance Results

Considering that the outage requirement can be met with dual-band macros only, relays can be deployed on the 2.6 GHz band to further improve network coverage and performance. Although not needed in terms of KPI target, network performance is investigated with a fixed number of 50 relays, for both in-band and out-band configurations, without applying any site planning gain.

In Fig. 4.17, user SINR distributions are shown for the dual-band macro layer case, considering the scenarios with only macros and 50 in-band relays. Similarly to the single-band macro case, the deployment of 50 in-band relays yields a gain of more than 3 dB on the average user SINR when compared to the macro-only scenario. In addition to this, the usage of the lower carrier at 800 MHz further enhances the macro users geometry especially at the cell-edge areas. The backhaul link SINR distribution is slightly improved compared to the single-band macro case as the different outage level – obtained with the second macro carrier – affects the deployment algorithm metrics and the selected relay positions.

The performance results related to the deployment of 50 in-band and out-band relays are outlined in Table 4.5. User outage can be halved when out-band relays are deployed together with the dual-band macros, and the user throughput rises

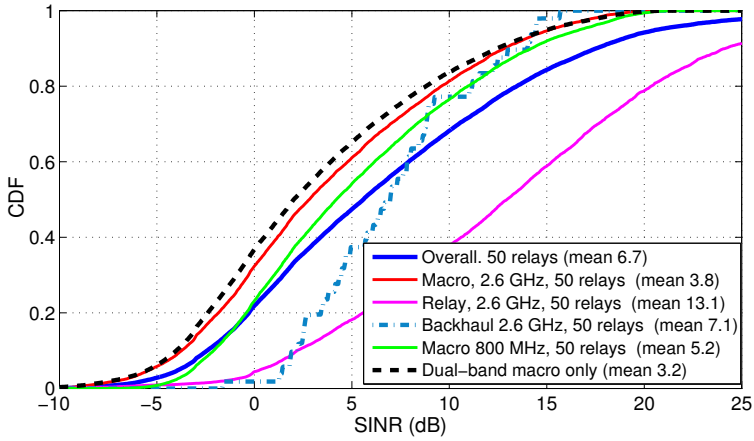

Fig. 4.17: SINR distributions for dual-band macro-only scenario (back dotted line) and in-band Rrlay deployment –direct, relay and overall user geometry, with Backhaul link geometry– for 50 relays.

Table 4.5: Performance results for in-band and out-band relays deployed with dual-band macros.

Deployment configurations	User Outage [%]	Throughput Gain over Dual-Band scenario
Dual-band only	3.8	–
50 in-band relays	2.3	+23%
50 out-band relays	1.7	+46.7%

by 46%, which is similar to the gains obtained by deploying out-band relays over single-band macros. The same trend as for single-band macro case is experienced with in-band relaying, where the performance gains are lower as compared to the out-band relays. Under the current traffic assumptions, relay deployment may be optional as the outage target is already fulfilled with dual-band macros. Yet, for higher traffic demand, relay deployment can be leveraged in parallel with the macro carrier upgrade to 800 MHz, to increasingly improve network coverage on the 2.6 GHz band.

4.5 Cost Analysis of Iso-Outage Scenarios

The main criterion for assessing the economic viability of different deployment alternatives is to select deployment configurations delivering the same outage per-

formance (5% +/– 0.5% at 500 kbps). To have a wider overview of possible deployment options, 4 deployment options including relay deployment and macro-only upgrades are investigated, and the corresponding performance results are outlined in Table 4.6. Besides the 17 macro sites located within the investigated area, 7 additional macro sites located outside the area borders are considered for cost analysis, as some of their sectors serve part of the users.

Table 4.6: Performance results related to the iso-outage scenarios.

Nr.	**Deployment Options**	**User outage**	**Average User Throughput**	**Total Spectrum**
(1)	24 single-band macro sites 50 in-band relays with Site Planning (7 dB)	5.4 %	971 kbps	20 MHz FDD
(2)	24 single-band macro sites 30 out-band relays no Site Planning	5.3 %	985 kbps	20 MHz FDD + 20 MHz TDD
(3)	Optimized Dual-Band 15 single-band macro sites 9 Dual-band sites	5.1 %	949 kbps	20 MHz FDD + 20 MHz TDD
(4)	Macro Densification 24 single-band macro sites 8 new single-band macro sites	5.2 %	1176 kbps	20 MHz FDD

With regard to relay deployment, the first deployment option is given by 50 in-band relays operating together with a single-band macro layer at 2.6 GHz. As pointed out in section 4.3, the outage requirement is met only if site planning gains are assumed on the backhaul link. From a cost perspective, such relays are regarded as "high-cost" relays as more effort is put on relay initial planning and network optimization, which increase the IMPEX component of the overall TCO. Out-band relay deployment is represented by the second scenario, in which no site planning gain is assumed, i.e. "low-cost" relays. It is important to note that the overall TCO model for out-band relaying includes the deployment costs related to upgrading the donor cell sites with an additional TDD carrier needed to operate the backhaul. With 30 out-band relays, 13 out of 24 sites host donor cells and are therefore upgraded to the second carrier, i.e. the adjacent 20 MHz band at 2.6 GHz operated in TDD mode and entirely dedicated to backhaul transmission.

The last two iso-performance scenarios are obtained through macro layer upgrades only. In the dual-band macro scenario, the cost is calculated on the assumption that the overall site is upgraded to 800 MHz although only some of the co-located sectors need to be upgraded to meet the outage target (see Subsection 4.4.1). The overall site upgrade is indeed more realistic from a deployment perspective than upgrading single sectors as current base station architectures include a compact three-sector RF module supporting multi-carrier [136]. Moreover, macro densification guarantees not only improved coverage but also higher capacity performance

with a gain of 24% over the dual-band macro scenario.

The TCO analysis is carried out for the previously described scenarios and according to the cost figures presented in Section 3.7. The cost values of the different deployment alternatives are depicted in Fig. 4.18, highlighting the different components of the overall TCO. The total cost also includes the expenditure related to the macro reference scenario, which is obtained by considering an LTE upgrade to all the existing 3G sites. OPEX is calculated over a period of 4 years in order to evaluate the impact of certain expenditures, such as site rental or backhaul expenses, over a more extended time frame. For this reason, OPEX is considerably dominant with respect to the other cost components.

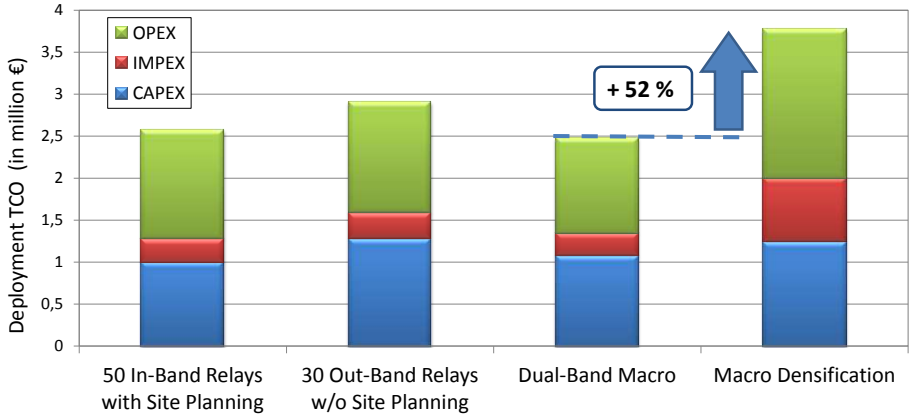

Fig. 4.18: TCO associated with the selected iso-outage scenarios, showing the split among the different cost components (CAPEX,IMPEX,OPEX). Running costs are taken into account for a time span of 4 years.

Macro densification gives the highest TCO, whereas in-band relays and dual-band scenario are the most cost-effective solutions. The deployment of 9 new LTE macro sites certainly penalizes the macro densification scenario due to extremely high fixed costs, such as civil works, site acquisition and equipment installation. As each new macro site is around 20 and 4 times more expensive than deploying one in-band relay and upgrading one site to the second carrier, respectively, macro densification is approximately 50% more costly than scenarios 1 and 3. Moreover, out-band relay deployment turns out to be more expensive than in-band relays: although fewer relays are deployed (30 against 50), and no site planning-related costs are considered, the TDD carrier has to be deployed at the macro site hosting the donor cell. This increases the cost of the macro infrastructure that is needed to feed the wireless backhaul since more than half of the sites are upgraded to the additional TDD carrier.

The deployment of in-band relays and the macro upgrade to the lower carrier

band perform similarly in terms of TCO, and they can both be considered as economically viable deployment solutions for the assumed network offered traffic. On one hand, it can safely be stated that the installation price associated to the multi-carrier upgrade is not expected to be particularly sensitive to the deployment scenario as it is mostly about performing both hardware and software upgrades on existing sites. The cost of relays, on the other hand, strongly depends on the specific deployment conditions, the considered country and equipment. Site rental and acquisition costs may vary significantly with regard to the selected deployment locations and reference country [47]. In this dissertation, the relay cost figures reflect the case in which relays are designed to guarantee easy installation and low equipment costs. When site planning is assumed, relay IMPEX is increased as initial planning and network optimization procedures are performed to ensure better backhaul SINR conditions. Additional costs related to the use of more directional antennas, which require higher installation and maintenance costs, are not taken into account, thus giving an optimistic case in terms of infrastructure costs for in-band relay deployment.

4.6 Summary and Conclusions from the Sub-Urban scenario

This chapter has analyzed the performance of downlink relaying for a realistic suburban area and under realistic spectrum availability assumptions. A minimum user data rate of 500 kbps is used as the main KPI for an offered network load of 1200 simultaneously active users. By considering the reference LTE macro site deployment co-sited with the existing 17 3G sites and transmitting at 2.6 GHz (single-band macro), 11% of the users are in outage, and this is mostly due to poorly covered areas located in the city outskirts. In order to reduce user outage below a target of 5%, different relay and macro deployment alternatives have been investigated in terms of performance and cost. The following conclusions can be drawn:

- A coverage-oriented deployment of in-band relays cannot significantly reduce user outage as the backhaul link acts as a bottleneck for the performance of relay users. By assuming a low-gain antenna (7 dBi) at the relay side, a large number of deployed in-band relays, e.g. 100 in the investigated area (6 relays/site), do not give considerable improvements in user outage, which saturates at around 6%. To further reduce user outage, it is crucial to enhance the backhaul link SINR through site planning or the installation of high gain antennas (significantly larger than 7 dBi). With a site planning gain of 7 dB exclusively applied on the backhaul link to the donor cell, 50 in-band relays (3 relays/site) enable the network to fulfill the outage

requirement.

- Out-band relay base stations using dedicated TDD spectrum for backhaul (not available for transmission towards the users) provide significant user outage and average user throughput improvements as compared to the in-band case. Indeed, thanks to a higher availability of radio resources on the backhaul link, 30 out-band relays (1.8 relays/site) are able to deliver a 5% outage without resorting to site planning gains.
- The use of low frequency spectrum (800 MHz) at the macro layer considerably improves network coverage, thereby achieving similar performance as out-band relays deployed together with macro cells in the 2.6 GHz band. On top of the dual-band macro layer, in-band and out-band relays can further improve the network performance, and the gains are in the same order of magnitude as in the single-band macro scenario.
- From a cost point of view, in-band relays can be profitable compared to macro densification and are as cost effective as LTE macro upgrade to the 800 MHz carrier frequency, when all these solutions deliver the same outage value. In-band relays have some cost advantages over out-band relays due to the fact that the backhaul link requires an additional carrier upgrade. Essentially, the additional cost associated with the dedicated backhaul carrier deployment exceed the cost savings obtained with a smaller number of deployed out-band relays.

The conclusions above are strongly related to the type of investigated scenario – the suburban area – and also the assumed traffic load. By selecting an initial outage level of 10%, the dual-band macro upgrade seem to be the right solution to tackle the outage problem and improve coverage. In-band or out-band can be alternative solutions in the short/medium term, but in case of extremely higher traffic demand, they would fail in delivering the expected outage because of the limited backhaul link capacity. To cope with exploding traffic growth, the combination of different deployment layers, such as relays, macro-carrier upgrade and also new macro sites, can be leveraged to boost network performance in a cost-efficient fashion. Moreover, from an operator's perspective, TDD spectrum exclusively used for relay backhaul transmission is quite unrealistic as that band can also be exploited to serve mobile users directly – assuming that they can support both TDD and FDD transmission. As an example, the 2.6 GHz asymmetric band could be used for indoor base stations (femto and pico cells) to serve high traffic indoor areas, mostly located in the downtown area, if the network runs out of capacity. All the previously mentioned deployment scenarios could be addressed in further studies with particular emphasis on long-term deployment solutions and higher traffic volume growth.

Chapter 5

Relay and Micro Deployment in a High-Traffic Metropolitan Scenario

5.1 Introduction

In the previous chapter the viability of deploying relays has been evaluated in a coverage-limited scenario, which is inherently suited for a two-hop relay connection on condition that excellent signal quality is guaranteed on the backhaul link. However, due to higher population density and fiercer competition among mobile operators, mobile data usage is much higher in dense urban areas than in suburban or rural scenarios. Therefore, high-traffic urban scenarios are the most critical with reference to offering sufficient capacity for data hungry devices and applications. Existing urban 3G deployments already present high macro site densities with average ISD below 500 m. On the one hand, this can guarantee acceptable signal coverage all over the network – such a scenario can be defined as interference-limited – but on the other hand, the available capacity may not be sufficient to support increasing traffic volumes.

The main target of this chapter is to investigate the deployment of outdoor small cells – typically deployed at street level below rooftop – in a realistic LTE dense urban scenario, which is located in the downtown area of a European capital, as illustrated in Fig.5.1. As one of the biggest obstacles and cost drivers for the

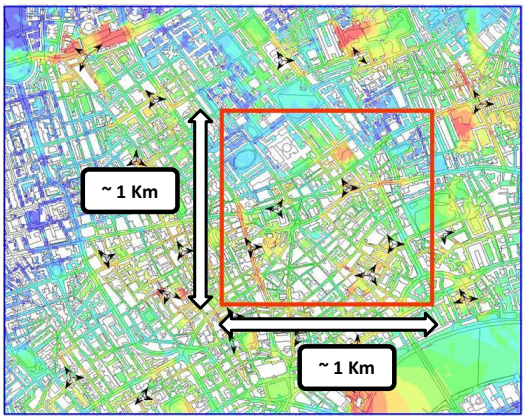

Fig. 5.1: Metropolitan area scenario with existing 3G site deployment and predicted path loss. The investigated area is delimited by the rectangle.

deployment of small cells is backhaul, the analysis focuses on the downlink performance evaluation of both relay and micro deployment in a selected high-traffic area of 1 km^2, or more intuitively the comparison in terms of performance and cost between the use of wireless and wired backhaul for small cell deployment. To improve the propagation modeling in the metropolitan area, path loss predictions for macro and relay backhaul link are based on ray tracing and aided by detailed 3D building information. Although wireless backhaul is extremely attractive from a cost perspective, the performance of relays has yet to be thoroughly evaluated, especially when spectrum availability is scarce and in-band relaying is the only applicable configuration. In particular, the case study is meant to provide answers to the following research issues concerning the outdoor small cell deployment in an LTE network:

- Focus on performance comparison between in-band relay deployment and the analogous case for micro base stations, i.e. co-channel micro deployment. This scenario is the most challenging in terms of spectrum resources, as relay, micro and macro cells share the same frequency band.

- Evaluate to what extent small cell network performance is sensitive to different transmission configurations, such as small cell transmission power, the use of additional LTE TDD spectrum for relay backhaul and macro user transmission, or the possibility of performing interference cancellation at the relay side to boost backhaul SINR.

- Compare, from a financial point of view, relay and micro cell deployments delivering the same outage performance. The TCO analysis is accomplished according to varied small cell cost assumptions.

The remaining part of the chapter is organized as follows: Section 5.2 deals with a detailed description of the scenario and the main simulation assumptions; in Section 5.3 simulation results are presented for both in-band and co-channel micro deployment, whereas Section 5.3 discusses the impact of backhaul capacity improvements on network performance; to conclude, Section 5.4 describes the TCO analysis for iso-outage scenarios before summarizing and discussing the recommended solutions in the last section.

5.2 The High-Traffic Metropolitan Scenario: The "Hot-Zone"

This section is dedicated to the description of the investigated area and the main simulation assumptions. The existing 3G deployment is showed in Fig.5.1. It is evident that, differently from the suburban scenario, the number of involved sites and the size of the network area are remarkably smaller. Due its the metropolitan nature and area size, the analyzed network area is referred to as "Hot-Zone" since traffic demand and mobile broadband usage are orders of magnitude higher than in the surrounding areas. Details about the reference LTE deployment are hereinafter provided, highlighting macro layout, propagation modeling, and traffic assumptions.

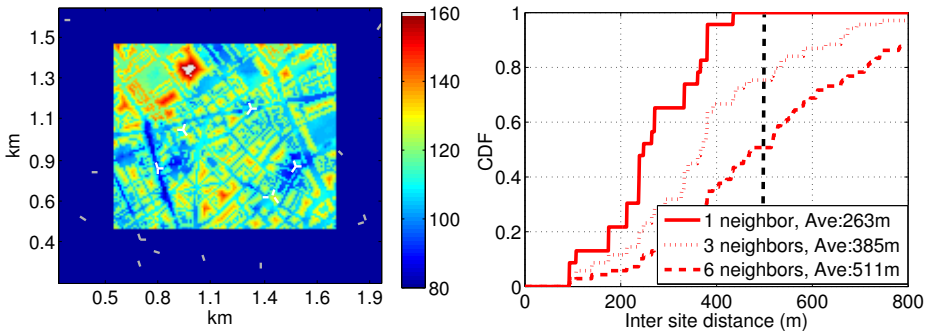

(a) Network Layout (b) ISD distribution

Fig. 5.2: Network layout (left) is shown through a best server link loss in dB obtained at 2.6 GHz, considering the presence of the building blocks. The ISD distribution (right) referred to closest sites is shown and compared with the fixed ISD employed in 3GPP Case I scenario (vertical dashed line at 500 m).

5.2.1 Network Scenario Description

The metropolitan network scenario is obtained from an existing 3G macro cellular deployment owned by a major mobile operator. The investigated area is shaped as a square with a size of 1 km^2 and a spatial resolution equal to 10 m x 10 m, as depicted in Fig. 5.2(a). The area contains 5 macro sites – each equipped with 3 sectors – but in order to avoid border-effects, one tier of interfering cells from base stations located outside the examined area is taken into account. A total number of 30 sectors cover the investigated area, but the 15 sectors (5 sites) within the area borders cover more than 75% of the area. The ISD between 2 neighbor macro sites is on average 260 m with a minimum distance of around 100 m, just as in typical dense urban macro deployments [49]. Fig. 5.2(b) shows the ISD distributions for the three and six nearest macro sites, respectively, and the average distance of the 6 closest neighbor sites is similar to the fixed ISD utilized in the interference-limited 3GPP scenario (Case I).

Each macro site is considered upgraded to LTE with optimized antenna down-tilt angles obtained from the 3G live network. Digital maps related to ground elevation and indoor locations are available to improve the propagation modeling accuracy. From the best server link loss map of Fig. 5.2(a) it is possible to distinguish the shape of the buildings or other indoor areas, which make up for approximately 50% of the analyzed network area. The main simulation parameters related to macro configuration and network scenario is summarized in Table 5.1.

Table 5.1: Main Simulation parameters

Parameter	**Value**
LTE System	Downlink FDD/TDD LTE, 2x2 MIMO
Supported Carrier Frequencies	2.6 GHz
Macro eNodeB Power	46 dBm per carrier
Network Layout	30 sectors covering the area 5 sites (15 sectors) located inside the area
Antenna configuration	LTE-like antenna pattern Half-power beamwidth: $\theta_{3dB} = 65°$ Gain: 18 dBi Cable Loss: network input data Vertical tilt: network input data
Antenna Height	Network input data
Terrain Height	Digital elevation map
Indoor Area	Clutter map input 50% indoor area percentage

5.2.2 Propagation Models

To accurately estimate link budgets, a 3D ray-tracing tool is used to evaluate path loss and antenna pattern effects with regard to the radio link between macro cells and terminals, i.e. users or relay backhaul receiver. Such a tool models the radio propagation at street level by considering realistic positions and heights of the buildings that are imported from the 3D building map. The ray tracing propagation models have been tuned and calibrated using measurement data from the investigated scenario, and this ensures higher accuracy compared to statistical propagation models. The path loss predictions are available at a height of 1.5 m for user terminals and 5 m with regard to the backhaul link for relays. The different heights are considered in order to capture the antenna height gains obtained by deploying relays above the ground level. Indoor attenuation is based on an exponential model for building penetration, which is similar to the model presented in [132].

Fig. 5.3 provides insights into the way user SINR is spatially distributed in the investigated area with regard to the reference macro layout. Based on ray tracing predictions at 2.6 GHz, the highest SINR values are perceived in proximity of the macro cells, along the main streets to which the sector antennas are directed. In these locations, the radio waves transmitted by the server cell are guided through building and ground reflections, whereas the interference signals are strongly attenuated due to the NLOS conditions. The investigated scenario can be regarded as interference-limited in most areas of the network; coverage holes are located in small-sized spots – mainly in the upper part of the map – as base station density is relatively lower and larger building sizes determine higher signal attenuation. Moreover, the SINR distribution under uniform traffic assumptions does not differ from the one obtained by considering the employed user density. As described in subsection 5.2.3, the users are evenly distributed between cell edge and cell center locations due to cell-level based traffic distribution.

As for outdoor small cells (relays and micros), the path loss on the access link is estimated by means of the statistical model proposed in Eq. 4.2 in the previous chapter, but the following modifications are introduced:

- The probability of being in LOS conditions decreases more steeply with increasing distance as compared to the suburban scenario. This is applied in order to model the street level propagation, which is highly affected by the presence of high and large obstacles. In fact, the LOS condition disappears for distances larger than 180 m (one third of the distance in the suburban case). The LOS probability is formulated as follows [62]:

$$Pr_{LOS}(d) = 0.5 - \min(0.5, 5\exp(-0.156/d)) + \min(0.5, 5\exp(-d/0.03)) \tag{5.1}$$

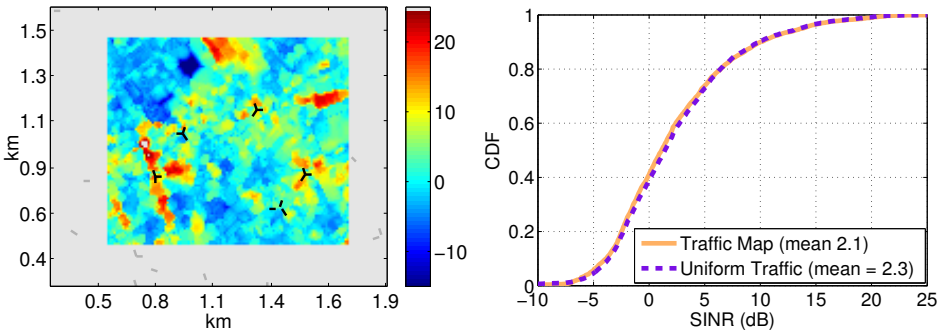

(a) Best Server SINR [dB]

(b) User SINR CDF

Fig. 5.3: Best server user SINR map (left) based on ray-traced path loss predictions. The SINR cumulative distribution functions (right) refer to both uniform and realistic user density maps.

- Similarly to the ray tracing model for macro cells, the outdoor to indoor penetration loss is applied only if users are located in indoor areas. As for small cells, the penetration loss is kept constant at 20 dB, without introducing any exponential signal attenuation to model the propagation through the indoor areas.

Statistical models for small cell propagation are utilized in order to reduce simulation complexity and time. This gives more flexibility when investigating the network performance for large small cell densities and understanding the potential of deploying such base stations. More accurate propagation models based on ray tracing are proposed in Part II of this dissertation.

5.2.3 Processing of Traffic Data and User Density Map

In this case study spatial traffic information is not available in the form of a pre-processed traffic volume map that is directly used to position the users throughout the network area. As described in Chapter 3 (refer to the second method in subsection 3.3.3), the spatial traffic characteristics are extracted from the measured cell traffic volumes that are subsequently associated with the corresponding macro cell coverage areas.

Firstly, cell traffic volumes are to be extracted from massive downlink data measurement campaigns collecting High Speed Downlink Packet Access (HSDPA) data volumes on an hourly basis over one week. Such information is available for all the 30 sectors that are serving the investigated area. Considering that data is mostly

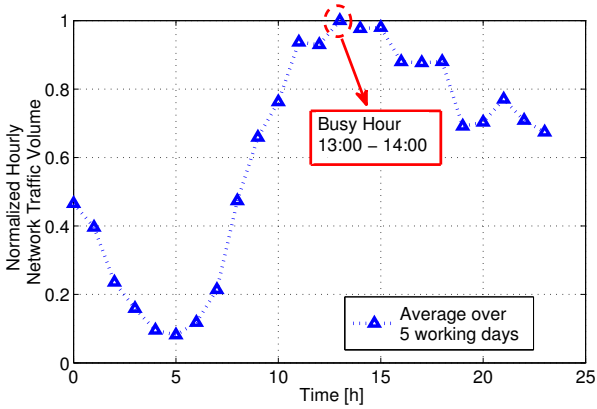

Fig. 5.4: Daily aggregated network traffic pattern, which is averaged out over 5 working days. The busy hour is recorded between 13:00 and 14:00, and the corresponding cell traffic volumes are used to generate the user density map.

consumed during working days, the average daily traffic profile shown in Fig. 5.4 is obtained by averaging out the daily traffic profiles over 5 days. Each point of the profile stands for the aggregate network traffic volume at a specific hour, and this value is normalized with respect to the highest traffic volume. The daily traffic peak, i.e. the busy hour, occurs between 1 and 2 pm, and this result differs from previous large-scale network traffic measurement data in which the peak was noted at 22 pm [15, 36]. This can be explained by the fact that the investigated area is mostly populated in the daytime, and most of the traffic is associated with business related activities, e.g. in shops and offices.

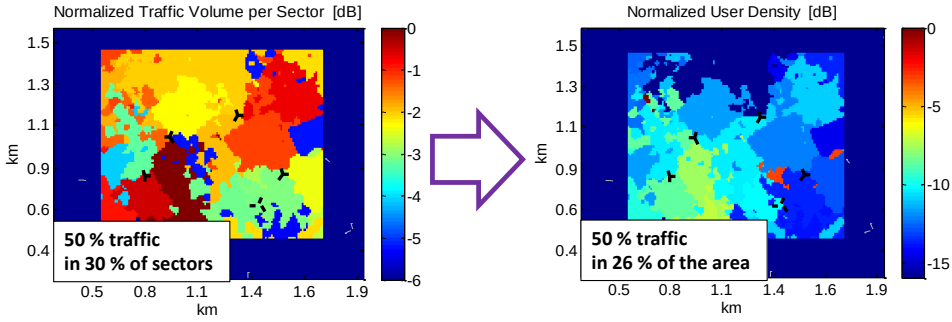

Fig. 5.5: Non-uniform user density map obtained from the downlink traffic volume map, which is derived by assigning the busy hour traffic volume of each cell to the corresponding cell coverage area.

Upon extracting the busy hour traffic volumes for each of the serving macro cells,

Eq. 3.3 is applied in order to generate the spatial traffic map, and this process is shown in Fig. 5.5. It can be inferred that the most loaded macro cells are located in the south-west area of the network and, similarly to the suburban case study, one third of the sectors deliver half of the network downlink traffic volume. As for its spatial distribution, half of the downlink traffic is concentrated on 26% of the network area, which is slightly less than the traffic sector distribution due to the limited coverage areas of high-traffic cells. Moreover, owing to the direct mapping of traffic volumes onto cell coverage areas, users are uniformly generated throughout the cell area. In this case study no additional information about traffic hot spots within a cell is available. Therefore, the utilized traffic distribution is solely based on cell level traffic, and based on the available indoor building map, *50% of the users are located indoor.*

5.2.4 Relay and Micro Deployment Assumptions

Relay and micro cells are both considered as small cell deployment options for the Hot-Zone case study. The radio resource sharing as well as the configuration assumptions for in-band and out-band relays are identical to the ones utilized in the previous case study (refer to sections 3.4 and 4.2.4 for details). Moreover, hybrid deployment of relays and micros is not addressed in this case study as the two types of small cells are deployed separately and compared in terms of performance.

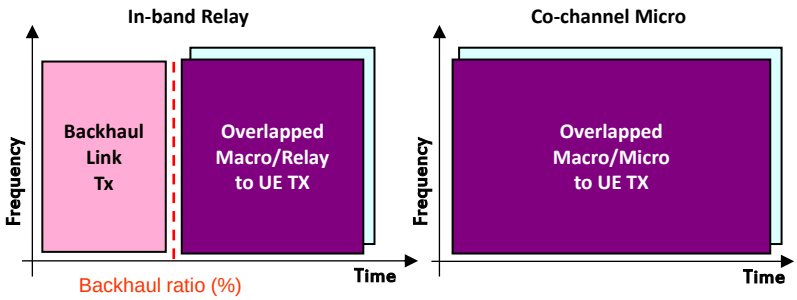

Fig. 5.6: Resource allocation for in-band relays and co-channel micros

Emphasis is put on the deployment case where macro and relays/micros are sharing the same radio resources, including backhaul relay transmission. The spectrum utilization for relay and micro cells complementing the overlay macro deployment is illustrated in Fig. 5.6: in-band relaying requires a certain amount of radio resources to be dedicated to backhaul transmission whereas a plain frequency reuse one is employed for relay and macro transmission towards the users; micro cells, instead, utilize all the spectrum resources to transmit data towards the users, and this configuration is defined as *co-channel* micro transmission, which entirely overlaps

with the macro. Micro backhaul is provided without squandering mobile spectrum, e.g. fixed line or microwave solutions on licensed bands, and the resulting backhaul capacity is sufficient to deliver the peak downlink data rates experienced on the access link. Furthermore, out-band relaying is also considered amid the various deployment options: in this case an additional adjacent TDD band is entirely dedicated to backhaul transmission – i.e. shared among the relays connected to the same donor –, whereas the relay access link utilizes all the spectral resources together with the macro just as micro cells.

Table 5.2: Relay and micro base stations parameter setting

Parameter	**Value**
Relay/micro power	30/37 dBm
Carrier frequency	2.6 GHz
Antenna Pattern Access Link, relay/micro	Omni Antenna Pattern 5 dBi antenna gain
Antenna Pattern Relay backhaul link	Directional antenna [137] Half-power beamwidth: $\theta_{3dB} = 55°$ Front-back ratio: $A_m = 20\ dB$ 12 dBi antenna gain
Antenna Height	5 m
Common deployment formula settings (relay and micro)	A_i = 100m x 100m ISD_{relay} = 100 m, ISD_{micro} = 80 m $ISD_{macro,relay}$ = 150 m,$ISD_{macro,micro}$ = 100 m Outdoor locations only
Relay specific Metric Setting	$wCov = 0.5$ $wOut = 2$ $wBH = 4$ disabled
Micro specific Metric Setting	$wCov = 0.5$ $wOut = 4$ wBH disabled

The main simulation assumptions about radio parameters and deployment algorithm settings are outlined in Table 5.2. Antenna pattern and height is identical for relays and micros when the access link is considered. Regarding relay backhaul antenna and overall deployment strategy, this case study relies upon different assumptions in comparison with the previously addressed suburban case study. The following enhancements are introduced:

- A more directional antenna is assumed at the relay side to enhance signal quality between donor cell and relay node. Based on [137], the half-power beamwidth is 15° narrower than the one utilized in the suburban scenario, thereby mitigating more effectively the interference power from neighbor cells. The antenna gain at the assumed frequencies is 12 dBi.
- Concerning the deployment algorithm, the selection of relay locations is performed by exploiting not only the coverage and outage weights, but also the one related to backhaul signal quality, wBH. This means that no site plan-

ning gains (utilized in the suburban case study) are applied to improve the backhaul signal quality as the deployment metric of Eq. 3.13 already considers the backhaul signal quality. A better backhaul link gives the opportunity to fully exploit the potential of in-band relays given that in-band backhaul connection generally acts as a bottleneck for the performance of relay users. All the available outdoor locations are evaluated to select the relay positions as the predicted urban propagation coverage is extremely sensitive to the presence of buildings and street layout. The deployment metric of Eq. 3.13 is calculated over the area A_i surrounding each candidate solution, and its size is aligned with the expected small cell coverage. Similarly to the suburban case, ISD between relay cells and reference macro sites are chosen to effectively spread relays over the investigated areas based on estimated coverage and transmission power. The overall small cell deployment strategy is, according to the metric weights outlined in Table 5.2, coverage-oriented, and the reader is referred to Appendix B.2 for details about the deployment algorithm calibration.

- With regard to micro cells, the deployment algorithm is optimized to fully exploit the opportunity of having no backhaul-limited performance. In other words, assuming that micros have other means for backhauling than utilizing mobile spectrum resources, their deployment is targeted at serving high-traffic areas and improving coverage performance without prioritizing the signal quality perceived on the wireless backhaul link. A performance comparison between optimized micro deployment and the case in which micros are deployed in the same positions as relays is shown in the results section.

In this case study all the outdoor locations are assumed to be available for small cell deployment without introducing any limitation for site availability or fixed-line backhaul connections. In a fully realistic deployment, the small cell positions may be shifted in proximity of the selected ones due to practical installation limitations or distance from fiber access or backhaul aggregation points.

5.2.5 Spectrum Allocation and Simulation Scenarios

As previously stated, the focus of the case study is on evaluating the performance of small cell deployment under limited spectrum availability, and the analyzed scenarios are outlined in Table 5.3. LTE spectrum is assumed to be available in the 2.6 GHz band, with most performance results obtained from the case in which a 20 MHz FDD band is to be shared amid macros and small cells. In order for specific deployment configurations to meet outage requirements, additional spectrum is considered along with the FDD band, and the assumption is that of relying on the adjacent TDD spectrum at 2.6 GHz. The additional carrier is utilized to

upgrade the macro layer, i.e. a dual-band configuration, or to support the out-band backhaul wireless connection. Therefore, users are assumed to support both FDD and TDD transmission when connected to the macro [138].

In general, the purchase of TDD spectrum at 2.6 GHz is less expensive than lower frequency spectrum, e.g. 700/800 MHz, as can be verified in [135], due to worse coverage in suburban and rural areas. Being attractive for operators from a financial perspective, the TDD carrier is chosen for this case study. When out-band relays are deployed, two options for using the additional TDD carrier are considered: the first one assumes that the unpaired spectrum is exclusively dedicated to the backhaul link without the possibility of serving macro users; the second one consists in dedicating TDD spectrum to the backhaul link only if the macro cells serve relays, i.e. a donor, whilst the non-donor ones are allowed to serve macro users. Obviously, the assumption is that of having a dual-mode FDD/TDD network where users can connect to both modes.

Table 5.3: Deployment scenarios and spectrum allocation for the different links

Network Deployment	**2.6 GHz (1)** (FDD, 20 MHz)	**2.6 GHz (2)** (TDD, 20 MHz)	Total bandwidth
Single-Band Macro Reference Scenario	macro direct	–	20 MHz FDD
Reference Scenario + **In-band relays**	macro direct relay access + backahul	–	20 MHz FDD
Reference Scenario + **Co-channel micros**	macro direct micro	–	20 MHz FDD
Dual-Band Macro	macro direct	macro direct	20 MHz FDD 20 MHz TDD
Dual-Band Macro + **Out-band relays**	macro direct relay access	macro direct backahul	20 MHz FDD 20 MHz TDD

5.3 In-Band Relay vs. Co-Channel Micro Performance

This section presents the network performance evaluation for different deployment alternatives assuming that only one carrier is utilized at both macro and relay/micro layer. Firstly, the single-band macro scenario is investigated in terms of user outage over different values of network offered traffic, thereby selecting the initial number of active users to be used as a reference for small cell deployment. Secondly, outage and capacity performance of in-band relays is presented for different relay densities, and similar results are given with respect to micro deployment. Lastly, a sensitivity study based on varied transmission power for both relay and micro nodes is performed to evaluate the impact of larger cell footprint on network

performance. For all the investigated deployment options, the performance target is to guarantee an outage level of at least 5%.

5.3.1 Macro Reference Performance

Prior to deploying relay or micro cells, the initial network load, expressed in terms of number of active users requiring a minimum data rate level, is selected upon evaluating the outage performance for different numbers of active users. Given the initial LTE deployment presented in the previous section, the network outage trend over the number of active users generated in the network is illustrated in Fig. 5.7: the minimum required data rate for the investigated high-traffic area is fixed at 1 Mbps and, as expected, network outage increases linearly with the number of users. Starting from a traffic load of 200 users, the reference LTE macro layer is able to fulfill, with one deployed carrier, the outage requirement of 5%, but after increasing the traffic load by 50% (300 users), the user outage triples. Such a trend is explained by the fact that most of the traffic load is served by a restricted number of cells, which are not able to provide users with a sufficient data rate. As the resource sharing algorithm firstly aims at guaranteeing the minimum data rate to *all* connected users, highly loaded cells rapidly run out of capacity, and user outage dramatically increases.

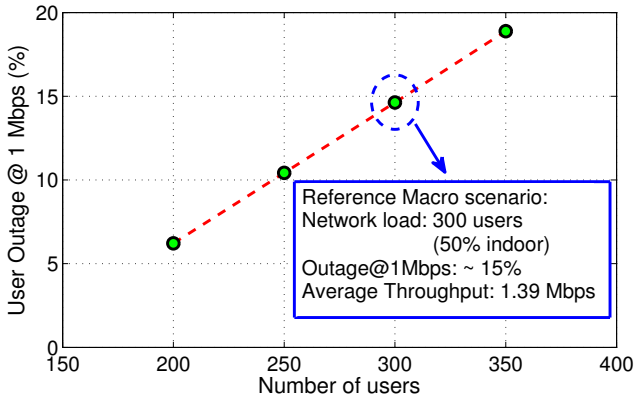

Fig. 5.7: User outage at 1 Mbps over different values of offered network load for a macro-only deployment (20 MHz at 2.6 GHz). The reference network load for evaluating small cell deployment is equal to 300 users with an initial outage value of 15%.

The reference traffic load for evaluating the performance of small cell deployment is set at 300 users, with a minimum data rate of 1 Mbps and a full buffer traffic model. The average number of served users per sector is around 10, with a peak of 30 users in the most loaded cell area. The initial outage level is then at around 15%

with a delivered average throughput of 1.4 Mbps. Further insights as to network load and user outage spatial maps are provided in Fig. 5.8, and it can clearly be seen how the highest cell outage levels stem from the most loaded cells. The most critical area for network performance is located in the south-west part of the map due to high traffic demand: it can be found that the two cells providing the highest outage are responsible for one third of the overall outage (approximately 5%), whereas the remaining outage is concentrated in 6 cells. The distribution of outage users across the macro cells points out that small cell deployment is to be prioritized in a limited number of macro cell areas. The main idea is to offload users from highly loaded macro cells towards small cells, which guarantee a higher spatial reuse of radio resources and a lower number of users per cell to be served. Obviously, backhaul capacity plays an important role with respect to exploiting the potential of relays, especially when part of macro radio resources are sacrificed to wireless backhaul.

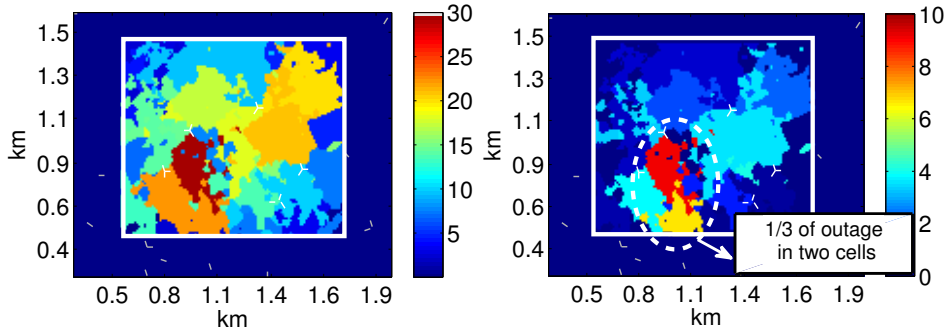

(a) Number of users

(b) Outage Users

Fig. 5.8: Average number of served user per cell (left) and outage user per cell (right) displayed over the cell coverage area.

5.3.2 In-Band Relay Deployment

Given an initial outage of 15%, in-band relay base stations are deployed to complement the existing macro layer and decrease the user outage. As previously explained, a coverage-oriented deployment of relays is pursued, meaning that it is targeted at improving coverage in those macro cell areas affected by high outage levels. The traffic assumptions also imply that users are uniformly distributed throughout each cell area of the reference macro deployment without any localized hotspot. Hence, the coverage-driven relay deployment prioritizes the positions at the cell edge areas, where signal quality is impaired by interference, as well as ensuring excellent backhaul connection. In this subsection relay transmission power is fixed at 30 dBm.

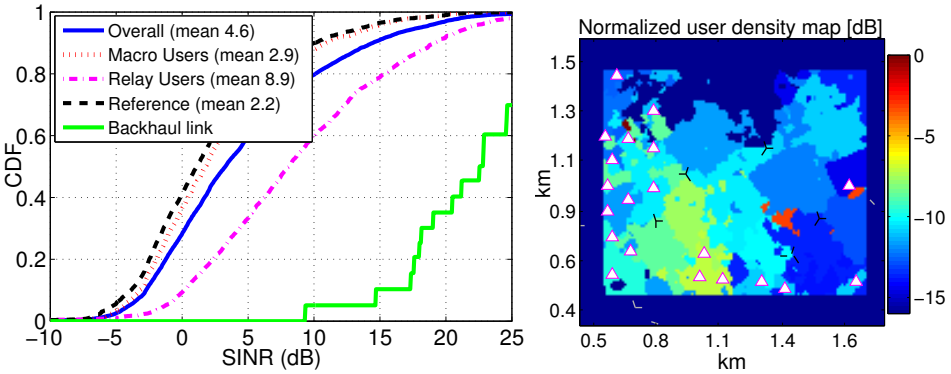

(a) SINR distributions

(b) In-band relay deployment snapshot

Fig. 5.9: Wideband SINR distributions (left) for macro reference scenario and in-band relay deployment (20 relays), showing direct, relay and overall user SINR together with backhaul link geometry. Relay positions in the network are shown on the right

Fig. 5.9(a) illustrates the SINR distributions for both macro-only and in-band relay deployment at 2.6 GHz with an illustrative number of 20 relays. The overall user SINR is improved by 2.4 dB as compared to the macro reference scenario, and this is mainly due to the fact that relay users experience higher SINR values than the macro users. Owing to the deployment algorithm settings, relays are mainly deployed in areas of the network where high interference or low received signal strength limits the downlink performance (refer to the SINR spatial map in Fig. 5.3(a)). In addition, the imposed minimum ISD with respect to other relays or existing macro sites guarantees sufficient isolation at 2.6 GHz amongst the deployed base stations, and the experienced SINR does not deteriorate.

The quality of the backhaul link is significantly better than the one experienced by macro and relay users, with a minimum value of around 9 dB. Backhaul geometry outperforms the one experienced in the suburban case study for two main reasons: the use of a directional antenna with a 12 dBi gain mitigates the impact of interference at the relay side and in addition to this, the deployment metric gives higher priority to those locations experiencing excellent SINR conditions on the backhaul. Though the macro cells affected by the highest outage are located in the southern area of the network, relay deployment cannot only be concentrated in those cells, as shown in Fig. 5.9(b). In the high-outage areas of the network, low-SINR is experienced in small spots, and the denser macro deployment limits, in this region of the network, the set of candidate locations experiencing high backhaul signal quality. For this reason, relay deployment cannot effectively offload part of the traffic associated with cells carrying most outage users.

In Fig. 5.10, user outage performance, average user throughput gains over the

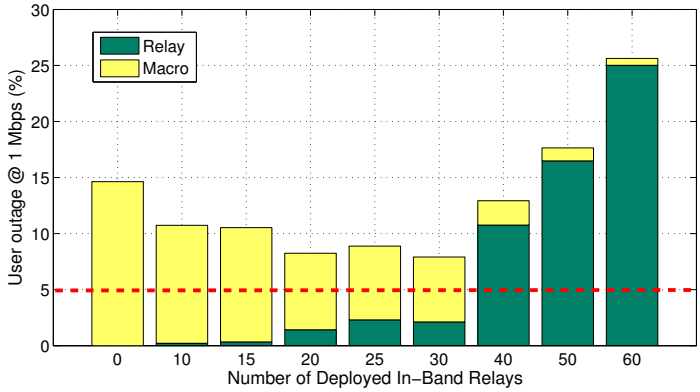

(a) User Outage

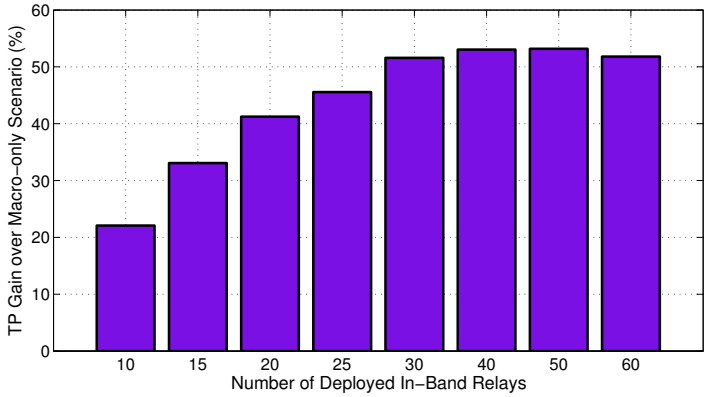

(b) User Throughput

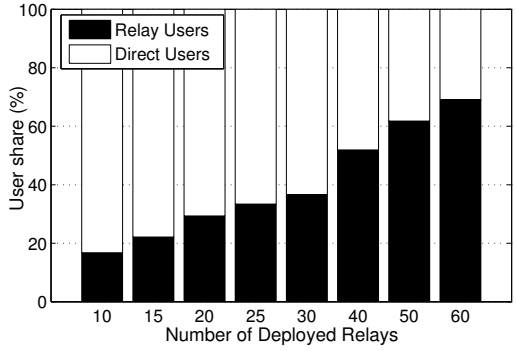

(c) Relay user share

Fig. 5.10: User Outage, Average Throughput (TP) and relay/macro user fraction over different numbers of in-band deployed relays. The outage is shown by splitting the contribution from macro and relay layers to the overall outage level. Relay transmission power level is set at 30 dBm.

macro-only reference scenario, and relay-to-macro user split are presented with reference to different numbers of deployed relays. The overall user outage is shown by considering the split between users connected to relays and those connected to macro cells. The outage level decreases with increasing number of relays before leveling out at around 8 % between 20 and 30 relays. It can be observed that below 30 relays, the majority of outage users belong to the macro layer, but when more than 30 relays are deployed, the overall user outage is basically caused by relays and increases steeply. With regard to average throughput, relays yield capacity gains as compared to the macro-only scenario. The throughput gains increase until 30 relays are deployed in the network, and it saturates at around 50%. Throughput enhancement is a direct consequence of improved user SINR whereas its saturation is due to the backhaul-limited relay transmission. The wireless backhaul fails to deliver the ideal aggregate throughput experienced on the relay access link, especially when the number of relays per donor increases.

By raising the relay density in the network, more users connect to relay nodes – 40 relays offload half of the users from the macro layer – but on the other hand, macro donor cell resources are to be shared amongst a higher number of connected relays. As a consequence, the amount of backhaul resources allocated to each single relay is lower and the relay transmission is strongly backhaul-limited. A highly dense relay deployment has a two-fold drawback: first, excellent backhaul SINR, e.g. larger than 10 dB, cannot be guaranteed to all relays due to a limited set of optimal candidate positions for backhaul connection; second, the assigned relay ISD requirements for mitigating inter-relay interference do not allow relays to be solely deployed in the most critical areas for user outage, and for this reason, they spread over other regions of the network where the two-hop connection does not significantly enhance network performance.

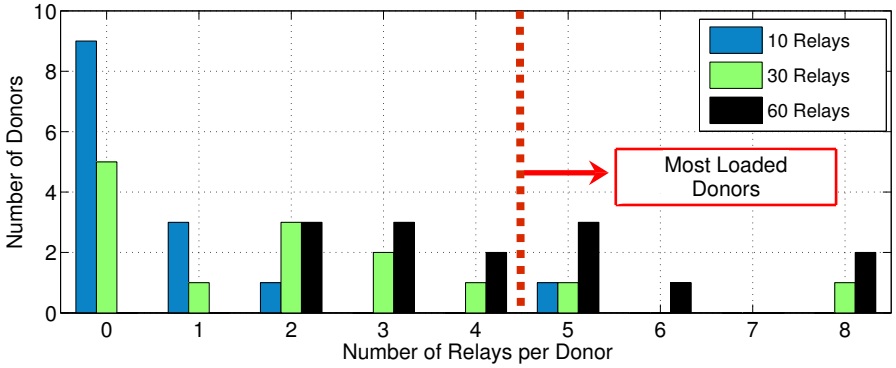

Fig. 5.11: Number of donor cells over number of connected relays per Donor for different number of relays (10,30,60) deployed in the network

Fig. 5.11 gives further insights as to how relays are distributed amongst the differ-

ent macro donor cells. Given a predefined set of potential donors – 14 donor cells obtained after deploying 60 relays –, the graph shows the number of donors serving the number of relays specified on the horizontal axis. With 10 relays deployed in the network, half of the relays are connected to one donor cell ensuring good relay backhaul geometry in spite of poor coverage performance for macro users; however, most of the potential donors are not utilized to establish the backhaul connection, i.e. 0 relays connected on the x-axis. As the number of relays is increased to 30 (more than 3 relays per active donor), they start being spread more uniformly all over the network, but a pair of donor cells turns out to be the most critical in terms of backhaul load, reaching a maximum of 8 relays to be fed. When the network is loaded with 60 relays (larger than 4 relays/donor), the number of donor cells loaded with more than 5 relays relays is considerably increased, and this leads to worse performance in terms of overall user outage.

In conclusion, in-band relays transmitting at 30 dBm are not capable of reducing the outage level below the 5%-target, and outage performance becomes worse as the relay density increases. The main limitations to relay performance are to be found in backhaul capacity bottleneck and also the traffic characteristics of the investigated scenario. In fact, high traffic load on a limited number of macro cells rather than lack of signal coverage is responsible for the achieved user outage in the reference scenario, and sacrificing macro capacity for wireless backhaul does not help to significantly decrease the number of unsatisfied users.

5.3.3 Co-Channel Micro Deployment

The same analysis carried out for relay nodes is repeated for co-channel micro deployment with a 30 dBm micro transmission power. The main target is to understand the performance gap between micro and relay performance in terms of both outage and capacity when the same of number of small cells is deployed. In order to maximize micro performance, the deployment algorithm setting prioritizes high outage and high traffic cell areas as well as relaxing the backhaul link constraint, as can be seen in Table 5.2.

Similarly to the previous subsection, Fig. 5.12 illustrates user outage and average throughput over an increasing number of deployed co-channel micros, and such trends are compared with the corresponding KPIs related to in-band relay deployment. It can be observed that micro base stations exhibit lower user outage values as compared to relay deployment, and user outage goes down when increasing the number of micros. Outage users are only connected to macro cells because, differently from the relay case, the micro access link throughput is not limited by the backhaul connection, and the micro user load is lower than the macro. This means that a limited number of users share micro spectrum resources, with an average micro user SINR that exceeds 10 dB (relay access and micro propagation

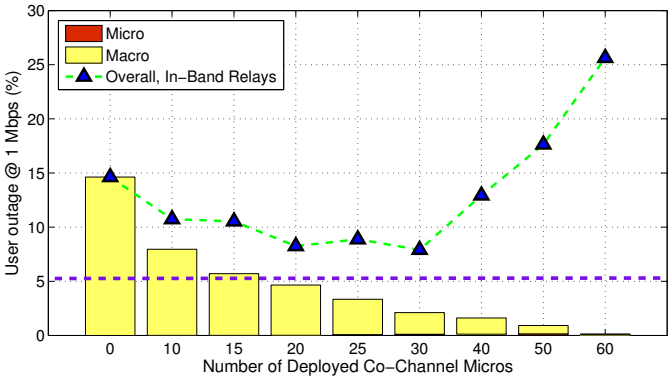

(a) User Outage

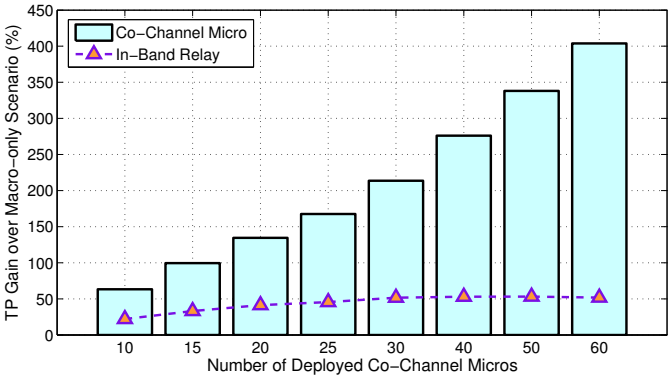

(b) User Throughput

Fig. 5.12: User Outage and Average Throughput (TP) over different numbers of co-channel deployed micros. The former is shown by splitting the contribution from macro and micro layers to the overall outage level. The relay performance obtained with the same number of relays as micros is shown with the dashed line.

models are the same). Moreover, the deployment of micros is also more flexible as there is no need for ensuring extremely good wireless backhaul connections. As a result, a denser small cell deployment can be pursued in highly loaded macro cell areas serving most of the outage users. By means of this, micro base stations are able to efficiently offload the most loaded macro cells, hence significantly enhancing the overall network performance. In principle, 20 micros are sufficient to bring down the outage level below the 5%-target and this goal cannot be achieved with a pure relay deployment. Similarly to outage performance, the capacity gains are one order of magnitude higher than those achieved with relays. The capacity gains increase linearly with the number of deployed micros until reaching a gain of 400% (5 times) over the macro-only scenario, with 60 micro base stations (4 Mi-

cros/cell on average). Moreover, only 10 micros are needed to equal the capacity gain (50%) obtained when deploying 30 relays.

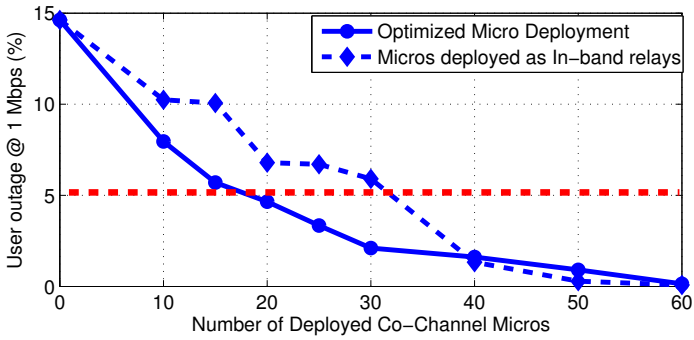

Fig. 5.13: Outage comparison between optimized micro deployment and the case where micros are deployed in the same positions of relays. The outage levels are evaluated over different numbers of deployed co-channel micros.

If micros are deployed in the same positions as relays, the network outage performance becomes worse as the potential of deploying micros is not fully exploited. Fig. 5.13 depicts the network outage trends when considering the previously shown optimized micro deployment and the case in which micros are deployed in the locations selected for relays. It can be seen that 10 additional micros are needed to hit the outage target when deployed as relays. When the number of small cells is below 30, the relay locations are chosen also on the basis of backhaul link geometry, but in this fashion they cannot solely be gathered in the high-traffic areas due to high backhaul interference levels. The outage trend with micros deployed as relays can also be seen as an upper bound for relay deployment performance, considering that the relay end-to-end connection is not backhaul limited. In order to narrow the performance gap with ideal wireless backhaul, significant improvements in backhaul transmission spectral efficiency are necessary or alternatively, large bandwidth spectrum is to be dedicated to backhaul transmission.

5.3.4 Sensitivity to Small Cell Transmission Power

This subsection addresses a network performance sensitivity study with respect to small cell transmission power for both in-band relay and co-channel micro deployment, without modifying the deployment algorithm settings. By raising the transmission power level from 30 dBm to 37 dBm, the relay or micro cell size becomes larger and more users connect to the small cells. As can be seen in Table 5.4, when relay transmission power is increased, relay user improvement is in the order of 6 percentage points. The average relay cell size does not considerably

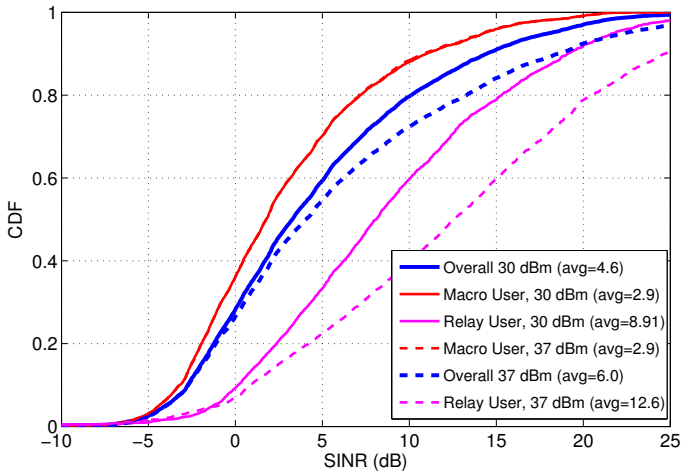

Fig. 5.14: SINR distributions for 30 in-band relays when applying two different transmission power levels (30 and 37 dBm).

Table 5.4: Share of users connected to relay layer.

Relay Number	10	15	20	25	30	40	50	60
Relay user share (30 dBm)	17%	22%	29%	33%	37%	52%	62%	69%
Relay user share (37 dBm)	19%	25%	33%	37%	41%	58%	68%	76%

enlarge due to strong macro layer signal strength and NLOS conditions experienced by relay/micro users at the cell edge. The same conclusions can be drawn from the user SINR distributions extracted for both transmission power levels in Fig. 5.14. Considering 30 in-band relays, SINR gains are evident only for relay users at cell center as in those locations users are likely to be in LOS with respect to the relay node. Instead, the SINR of the worst users is not affected by increased transmission power.

Fig. 5.15 illustrates outage and average throughput performance for relay and micro deployment at both 30 and 37 dBm as transmission power levels. Overall, it can be inferred that the user outage performance essentially maintains the same level in both relay and micro deployment scenarios. The reason is that the number of users offloaded to small cells does not substantially increase with higher transmission power, and in addition to this, the SINR of cell-edge users, who are most likely in outage, is not improved. As for relays, user outage becomes worse with increased transmission power as the slight increase in relay user share is not sustained by backhaul link capacity; as a result, the additional relay users are deemed to be in outage.

As regards user throughput, capacity improvements can be attained by increasing the small cell power due to better user geometry experienced in proximity of the small cells. When relays are deployed, the backhaul-limited nature of the connection throttles the capacity gains, which are mainly due to those macro cells having a small portion of users covered by the enlarged relay cell footprint. Owing to the unlimited backhaul capability, micro cell performance fully benefits from the increased transmission power, as the improved average micro user SINR yields higher data rates. With more than 30 deployed micros and micro user share in the order of 40%, capacity gains over the macro reference scenario improve by 50-100 percentage points as compared to setting the power level at 30 dBm.

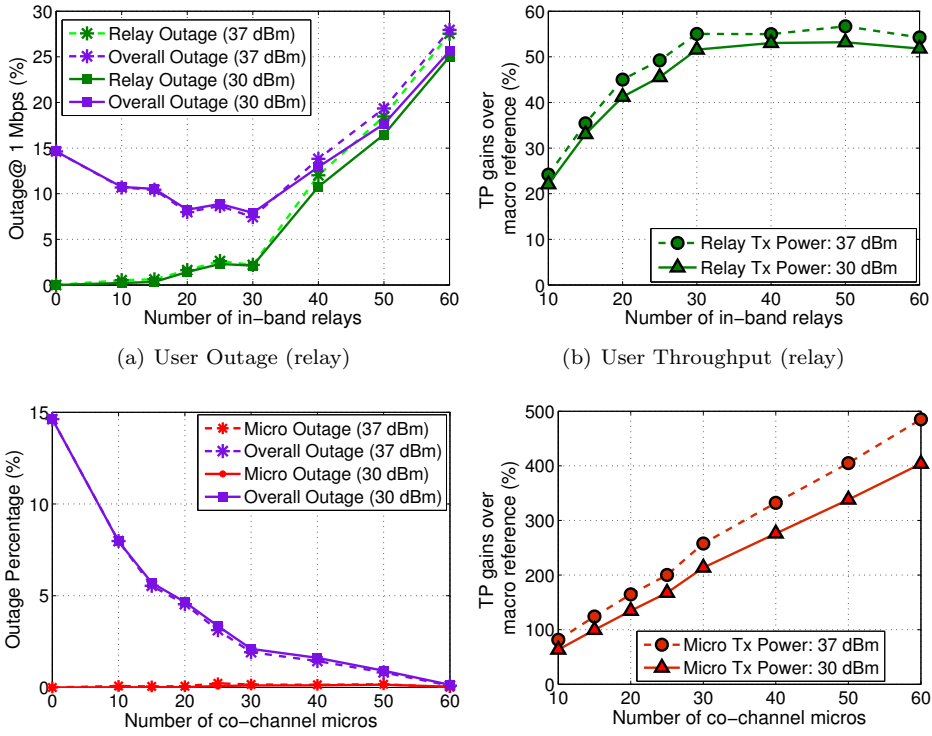

(a) User Outage (relay)

(b) User Throughput (relay)

(c) User Outage (micro)

(d) User Throughput (micro)

Fig. 5.15: User Outage and Average Throughput (TP) for both relay and micro deployment, showing the KPIs at both 30 and 37 dBm as transmission power. Overall user outage is presented together with the contribution of relay, or micro, layer.

5.4 Relay Deployment Potential Improvements

In this section two possible alternatives to enhance the backhaul link capacity are investigated. The former is obtained by adding 20 MHz of TDD spectrum at the macro layer, which can be used to feed the out-band relay wireless backhaul; the latter deals with the assumption that at the relay side the main interferer is suppressed with advanced antenna configurations leading to improved backhaul signal quality.

5.4.1 Additional Spectrum for Backhaul: Out-Band Relays

Adding more spectrum at the macro layer is generally the most direct way to enhance capacity. The use of additional TDD spectrum located in the 2.6 GHz band – this means that propagation conditions are the same as in the FDD band – is investigated according to different configurations. The first one is about upgrading all the existing macro cells to the second carrier and utilizing such spectrum for backhaul link transmission only, without serving regular users. As in the previous suburban case study, a full-duplex out-band relaying is assumed, meaning that all the spectrum is used for downlink transmission on the access link. The relay positions are the ones selected in the in-band relay scenario.

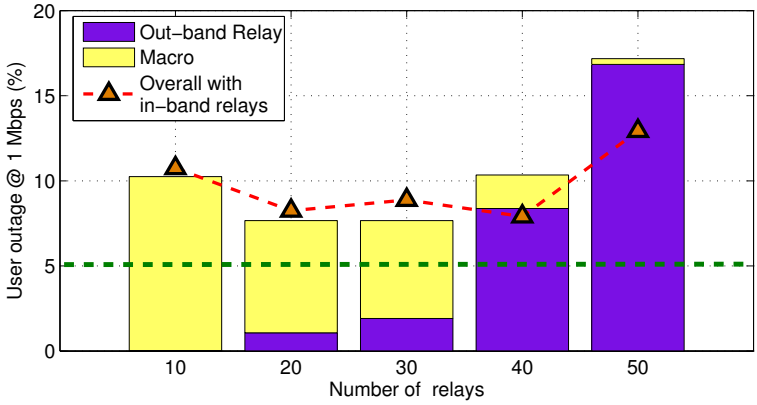

Fig. 5.16: User Outage for out-band relay deployment, showing the split between macro and relay outage. Added TDD spectrum is entirely dedicated to backhaul transmission; overall outage obtained with in-band relays is also shown for comparison.

Assuming that interference originates from all the macro cells, including the ones not serving relays, the perceived backhaul SINR is the same as in the in-band relaying case, i.e. a worst-case scenario. From Fig. 5.16 it can be concluded that the use of a dedicated spectrum does not yield significant improvements in user

outage when compared to in-band relaying: being the TDD spectrum available only for half the time, the 20 MHz bandwidth is not sufficient to considerably improve backhaul data rates, especially for those donor cells serving more than 5 relays. This behavior is even more evident when the number of relays is increased and more users connect to relay base stations. Differently from in-band relays, the out-band configuration does not allow relays to further extend the backhaul link ratio at the cost of macro and access link resources due to the fixed dedicated spectrum. In this fashion, relay backhaul capacity cannot be further improved, and the number of relay users in outage increase more steeply than with in-band relays.

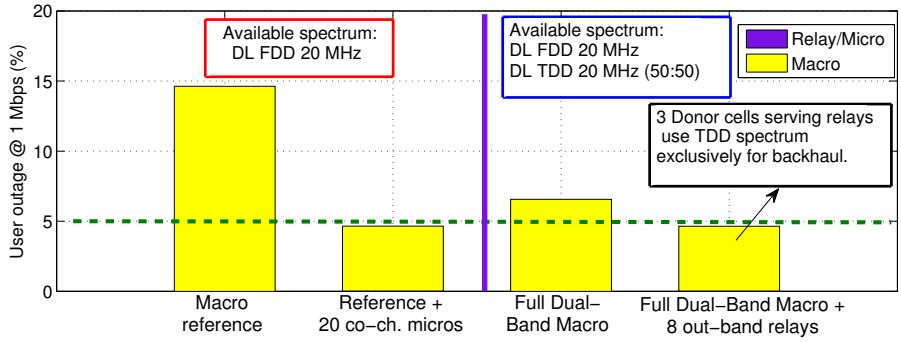

Fig. 5.17: Outage performance comparison between single band and dual-band macro layer scenarios together with small cell deployment. In the dual-band scenario, TDD spectrum is normally used to serve macro users, but in case of donor cell, the additional carrier is entirely dedicated to feed the relay backhaul. With 8 out-band relays, only 3 donor cells are involved, whereas the remaining cells serve macro users on TDD spectrum.

However, based on the assumption that user terminals can support both TDD and FDD operation mode, the additional carrier can be exploited to also serve macro users. Fig. 5.17 shows user outage performance for dual-band macro scenarios, with and without relays, in comparison with the reference single-band macro scenario and micro deployment with 20 co-channel micro base stations. If all macro cells are upgraded to second carrier, the user outage declines from 15% (reference scenario) to 6.6% without deploying small cells, which gives better performance than any of the investigated in-band relay configurations. Most of the outage still originates from the high-traffic areas where the serving macro cells run out of capacity; however, as the additional capacity is uniformly distributed all over the network, user outage reduces in all the serving macro cells and the overall performance draws near the 5%-outage target. In order to further decrease user outage, 8 out-band relays are to be deployed along with dual-band macros, and the overall outage is approximately 5%. This performance result is obtained by utilizing the TDD spectrum not only for relay backhaul but also macro users: this compromise is achieved by allocating the TDD spectrum resource exclusively to the backhaul link only if the macro cell has connected relays, i.e. a donor, oth-

erwise such resources are dedicated to macro users. With 8 deployed relays, the wireless backhaul is provided by 3 donor cells transmitting on the TDD band.

5.4.2 Potential of Interference cancellation

Another solution to enhance backhaul data rates is given by the suppression of the interference signals on the downlink at the relay side. To suppress the dominant interferer, advanced Interference Rejection Combining (IRC) receivers are needed at the relay receiver, based on multi-antenna configurations [139, 140]. The main idea behind the receiver design is to optimally combine the received signals at the terminal antenna ports [141, 142]. Implementation and feasibility of IRC receivers are outside the scope of this dissertation, but the main target is to evaluate the potential benefit of having the main interferer on the backhaul link suppressed. Therefore, the effect of using advanced receiver on perceived backhaul SINR is ideally modeled, for the $i-th$ relay, as follows:

$$SINR^{i}_{BH,enhanced} = \frac{P_{donor,i}}{(\sum\limits_{s\in\mathcal{S}_k} I_s) - I_{max} + N} \quad with\ I_{max} = \max_{s\in\mathcal{S}_k}\{I_s\} \tag{5.2}$$

where $P_{donor,i}$ is the received power from the serving donor, I_s is received interference power from the $s-th$ interferer, and I_{max} the received power from the dominant interferer, which is the sole one to be subtracted from the overall received interference power. By considering the same locations for 30 in-band relays, Fig. 5.18 shows the improvement in backhaul SINR shifting from the ordinary receiver to the enhanced one suppressing the strongest interferer. Depending on the power level difference between main interferers and the weaker ones, the SINR gains range from 3 dB to up until 7 dB giving a corresponding wideband throughput improvement in the order of 25-80%.

Fig. 5.19 shows the network KPIs for ordinary and enhanced backhaul over different numbers of deployed in-band relays. Relays are deployed as in the previous cases (see Table 5.2), and the transmission power is set at 30 dBm. The increased data rate experienced on the backhaul link enables the relay nodes to enhance the performance of relay users and the number of relay users in outage declines. Yet, the outage hits its minimum at 7% with 30 relays, 1 percent point less than the corresponding performance with ordinary backhaul. The reason is that most relay cells cannot be extensively deployed in high-outage cells due to the backhaul link quality constraint. As shown in Appendix B.2, the backhaul SINR considerably decreases if relay cells tend to be deployed as micros, and the enhanced backhaul would not suffice to reduce the user outage as effectively as micro cells.

When increasing the relay density, outage improvements with reference to the

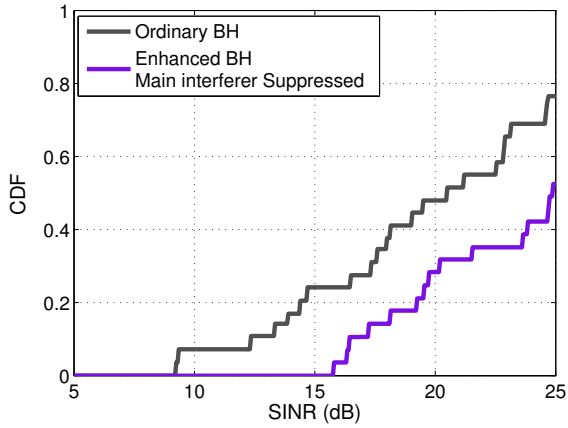

Fig. 5.18: Backhaul SINR distributions for reference and enhanced set-up (30 in-band relays). The latter is obtained by suppressing the main interferer, thus enhancing the backhaul signal quality.

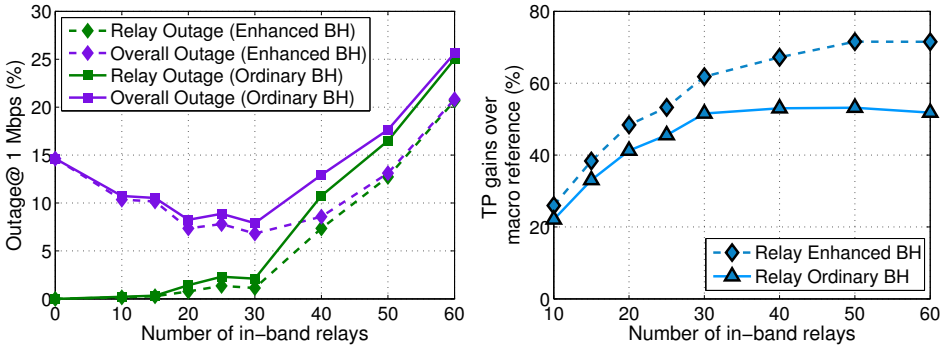

(a) User Outage (b) User Throughput

Fig. 5.19: User Outage and Average Throughput (TP) performance for ordinary and enhanced backhaul transmission over number of in-band relays. Overall user outage is presented together with the contribution of the relay layer.

regular backhaul configuration become more marked showing a gain of 5 percentage points over the ordinary backhaul scenario. In this case more relays share the backhaul link, and therefore the backhaul capacity improvement makes it possible to have a lower number of relay users in outage, albeit not sufficient to hit the outage target. Another aftermath is that average user throughput improves in a similar way thanks to higher data rates experienced by relay users. By deploying 20 relays with enhanced backhaul, the same throughput performance as 30 relays with ordinary backhaul is achieved. After the user throughput starts saturating,

the gain over the macro reference scenario reaches 60%, improving by 20 percent points as compared to the ordinary backhaul case.

5.5 Cost Analysis for Iso-Outage Scenarios

Based on the approach followed in the previous suburban case study, the cost analysis is carried out for iso-performance deployment options delivering an outage level within the interval 5% +/– 0.5%. The viability study is focused on the comparison between relay and micro deployment. According to previously presented performance results, two deployment solutions are selected as iso-outage scenarios: the reference single band macro scenario along with 20 co-channel micros, and a full dual-band macro upgrade together with 8 out-band relays. For each of the deployment solutions, two different cost assumptions are considered with regard to the small cell cost structure. Relay and micro cells can be regarded as "high-cost" or "low-cost", and both cases are considered to highlight the TCO sensitivity to different deployment assumptions. The selected scenarios are outlined and labeled in Table 5.5 together with outage and average throughput performance indicators.

Table 5.5: Performance results related to the iso-outage scenarios.

Nr.	Deployment Options	Small cell cost	User outage	Average Throughput	Total Spectrum
Sc. 1	17 single-band macro sites **20 co-channel micros**	low cost	4.7 %	3.3 Mbps	20 MHz FDD
Sc. 2	17 single-band macro sites **20 co-channel micros**	high cost	4.7 %	3.3 Mbps	20 MHz FDD
Sc. 3	17 dual-band macro sites **8 out-band relays**	low cost	4.6 %	2.4 Mbps	40 MHz FDD/TDD
Sc. 4	17 dual-band macro sites **8 out-band relays**	high cost	4.6 %	2.4 Mbps	40 MHz FDD/TDD

Also in this case study, the overall TCO is calculated by considering a time span of 4 years for OPEX, and the employed cost figures are presented in Table 3.1 in Section 3.7. Obviously, in each of the analyzed scenarios, the total cost comprises the expenses needed to set up the reference scenario, which consists in upgrading all the current 3G macro sites to LTE. Besides the 5 macro sites located inside the network area, the surrounding sites are considered when calculating the reference scenario TCO. The difference between high and low-cost relays lies in the assumed planning and optimization costs. With respect to relays, a micro cell is between 2 and 5 times more expensive, based on different site acquisition and backhaul assumptions. In particular, the high-cost version includes a more expensive installation of the backhaul connection (e.g. trenching fiber) and higher micro site rental price. This adds up to an overall cost that is close to the expenditure needed

to deploy an LTE additional carrier.

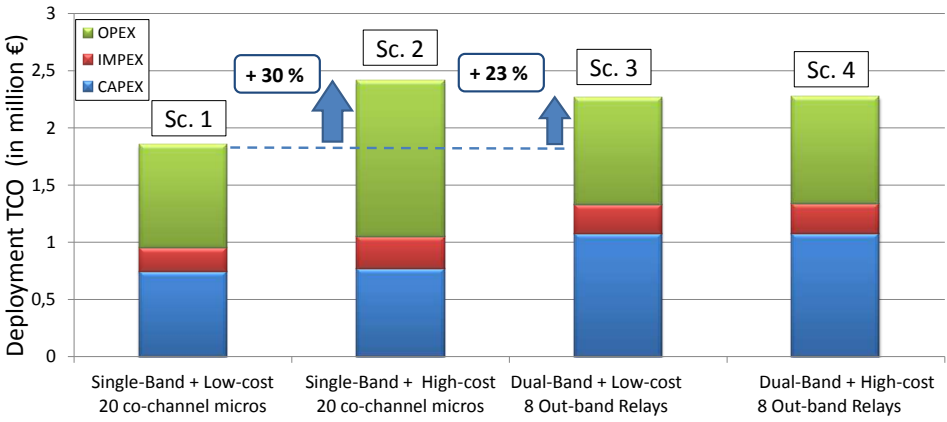

Fig. 5.20: TCO associated with the selected iso-outage scenarios involving micro and relay deployment for different cost assumptions. Running costs are taken into account for a time span of 4 years.

The TCO results associated with the 4 investigated scenarios are illustrated in Fig. 5.20, showing the split between the different cost components. It can be seen that the low-cost micro scenario turns out to be the least expensive, with a 30% saving as compared to deploying high cost micros. In the high-cost micro scenario, network costs are dominated by both IMPEX and OPEX due to backhaul and site rental expenses for micro base stations – the cost of each high-cost macro is 2.7 times higher than low cost. This leads to the highest TCO amongst all the investigated solutions. The cost of out-band relays along with a dual band overlay macro layer is in between the two micro scenarios, with a cost increase of around 23% with reference to the low-cost micro case. The difference between high-cost and low-cost relay deployment scenarios is not significant as the cost of deploying 8 relays is overcome by all the expense needed to upgrade the full macro network to the second TDD carrier. It can also be inferred that the break-even point in terms of network costs between relay and micro deployment can be found between the assumed micro cost structures. In general, backhaul installation and related running costs may vary considerably, depending on a lot of parameters, such as the investigated country, outdoor site location, the available backhaul medium (leased or self-built). In this study, micro cells are surely profitable if the sum of OPEX and IMPEX is equal or lower than the midpoint between high-cost and low-cost micros.

Overall, micro deployment is a viable solution with respect to relay deployment as long as the site and backhaul-related costs are contained. In addition to this, it is also worth considering the average throughput performance, which can fur-

ther differentiate micro and relay scenarios. The iso-performance scenarios are, as mentioned earlier, built on the same outage requirement, but 20 co-channel micros are able to deliver an average user throughput of 3.3 Mbps, which is 38% higher than in the relay scenario employing one additional carrier. As shown in subsection 5.3.3, network capacity gains of up to 5 times over the macro reference can be achieved with denser micro deployment. Instead, the relay throughput performance is generally one order of magnitude lower than in the micros, and it tends to saturate at higher densities. From a deployment strategy perspective, co-channel deployment of micro base stations certainly outperform relays in overall system spectral efficiency as enhanced throughput performance can be achieved, at the same outage level, with less available spectrum. This is of fundamental importance in the long-term when traffic demand and minimum required data rates are predicted to increase from the assumed levels.

5.6 Summary and Conclusions from the Metropolitan Scenario

This chapter has investigated and compared the deployment of relay and micro base stations in terms of downlink radio performance and network cost. A realistic metropolitan area of 1 km^2 is available for the study along with a dense deployment of 5 LTE sites, co-located with the existing 3G ones. For a minimum data rate of 1 Mbps and 300 simultaneously active users, the reference macro deployment transmitting at 2.6 GHz over a 20 MHz FDD band achieves an initial outage level of 15%. Outage users are mainly located in the high traffic areas which force the serving macro cells to run out of capacity when delivering the minimum data rate. To reduce the outage level towards the the 5%-target, relays or micros are introduced, and it can be concluded that:

- The results indicate that the use of in-band relays can at most halve the user outage, reducing it to 8 % with 20 Relays (1.3 relays/sector). Although good backhaul link quality can be achieved through accurate positioning of relays, deploying a larger number of relays does not have a beneficial effect on user outage due to increased load on the backhaul link. Also, the capacity gain saturates at around 50% compared to the macro-only case. It is noted that the main cause for having outage users is the high traffic load within few macro cells rather than having coverage holes.
- Increasing the relay transmission power or suppressing the dominant interference signal on the backhaul link do not bring the outage level below the required threshold. Interference cancellation gives benefits mostly when donors are loaded with multiple relays but the backhaul capacity improvement is not sufficient to abate relay user outage.

- To hit the outage target, an additional TDD carrier is to be deployed at the macro layer and used for both backhaul and ordinary user transmission. In this fashion, a full dual-band macro upgrade with 8 out-band relays (served by 3 different donors) are able to decrease user outage to 5%.
- Under the assumption of no backhaul constraints, micro cells sharing the same band with the macro can significantly reduce user outage and guarantee substantial capacity gains of up to 5 times with 4 micros/sector. 20 co-channel micros (1.3 micros/sector) are needed to reach the outage target, and better average performance can be obtained by increasing the micro transmission power due to improved signal quality and increased number of offloaded users to the micro layer.
- Considering two different cost structures for both micros and relays, low-cost micro deployment is the least expensive solution with respect to out-band relays operated on a 2-carrier macro deployment. Being the micro cost driven by backhaul, the TCO trends are extremely sensitive to the backhaul cost assumptions, but the midpoint between low-cost and high-cost micros is sufficient to render micro deployment financially more appealing than relay deployment together with enhanced average throughput performance.

The bottom line of the metropolitan case study is that micro deployment seems to be a more viable solution than relays, especially from the performance side. Relays can be helpful to solve specific and localized coverage issues but their capacity benefits saturates from a certain relay density onwards. To fully assess the viability of micro deployment, it would be interesting to evaluate network performance under more stringent throughput requirements and increased traffic demand. In the long-term, one carrier does not suffice to deliver the expected throughput and extremely dense co-channel micro deployment may not help in reducing user outage to the expected levels. In this situation acquiring additional spectrum and smart inter-tier coordination to avoid interference and optimize user offload are the key solutions to meet the performance targets. In addition to this, indoor low-power small cells are expected to give an additional boost to user experience by increasing network capacity. The joint deployment of outdoor and indoor small cells is addressed in the next part of this dissertation.

Part II

Analysis of Indoor Deployment for a Metropolitan Scenario

Chapter 6

Building the Indoor Deployment Framework: Models, Assumptions and Reference Scenario

6.1 Introduction

The second part of this dissertation focuses on the potential of deploying low power indoor base stations, i.e. femto cells, to meet the increasing demand in mobile broadband services. Along with outdoor small cells, the deployment of femto cells is a key solution as to offloading big portions of network mobile traffic through fixed-line backhaul owned by the user or belonging to the enterprise building. In order to properly assess the performance of indoor area deployment, more advanced models related to indoor propagation, building layout and indoor traffic distribution are required. The deployment strategy for indoor nodes can be optimized with regard to increasing the amount of data offloaded towards indoor cells in high-traffic areas. Similarly to the deployment solutions previously addressed, radio performance and cost effectiveness of femto cells is evaluated by means of a case study, which is built upon a realistic dense urban scenario with intensive mobile data consumption.

Firstly, this chapter deals with the description of the large-scale macro urban scenario, which is used as reference for the deployment study, and it basically serves as a complement to the scenario modeling of Chapter 3. In particular, Section 6.2 describes the macro reference deployment layout, the new propagation models utilized for both outdoor and indoor cells, and the enhanced spatial traffic modeling that takes into account the indoor-to-outdoor traffic split and multi-floor user locations. Then, novel deployment strategies for small cells (micros and femtos) are presented in Section 6.3. As for radio resource sharing and physical layer considerations, the same models introduced in Chapter 3 are considered, and they are, for this reason, omitted in this chapter.

Lastly, the performance result for the reference macro deployment is presented according to different traffic growth assumptions. In addition to this, a macro upgrade to second carrier together with underlaid co-channel micro deployment is evaluated on the large scale deployment scenario so as to fulfill the outage requirement (see Section 6.4). This preliminary study is performed to identify, as discussed in Section 6.5, the hot-zone area that serves as deployment scenario for femto deployment in Chapter 7, where the viability of deploying femto cells in place of or together with outdoor micro cells is investigated.

6.2 The Reference Scenario

This section deals with the description of the selected metropolitan scenario. The reference macro deployment and available building location are presented together with the traffic assumptions that are considered when evaluating the network radio performance. Details about propagation and indoor user location modeling are also provided.

6.2.1 Large-Scale Metropolitan Scenario

By following the same approach as in the previous case studies, the reference LTE macro cellular deployment is obtained from an existing 3G operating network located in a major European capital city. Each site is assumed to be upgraded to LTE, keeping the same downtilt and bearing angles for each antenna sector. As can be seen from Fig. 6.1, the investigated area size is in the order of 4x3 km, but it does not have a regular shape. In this study the borders of the investigated areas are tailored to the coverage areas of the macro sites that are located within the investigated area. By estimating the macro cell coverage at 800 MHz, network users are served only by the macro cells lying within the map "mask", whereas the outer ones contribute as interferers to the overall network performance. The total number of macro sectors is 233 whereas 118 are located inside the investigated

area, with an average ISD of 340 m. The main simulation parameters for the overall scenario are shown in Table 6.1.

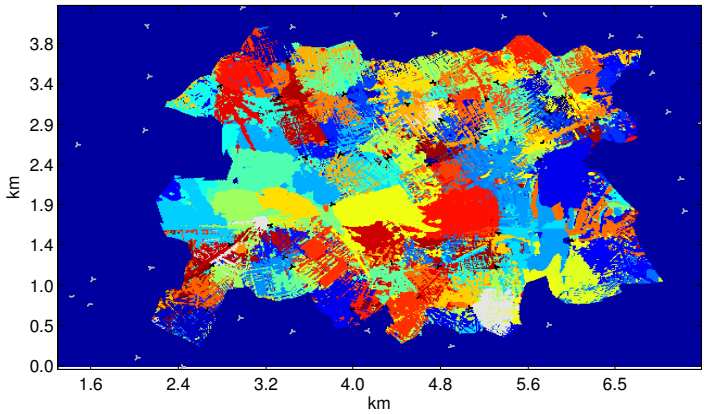

Fig. 6.1: Best server map for the macro reference scenario where a different pixel color is associated with the specific macro cell which covers that pixel. The shape of the investigated area is obtained by estimating macro cell coverage at 2.6 GHz.

Table 6.1: Main Scenario Assumptions and Parameters

Parameter	**Value**
LTE System	Downlink FDD LTE, 2x2 MIMO
Carrier Frequencies	2.6 GHz/20 MHz, 800 MHz/10 MHz
Macro eNodeB Power	46 dBm per carrier
Network Layout	233 sectors in total 118 sectors covering the investigated area
Antenna Pattern	Realistic Antenna Pattern network input data: tilting angles, antenna gains, cable losses
3D Building Map	5661 buildings Overall Indoor area percentage: 34% Floor height: 3.1 m Average Floor number: 5 Average 2D building area: 760 m^2

To better model indoor propagation and indoor traffic distributions, a detailed 3D building map is employed with a resolution of 10 m x 10 m. Building location information is based on height and the coordinates of the building block edges, which renders it possible to identify the outdoor areas surrounded by building blocks, such as courtyards or streets. More than 5000 buildings can be identified in the area, and the average covered area for each building is in the order of 700 m^2. In total, 34% of the area is covered by buildings, and the average number of floors per building is around 5. The latter has been obtained by assuming a fixed floor height of 3.1 m for each building. The number of floors are needed when

distributing the users across multiple floors, applying floor penetration and floor height propagation gains, as explained in the next subsection.

6.2.2 Modeling Outdoor and Indoor propagation

Two different propagation models are utilized with regard to the sort of transmitting base stations. These can be divided into outdoor and indoor cells. In this case study, macro and micro cells are deployed outdoor – relays are excluded – whereas femto base stations are deployed only in indoor areas. For the outdoor cells, a ray-tracing tool is used to estimate the propagation losses together with indoor penetration corrections, whilst femto path loss is calculated by means of a statistical model described below.

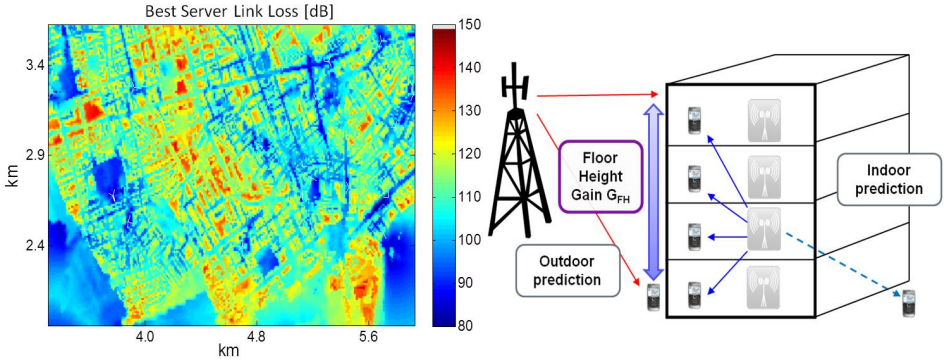

Fig. 6.2: Spatial map (left) showing the macro best server link loss at 2.6 GHz at a height of 1.5 m (ground floor). When users are located on upper floors (right), a deterministic floor height gain is applied based on the outdoor prediction at the ground floor.

Fig. 6.2 illustrates, on the left, the macro best server link loss map for both indoor and outdoor areas at 2.6 GHz and ground floor height. In essence, the 3D ray-tracing tool is used to evaluate the radio propagation at street level and antenna pattern effects with regard to the radio link between outdoor cells and outdoor pixels. To estimate the indoor signal level, the indoor penetration loss within the building is calculated through an indoor additional loss (in dB) that is added to the outdoor path loss prediction. The indoor penetration, $IndL_{lk}$ (used in Eq. 3.9, becomes:

$$IndL_{lk} = \alpha \cdot d_i + L_{extwall} - G_{FH} \quad [dB] \tag{6.1}$$

where d_i is the distance (in meters) from the indoor location k to the external

wall observing the highest received signal strength from cell k. $L_{extwall}$ defines the penetration loss through the external wall (set at 20 dB). The indoor penetration is exponential in the linear domain according to exponent α, which is set to 0.6 [62, 132]. The path loss predictions are available at a height of 1.5 m, and the received signal strength at the higher floors is modeled by applying a floor height gain, G_{FH}, of 3.4 dB/floor [132, 143, 144]. The floor height model is valid for transmitters deployed above rooftop and therefore it is only applied to the macro cells, i.e. $G_{FH} = 0$ dB/floor for micro cells as confirmed in [145].

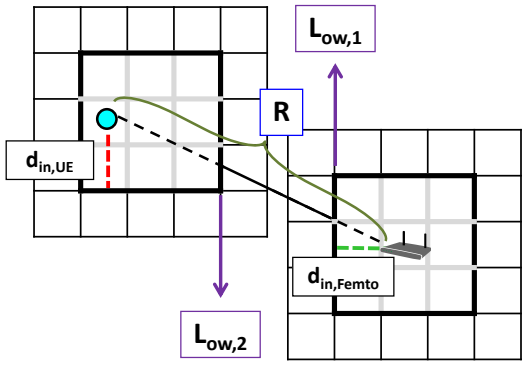

Fig. 6.3: Femto Propagation

With regard to indoor femto cells, a statistical model based on [62] is considered, and it is defined as follows:

$$PL_{dB}^{femto} = \max(38.46 + 20log_{10}(R), 15.3 + 20log_{10}(R)) + \alpha \cdot d_{2D,ind} + \ldots \\ \ldots + 18.3n^{(n+2)/(n+1)-0.46} + \sum_{i} L_{ow,i} \tag{6.2}$$

where R is the total distance in meters between the femto cell and a user (indoor or outdoor); $d_{2D,ind}$ is the distance covered inside the buildings, which is given by the sum of two indoor paths if user and femto are located in different buildings as illustrated in Fig. 6.3; α is set to 0.6, the same as for macro indoor penetration; $L_{ow,i}$ is a penetration loss of 20 dB due to each penetrated external building wall (two at most if user and femtos are inside different building blocks). The penetration loss across different floors is also taken into account and depends on the number n of penetrated floors.

6.2.3 The Outdoor-to-Indoor Traffic Split

In this case study particular emphasis is put on indoor traffic modeling as the potential of indoor offloading is strictly dependent on how traffic is distributed

over indoor areas. The final user density map is obtained by combining coarse spatial traffic information with 3D building data, as illustrated in Fig. 6.4. The processing steps are outlined as follows:

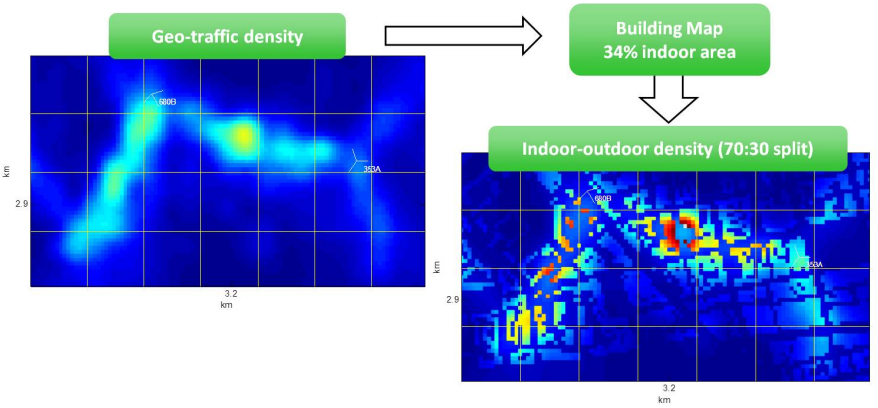

Fig. 6.4: Traffic data processing needed to obtain the final user density map. An outdoor-to-indoor traffic split of 70% is assumed.

- An initial 2D user density map is considered, being $s_{l,k}$ the user density in the generic pixel (l,k). Such a map is derived with a resolution of 50 m x 50 m from extensive geo-location based measurements under busy hour traffic conditions. No information is included with regard to traffic volume generated from indoor locations.

- On top of the user density distribution, 70% of the traffic is assumed to be generated from indoor areas [146] and the remaining part from the outdoor. To achieve this, building locations are utilized to weigh the indoor pixels when calculating the intermediate 2D user density map. Given the initial user density $s_{l,k}$ for the generic pixel (l,k) and an indoor ratio β_{Ind} equal to 0.7, indoor and outdoor user density are expressed, for the corresponding pixels, as follows:

$$
\begin{aligned}
s_{i,j}^{ind} &= \frac{\beta_{Ind} \sum_{l,k} s_{l,k}}{\sum\limits_{l,k \in \mathcal{L}^{ind}} s_{l,k}} \cdot s_{i,j} \\
s_{i,j}^{out} &= \frac{(1-\beta_{Ind}) \sum_{l,k} s_{l,k}}{\sum\limits_{l,k \in \mathcal{L}^{out}} s_{l,k}} \cdot s_{i,j}
\end{aligned}
\tag{6.3}
$$

where $\mathcal{L}^{ind}$ and $\mathcal{L}^{out}$ stand for the set of indoor and outdoor pixels respectively.

- For indoor users, the indoor traffic density can be further distributed amongst the various floors of the buildings. Considering that ground floors are usually commercial spaces that generate more traffic than higher floors, 50% of the indoor active users are assumed to be located at the ground floor whilst the remaining part is equally distributed amongst the upper floors.

Fig. 6.5(a) depicts the final user density map, showing only the 2D distribution from Eq. 6.3. It can be seen that two highest traffic areas are located in the western part of the investigated area, and half of the network traffic volume is consumed within those areas. The size of the hot-spots is in the order of 1 km^2. The impact of introducing the indoor user split on traffic spatial distribution is illustrated in Fig. 6.5(b): by shifting from the initial 2D traffic without traffic split to the one with embedded indoor user ratio, the percentage of the area generating half of the network traffic decreases from 17% to 11%. It means that network traffic becomes more concentrated in indoor areas where femto cells are expected to offload the overlay macro and micro network.

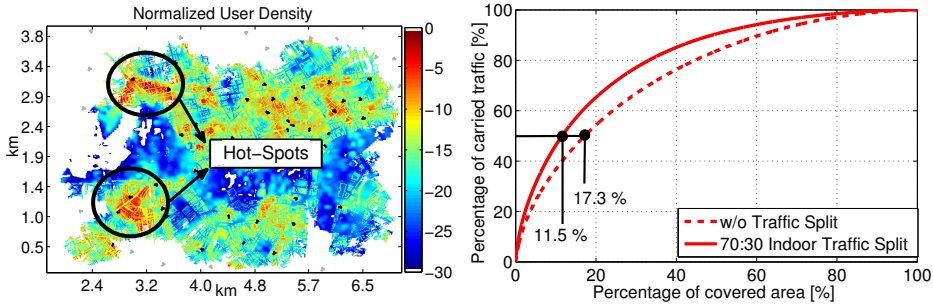

(a) User Density with Indoor Traffic Split

(b) Spatial Traffic CDF

Fig. 6.5: Traffic spatial map of the investigated area (left) together with the comparison of different traffic distributions obtained with and without indoor traffic split.

6.3 Small Cell Deployment Strategies

When deploying new micro and femto cells, the main goal is to find the deployment locations such that the overall downlink network outage, i.e. the percentage of users that experience a data rate below a predefined minimum required, is decreased. Two different deployment strategies have been used for micros and femtos, respectively, on the basis of the different transmission power and deployment constraints.

Micro cells are only deployed outdoor according to the SMART algorithm, the details of which can be found in [147]. The algorithm is made up of two steps: the first is a fast non-iterative algorithm that selects the first set of locations based on network outage spatial information; given the initial set of positions, the second step consists of a meta-heuristic algorithm that iteratively shifts the positions of the new micro cells to new locations in the study area. In the meta-heuristic search, the network performance is re-simulated for each iteration, and the algorithm ends when the best network outage is achieved or the maximum number of iterations is exceeded. A constraint for the set of available locations is given by the fact that micro cells are to be deployed outdoor.

Due to the expected high number of femto cells involved, the femto deployment strategy is based on a simpler traffic-driven deployment algorithm. Femto cells are deployed according to the algorithm described in Section 3.6; the only difference is in the deployment metric related to each candidate position as it is only driven by user density information. The employed metric is formulated as follows:

$$DM_i = \sum_{r,l \in A_i} \bar{s}_{r,l} \tag{6.4}$$

where $\bar{s}_{r,l}$ is the normalized user density in a generic pixel. The selected strategy purely based on traffic is aligned with the following deployment assumptions that are considered in this case study:

- Femtos operate in OSG mode, meaning that any user of a given operator network can connect to femtos without any access restriction.
- Femto deployment is evaluated in a traffic hot-zone area where indoor cells are supposed to provide high capacity in public hot-spots such as shopping malls, hotels and offices.
- Femtos are seen as an enterprise or metro public space solution rather than for residential areas. This means that operators are able to control the access and plan where the femto cells are going to be deployed, which is generally not the case for residential femto deployment.

Furthermore, femtos are deployed only at indoor locations and only at the ground floor of the corresponding buildings. The ground floor only deployment approach has been chosen because 50 % of the indoor users are assumed to be located at the ground floor. In fact, spreading the femtos over several buildings makes it possible to improve coverage and increase the number of offloaded users. Moreover, the macro signal is stronger at the upper floors, and this would penalize femtos in those locations, especially for highly interfered co-channel deployment. The full

deployment algorithm setting is presented in the next chapter, whereas further details about outage driven deployment and femto user statistics are provided in Appendix B.3.

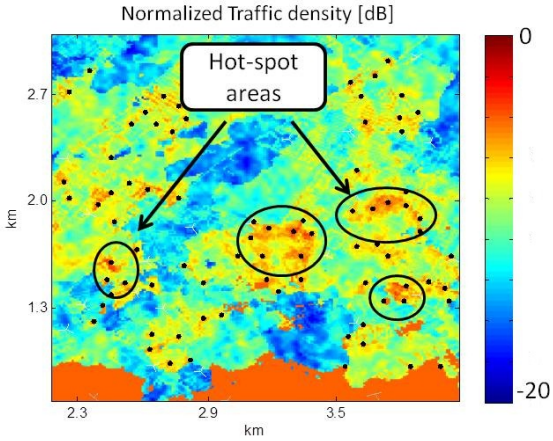

Fig. 6.6: Femto traffic-driven deployment giving priority to the high traffic locations highlighted with the circles. Femto nodes are depicted with the small black spots.

6.4 Large-Scale Deployment Performance

This sections present the network evaluation of different deployment options, considering the network area described previously. Starting from the reference single-band macro, macro carrier upgrades and co-channel micro deployment are investigated with the purpose of fulfilling the outage target. A mobile broadband traffic forecast model is employed to set the LTE network traffic load and identify the point at which the traffic growth cannot be sustained by the reference macro deployment. The goal of this analysis is to spot the most critical network areas, on which the indoor deployment study of Chapter 7 is focused.

6.4.1 Traffic Assumptions

The mobile broadband traffic growth with respect to the traffic volume of 2011 is shown in Fig. 6.7, and a model is employed to set the number of active users in the network area. As traffic growth prediction is out of the scope of this dissertation, the employed traffic forecast model and all the assumptions behind it can be found in [148] and references therein. For this specific case study, the overall traffic

growth is given by the sum of LTE and HSPA downlink traffic predictions, and it can been seen that the two curves cross after almost 8 years when the increased LTE penetration yields a higher traffic volume than HSPA. As for LTE, the traffic growth trend can be expressed as follows:

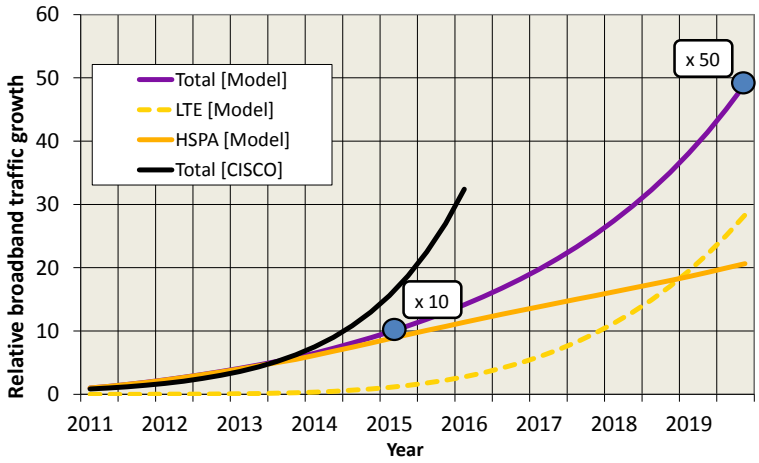

Fig. 6.7: Mobile broadband traffic forecast showing the split between LTE and HSPA growth curves for a time span of 9 years, in comparison with the more aggressive global traffic growth predicted by Cisco [149]. The relative total traffic growth from the initial year is highlighted in the text boxes, and at the end of the period a "50x" traffic growth from the starting year is predicted

$$T_{LTE}(t-t_1) = S_{Ntw}(t_1) \cdot P_{LTE}(t-t_1) \cdot Y^{(t-t_1)} \tag{6.5}$$

where t_1 is the initial year and t the time expressed with a granularity of one year. The traffic increase is given by a combination of different factors that are described below:

- $S_{Ntw}(t_1)$ is the total subscriber base – i.e. the total number of potential broadband users – in the considered network area at the initial year.
- $P_{LTE}(t-t_1)$ stands for the LTE connectivity ratio (or penetration) model for the selected time period, and it is relative to the reference starting time. Such a curve is modeled as Gompertz function [150] and starts increasing significantly after 4 years since the initial time step. The main parameter setting can be found in [148].
- Y represents the per subscriber yearly traffic growth, which is generally set based on publicly available forecast data and/or the specific operators'

expectations for the analyzed network. In this case study, Y is set to 1.45, i.e. the traffic per subscriber increases by 45% every year.

When simulating the network performance, only a fraction of the subscriber base is considered. In fact, the relevant parameter for evaluating network performance is the number of simultaneously active broadband users. For the initial year, the available 3G downlink traffic volume generated in the busy hour is used to estimate the average sector throughput, from which the number of active users is calculated based on the minimum data rate to be guaranteed. Different user terminal, subscription and application types are not considered in the model. To calculate the traffic load over time, the number of active users available at the initial year is multiplied by the adoption penetration curve $P_{LTE}(t - t_1)$.

Although global traffic forecast information is available [149], mobile network deployments and radio access capabilities can be at various stages of implementation depending on the different operators, market maturity or geographical region. Hence, the main advantage of the above traffic growth model is that of calibrating and adapting the related parameters to the specific case study in order to better plan the needed capacity enhancements.

6.4.2 Spectrum Allocation and Initial Macro Deployment Performance

With regard to spectrum availability, two bands of LTE paired spectrum at 800 MHz and 2.6 GHz are considered with a bandwidth of 10 and 20 MHz respectively. The minimum data rate is fixed at 1 Mbps, and the corresponding outage level target is fixed at 10%, or alternatively 90% mobile broadband coverage, according to the guidelines suggested by a regulator in [151] to promote competition in mobile markets. Macro base stations are allowed to transmit at both carriers, whereas micro cells are deployed only at 2.6 GHz sharing the spectrum with the macro overlay, as shown in Table 6.2. The transmission power of the small cells is 30 dBm, their transmission bandwidth can be selected between 5 and 20 MHz, and a 5 dBi omni antenna is utilized. The spatial user density map is only based on geo-location based measurements, without imposing a 70% indoor split (see Fig. 6.5(b)). Under these assumptions, 44% of the users are located inside the buildings. When indoor, users are deployed at ground floor with a 50% probability, as explained in Subsection 6.2.3.

Table 6.3 summarizes the network KPIs in the single-band macro scenario for different total traffic growth scenarios (three, ten and fifty-fold traffic increase) that can be referred to the overall mobile broadband traffic trend in Fig. 6.7. It is clear that the user outage performance increases with increased traffic load as

Table 6.2: Deployment scenarios and related spectrum allocation

Network Deployment	800 MHz (FDD, 20 MHz)	2.6 GHz (FDD, 20 MHz)	Total bandwidth
Single-Band Macro	Macro	–	20 MHz
Dual-Band Macro	Macro	Macro	30 MHz
Dual-Band Macro & Co-channel Micro	Macro	Macro Micro (30 dBm)	30 MHz

a higher number of users share the same macro resources and the average user throughput decreases. Up until a total 10-fold traffic growth, a 10 MHz band gives enough capacity to keep the percentage of unsatisfied users below the target. Yet, the number of users explodes for a "x50" traffic growth due to increased LTE adoption, and under these conditions, the single-band macro layer is no longer able to fulfill the outage target. For this traffic increase, approximately half of the users are in outage, and these are mainly located in the high traffic areas of the investigated scenario. To reduce user outage, additional spectrum in combination with small deployment in the hot-spot areas needs to be considered. Henceforth, network performance will be evaluated for a traffic growth of 50 times, as the corresponding traffic load is the most critical for the overall network performance.

Table 6.3: Single-band macro performance at 800 MHz for different traffic growth scenarios. The employed traffic map does not include the indoor split.

Traffic Growth	"x3"	"x10"	"x50"
LTE User Number	38	676	3002
Minimum data rate (Mbps)	1 Mbps	1 Mbps	1 Mbps
Outage data rate (%)	1%	9.3%	52%
Average user th'put (Mbps)	9.9 Mbps	2.8 Mbps	0.5 Mbps

6.4.3 Performance Results for Dual-band Macro and Micro Deployment

Based on the 50-fold traffic increase, network outage at 1 Mbps for a full dual-band macro network upgrade with and without micro underlay is presented in Fig. 6.8. The performance results are presented according to two different user density distributions: the first is without assigned indoor traffic split (plain geo-location traffic), whereas in the second case 70% of the traffic originated from indoor areas. When considering the macro-only scenario, the deployment of an additional band of 20 MHz at 2.6 GHz enables the network to reduce the outage to 22%, that is less than half as compared to the 800 MHz-only deployment. Moreover, although a higher number of outage users are located indoor, the overall

user outage is not sensitive to the different traffic distributions. In other words, the more concentrated traffic does not have any effect on the macro layer as the macro cell areas are significantly larger than the single building blocks, and the relatively dense macro deployment in the high traffic areas prevents the indoor areas from being coverage-limited.

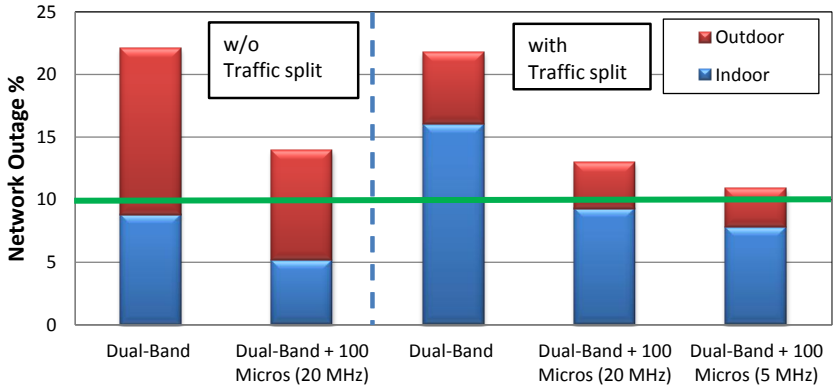

Fig. 6.8: Network outage at 1 Mbps showing the split between indoor and outdoor outage users for macro dual-band and co-channel micro deployment scenarios. Micro transmission bandwidth is set to 20 MHz (equal to the macro) or 5 MHz with a transmission power of 30 dBm. Overall outage is shown through the split between outdoor and indoor outage users.

To further decrease user outage, 100 micro cells are to be co-channel deployed with the macro layer at 2.6 GHz, according to the outage-driven deployment algorithm previously described. By utilizing the full band of 20 MHz, user outage does not go below 13% and, similarly to the macro layer, it does not vary significantly with reference to the indoor traffic split. Although a larger number of users is generated indoor, the number of users offloaded to micro cells is not significantly improved. The reason is that half the indoor users are generated on the upper floors, and in these locations micro coverage is impaired by stronger macro signals due to the assumed floor height gain – not applied to micros.

Co-channel micro deployment can meet the target if the transmission bandwidth is reduced to 5 MHz keeping the same transmission power. In this scenario the impact of different transmission bandwidth between micro and macro cell on user SINR is considered by means of a simple model: the interference power originating from micro towards macro and vice versa, is linearly scaled according to the ratio between the larger and smaller band, i.e. one fourth. A gain in terms of user SINR can be seen in Fig. 6.9, where the micro G-factor improvement is more pronounced than the macro at 2.6 GHz. This is due to the fact that the macro cells are the main interferers for micro users, and the reduced transmission bandwidth allows micro to serve more users (+4% in micro user split), as shown in Table 6.4.

The overall user outage is reduced to the predefined target, but shrinking the micro bandwidth has in return several drawbacks: with 5 MHz, micro cells begin having users in outage as the available capacity does not suffice to serve all users with 1 Mbps and this could be a limitation for higher traffic demand; then, the average user throughput is lower than in the 20 MHz case since micro users cannot experience high peak data rates due to the reduced available capacity. In general, a trade-off between reduced interference and a full frequency reuse is necessary to achieve a network performance level that is acceptable from both a coverage and capacity perspective.

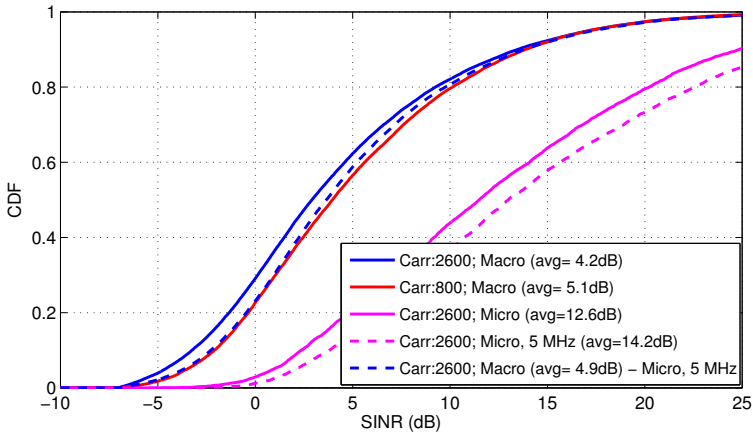

Fig. 6.9: SINR distributions for macro and micro users after deploying 100 micro cells with different transmission bandwidth (20, 5 MHz). A 70% indoor traffic split is assumed

Table 6.4: Network performance insights for different deployment scenarios, assuming a 70% indoor traffic split.

Network Statistics	Dual-Band Macro (DB)	DB + 100 Micros (20 MHz)	DB + 100 100 Micros (5 MHz)
Macro Outage	21.7%	12.9%	9.4%
Micro Outage	–	0%	1.4%
Average user th'put (Mbps)	1.2 Mbps	2.4 Mbps	1.5 Mbps
Micro user split (%)	–	15%	19%

6.5 Discussion

The performance analysis conducted in the large-scale urban scenario demonstrated that a multi-carrier macro layer is able to cope with increasing traffic demand when outdoor micro cells are deployed at street level. For a traffic increase by a factor of 50 from today's levels, the most critical areas in terms of network outage are located in those zones of network where the traffic demand is significantly higher than in the rest of the network, as shown in Fig. 6.10. Almost half of the 100 deployed micros are deployed inside the high traffic area located on the north-west corner of the investigated area. From the performance results it can be concluded that in such a dense network deployment it is recommendable to reduce interference between the different deployment layers so as to improve the radio performance and favor user offloading towards the small cells. In this fashion, the outage target on the large-scale deployment can be guaranteed, but it is also true that in the hot-zone areas the outage level relative to few numbers of macro sites located therein can exceed the required level.

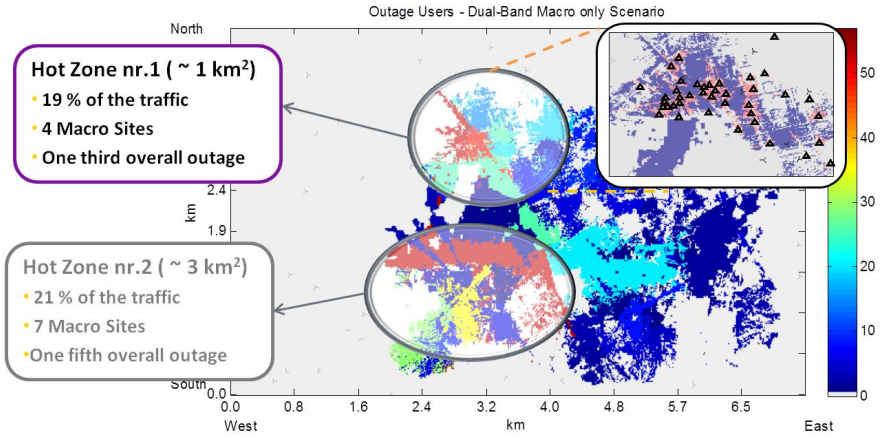

Fig. 6.10: User outage spatial map for the large-scale macro-only deployment, showing the contribution of the high-traffic areas. An example of micro deployment within one of the Hot-Zone areas is provided.

In the next chapter the radio network performance is investigated by focusing the attention only on the northern high-traffic area illustrated in Fig. 6.10, which is responsible for one third of the overall network outage in the macro-only scenario. The target is to assess the potential of combining the macro layer deployment not only with outdoor micro cells, but also indoor femto cells operating in OSG mode in a dense hot-zone urban scenario. Due to the significantly increased deployment density and more aggressive traffic demand from indoor areas, the usage of the available spectrum among the different deployment layers becomes crucial as to

striking a balance between network coverage and capacity improvements.

Chapter 7

Multi-Layer Heterogeneous Deployment in a Hot-Zone Urban Scenario

7.1 Introduction

In order to accommodate the fast growth of mobile traffic, both outdoor and indoor small cell deployment solutions are envisaged to considerably enhance network coverage and capacity. The overall target of this chapter is to investigate and compare the downlink performance of different LTE heterogeneous network deployment solutions and, differently from previously addressed case studies, particular emphasis is put on OSG indoor femto cells. The analysis is carried out in the hot-zone network scenario mentioned in the previous chapter in Section 6.5. Such a high traffic area extends over 1.27 km^2, and it makes up for around one fifth of the overall traffic demand estimated over the large-scale deployment area (ca. 12 km^2). Due to the extremely high and concentrated traffic, it is challenging for a macro-only deployment to provide users with the expected data rates. For this reason, a dense cluster of low-power cells at street and indoor level – micro and femto cells respectively – is expected to offload the overloaded macro layer especially if most of the traffic originates from indoor locations. This study assumes the deployment of indoor OSG femtos as no access restriction is applied to the connected users.

In light of the beneficial effects of offloading on the user experience, several performance and cost-related aspects are to be addressed when investigating the viability of multi-layer heterogeneous networks. In this chapter, the analysis of such deployment solutions is tackled according to the following:

- Various heterogeneous deployment solutions are considered to guarantee the network coverage targets. These are given by outdoor micro-only, indoor femto-only and joint micro-femto deployments, which underlay a dual-band macro deployment built on the existing 3G network. A traffic growth of 50 times from today's level is assumed, as explained in the previous chapter.

- In order to evaluate the impact of interference amongst the different deployment layers, radio performance evaluation is carried out through different spectrum allocation schemes, assuming two available LTE spectrum bands. The main target is to identify the scheme that achieves the best trade-off between user offloading and network coverage performance.

- Iso-outage scenarios are ultimately compared in terms of infrastructure costs to understand how the different solutions could impact the operator's mobile network evolution in the long-term.

Although being one of the most important technical challenges, more complex interference management techniques, such as eICIC or advanced traffic steering algorithms, are beyond the scope of this dissertation. Having in mind that those techniques could yield performance gains, the analysis is mostly focused on identifying the most suited multi-layer deployment solutions and examining their cost-effectiveness. The chapter is structured as follows: macro reference scenario performance is addressed in Section 7.2, outdoor micro deployment in Section 7.3, indoor femto deployment in Section 7.4, and joint micro-femto deployment in Section 7.5; the TCO analysis is described in Section 7.6 and the final conclusions in Section 7.7.

7.2 Reference Hot Zone Scenario Performance

This section includes the description of the Hot-Zone area in terms of involved macro sites and building related information. Then, radio performance results are presented with regard to the reference macro scenario, which are used as a baseline when evaluating performance gains associated with small cell deployment.

7.2.1 Scenario Description

The Hot-Zone area is located within the large-scale scenario presented in Section 6.2 where further details on macro layout, propagation modeling and user density can be found. As shown in Fig 7.1, the investigated area size is 1,27 km^2, and the shape is obtained by considering the area covered by the macro cells located inside the investigated area. The number of macro sites is 4, and the irregular shape of the area is due to the scattered coverage areas estimated through 3D raytracing models. The surrounding base stations are considered as interferers in order to have valid performance statistics for users close to the area edges. More than 900 buildings are located inside the area, covering 36% of it.

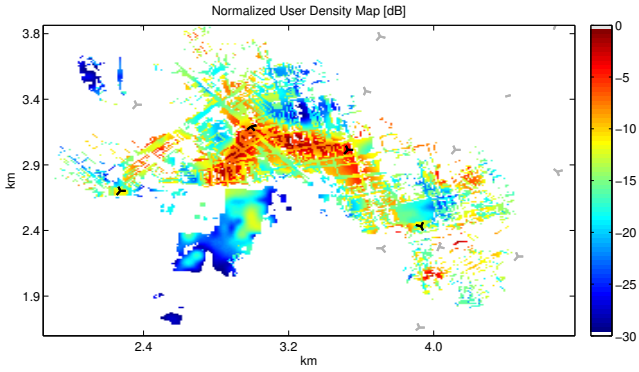

Fig. 7.1: Normalized user density map for the investigated hot-zone area including 4 macro sites, depicted in black. 70% of the users are assumed to be located in indoor areas.

As for traffic assumptions, a "x50" traffic traffic growth for LTE is considered (refer to Section 6.4 for details), leading to a user load of 558 users to be served. The Hot-Zone area carries around one fifth of network traffic and is responsible for one third of the overall macro outage when considering the large-scale macro network deployment. Moreover, 70% of the users are assumed to be located inside the buildings, as can been seen in the normalized user density map shown in Fig 7.1, and half of the indoor users are placed at the ground floor.

7.2.2 Macro Deployment Performance Results

Macro performance results are evaluated in terms of outage and average user throughput for a minimum required data rate of 1 Mbps, and similarly to the large-scale deployment study, the outage target is fixed at 10%. With regard to the reference macro deployment, two carriers are available at both lower and higher frequency bands, i.e. 800 MHz and 2.6 GHz, as in a typical European LTE

Table 7.1: Main Scenario Assumptions and Parameters

Parameter	Value
LTE System	Downlink FDD LTE, 2x2 MIMO
Supported Carrier Frequencies	2.6 GHz (20 MHz), 800 MHz (10 MHz)
Network Layout	4 sites (large network with 118 sectors)
Traffic Assumptions	"x50" traffic growth 558 users 70/30 indoor traffic split 50% at ground floor
3D Building Map	915 buildings Indoor area percentage 36%
Minimum data rate Outage target	1 Mbps 10%

deployment. From Fig. 7.2 it can be inferred that user SINR does not vary at the different frequency bands: this means that the Hot-Zone is strongly interference-limited due to the extremely dense macro deployment and traffic distribution, at both outdoor and indoor locations.

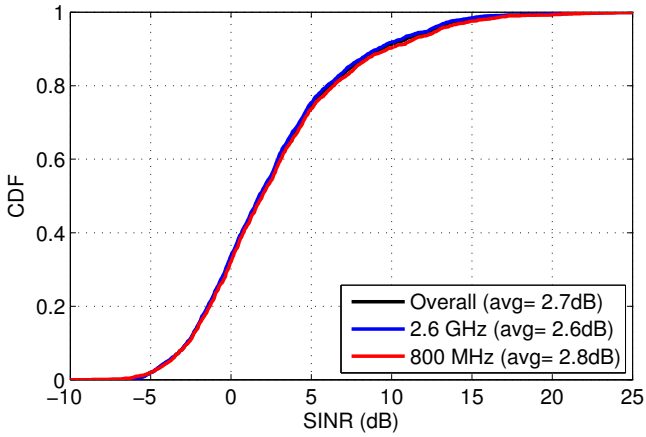

Fig. 7.2: User SINR perceived at both 800 MHz and 2.6 GHz for the reference macro deployment.

The main KPIs are shown in Table 7.2 for both single-band and dual-band macro deployment. When deploying only the lower frequency carrier, only 25% of the users are served with at least the minimum data rate: macro cells serve on average approximately 46 users, and the 10 MHz band does not provide sufficient radio resources to be split amid the connected users. As most users cannot achieve any downlink throughput, the average user throughput collapses well below the minimum data rate threshold. By deploying additional spectrum at 2.6 GHz on a 20 MHz band, user outage significantly drops, stopping at 42% , well above

Table 7.2: Network performance for macro-only deployment having single and dual-band configurations. The dual-band macro deployment is used as reference scenario when evaluating the network performance of the different heterogeneous deployment options.

Network Configuration	User Outage	Average User Throughput
Single-Band Macro 800 MHz (10 MHz)	73%	0.29 Mbps
Dual-Band Macro 800 MHz (10 MHz), 2.6 GHz (20 MHz)	42%	0.65 Mbps

the 10%-target. Although the overall spectrum is tripled, the offered traffic load is so massive that the available radio resources are not even capable of halving the user outage from the level achieved with single-band macro. On a similar trend, user throughput increases up to 0.6 Mbps, which is still below the minimum required data rate. Assuming that no additional carrier is available, a small cell underlay achieving massive cell splitting is needed to further reduce the number of outage users and boost network capacity. The dual-band macro performance will hereinafter be used as a reference scenario when presenting micro and femto deployment offloading gains.

7.3 Outdoor Micro-Only Deployment Results

This section is dedicated to the downlink performance evaluation of outdoor micro base stations in the Hot-Zone scenario. Micro cells are deployed according to the algorithm presented in Section 6.3, and the search of candidate positions guarantees a minimum ISD of 50 m. The transmission power is set at 30 dBm, and a 5 dBi omni antenna is employed. Considering the availability of both 800 MHz and 2.6 GHz spectra, different spectrum allocation schemes determine the simulation scenarios illustrated in Fig. 7.3: the co-channel case presents full frequency reuse between macro and micro cells over the 20 MHz bandwidth; in the out-band case, the 2.6 GHz band is only allocated to micros, whereas in dedicated channel scenario the higher frequency band is split into two orthogonal chunks of 10 MHz, which are separately assigned to micro and macro layers.

7.3.1 Co-channel Micro Deployment

Fig. 7.4 illustrates network outage over a different number of deployed co-channel micros together with the percentage of offloaded users to the micro layer. The outage values are shown by considering the split between indoor and outdoor

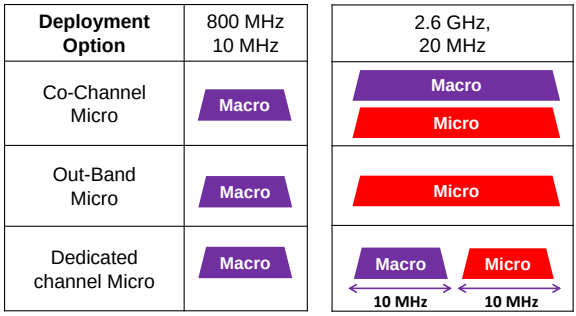

Fig. 7.3: Micro Deployment simulation scenarios

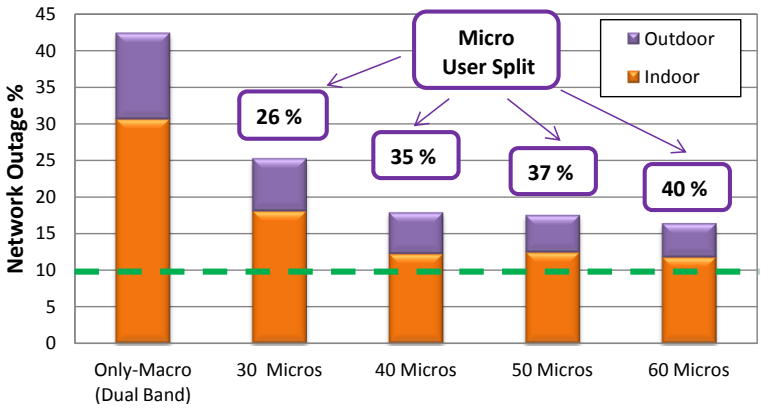

Fig. 7.4: User outage at 1 Mbps over different numbers of co-channel micros, showing the outage share of indoor and outdoor users; micro cells are deployed on top of the dual-band macro layer. The percentage of users offloaded to micros is shown in the text boxes.

outage users. By increasing the number of co-channel micros, it can be seen that network outage decreases as users are offloaded to the micro cells, and a larger amount of capacity is available at the macro layer. Due to micro and macro layers interfering with each other, the outage performance does not improve considerably with increased micro density, saturating at around 16%. In fact, the dense macro deployment and the floor height gain associated with users located at the upper floors limit the micro coverage.

As a result of increased interference on the 2.6 GHz carrier, macro users tend to be assigned to the 800 MHz - the “escape carrier” - because of higher experienced SINR. Yet, the lower bandwidth and higher load at 800 MHz leave the macro layer congested and part of the users in outage. Micro user load does not exceed 5 users/cell, and the 20 MHz band is sufficient to provide all users with the minimum

data rate. Hence, outage is entirely caused by the macro layer, and most outage users are located indoor due to the assumed indoor traffic split and also better macro coverage at the higher floors.

As can be seen in Fig. 7.5, average user throughput performance is considerably enhanced with respect to the macro reference scenario. With only 30 micros, the user throughput becomes almost 4 times the data rate experienced with macro deployment, reaching 2.5 Mbps. The reduced user load per cell allows users to be assigned higher shares of resources, thus achieving higher downlink data rates. This trends holds for larger numbers of micros as the user data rates benefit from higher cell densities. By doubling the number of micros, user average throughput rises by 80% as compared to the 30 micros scenario.

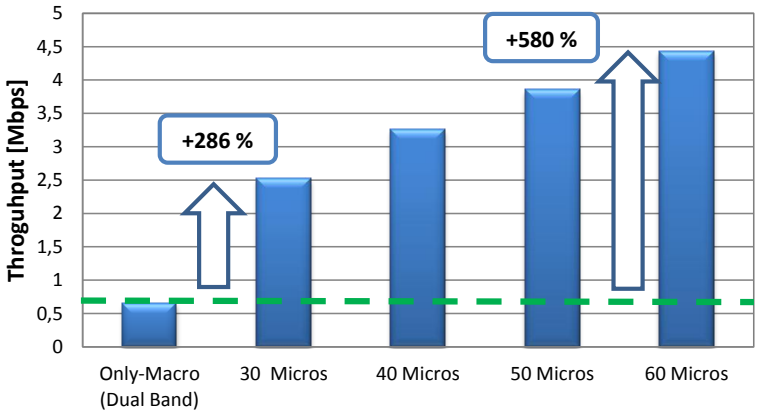

Fig. 7.5: Average user throughput gains over macro reference for different numbers of deployed co-channel micros. Micro cells are deployed on top of the dual-band macro layer

7.3.2 Out-band Micro Deployment

By removing the macro carrier at 2.6 GHz and dedicating the higher frequency band solely to micro transmission, the percentage of users offloaded to the micro layer considerably increases in comparison with the co-channel scenario. Micro cell coverage is not limited by macro interference although this comes at cost of reduced capacity at the macro. In Fig. 7.6, user outage sensitivity to different values of micro SINR bias is shown when 40 out-band micros are deployed. Firstly, without any bias, micro users share exceeds 50%, but, differently from the co-channel case, the macro layer is equipped with only one carrier. The higher number of users offloaded to micros does not outweigh the reduced macro spectral resources, i.e. 10 MHz at 800 MHz instead of 30 MHz over both frequency bands in the co-channel case. As a result, only macro users are in outage, without meeting the required

target. To further improve the user outage, higher SINR offsets can be used to steer more users towards the micro layer. However, the use of aggressive cell selection biases may cause a high number of radio link failures when performing hand over in high mobility scenarios. For this reason, an SINR bias of 3 dB is hereinafter selected when presenting micro performance results.

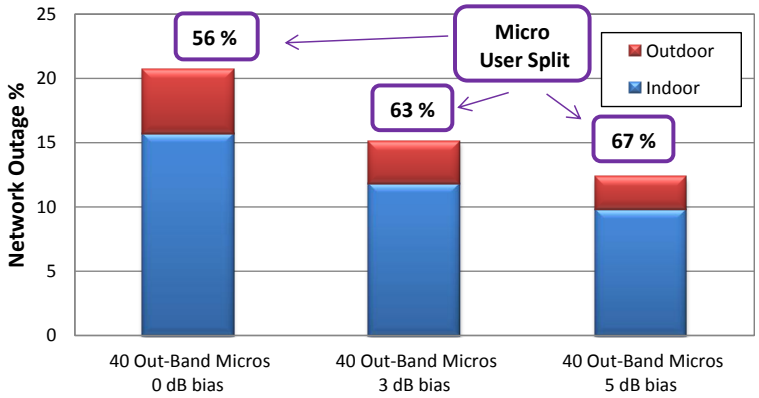

Fig. 7.6: User outage sensitivity to micro SINR bias, having deployed 40 out-band micros. The percentage of users offloaded to micros is shown in the text boxes whereas user outage is illustrated showing the split between indoor and outdoor users.

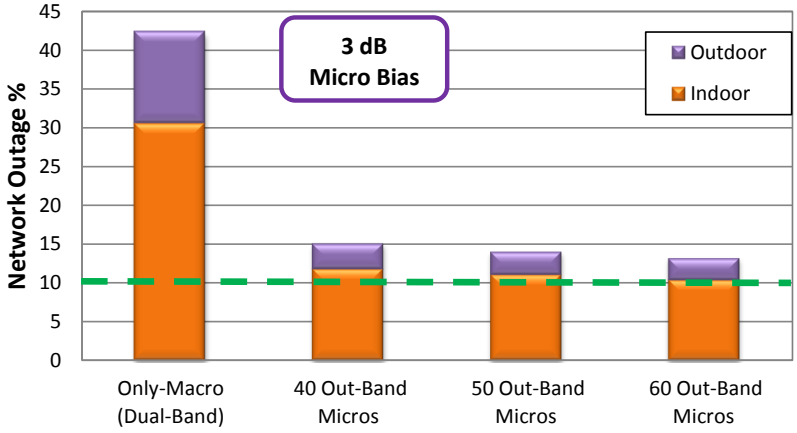

Fig. 7.7: User outage at 1 Mbps over different numbers of deployed out-band micros, showing the split between outdoor and indoor users. Micros are deployed together with a single-band macro layer. The micro SINR bias is 3 dB.

User outage over number of deployed out-band micros with a cell selection bias of 3 dB is depicted in Fig. 7.7. 60 out-band micros do not suffice to reduce the outage below the 10% target, with almost all outage users being located in indoor areas and served by macro users. Further insights as to micro users split and

average throughput comparing co-channel and out-band scenarios are provided in Fig. 7.8. User offloading is not considerably sensitive to the number of deployed micro cells as the interference between micros puts a limit to micro coverage for high cell densities. In the out-band scenario, the percentage of offloaded users is almost doubled with reference to co-channel micros for low micro densities. Further, the possibility of fully exploiting the 20 MHz micro band enables the users to achieve higher data-rates than in the co-channel case – 50-100 percent points improvement in throughput gains over reference –, without an additional carrier at the macro layer. Although not shown in this section, the user load at micro layer can be sustained by each micro cell, and outage users are basically connected to the macro layer.

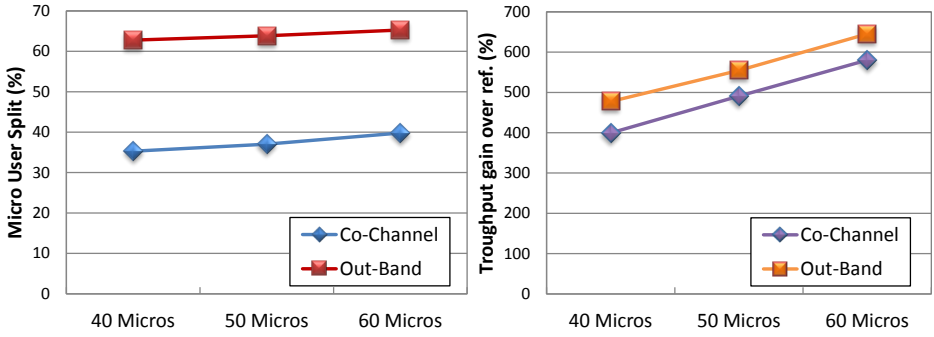

(a) Micro Users Split (b) Throughput Gains

Fig. 7.8: Micro users split and average user throughput gains over reference, comparing out-band and co-channel micro deployment.

7.3.3 Dedicated Channel Micro Deployment

The compromise between co-channel and out-band micro deployment is given by the dedicated channel configuration scheme. The 20 MHz band at 2.6 GHz is split between two orthogonal chunks and assigned to macro and micro layer respectively. From an interference perspective, this configuration is similar to the out-band micro as no interference originates from the macro layer, but part of the higher frequency spectrum is allocated to macro layer to enhance macro user data rates. A cell selection bias of 3 dB is applied to micro cells, which leads to offloaded user percentages that are in the same range as in the plain out-band deployment.

Fig. 7.9 illustrates the outage performance for different numbers of micro cells deployed on a dedicated channel along with with dual-band macro. With this allocation scheme, 35 micros are able to bring the user outage below the 10% level, and such a scenario is selected amongst the ones to be compared in terms of

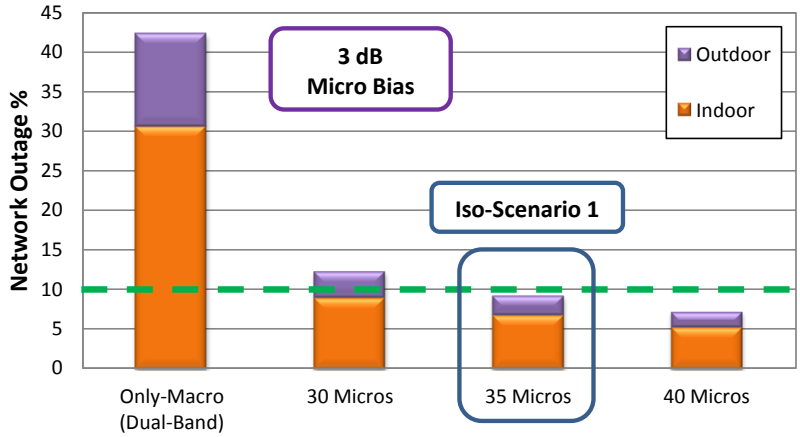

Fig. 7.9: User outage at 1 Mbps over different numbers of micros deployed on dedicated channel, showing the share between indoor and outdoor users. The micro SINR bias is 3 dB and the scenario selected for cost analysis is highlighted with the rectangle.

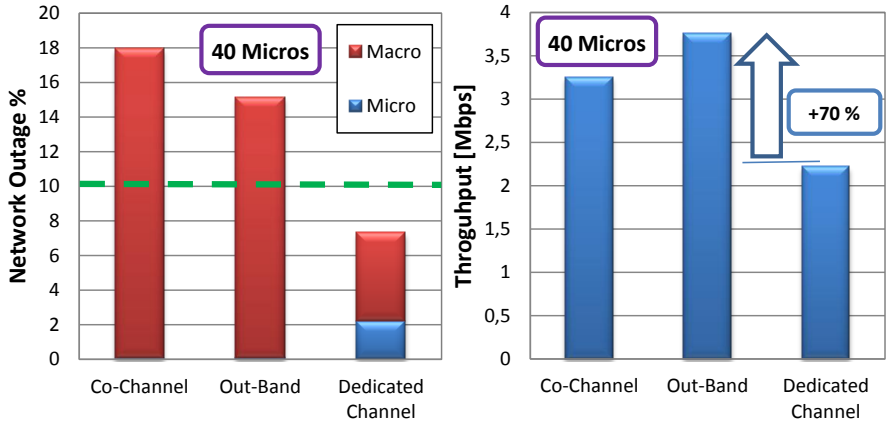

(a) User Outage (b) User Throughput

Fig. 7.10: User outage and throughput comparison between the different micro deployment schemes, assuming 40 deployed micros.

network costs. By keeping the micro user share above 60%, macro users can now share additional frequency resources with respect to out-band micro deployment, and the overall outage performance improves for higher micro densities. Fig. 7.10 compares the main KPIs obtained with 40 micro cells according to the three investigated deployment schemes. It can be inferred that utilizing the full band at 2.6 GHz for micro transmission (co-channel and out-band) enables all micro users

to be served with at least the minimum required rate, whereas the macro layer lacks the amount of resources needed to fulfill the outage target. When half of the higher frequency band is allocated to micros, the overall user outage significantly decreases, but one third of it is due to micro cells. In this case, the micro spectral resources are not enough to satisfy all users, and the data rates experienced at the micro layer become lower. As a consequence of this, the capacity performance is lower than the case where the entire 20 MHz transmission band is allocated to micro cells. For example, the average user throughput improves by 70% with 40 out-band micros as compared to the dedicated channel although the outage target is not fulfilled.

7.4 Indoor Femto Deployment Performance Results

Following the same approach as in micro-only deployment, indoor OSG femto cells are deployed according to the spectrum allocations schemes presented in Fig. 7.11: co-channel, out-band and dedicated channel femto deployments. The deployment strategy is entirely traffic driven, as described in Section 6.3, and the indoor locations are selected imposing an ISD constraint of 20 m. The transmission power is fixed at 20 dBm with the assumption of no downlink power control and no coordination amongst the different deployment layers. Omni-directional antennas are considered. Femtos are deployed only at ground floor where half of the indoor users are assumed to be. The reader is referred to Appendix B for further details about femto user SINR and deployment strategies.

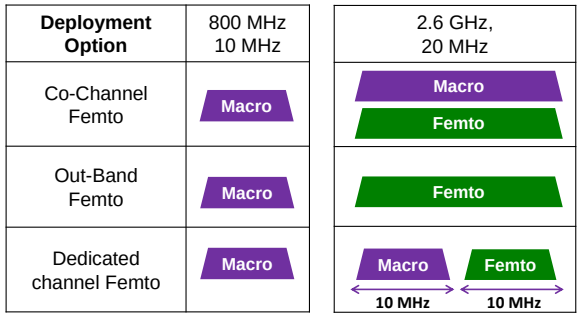

Fig. 7.11: Femto deployment simulation scenarios

7.4.1 Co-channel Femto Deployment

Network outage is illustrated in Fig. 7.12 by dividing the overall outage between indoor and outdoor users. Similarly to the previously described micro deployment, a highly dense co-channel deployment of femtos does not give significant outage improvements, and 1000 co-channel femtos (787 femto/km^2) can reduce the network outage slightly below 20%. In the co-channel case, femto coverage is strictly confined not only within the building area, but also at the ground floor as the interference generated by macro cells is stronger at the higher floors. As the femto footprint is extremely limited, i.e. an average effective coverage radius of 16 m, it is necessary to deploy a higher number of femtos than active users in order to capture the spatial variations of traffic density on both the 2D plane and vertical floors. The percentage of offloaded users towards co-channel deployed femtos does not exceed 40%, and this amount is not sufficient to ease the user load at the macro layer.

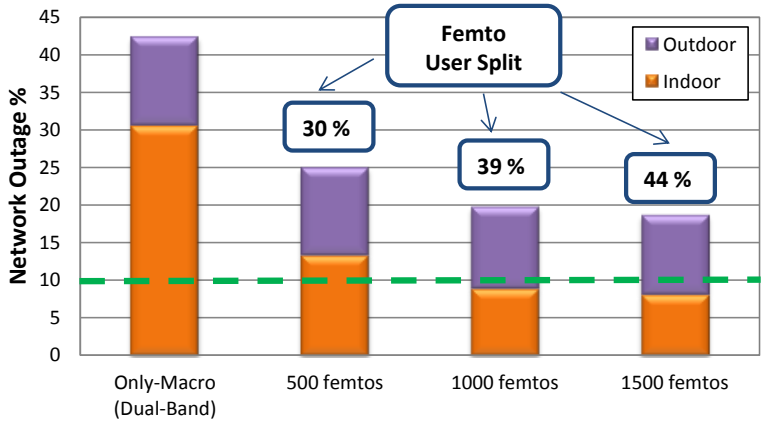

Fig. 7.12: User outage at 1 Mbps over different numbers of deployed co-channel femtos, showing the outage share of indoor and outdoor users. Femtos are deployed together with the dual-band macro layer. The percentage of users offloaded to femtos is shown in the text boxes.

With co-channel femto deployment, the outdoor outage constitutes around half the overall outage level. This is due to the fact that almost all outdoor users are served by macro cells that do not have enough capacity to serve all the connected users. This trend is different from the micro deployment scenario where the user outage is dominated by indoor users that cannot be offloaded to micro cells. Increasing the number of co-channel femtos does not yield significant gains in terms of femto user intake, and the outage performance saturates. Macro user SINR at 2.6 GHz is severely impaired by femto interference, as illustrated in Fig. 7.13(a). Prior to applying the load balancing algorithm to distribute the users between the two macro carriers, the SINR perceived at 2.6 GHz is, for 60% of the potential macro

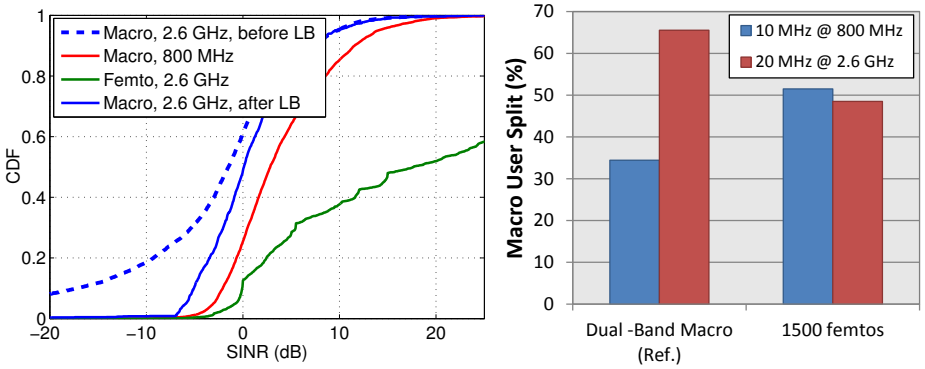

(a) User SINR with 1500 femtos (b) Macro user share

Fig. 7.13: User SINR (left) for uniform traffic distribution and macro users split (right) between the two macro carriers upon applying the multi-carrier load balancing (LB); 1500 deployed femtos are considered. User SINR is shown at 2.6 GHz before and after running the load balancing algorithm, whereas no significant differences are experienced at 800 MHz.

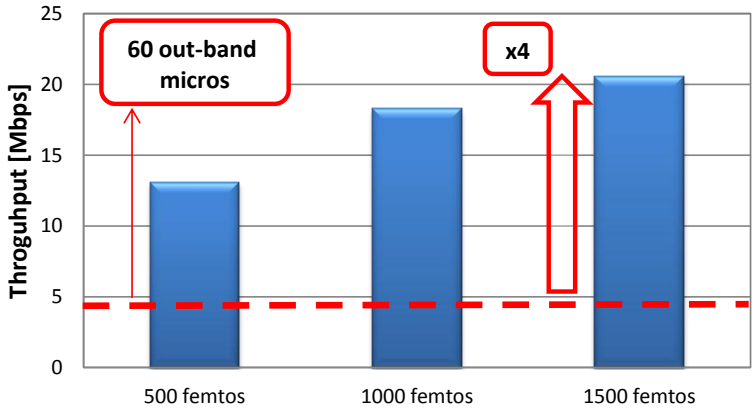

Fig. 7.14: Average user throughput over deployed co-channel femtos, compared to throughput performance obtained with only 60 out-band micro cells (red dashed line).

user locations, below 0 dB. Upon performing the load balancing, Fig. 7.13(b) shows that macro users are equally split between the two carriers when femtos are deployed. But this penalizes the 800 MHz escape carrier in terms of outage as only 10 MHz are available compared to 20 MHz at the higher frequency carrier. The performance evaluation is carried out assuming full interference from femtos not serving any user as a worst case scenario.

As for average throughput performance, most femtos serve less than 2 users, thus

delivering peak data rates to femto users thanks to excellent SINR in proximity of the indoor cells. The average data rates exceed 10 Mbps, peaking at 20 Mbps with 1500 co-channel femtos, as illustrated in 7.14. This enables co-channel femto deployment to improve user throughput by 4 times when compared to out-band micro deployment. Co-channel femtos yield a significant capacity boost, but the number of offloaded users must be improved so as to reach the outage target.

7.4.2 Out-band Femto Deployment

When femtos are deployed on the macro-free carrier at 2.6 GHz, femto coverage inside the buildings enlarges, and also outdoor users in close proximity of the buildings can be served by the closest indoor femto cells. Following the same approach as in micro deployment, an SINR femto cell bias of 3 dB is employed. Fig. 7.15 shows the outage performance obtained with different numbers of deployed out-band femtos. The percentage of offloaded users reaches around 70% with the densest femto deployment, i.e. 30 percent point higher than with co-channel femtos. As a result, the user outage achieves the 10%-target when 1500 femtos are deployed (1181 femto/km^2). Moreover, network outage is equally split between outdoor and indoor users (located at the upper floors) that are connected to the macro layer, whereas femto cells do not serve outage users.

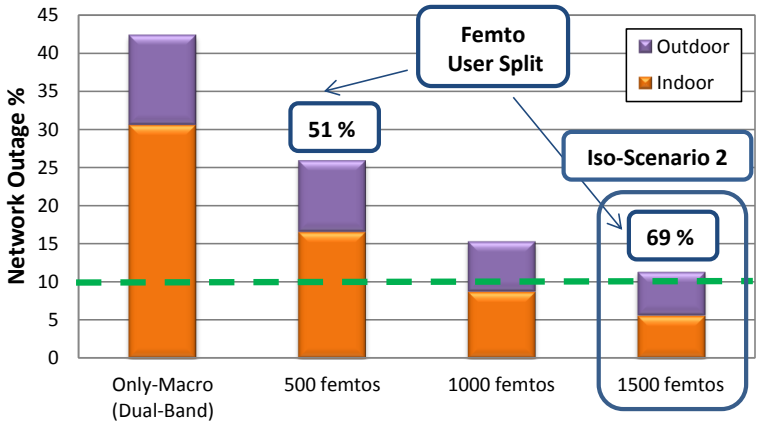

Fig. 7.15: User outage at 1 Mbps over different numbers of deployed out-band femtos, showing the outage share of indoor and outdoor users. Out-band femtos are deployed along with single-band macro cells. The percentage of users offloaded to femtos is shown in the text boxes. The iso-outage scenario is highlighted with the rectangle.

The improved femto offloading enables the network to deliver higher average throughput with regard to the co-channel case, as shown in Fig. 7.16. Despite only one carrier deployed at the macro layer and higher user load for femto cells,

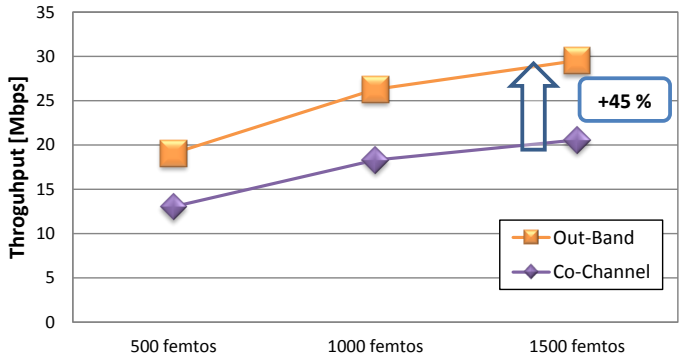

Fig. 7.16: Average user throughput over deployed femtos, compared to throughput performance obtained with the same number of co-channel femtos.

throughput gains of up to 45% can be achieved, reaching an average data-rate of 30 Mbps. As no access restriction is employed on femtos, the use of a femto-dedicated carrier allows users to fully benefit from the highly dense femto deployment. Yet, to sufficiently cover the indoor buildings and reach the outage target, an average of almost 2 femtos per building shall be deployed (1500 femtos in 915 buildings).

7.4.3 Dedicated Channel Femto Deployment

Following the same trend experienced with micro deployment, the deployment of macro and femto layer on orthogonal frequency channels in the 2.6 GHz band achieves the best outage performance. The enhanced capacity at the macro layer allows the network to fulfill the outage target by deploying around 500 femtos. Such a scenario is selected to carry out the cost analysis in Section 7.6. In Fig. 7.17 it can be seen that the user outage at 1 Mbps constantly decreases as the femto density becomes higher. Moreover, although femtos transmit on half of the available bandwidth at 2.6 GHz, femto users are not in outage because of the dense deployment and low user load per femto.

As for the throughput performance comparison illustrated in Fig. 7.18, it can be inferred that reducing the transmission band of femtos has a negative impact on average user throughput. For 500 deployed femtos, a throughput gain of 70% over the dedicated channel scenario can be achieved with plain out-band femto deployment. In the this case, the 20 MHz bandwidth renders it possible for femto users to boost the average user throughput even though user outage is well above the target. The same reasoning is valid for co-channel femto deployment, but the user throughput performance is worse. In fact, a lower number of users can be offloaded to femtos nodes due to co-channel macro interference.

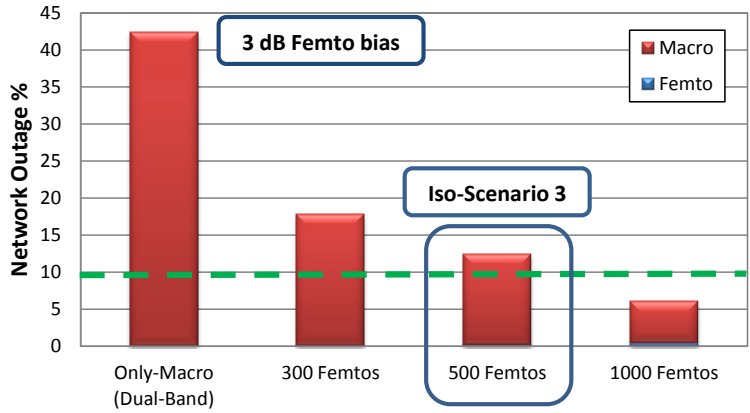

Fig. 7.17: User outage at 1 Mbps over different numbers of femtos deployed on dedicated channel, showing the outage share of indoor and outdoor users. The percentage of users offloaded to femtos is shown in the text boxes. The iso-outage scenario is highlighted with the rectangle.

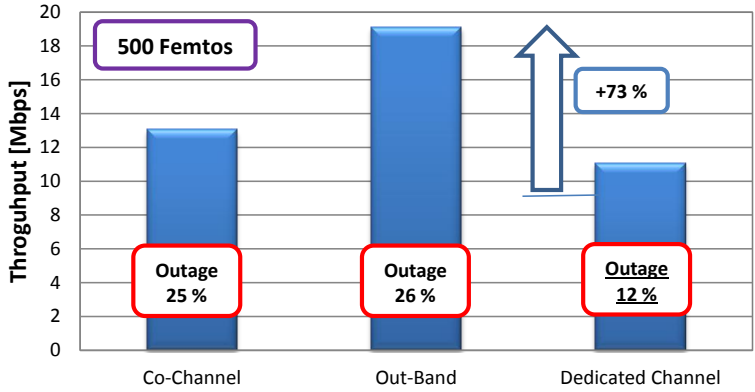

Fig. 7.18: Average user throughput comparison between the different femto deployment schemes, assuming the deployment of 500 femtos.

7.5 Joint Micro-Femto Deployment

The spectrum allocation schemes proposed for joint micro-femto deployment are illustrated in Fig. 7.19: micro and femto cells are deployed at 2.6 GHz in a co-channel or dedicated channel fashion without any macro overlay on the same band. Based on previous learning from micro and femto-only deployments, dual-band macros are not considered in this scenario since such a configuration considerably limits the offloading potential to small cells. In addition, an SINR bias of 3 dB is used for both micro and femto cells in both the spectrum allocation schemes, in

order to favor user offloading from macro to small cells.

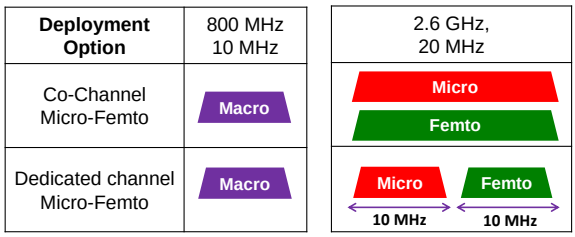

Fig. 7.19: Femto deployment simulation scenarios

Fig. 7.20 shows the outage performance for co-channel and dedicated channel joint deployment of micros and femtos. By fixing the number of micros to 40, both deployment schemes are able to reach the outage target, but deploying femtos and micros on separate frequency chunks outperforms the co-channel scenario. This means that 300 femtos are sufficient to hit the 10% level, sparing 200 femtos as compared to the co-channel case. As previously seen, utilizing less spectrum for micro transmission causes a minor part of micro users to be left in outage, due to fewer available radio resources. However, the outage is entirely dominated by macro users as observed in previous deployment scenarios.

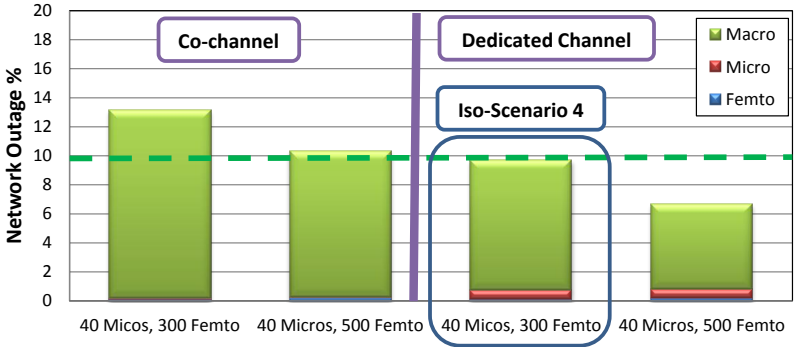

Fig. 7.20: User outage at 1 Mbps over different numbers of jointly deployed micro and femto cells for both co-channel and dedicated channel scenarios, showing the outage split amid the deployment layers. The iso-outage scenario is highlighted with the rectangle.

With regard to the share of offloaded users (see Fig. 7.21), isolating femto and micro transmission allows more users to connect to small cells, reaching a peak of 80% offloaded users with 40 micros and 500 femtos. However, as small cell transmission is not interfered by macro cells, the overall percentage of offloaded users is not extremely sensitive to different deployment schemes. The difference in small cell users share between co-channel and dedicated channel deployments is in the order of 6-8 percent points. This additional percentage of offloaded

users is connected to micros, especially from the outdoor areas, as no interference originates from the femto layer.

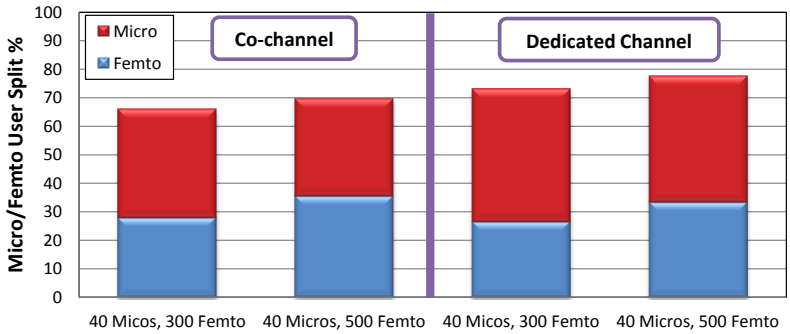

Fig. 7.21: Micro and femto user share over different numbers of jointly deployed micro and femto cells for both co-channel and dedicated channel scenarios.

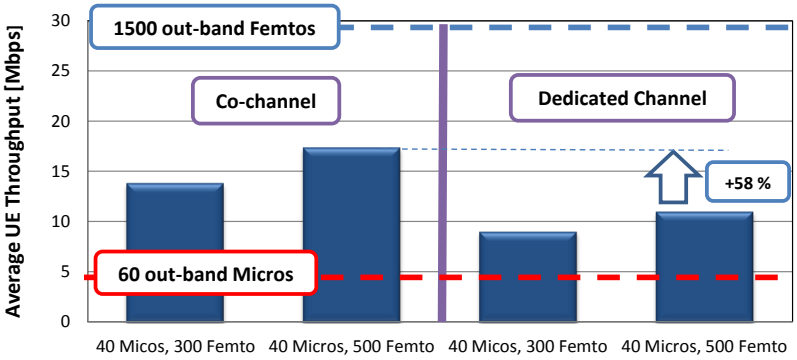

Fig. 7.22: Average User Throughput performance over different numbers of jointly deployed micro and femto cells for both co-channel and dedicated channel scenarios. Data rates achieved with micro and femto-only deployment are shown for comparison.

With the same trend as in micro and femto-only deployments, the full frequency reuse case yields gains in terms of user average throughput with reference to micro and femtos deployed on dedicated bands. The performance gain is in the order of 50%, as can be seen in Fig. 7.22. In general, the user average data rates achieved with joint micro-femto deployment lie in between the performance obtained with micro or femto-only deployment schemes. In fact, without joint deployment, out-band micro-only deployment cannot reach a sufficiently high base station density to achieve high data rates; femto-only deployment, on the other hand, represents the other extreme where the average user load per cell is significantly lower than in the other deployment solutions.

7.6 Cost Assessment of Iso-Performance Scenarios

By following the cost assessment methodology explained in Section. 3.7, deployment scenarios delivering the same user outage level are compared in terms of network infrastructure costs. The iso-outage scenarios have been selected and highlighted throughout the performance analysis of the different heterogeneous deployment solutions. The section presents both the infrastructure cost assumptions and the TCO analysis.

7.6.1 Deployment Cost Structure Assumptions

The cost figures related to the different deployment configurations are outlined in Table 7.3. Along with macro upgrades and micro deployment, two different cost structures are proposed for femto deployment. For both of them it is assumed that backhaul costs are not sustained by operators as the existing residential/enterprise broadband fixed connection can be directly leveraged as backhaul towards the core network; then, the cost difference is given by higher equipment quality and more expensive femto installation and planning costs inside the building.

Table 7.3: TCO estimates for the different deployment layers, showing the split of the different cost components. The final TCO is calculated assuming 4 years of running costs, and the far right column shows the TCO values normalized to the cost of low-cost micros.

Deployment Options	**CAPEX** in k€	**IMPEX** in k€	**OPEX** in k€	**TCO** in k€	**Normalized** TCO
LTE upgraded site	18.5	12.5	5.6	53.5	9.9
LTE second carrier	12	8.5	1.6	27	5
High-cost Micro	7.5	2.3	3.2	22.7	4.2
Low-cost Micro	1.5	1.5	0.6	5.4	1
High-cost Femto	0.22	0.38	0.05	0.8	0.15
Low-cost Femto	0.07	0	0.02	0.15	0.03

As for the outdoor cells, it can be noted that the absolute cost expenditures are lower with respect to the cost figures proposed in Section 3.7 and applied to the previous case studies. One of the reasons is that the above cost figures have been estimated one and half year later than the previous ones, and this results in increased knowledge about equipment costs together with related price erosion. Then, reduced costs are also due to different assumptions on backhaul-related and site expenses: the case study is run according to a considerable traffic growth from today's traffic levels, which is likely to take place in a time period of 10 years; hence, it assumed that, by that time, backhaul connection and installation

costs, e.g. fiber, are significantly lower in comparison with the current ones. The difference between high and low cost micros is also taken to the extremes as the low cost version assumes extremely low equipment and site rental costs. In addition, the cost ratio of LTE macro upgrades with respect to the high-cost micro cell is in the same order of magnitude as in the previous case studies.

7.6.2 TCO Analysis

The iso-outage scenario to be analyzed in terms of cost infrastructure are presented in Table 7.4, together with network main KPIs and offloaded users from macro layer. The solutions include heterogeneous deployments having micro or femto-only scenarios as well as one configuration presenting both of them. The selected deployment solutions are the ones delivering an outage performance that is the closest to the 10% target level. Scenario 2 and 3 are 1 and 2% above the required level, respectively, due to the granularity used with the number of deployed femtos. As user outage is remarkably sensitive to femto density with out-band and dedicated channel femto configurations, the outage target can easily be met with relatively small number of additional femtos. Therefore, this is expected not to substantially affect the trends and conclusions related to the cost analysis.

Table 7.4: Performance results related to the iso-outage scenarios. The number of offloaded users to small cells is inserted in the rightmost column

Nr.	Deployment Options	User outage	Average Throughput	Offloaded users
Sc. 1	4 dual-band macro sites **35 ded.-channel micros**	9.3%	2.1 Mbps	63%
Sc. 2	4 single-band macro sites **1500 out-band femtos**	11.3%	29.5 Mbps	69%
Sc. 3	4 dual-band macro sites **500 ded. channel femtos**	12.3%	10.1 Mbps	51%
Sc. 4	4 single-band macro sites **40 micros** , **300 femtos** , ded.channel	9.7%	8.9 Mbps	72%

Fig. 7.23 illustrates and compares the network infrastructure costs with reference to the selected iso-performance scenarios, showing the cost split amid the different deployment layers. Each existing 3G macro site is upgraded to LTE, whilst, as a first analysis, high-cost micros and femtos are assumed when calculating the TCO. The cost analysis shows that the scenario combining dual-band macro sites with femto cells on dedicated channels is the least expensive, whereas the extremely dense deployment of out-band femtos yields the highest costs, almost twice as much as femtos on dedicated channels. The cost associated with micro-only deployment is in between the TCO figures obtained with the two femto deployment solutions. Since a high cost micro is 28 times more expensive than a high-cost femto, deploying 35 micros instead of 500 femtos doubles the cost needed for small

cells, and the overall TCO, including the macro, is 54% higher than the least expensive femto-only deployment. The joint deployment of micro and femto cells turns out to be approximately as costly as out-band femto deployment. Similarly to out-band femto deployment, sparing the additional carrier upgrade at the macro layer does not suffice to compensate the investment needed to deploy small cells – the cost of a macro site carrier upgrade is similar to that of a high-cost micro. Hence, the hybrid deployment of micros and femtos is entirely dominated by the 40 high-cost outdoor micro cells.

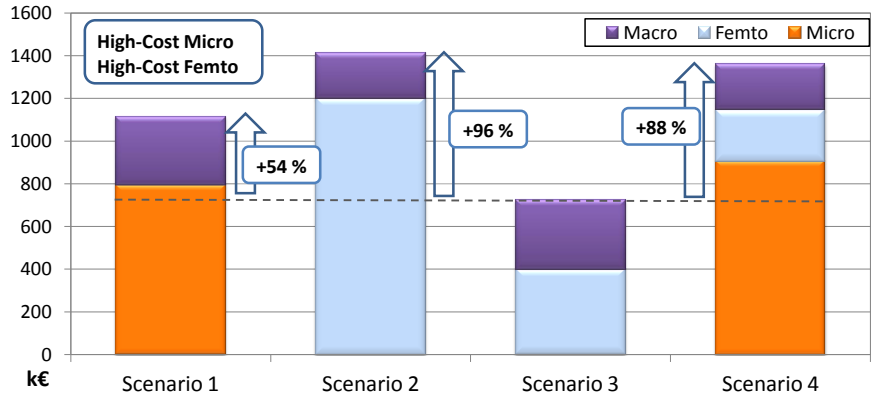

Fig. 7.23: TCO analysis for the 4 investigated scenarios, showing the cost split between the different deployment layers. High-cost structures are assumed for both micro and femto cells. Running costs are taken into account for a time period of 4 years.

In order to further investigate the viability of the selected solutions, the TCO sensitivity to different cost assumptions is illustrated in Fig. 7.24, taking into account different combinations of high-cost and low-cost cost structures outlined in Table 7.3. The scenario presenting only out-band femtos is omitted from this analysis as femto cells on dedicated channel yield a lower cost. As regards the micro-only scenario, deploying low-cost micros makes it possible to significantly reduce the infrastructure costs. As a low-cost micro is 4 times less expensive than a high-cost one, the overall TCO can be halved in comparison with the high-cost micro scenario. In addition, the macro LTE upgrade cost starts being dominant when low-cost micros are deployed.

For the femto-only deployment scenario, it can be observed that it is more expensive to deploy high-cost femtos than deploying only low-cost micros (ca. 50%). With low-cost femtos, the cost of which is $1/5^{th}$ of the high-cost one, the overall TCO can be reduced below the low-cost micro deployment scenario with a cost saving of around 20%. Low-cost femtos yield the lowest TCO as compared to the investigated scenarios, and macro related costs dominate the overall infrastructure expenditure.

When low-cost micros are deployed together with femtos, it can be inferred that the joint micro-femto deployment scenario is competitive in terms of cost. The cost saving obtained from not deploying an additional macro carrier impacts the overall TCO especially when this is combined with the possibility of deploying less expensive femtos. In this case, the joint micro-femto deployment achieves a cost performance that equals the one obtained with the deployment of only low-cost micros.

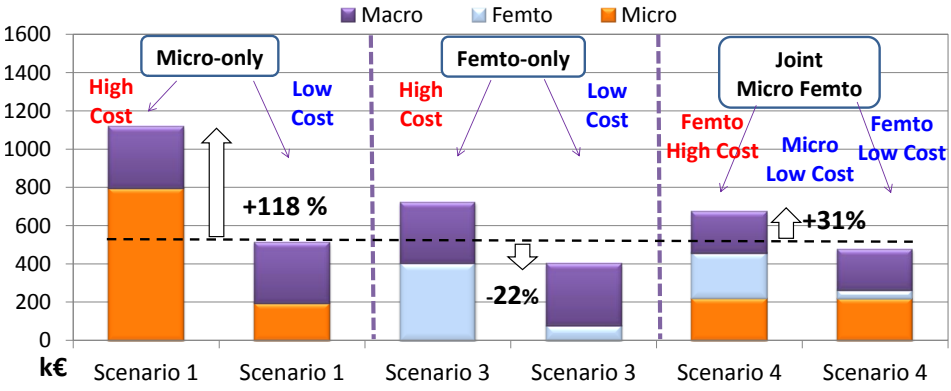

Fig. 7.24: TCO sensitivity small cell cost structures, showing the cost split between the different deployment layers. Running costs are considered over a period of 4 years.

To sum up, femto-only deployment gives the best TCO performance in all the investigated scenarios. Such a solution is particularly advantageous when compared to the deployment of high-cost outdoor micro cells. When the cost of outdoor micros decreases, the cost differences amongst all the selected deployment options tend to shrink, especially in the scenarios where low-cost indoor cells are deployed. Moreover, average throughput is an additional performance indicator that can be used for evaluating the potential capacity enhancements in the long term. From this perspective it is evident that massive deployment of indoor OSG femtos can significantly boost network capacity. In essence, it is possible to achieve data rates that are from 5 to 14 times higher than the throughput achieved with only micros on dedicated channel. The joint deployment of micros and femtos on separate frequency channels yields a throughput performance that is aligned with the femto-only deployment scenario when femtos are deployed on dedicated channel over a dual-band macro overlay. This scenario maximizes the number of offloaded users to small cells, thereby improving network coverage for both indoor and outdoor users. Throughput performance could be further enhanced by deploying femto and micro cells in a co-channel fashion at 2.6 GHz as shown in Fig. 7.22, but an additional number of femtos – approximately 200 – is to be deployed to meet the outage requirement.

7.7 Conclusions and Recommendations

This case study has investigated and compared the LTE downlink performance of several heterogeneous deployment schemes in a realistic Hot-Zone metropolitan scenario, which is served by 4 macro sites. By assuming a 50-fold traffic growth with 70% of the users located indoor and a minimum required user data rate of 1 Mbps, it can be found that 42% of the users are in outage for the reference dual-band macro layer transmitting at 800 MHz and 2.6 GHz. To effectively decrease the outage level to the 10%-target, different heterogeneous deployment solutions can be considered, such as micro cells, indoor OSG femto cells, and their combination. Having a considerably dense network deployment, it is recommended that small cells be deployed on frequency channels that are not shared with the overlay macro cells. This spectrum allocation renders it possible to protect small cells from the strong macro interference, which limits the small cell coverage. As for TCO, the cost-effectiveness of the different iso-outage solutions varies considerably depending on the assumed small cell cost structure. In general, femto-only deployment is the most cost-effective solution for both high and low cost femto models, but the network cost differences narrow if low-cost micros can be deployed.

In particular, the following detailed conclusions can be drawn from the performance and cost analysis:

- Co-channel micro deployment performance is significantly impaired by macro interference. In order to meet the outage requirement, the 20 MHz band at 2.6 GHz is to be split into two orthogonal dedicated frequency channels that are assigned to micros and macros separately. In this fashion, 35 micros, i.e. 3 micros per macro sector, are needed to hit the outage target although average data rates are lower as compared to co-channel micro deployment or full out-band micro deployment dedicating the full 2.6 GHz band to micro transmission. An SINR bias of 3 dB is suggested for micros during the cell selection phase, to improve user offloading.
- Similarly to micro-only deployment, femtos deployed on macro-free frequency bands achieve the best outage performance, also with the use of a 3 dB cell selection bias. By equally splitting the higher frequency band between macro and micro transmission, 500 femtos (i.e. 400 femto/km^2) on dedicated channel hit the required outage target with average throughput gains of approximately 5 times as compared to micro-only deployment. The outage requirement can also be fulfilled with out-band femtos transmitting on the full band at 2.6 GHz where macro are deployed only at 800 MHz. In this case, the number of required femtos, as well as the capacity improvements, is 3 times that of the dedicated channel scenario (1200 femto/km^2).
- The hybrid deployment of micros and indoor femtos - with each layer transmitting on dedicated frequency resources - gives similar capacity improve-

ments as femtos on dedicated channels, with the advantage of deploying the macro layer with only one carrier. To achieve the outage target, 40 micros (more than 3 micros per macro sector) and 300 femtos (240 femto/km^2) are to be deployed on dedicated channels.

- From the TCO perspective, the deployment solutions based on micro deployment are extremely sensitive to the micro cost structure. In case of high-cost micros, micro-only and joint micro-femto deployments can be around 50 and 90% more expensive than deploying high-cost femtos on a dedicated channel, respectively. In case low-cost micros can be provided, the cost gaps become smaller, and low-cost femtos shall be deployed in order to have a more cost-effective deployment than micro-only, i.e cost savings of around 20%. With low-cost micros and femtos, the joint micro-femto deployment cost is in between the micro and femto-only scenarios, but the capacity improvements are in the same range as with femto-only deployment.

As already stated in the introductory section, the performance evaluation of heterogeneous deployment solutions has been carried out without considering LTE-Advanced techniques for interference management. These can be exploited to optimize network performance when small cells share the frequency resources with macros [27]. By partially muting macro transmission in the time domain [35], macro interference on outdoor micro cells can be mitigated, and range offsets can be used to extend micro coverage. The advantage of this feature is that muting ratios and offsets value can be tuned according to how the user load is distributed between the two layers. Obviously, fast information exchange about muting pattern and cell load between macro and micro cells via X2 interface is needed to coordinate interference. Moreover, user mobility represents another variable to be considered when evaluating dense deployment scenarios, as radio link failures can seriously affect user experience [26].

As for indoor cells, it is understood that with dense OSG co-channel femto deployment, femto coverage is limited, and macro users' performance on the shared carrier is significantly impaired by interference. In such a scenario, calibrating the femto transmission power [152] as well as utilizing more advanced IRC receivers at the terminal side could decrease the interference level received by macro users. Moreover, as briefly illustrated in Appendix B.4, some simple load-balancing policy for co-channel femto deployment can efficiently balance the user load between macro and femto layers and avoid that a large amount of users "escape" to the femto-free macro carrier.

Chapter 8

Conclusions and Future Work

The viability of different heterogeneous deployment solutions including outdoor and indoor small cells has been evaluated on a set of LTE case studies. Considering realistic network deployments, the overall target was that of providing mobile operators with deployment guidelines as to how to meet traffic demand in a cost efficient manner. This brief final chapter is meant to summarize the main findings from the two main parts of the dissertation in the form of concise "take-home" messages or general recommendations. After that, a few aspects that could be investigated for further studies are provided in order to improve the existing models or broaden the scope of the deployment study.

As the outcome of each case study has been discussed in detail at the end of each related chapter, this sections summarizes the main conclusions and guidelines related to the two main research areas: one for outdoor deployment and one for the additional indoor layer, which is in line with the order of the presented case studies. The network performance evaluation is valid for an LTE system and limited to downlink performance only. The main performance indicator is network coverage, which is expressed in terms of user outage with reference to a required minimum data rate. The cost evaluation has been performed on deployment solutions achieving the same coverage performance. The final recommendations mobile operators should follow when introducing small cells in the network are highlighted in italic text.

8.1 Conclusions and Final Recommendations

Based on the research problems outlined in Chapter 1, it can be concluded that:

What type of small cells can keep up with the traffic growth?

- *Deploy relays to solve localized coverage issues as no substantial capacity gain can be provided.*

  When deploying in-band relays at 2.6 GHz, user outage can be effectively reduced in coverage-limited suburban scenarios. The performance tends to saturate with increased number of relays due to increased load on the backhaul link. In the interference-limited urban scenario, relay performance is substantially worse as the most critical outage areas are confined within few cells. In this case high traffic load rather than lack of coverage is the primary reason for high outage levels. The use of dedicated TDD spectrum for out-band backhaul transmission improves the relay performance compared to the in-band case, but capacity gains are substantially lower than micro or femto deployment.

- *If available, additional macro low-frequency spectrum can be deployed instead of relay cells*

  Deploying an additional carrier in the low frequency band, e.g. 800 MHz, gives a similar performance to that achieved by deploying out-band relays with dedicated TDD spectrum for backhaul. Obviously, the macro carrier upgrade solution depends on whether the mobile operator acquires the license to transmit on low-frequency spectrum.

- *Dense deployment of micro and OSG femto cells is the optimal solutions to serve hotspot areas and, in the long term, accommodate increasing traffic demand.*

  For outdoor deployment in Hot-Zone scenarios, co-channel micro deployment significantly outperforms in-band or out-band relay performance in terms of reducing outage and boosting network capacity (up to 5times for identical small cell densities). To achieve this, the micro backhaul connection must be capable of supporting the data rates experienced on the access link.

  In highly dense small cell deployment scenarios with high traffic consumption, the coverage target can be met not only with micro deployment but also femto-only and joint micro-femto deployment configurations. When achieving the same coverage performance, it can be seen that OSG femtos deliver the highest user average data rates due to low user load per femto cell. The capacity gains over micro-only deployment can be up to 5 times, whereas the joint micro-femto deployment performance lies in the middle between micro and femto deployment.

How shall small cells be deployed in realistic scenarios?

- The backhaul link is the true bottleneck limiting the performance of relay cells. This translates into *the need of carefully planning the relay positions as well as installing directional antennas with gains above 7 dBi* to effectively filter interfering signals and enhance the backhaul SINR.

- *In order to meet the outage target, densely located small cells need to be deployed on spectrum that is free from macro interference. In this way, all the small cell deployment combinations – micro-only, femto-only and hybrid micro-femto deployments – can reduce the outage below the target.*

  Co-channel deployment of micro or femto cells together with the macro layer significantly limits the outage performance of small cell deployment as the coverage of small cells is dramatically impaired by macro interference. To increase network performance under extremely dense deployment conditions, small cells have to be deployed on a dedicated frequency band. When deploying only micros or only femtos to meet the outage target, the spectrum allocation scheme that optimizes the number of deployed small cells is given by the split into two orthogonal channels of overall transmission band. One is dedicated to macro transmission and one to the deployed small cell. In this fashion, the macro layer performance is better than the case where the overall band is allocated to small cells, thus reducing the number of deployed small cells. A similar strategy is beneficial with joint deployment of femtos and micros.

- *In case of small deployment on a macro-free carrier, a cell selection bias (e.g. a 3 dB SINR bias) applied at the small cells is recommended to further enlarge the footprint of the low power nodes and improve user offloading.*

Which small cell deployment configuration is the most cost-effective?

- *Macro upgrade to additional low frequency spectrum is as cost-efficient as relay deployment. For similar coverage performance, co-channel micro deployment is economically profitable compared to relays on condition that a trade-off between high and low-cost micro backhaul, nearer to the lower bound, is achieved.*

  From an infrastructure cost point of view, in-band relay deployment is more profitable than macro densification in the coverage-limited scenario, and it gives similar performance to upgrading the macro layer with an additional carrier in the low frequency band. When guaranteeing the same coverage requirement, co-channel micro cells can achieve better cost performance than deploying both an additional TDD macro carrier and out-band relays in

urban Hot-Zone areas. By estimating two cost extreme cases for micro deployment, this occurs if the micro backhaul related costs can be kept closer to the proposed low-cost micro estimate.

- *For high small cell densities, massive OSG femto cell deployment is the most cost-effective solution*

  In Hot-Zone areas, indoor femto-only deployments yield the best cost performance (together with the highest data rates) on condition that running costs are kept low by leveraging the customer's broadband connection at the indoor premises. Micro-only or joint micro femto deployment can yield a competitive cost performance only under low-cost micro assumptions, and this becomes a stringent requirement to ensure the viability of micro deployment.

8.2 Recommendations for Small Cell Studies

The methodology and outcome of the thesis can also be utilized to improve the simulation setup and update the simulation assumptions of regular 3GPP network scenarios [62, 153]. The use of real network layouts and traffic distributions based on measurements allow operators to more easily understand the potential of small cell deployment. Thus, network inhomogeneity and more complex propagation assumptions could be applied to regular scenarios for a more accurate approximation of real life deployment characteristics related to small cell deployment. Briefly, the most important suggestions revolve around the following:

- Introduce different macro ISD within the same simulation scenario, e.g. 100 250 and 500 m, to render the network layout more inhomogeneous. Different cell sizes and macro site positions would give a more realistic modeling of cell density and also interference from surrounding macro cells. For example, the relay case studies have shown how interference on the relay backhaul link influences the selection of the relay site and its performance, without having the possibility of positioning relays precisely on regular cell-edge borders or deploying more than 5 relays per macro donor cell.

- Consider spatial inhomogeneous traffic (e.g. log-normally distributed), having that the distribution of traffic across the reference macro cells is non-uniform (e.g. 50% of traffic in 20-30% of the cells). This leads to a more targeted small cell deployment that combines sparse and dense small cell deployment within the same scenario.

- Take into account the use of different frequency bands, and tune the propagation losses so that the difference in path loss between, for instance, 800

MHz, 2.6 GHz and 3.5 GHz is accurately modeled. This is particularly important for coverage-limited scenarios and small deployment at higher frequency bands.

- Place multiple buildings in the investigated area in such a way that the indoor area percentage is in line with an average urban environment. As for high-rise building, it becomes crucial to introduce floor height gains for macro transmission over rooftops. Moreover, outdoor small cell coverage prediction can be improved by introducing vertical antenna pattern to radiate the signal towards multi-floor buildings.

8.3 Future Work

This final section looks at different aspects and topics that could be of particular interest to extend the presented work. The suggestions revolve around the methodological approach of the deployment study and the possibility of introducing new deployment features that have not been included in this dissertation.

When adopting a holistic approach to carry out a techno-economic analysis of different deployment solutions, it is clear that an additional effort can be spent on improving the specific modeling blocks. For instance, more accurate propagation and scenario models for small cells, especially in indoor areas, would help estimate small cell coverage in a more realistic way than statistical models. Another critical aspect is related to the backhaul link, particularly in strongly shadowed scenarios. In fact, the largely spread angle of arrival for the received signal makes the antenna pointing towards the donor more complex as compared to LOS conditions. In addition, more advanced iterative deployment algorithms can be utilized to optimize the positioning of small cells at the cost of increased simulation complexity, similarly to the micro cell deployment described in Chapter 6.

Regarding the case study methodology, an interesting approach would be that of evaluating network performance and required upgrades over a multi-year period in a realistic network scenario, based on different traffic growth predictions (e.g. steady or aggressive). In this way, it would be possible to combine different types of small cells according to the predicted traffic demand, and identify the most cost-effective solution over a certain amount of years. Furthermore, different KPIs and receiver assumptions associated with different users could be the first step towards modeling the fact that users have different devices, subscriptions and behavior when consuming data services. On top of this, evaluating uplink performance could be an additional step as the requirements on uplink traffic are also increasing at a fast pace.

Several deployment options have not been considered in this dissertation. For

example, the deployment of indoor pico cells covering large indoor areas with a transmission power level between 20 and 30 dBm can be investigated, on condition that accurate models about hotspot location and propagation losses are available. Another realistic option is that of deploying CSG femto cells, especially in residential areas, although interference management schemes may be needed in the co-channel deployment case to safeguard the users who do not belong to the femto subscriber group. However, the most important future step is to evaluate the viability of deploying indoor (and also outdoor) WiFi access points, which already have a dominant market position. The 802.11n version of the standards can theoretically guarantee peak data rates that are similar to the one ensured by the first release of LTE, but WiFi nodes transmit on unlicensed spectrum. Relying on realistic performance models including interference from other user-deployed WiFi nodes, the target would be to investigate whether WiFi access points are more cost-effective than femto cells or they should both be deployed to meet increased traffic demands in the long-term.

When considering advanced features for small cell co-channel deployment, one possibility is to model the impact of advanced interference cancellation schemes based on inter-cell coordination between macro and micro/pico cells (LTE eICIC). By temporarily muting macro transmission or lowering the transmission power of surrounding macro sites, micro co-channel deployment can benefit from reduced interference while extending micro cell coverage. Moreover, if coordination between macro and small cells can be guaranteed, advanced traffic steering policies can be envisaged to optimize the traffic offload towards the small cells. Regarding relays, the use of advanced antenna techniques, such as beamforming or Spatial Division Multiple Acess (SDMA), could be explored as a potential means of improving the backhaul link capacity although the behavior of such solutions in realistic scenarios is partially unknown.

Appendix A

Network Simulator Structure and Simulation Accuracy

This appendix presents the description of the simulator utilized to estimate the radio performance of the investigated deployment scenarios. The target is to gain a better understanding of the simulation method and the different steps needed to evaluate the performance indicators. In addition to this, considerations about simulator calibration and simulation accuracy are provided.

A.1 Network Simulator Description

The main KPIs, namely user outage and average user throughput, are estimated by means of a static Monte-Carlo based downlink network simulator that has been developed during the course of the PhD project. In each snapshot of the Monte-Carlo simulation a realization of the user density spatial distribution is obtained, thereby assigning the position of the users over the network area. Fig. A.1 shows the flowchart of main simulation steps and iterations, from network input data loading to the collection of the final statistics. The models behind each simulation block are described in Chapter 3.

The first simulation step deals with the initialization of the network scenario. This means to load the existing macro layout, including radio parameters (supported

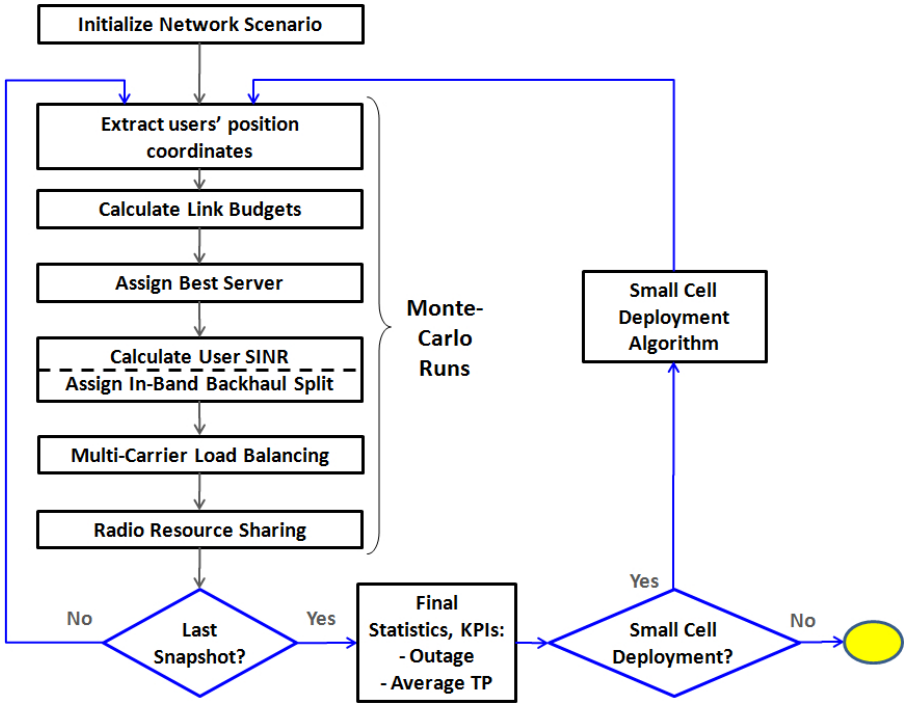

Fig. A.1: Overview of the simulation flow related to the developed static network simulator. Different realizations of the user density distribution are extracted in each of the Monte-Carlo runs, and the final statistics are collected by averaging out the radio performance obtained over the different snapshots. When small cells are deployed, the reference macro performance serves as an input to the deployment algorithm block.

frequencies, antenna patterns, feeder losses, etc.) and position coordinates. At this stage, terrain and clutter maps can be loaded to consider the height difference between transmitter and receiver, and the location of indoor areas. After setting up the network scenario, a random set of users is generated according to the utilized user density map. This is repeated for each snapshot of the Monte-Carlo simulation with the assumption that random variables associated with user location are independent and identically distributed (i.i.d.).

Given the position of users, the link budget between each user and each transmitting cell is calculated, based on path loss and antenna radiation patterns. The path loss is estimated according to statistical models or preloaded path loss maps obtained with raytracing. The link budget is used to calculate the received signal power in the donwlink at the user side, for each base station and at each transmission frequency. By means of this, each user is assigned to the cell delivering the best wideband SINR performance. In this admission process, the SINR is calculated by assuming that each cell transmits at a certain fraction of the max-

imum power, i.e. the power used to transmit the LTE common pilot channels[1]. Moreover, a cell SINR bias can be applied to different types of base stations so as to extend the cell coverage.

The following simulation block addresses the calculation of the SINR experienced on the traffic channel, with full transmission power and under infinite buffer traffic assumptions. If in-band relays are deployed, such information is utilized to tune the backhaul link time ratio and jointly optimize the performance of users connected to relay cells and the overlay macro donor cell (refer to subsection 3.4.2 for details). At this point, user SINR and corresponding wideband throughput performance are utilized to assign cell resources to the users. If multiple carriers are deployed at the macro layer, users are first allocated to one of the carriers according to the proposed load balancing algorithm. Then, cell radio resources are assigned to the connected users based on a scheduling algorithm that is aimed at providing each user with the predefined minimum data rate.

The network simulation is repeated according to a specified number of Monte-Carlo iterations. Once all runs are completed, the final statistics are collected, and the main KPIs are given by user outage and average user throughput. These values are obtained by averaging out the network performance indicators over the different simulation runs. In case small cell deployment is enabled, the preliminary macro simulation is used to provide the input to the small cell deployment algorithm (macro outage and network SINR coverage). Upon selecting the locations of the small cells, the network simulation runs are performed again with the enhanced network deployment, and the final statistics including small cells are generated.

A.2 Network Simulator Validation and Accuracy

To validate the output of the employed static network simulator, a G-factor[2] distribution has been compared with the one obtained in an LTE-A system level simulator that has been validated and calibrated in previous studies [118, 155]. In order to compare the two simulators, a typical hexagonal macro scenario with a 500 m ISD is assumed according to the radio transmission parameters suggested in [62]. Fig. A.2 shows the resulting G-factor cumulative distribution for a limited number of snapshots, where 10 users per macro cell are uniformly distributed over the cell area. It can be stated that the alignment between the two G-factor distributions can be considered acceptable within the simulation accuracy, with absolute differences being below 1 dB.

[1]The calculated SINR is proportional to the Reference Signal Received Quality (RSRQ) that each user equipment measures on the LTE reference symbols to estimate the channel signal quality [154].

[2]This corresponds to a wideband SINR calculation, assuming full load from interfering cells and averaging out the received signal power over fast fading

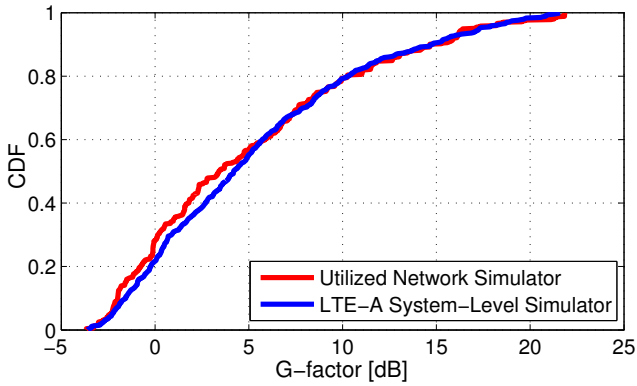

Fig. A.2: G-factor cumulative distributions for the utilized static network simulator and an LTE-Advanced system-level simulator utilized in [118, 155].

Another important aspect is the statistical relevance of the presented simulation results, which consists in assessing the confidence interval for each of the presented KPIs. By denoting X^i_{KPI} as the KPI value obtained at the $i-th$ run of the Monte-Carlo simulation, the average network performance is estimated by means of the sample mean estimator:

$$\hat{\mu}_{est} = \sum_{i=1}^{N} \frac{X^i_{KPI}}{N} \tag{A.1}$$

where N is the number of runs. Besides the sample mean estimator, it is possible to define the sample variance as follows:

$$\hat{\sigma}^2_{est} = \frac{\sum_{i=1}^{N}(X^i_{KPI} - \hat{\mu}_{est})^2}{N-1} \tag{A.2}$$

The sample mean estimator, $\hat{\mu}_{est}$, is an approximation of the true mean value of the considered KPI, $\bar{X}$. In each run of the Monte-Carlo simulation, X^i_{KPI} is obtained by considering a realization of the traffic density distribution and, in some scenarios, the random variables associated with the probability of LOS between relay (or micro) cells and the user (refer to equations 4.3 and 5.1). As explained in [156], it is possible to calculate the confidence interval in which the difference between the true mean $\hat{\mu}_{est}$ and the sample mean $\bar{X}$ is contained with a probability of 95%. This condition can be expressed as follows:

$$Pr\{\left|\bar{X} - \hat{\mu}_{est}\right| < 1.96\frac{\hat{\sigma}_{est}}{\sqrt{N}}\} = 0.95 \tag{A.3}$$

Therefore, the quantity $d = 1.96\hat{\sigma}_{est}/\sqrt{N}$ represents half the 95% confidence interval, i.e. $\hat{\mu}_{est} \pm d$. To provide insight into the simulation accuracy of the presented numerical examples, the Hot-Zone scenario investigated in Chapter 5 is selected as a reference for the statistical analysis of the simulated data. The reason is that such scenario presents a more spread spatial distribution compared to other scenarios, and also probabilistic path loss models. This implies that more realization of the statistical distributions are needed to achieve an acceptable simulation accuracy.

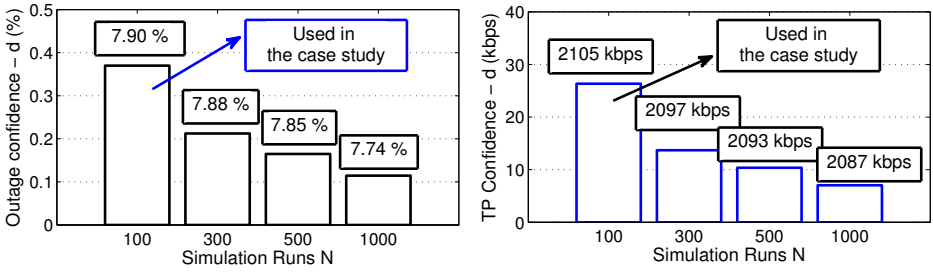

(a) User Outage

(b) Average User Throughput

Fig. A.3: Half length of the 95% confidence interval, d, for both the user outage and average user throughput for a selected Hot-Zone scenario featuring 50 in-band relays. The simulated sample mean estimators are indicated in the text boxes, and the confidence intervals have to be applied on top of them.

By considering the main KPIs, user outage and average user throughput, the sensitivity of the 95% confidence interval to the number of simulation runs is shown in Fig. A.3, for 50 in-band relays[3]. With regard to user outage, it can be seen that 100 snapshots give a 95% confidence interval with d lower than 0.4%. This means that the presented outage performance can be expressed as 7.9±0.37%. The accuracy increases with a larger number of snapshots, and the same behavior can be observed for the average user throughput. With the lowest number of runs, the confidence interval d, which is equal 26 kbps, is less than 1.5% the simulated throughput value.

In this dissertation the final statistics have been collected after 100 simulation snapshots in all the investigated scenarios. The achieved simulation accuracy is considered to not affect the presented performance and cost analysis trends and the recommended network evolution strategies.

[3]The user outage performance can be observed in Fig. 5.10(a) in Chapter 5

Appendix B

Further Insights on Network Performance Results

The target of this appendix is to complement the network performance results presented in the previous chapters. Emphasis is put on the calibration of the heuristic deployment algorithm (refer for details to subsection 3.6), which is needed to reduce the user outage. In addition to that, further details on femto user locations and inter-layer load balancing are provided, based on the indoor deployment case study presented in Chapter 7.

B.1 Relay Deployment Insights for the Suburban Case Study

In the suburban case study (see Chapter 4) the utilized input parameters for the deployment formula of Eq. 4 are listed in Table 4.2. The parameters were selected according to a coverage oriented approach for relay cells. To properly tune the heuristic deployment algorithm, a sensitivity study has been carried out based on different values of the deployment parameters. The selected scenario presents 50 in-band relays together with a single-band macro layer, as shown in subsection 4.3.2. The highlights from the sensitivity study are depicted in Fig. 4 for the parameters $wCov$ and $wOut$, although a similar analysis has also been conducted – but not presented in this dissertation – for other input parameters such as relay minimum

ISD or the metric area A_i for the $i-th$ candidate location. It can be seen that the user outage is remarkably more sensitive to the outage weight than the coverage one. The reason is that $wOut$ allows the deployment algorithm to prioritize areas covered by high outage macro cells. On top of this, the choice of the coverage weight can be optimized to strike the balance between the low SINR regions and user spatial density.

Scenario	wCov	wOut	Outage
Macro only	-	-	10.8 %
50 in-band relays (Traffic)	0.2	2	11.1 %
50 in-band relays (Coverage)	**0.8**	**3**	**7.3 %**

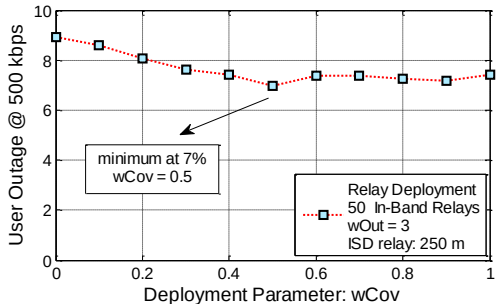

Fig. B.1: Deployment formula calibration for in-band relay deployment (50 relays) in the suburban scenario presented in Chapter 4. After choosing the parameter setting highlighted in the table located on the left, the user usage sensitivity to the parameter $wCov$ is studied so as to select the best value for user performance.

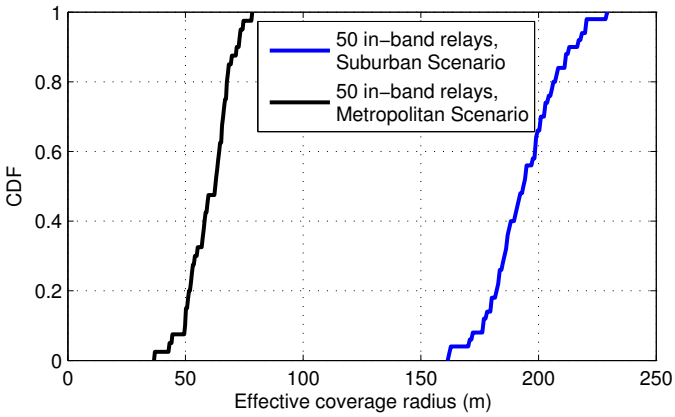

Fig. B.2: Relay Effective coverage radius distribution for the suburban scenario, considering 50 in-band relays. The curve is compared to the relay deployment performed in the Hot-Zone scenario of Chapter 5 for the same number of deployed relays.

Another insight on in-band relay deployment is given by the relay coverage area extension in different deployment scenarios. Fig. B.2 shows the cumulative distribution of the relay effective coverage radius, i.e. the radius of the ideal circle having the same area as the one covered by the relay, when 50 in-band relays are deployed. In the suburban (coverage-limited) scenario the coverage radius is

approximately 3 times larger than in the Hot-Zone scenario (addressed in Chapter 5) due to sparser macro deployment, higher relay transmission power, and larger minimum relay ISD. For the same reasons, it can also be observed that the variation of effective coverage radius is more pronounced in the coverage-limited scenario than in the metropolitan one.

B.2 Deployment Algorithm Calibration in the Hot-Zone Case Study

A similar process for selecting the deployment algorithm input parameters has been repeated to position relay cells in the Hot-Zone case study of Chapter 5. The deployment algorithm has been, also in this case study, tuned based on in-band relay deployment performance. By setting the coverage $wCov$ to 0.5 as in the suburban case study, the backhaul link SINR and macro outage are both considered to optimize the relay positioning. Fig. B.3 shows the user outage sensitivity to different combinations of wBH and $wOut$, together with the impact on relay backhaul SINR. This example is based on 20 deployed in-band relays.

wOut	wBH	Outage (macro reference **14.6 %**)
3	1	19.3 %
3	3	10 %
2	3	8.4 %
2	**4**	**8.2 %**

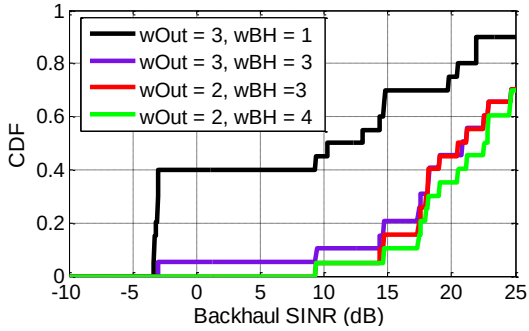

Fig. B.3: Deployment formula calibration for in-band relay deployment (20 relays) in the urban scenario presented in Chapter 5. The utilized parameter setting is highlighted in the table located to the left ($wCov$ is fixed at 0.5), whereas the sensitivity of the backhaul signal quality to the deployment strategy is depicted in the right figure.

The sensitivity study points out the impact of ensuring high backhaul SINR on the overall relay network performance. With wBH set to 1, half the relays perceive a backhaul SINR that is lower than 10 dB. This results in an overall user outage that exceeds the level achieved with the macro-only deployment. To relieve the backhaul link capacity bottleneck, wBH is to be increased with a higher priority than the outage weight. By raising the backhaul weight from 1 to 4, the backhaul SINR can improve by more than 10 dB, and the user outage can be reduced by around 10 percent points.

B.3 Femto Deployment Insights

This section provides further details on femto deployment strategies and user performance for different femto configurations, assuming the same network scenario of Chapter 7. Fig. B.4(a) compares different femto deployment strategies for co-channel femto deployment, showing traffic-driven (used when presenting the case study results) and outage-driven deployments. The latter is implemented by utilizing the outage user density map instead of plain user density, based on the reference macro-only performance. It can be inferred that the outage driven deployment does not yield significant gains in terms of user outage. This is due to the fact most users are placed indoors, and outage users are basically located in high traffic locations. As a consequence, traffic and outage spatial distributions tend to overlap. Moreover, Fig. B.4(b) shows the network outage performance for co-channel femto deployment (1000 access points) when employing different transmission bandwidths. By reducing the femto transmission bandwidth from 20 to 5 MHz, macro users are less interfered by co-channel femtos, and this translates into better macro performance with regard to user outage. Although femtos have less spectral resources, the average femto user load is not so high that femto users cannot be provided with the minimum data rate. However, the performance improvement does not allow the network to hit the 10% outage target.

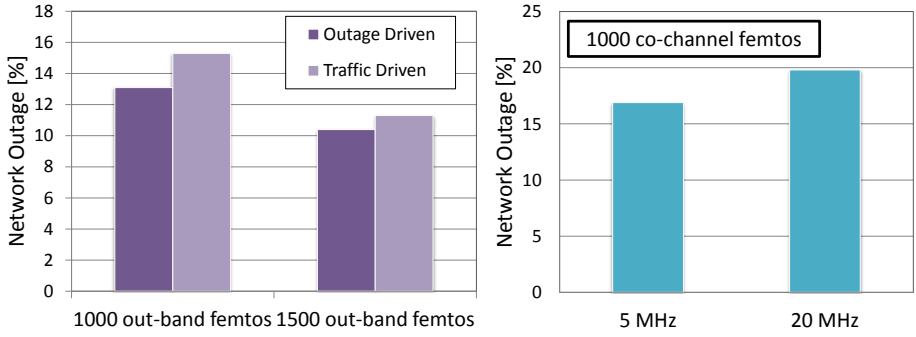

(a) Deployment Strategy (b) Femto Bandwidth

Fig. B.4: User outage sensitivity to different out-band femto deployment strategies (left) driven by traffic or outage, and reduced transmission bandwidth for co-channel deployed femtos (right).

Co-channel femto user geometry is shown in Fig. B.5(a), for femto outdoor, indoor ground floor, and indoor upper floors users. Given 1000 femtos deployed at the ground floor, most femto users – approximately 90% as shown in Fig. B.5(b) – are located indoors. Outdoor users experience worse SINR conditions than the indoor ones as the femto signal is attenuated by the building external wall, and interference from macro cells is also higher. With regard to indoor users, it can be seen that the highest femto SINR is experienced at the ground floor due to the

proximity of the transmitting cell. However, on the upper floors, femto user SINR decreases because of the floor penetration signal losses and the macro interference that increases with the receiver height. When out-band femtos are deployed, the indoor cells extend their coverage, not only indoors, but also outdoors. Indeed, Fig. B.5(b) shows that the share of outdoor users increases when shifting from co-channel to out-band by around 10% points.

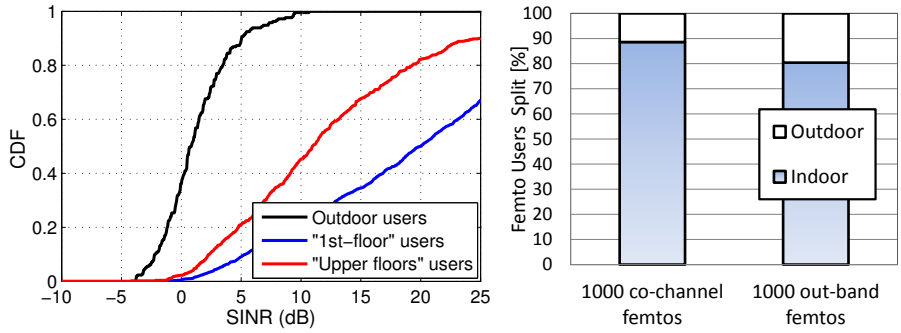

(a) Co-Channel Femto User SINR

(b) Femto Users Split

Fig. B.5: Insights on femto users SINR with 1000 co-channel deployed femtos (left) for different user locations, and outdoor/indoor femto user split (right) for co-channel and outband femto deployment.

B.4 Inter-Layer Load Balancing for Co-Channel Femto Deployment

Smart and adaptive user load balancing between different deployment layers, such as from macro to small cells, has not been explicitly addressed in this dissertation. Under co-channel deployment assumptions, the coverage of small cells is significantly limited by the macro cells transmitting at higher power, and the increased interference level impairs the network performance. Assuming, for example, the deployment scenarios described in Chapter 7, it is known that part of the users who would connect to small cells on the shared band at 2.6 GHz are ultimately connected to the dedicated macro "escape carrier" due to better SINR conditions

A simple, yet effective option to better balance the load between users is given by an SINR threshold that is used to force the inter-frequency hand-over from the macro escape carrier to the small cells. Fig. B.6 shows the impact of utilizing this inter-layer load balancing policy on a combined deployment of 40 micros and 1000 femtos sharing their transmission band at 2.6 GHz with the macro layer (refer to Table 7.1 for the full scenario set-up). The SINR threshold is applied, as an

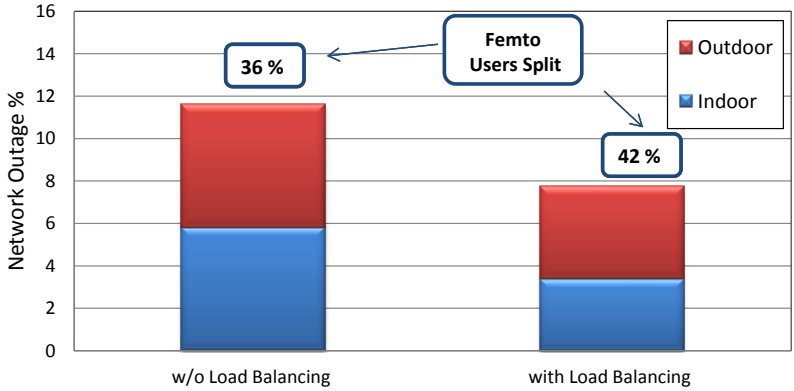

Fig. B.6: User outage performance with and without inter-layer load balancing in a scenario featuring a co-channel deployment of macro, pico and femto layer. The SINR threshold is set at 0 dB.

example, to the femto layer only, and it is set at 0 dB. The threshold applies to all the users connected to 800 MHz, but having a femto cell as potential best server on the 2.6 Ghz band. These are forced to connect to the femto layer if the femto SINR exceeds the 0 dB SINR threshold. By means of this, the percentage of users connected to femtos increases by 6 percent points, and as a result the overall user outage decreases from 12 to 8%.

The simple algorithm shows that a smarter distribution of the user load amongst the layers is beneficial for the network performance. Obviously, the implementation of such a feature requires tight coordination between the different deployment layers, and it can be extended to all types of deployed small cells. In addition, information about cell load can be exploited to adaptively and dynamically set the hand-over threshold so as to optimize the network KPIs.

Appendix C

Deployment Cost Breakdown for TCO analysis

The appendix provides the detailed price list that is utilized for the TCO analysis of iso-performance scenarios. These are compared under the assumption that the network upgrades are deployed in the same year, and the running costs are considered over a period of 4 years. As described in Section 2.6, the radio access cost structure is made of three main components, and the overall TCO is calculated, for each of the investigated scenario, as follows:

$$TCO = \sum_{i=1}^{N_{BS}} (CAPEX_i + IMPEX_i + 4 \cdot OPEX_i) \tag{C.1}$$

where N_{BS} is the total number of base stations deployed in the network area. The OPEX is assumed to be a fixed value for each of the considered years. For the sake of simplicity, the multiplying factor of the running costs is equal to the number of years, although the overall OPEX can be discounted in case the Discounted Cost Flow model is applied [157]. For example, for a fixed yearly discount rate of 10%, the 4-year multiplying factor for OPEX becomes 3.5, but such estimation is strictly correlated with the assumptions behind the discount rate estimate.

The cost assumptions utilized in Part I and Part II are outlined in Fig. C.1 and C.2, respectively. The assumption behind the selected figures have been explained

in Section 3.7 and Section 7.6. The proposed cost structure is the same for all the investigated deployment solutions, but specific cost figures are assigned to each type of base station and macro upgrade. Within the same type of deployment solutions, the cost associated to a specific small cell or macro upgrade is the same independently of the position occupied in the network.

General Parameters	Newly deployed LTE Site	LTE site (reuse HSPA site)	LTE upgrade to 2nd carrier	Relay (High Cost)	Relay (Low Cost)	Micro (High Cost)	Micro (Low Cost)
Power Consumption (in Watts)	850	850	1000	120	120	120	120
Electricity costs (EUR/KW/hour)	0,15	0,15	0,15	0,15	0,15	0,15	0,15
CAPEX (€)	46000	35000	26500	3100	3100	8500	7500
Equipment (1+1+1)	18000	18000	18000	3100	3100	4000	4000
Backhaul (SDH MW connection)	17000	17000	8500	0	0	4500	3500
Auxiliary equipments (antenna + mast, battery, power supply)	11000	0	0	0	0	0	0
Others - Femto/WiFi GW	0	0	0	0	0	0	0
IMPEX (€)	53500	9000	5750	1380	750	6448,8	2448,8
Site acquisition	5000	0	0	350	350	371	371
Backhaul deployment	6500	6500	3250	0	0	4350	350
BTS installation/ Deployment	10000	2500	2500	400	400	318	318
Initial planning and network optimization	0	0	0	630	0	667,8	667,8
Site preparation	32000	0	0	0	0	742	742
OPEX (€) - One Year	19816,9	10916,9	2314	1210	1210	7789,68	2029,68
Site Rental	16000	8000	0	650	650	1272	1272
Operation and maintenance (BTS, tower, site, etc.)	1400	500	500	400	400	6360	600
Electricity Cost	1116,9	1116,9	1314	160	160	157,68	157,68
Backhaul maintenance	1300	1300	500	0	0	0	0
CAPEX split (%)	38,55	63,73	76,67	54,48	61,26	37,38	62,61
IMPEX split (%)	44,84	16,39	16,64	24,25	14,82	28,36	20,44
OPEX split (%)	16,61	19,88	6,69	21,27	23,91	34,26	16,94

Fig. C.1: Deployment cost breakdown of fixed and running costs (in Euros) for the deployment options considered in first part of the dissertation. At the bottom of the table CAPEX, IMPEX and OPEX cost splits with reference to the total one-year TCO are considered

General Parameters	LTE site (reuse HSPA site)	LTE upgrade to 2nd carrier	Micro (High Cost)	Micro (Low Cost)	Femto (High Cost)	Femto (Low Cost)
Power Consumption (in Watts)	850	850	80	80	12	12
Electricity costs (EUR/KW/hour)	0,15	0,15	0,15	0,15	0,15	0,15
CAPEX (€)	18500	12000	7500	1500	220	70
Equipment (1+1+1)	15000	12000	4000	1000	200	50
Backhaul (SDH MW connection)	2000	0	3500	500	0	0
Auxiliary equipments (antenna + mast, battery, power supply)	1500	0	0	0	0	0
Others - Femto/WiFi GW	0	0	0	0	20	20
IMPEX (€)	12500	8500	2330	1500	380	0
Site acquisition	0	0	350	350	0	0
Backhaul deployment	500	0	350	250	0	0
BTS installation/ Deployment	12000	8500	300	300	0	0
Initial planning and network optimization	0	0	630	300	180	0
Site preparation	0	0	700	300	200	0
OPEX (€) - One year	5616,9	1616,9	3205,12	605,12	20	50
Site Rental	1000	0	100	100	0	0
Operation and maintenance (BTS, tower, site, etc.)	2000	500	1000	300	20	50
Electricity Cost	1116,9	1116,9	105,12	105,12	0	0
Backhaul maintenance	1500	0	2000	100	0	0
CAPEX split (%)	50,52	54,26	57,54	41,61	35,48	58,33
IMPEX split (%)	34,14	38,43	17,87	41,61	61,29	0,00
OPEX split (%)	15,34	7,31	24,59	16,79	3,23	41,67

Fig. C.2: Deployment cost breakdown of fixed and running costs (in Euros) for the deployment options considered in second part of the dissertation. At the bottom of the table CAPEX, IMPEX and OPEX cost splits with reference to the total one-year TCO are considered

Appendix D

Study on Relay Link Measurements and Positioning

Evaluation of Potential Relay Locations in a Urban Macro-Cell Scenario with Applicability to LTE-A

Ignacio Rodriguez, Claudio Coletti, Troels B. Sørensen

Radio Access Technology Section (RATE)
Deparment of Electronic Systems
Aalborg University, Denmark
{irl, cco, tbs}@es.aau.dk

***Abstract*— Relay base stations are expected to play an important role in extending coverage for beyond 3G networks, such as LTE-A. However, the signal quality experienced on the backhaul link between the macro-cell and the relay node has a major impact on the performance of the multi-hop transmission. This paper presents a measurement-based study focusing on the performance evaluation of the relay backhaul link for different potential relay locations and antenna configurations in a real urban macro-cell scenario. Based on the assumption that a similar network deployment would apply for LTE-A, a fully operational 3G network has been used for measuring both received signal strength and Signal-to-Interference-Ratio (SIR). Furthermore, the results have been used to estimate the performance of the multi-hop transmission under simplifying assumptions. The experimental results show that by increasing the relay height from 2.4 m to 5 m, the received signal strength improves on average by 1.7 dB for omnidirectional antennas. When a directional antenna is mounted at 5 m and pointed towards the serving macro cell, significant SIR gains (around 5.9 dB) and throughput improvements are achieved at the locations where the relay node and the macro-cell are in Line-of-Sight (LOS).**

I. Introduction

Relays have been extensively studied as a part of the 3rd Generation Partnership Project Long Term Evolution-Advanced (3GPP LTE-A) over the last few years [1]. In order to keep up with the always increasing data traffic demand, the deployment of relay base stations is envisioned to be an attractive feature for improving network coverage and also enhance user data rates [2–4]. As most of the available LTE spectrum will be released at higher frequency bands (e.g. the 2.6 GHz band), higher attenuation on the link between the user terminal and the serving macro-cell may result in network coverage issues. Therefore, increasing the density of the existing macro network with low-powered relay nodes is expected to boost the performance of cell-edge users with reasonable expenditure as compared to the major investments needed for deploying new macro site or acquiring lower frequency spectrum. Moreover, one of the limiting factors (and cost drivers) for small cell deployment is backhaul, since wired fiber access is in most cases cost-prohibitive or not feasible. From this perspective, relay wireless backhauling that uses LTE spectrum provides a competitive edge against wired backhaul although this comes with trade-off in capacity and shared radio resource usage.

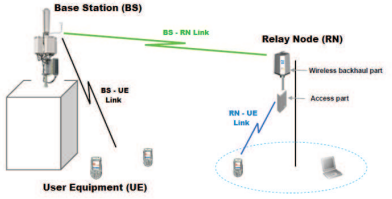

Fig. 1: Overview of the different transmission links involved in a relay-enhanced network.

By deploying relay nodes (RN), the distance between base station (BS) and user equipment (UE) is split into two hops, as shown in Fig. 1, thus reducing overall path loss between the UE and the BS. In a relay-enhanced network, there exist three different types of radio links: direct link (BS-UE), backhaul link (BS-RN) and access link (RN-UE). When considering the path loss associated with the previously mentioned links, the direct link between BS and UE is in general modeled with confidence thanks to previous extensive measurement-based investigations, e.g. [5], and the statistical models derived thereof. However, when the propagation occurs from over roof-top to street lamp post height, as illustrated in Fig. 2 for a typical backhaul link, the existing statistical models are less accurate [6]. Furthermore, some of the issues related to the backhaul link modeling are given by the use or assumption of planned relay node positions and/or directional characteristics of the link. Relay site planning is generally needed to boost the performance of the backhaul link so that it does not act as a bottleneck for relay access link transmission [3]. Because of this, a larger set of empirical data is required for extrapolating an accurate channel model for relay site planning.

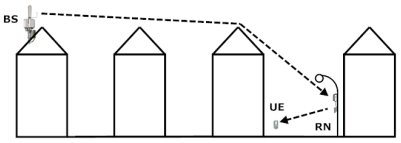

Fig. 2: Propagation mechanism in a urban relaying scenario.

This paper focuses on the performance of the backhaul link based on a measurement campaign conducted in a realistic urban scenario. A fully operational 3G network has been used for conducting the measurement campaign, and the main target is to show how sensitive relay deployment is with respect to receive antenna height, receive antenna type (omnidirectional or directional) and expected overall performance for different potential relay locations. Differently from [6] and [7], the results from the measurements include not only received signal strength but also the experienced Signal-to-Interference-Ratio (SIR), which describes the effect of interfering neighboring sites on the performance of the backhaul link. The measured SIR values are then utilized to estimate the achievable data-rates over the multi-hop transmission when different relay locations are considered. The remaining part of this paper is organized as follows: Section II describes the measurement campaign performed, Section III illustrates the results from the measurement campaign results, Section IV gives an overview of the achievable relay performance, and finally, Section V provides a conclusion.

II. Measurement campaign

The measurement campaign was performed in the city centre of Aalborg, Denmark. The environment, illustrated in Fig. 3 is a typical urban medium city where average building height and street width are about 15-18 m (3-4 floors) and 7-12 m, respectively. Measurements were made on the 2100 MHz High-Speed Downlink Packet Access (HSDPA), Wideband Code Division Multiple Access (WCDMA) network of the telecommunications operator Telenor.

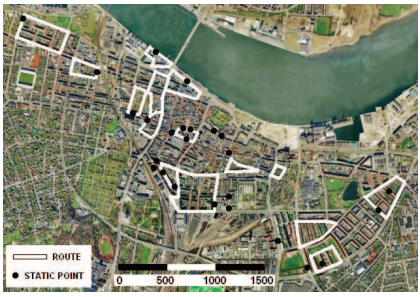

Fig. 3: Aerial view of the measurement area.

For this area, base stations are normally located above roof-top. 15 different nodes (45 cells) placed around the city centre were included in the campaign. The average inter-site distance is approximately 600 m. Transmit antennas are typical sectorial with 65° half-power beamwidth in azimuth and 5° in elevation, and a maximum gain of 18 dBi. The maximum transmitted power is set at 43 dBm.

At the reception end, two different types of antennas were used: two omnidirectional dipole antennas, with a gain of 2 dBi, were mounted on a van to perform drive measurements at 2.4 m and 5.0 m height. In addition to this, a directional antenna, with 8 dBi of gain and a beamwidth of 80° in azimuth and 60° in elevation, was mounted on a 5 m high mast in order to simulate a lamppost relay and perform static measurements. The whole measurement setup is illustrated in Fig. 4.

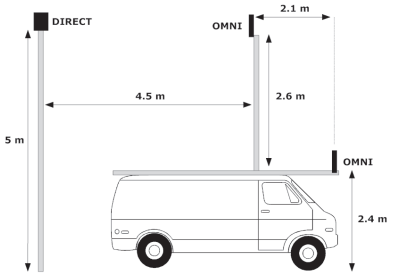

Fig. 4: Measurement setup with 3 different receive antennas.

The drive measurements consisted in driving the 15 different routes indicated in Fig. 3 across the city. These routes were located at cell-edge and included different kinds of propagation scenarios such as In-between-Building (IN-BB) or Line-of-Sight (LOS). The objective was to evaluate height gain, so the highest power signal from the different base stations was recorded at these two different heights (2.4 m and 5.0 m). The average length of the routes was 750 m, the average speed was 14 km/h and the sampling speed was 20 samples/s; effectively, there were 3857 samples available for comparison on each of the routes.

The static measurements were performed at the 25 different locations shown in Fig. 3. The positions were selected on a qualitative basis to include different, and what was deemed typical, relay positions for a lamp post mounted relay. In this sense, the chosen positions reflect the practical situation, where performance optimized planning is usually not possible. The directional antenna was pointed in the direct LOS direction towards the base station (sector) with the highest average signal level in the area - named hereafter “the donor base station”. According to propagation conditions, the measured positions can be classified as follows:

- LOS: direct view of the donor base station (clear LOS) or directional antenna pointing to a main street directly illuminated by the donor base station (almost LOS).
- IN-BB: typical In-between-Building locations or environments where it is possible to point the directional antenna along a street towards the desired donor base station. This is the most probable location for relay deployment (typical pedestrian street, commercial areas, etc.). An example of this scenario can be seen in Fig. 5.
- OTHER: Non-Line-of-Sight (NLOS) or severely shadowed environments (very narrow streets between tall buildings) where the link between the directional antenna and the desired donor base station is obstructed.

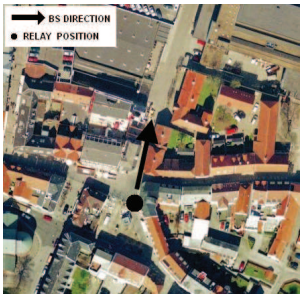

Fig. 5: Potential location for relay deployment in a pedestrian street inside a commercial area.

III. Analysis and Discussion of Measurement Results

Measurements focused on Received Signal Code Power (RSCP) and Interference Signal Code Power (ISCP). From these two parameters, Signal-to-Interference-Ratio (SIR) is defined in WCDMA as indicated in Eq. (1) with a spreading factor (SF) equal to 256 [8].

$$SIR = RSCP - ISCP + 10 \cdot log_{10}(SF) \quad (1)$$

Results are presented and analyzed for the drive measurements in the first place (omnidirectional antennas at different heights), and then for the static measurements (directional antenna and omnidirectional antenna at same height). Although the values are extracted from a 3G network, the conclusions drawn from the measurements would be applied to an LTE-A system. RSCP ans ISCP are averaged over a 5 MHz bandwidth, but the differences in signal strength between two different antenna configurations are representative also for larger bandwidths, such as 20 MHz for LTE-A. Then, the measured SIR can be used to estimate the corresponding wideband SIR for an LTE-A system, as explained in Section IV.

A. Height gain with omnidirectional antennas.

To evaluate the effect of the receive antenna height, the measurements from the omnidirectional antenna at 5.0 m were compared sample by sample with the measurements from the omnidirectional antenna at 2.4 m. This comparison was done in terms of received power (RSCP) and SIR as indicated in Eq. (2) and Eq. (3).

$$RSCP\text{-}HG = RSCP_{\ OMNI\ 5m} - RSCP_{\ OMNI\ 2.4m} \quad (2)$$

$$SIR\text{-}HG = SIR_{\ OMNI\ 5m} - SIR_{\ OMNI\ 2.4m} \quad (3)$$

where RSCP-HG (RSCP Height Gain) and SIR-HG (SIR Height Gain) indicate the gain in signal level or SIR at 5.0 m compared with the signal level or SIR at 2.4 m, respectively.

Fig. 6 shows the average RSCP-HG for each route. Received power is on average 1.77 dB higher at 5.0 m than at 2.4 m. These power height gain results are in agreement with [6] and [7]. Received power increases with height, or in other words, link path loss decreases with increased receive antenna height. For some routes, this value is around 3 dB which is the typical floor height gain considered in many studies [9].

The irregular result observed in Route 15 is explained by the complex propagation condition at some points of the route, where the classification condition was not always IN-BB as in the other cases.

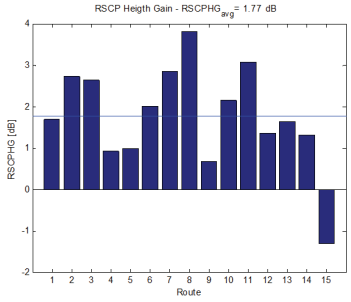

Fig. 6: RSCP Height Gain

The average SIR-HG for each route can be seen in Fig. 7. The measured SIR is on average 1.83 dB lower at 5.0 m than at 2.4 m. This means, that received power is higher at 5.0 m, but also interference from other base stations, which leads to a lower SIR.

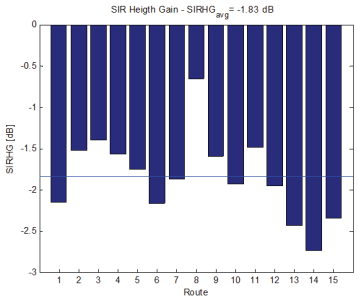

Fig. 7: SIR Height Gain

B. Directional antenna vs. omnidirectional antenna.

The impact of different antenna types was investigated on the static positions. In this case, the measurements from the directional antenna at 5.0 m are compared with the measurements from the omnidirectional antenna at same height as previously explained.

This comparison is done as in the previous section, in terms of RSCP and SIR as indicated in Eq. (4) and Eq. (5).

$$RSCP\text{-}TG = RSCP_{\ DIRECT\ 5m} - RSCP_{\ OMNI\ 5m} \quad (4)$$

$$SIR\text{-}TG = SIR_{\ DIRECT\ 5m} - SIR_{\ OMNI\ 5m} \quad (5)$$

where RSCP-TG (RSCP Type Gain) and SIR-TG (SIR Type Gain) indicate the gain in signal level and SIR from the directional antenna at 5.0 m compared with the signal level and the SIR from the omnidirectional antenna at the same height, respectively.

The different patterns have an impact in both RSCP and SIR, but more highlighted in SIR, since the directional antenna is expected to be capable of filtering interference with respect to the omnidirectional antenna.

Fig. 8 shows RSCP-TG for the 25 different positions measured. It can be seen that in both LOS and IN-BB situations, RSCP-TG is larger than 0 dB, which means that received power level is higher for the directional antenna than for the omnidirectional antenna. For the considered static positions, RSCP-TG is on average 6.33 dB for LOS and 3.70 dB for IN-BB. This difference can be explained by the fact that multi-path is more pronounced in IN-BB locations and thus means that despite of the lower gain of the omnidirectional antenna, it is capable of collecting more power from different reflections. This behavior is even more marked in the OTHER locations where RSCP-TG is smaller than 0 dB.

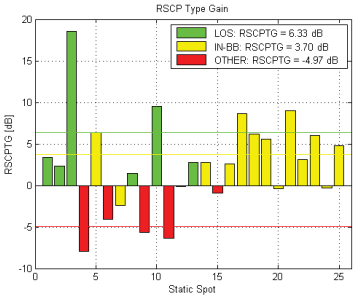

Fig. 8: RSCP Type Gain

Fig. 9 illustrates SIR-TG for all the different measured locations. For the locations where SIR-TG is larger than 0 dB, it can be concluded that the directional antenna is capable of filtering interference compared to the omnidirectional located at the same position. SIR-TG is on average 5.82 dB for LOS and 1.73 dB for IN-BB. This means that it is possible to filter more interference when pointing directly to the desired donor base station in LOS conditions than in typical IN-BB situations where relays are expected to be deployed.

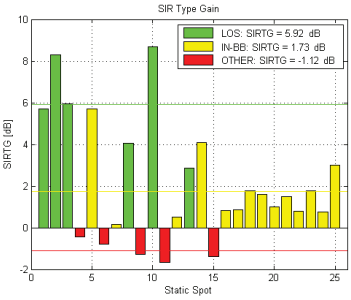

Fig. 9: SIR Type Gain

As it can be seen for OTHER locations, the directional antenna presents a lower SIR than the omnidirectional, indicating that the directional antenna is incapable of filtering interference in environments that are highly affected by shadowing.

Focusing on the IN-BB locations, the directional antenna does not give a significant gain in terms of SIR compared with the omnidirectional. In some cases, the problem comes when deciding where to point the directional antenna since the direction to the desired donor base station can be blocked by a building. This means, that more accurate positioning of the relay node is needed so that a clear desired signal from the selected donor can be received (i.e. pointing the directional antenna along a street towards the donor base station).

IV. Relay performance evaluation

To analyze the benefits of using a RN instead of a conventional direct link (BS-UE), a study has been carried out based on the previous measurements assuming that the observed statistics and scenario would apply to an LTE-A deployment of relay nodes. One LOS and four IN-BB locations have been selected to compare the actual performance of the direct link from a BS to a UE placed at 2.4 m height with a relayed link (BS-RN-UE) where the RN uses a receive directional antenna placed at 5.0 m. At each of the potential RN locations, the lowest 5%-ile SIR on the direct link from UEs located in the dominance area of the RN is selected, assuming a maximum radius of 44 m for the relay cell. Then, the performance on the direct link will be compared with the relayed link. The SIR values on the different links are shown in Table I.

A. Performance modelling.

In order to consider the wideband SIR (SIR_{wb}) values that are experienced on the traffic channel of an LTE-A transmission in the downlink, the measured SIR must be corrected by considering the spreading factor on the HSDPA traffic channel ($SF = 16$) in Eq. (1). Moreover, considering also that the RSCP is calculated on the pilot bits while the ISCP is calculated considering orthogonal and non-orthogonal

parts, it is necessary to re-scale the overall power which can be received on the traffic channel by a factor of approximately 10. The resulting SIR_{wb} can be mapped into throughput (TP) using a simple model based on a modified Shannon capacity formula [10] such as indicated in Eq. (6).

$$TP = 0.18 \cdot M \cdot \beta \cdot min \left\{ 10.5 \ , \ log_2 \left(1 + \frac{10^{\frac{SIR_{wb}}{10}}}{\mu} \right) \right\} \quad (6)$$

where $M = 100$ is the number of physical resource blocks occupied in a 20 MHz LTE-A transmission, and $\beta = 0.64$ and $\mu = 1.67$ parameters for the mapping in a macro scenario.

The overall throughput for the different links is indicated in Eq. (7) for the direct link and in Eq. (8) for the relayed link.

$$TP_{direct} = TP_{BS-UE} \quad (7)$$

$$TP_{relayed} = min\left(TP_{BS-RN}, TP_{RN-UE}\right) \quad (8)$$

Assuming that the UE is in close proximity of the RN, i.e. LOS conditions and significantly high SIR compared to other links, the performance over the complete relayed link is limited by the throughput experienced in the backhaul link as specified in Eq. (9). From this value, it is possible to calculate the effective throughput (TP_{eff}) by supposing half-duplex mode of operation. As realistic traffic load is not considered at the donor base station in terms of connected UE or multiple relays, a 50:50 time split between backhaul and access transmission subframes is assumed to calculate the end-to-end throughput. In this case, $TP_{eff,relayed}$ is half of $TP_{relayed}$ as indicated in Eq. (10).

$$TP_{relayed} \approx TP_{BS-RN} \quad (9)$$

$$TP_{eff,relayed} = 1/2 \cdot TP_{relayed} \quad (10)$$

To compare the performance over the two different end-to-end links, two metrics are defined: SIR gain (ΔSIR) and throughput gain (ΔTP).

TABLE I: Estimated SIR and throughput gains by using a relay at different potential locations.

$\mathbf{SIR_{BS-UE}}$ [dB] **UE : 2.4 m, 5%-ile**	**Relay Type**	$\mathbf{SIR_{BS-RN}}$ [dB] **RN : 5.0 m**	**ΔSIR** [dB]	**ΔTP** [%]
3.50	LOS	15.00	11.50	109
10.40	IN-BB	16.57	6.17	-11
5.60	IN-BB	14.59	8.99	44
4.30	IN-BB	10.11	5.8	13
2.10	IN-BB	7.61	5.51	21

B. Performance evaluation results.

The different SIR gain values shown in Table I are according to the type of location. In LOS, the highest gain is achieved (11.5 dB). In the IN-BB situations studied, this gain is lower and varies depending on the location. The average value of this gain in IN-BB conditions is 6.61 dB. As expected, the LOS relay, with the highest SIR gain leads to the highest throughput gain (109%). For this potential location, the RN can double the throughput experienced by a UE connected to it. One of the IN-BB potential locations presents a negative throughput gain (-11%), which means that for that particular location, SIR on the backhaul link is not sufficient to achieve a gain from relay deployment. For the other IN-BB locations, the average throughput gain is 26%, which is more than 3 times smaller than the one experienced in the LOS case.

V. Conclusion

This study analyzed the performance of the wireless backhaul link in an LTE-A relaying scenario by investigating the impact of the receive antenna at different potential relay locations. The performance evaluation has been based on measurements made in a real urban 3G macro-cell radio network, with relay positions chosen for typical LTE-A extension of the network. The analysis results show that both relay antenna height and type have an impact on the base station to relay link. Received power increases with height, with an average gain of 1.7 dB by increasing antenna height from 2.4 m to 5 m. The use of a directional antenna allows for filtering interference, obtaining an average SIR gain of 5.9 dB in LOS and 1.8 dB in in-between building locations compared to the omnidirectional antenna. By increasing SIR using directional antennas, the overall throughput experienced by a user connected to the relay is improved. It can be concluded that LOS conditions are required to enhance the cell-edge performance of relayed networks. If relays cannot be deployed in LOS conditions, more accurate positioning of the relay backhaul antenna has to be performed (i.e. increased antenna height), which would also affect the deployment costs.

Acknowledgment

The authors express their gratitude for the assistance from the telecommunications operator Telenor in performing the live network measurements.

References

[1] 3GPP, *TR 36.814 V9.0.0, Further advancements for E-UTRA physical layer aspects (Release 9)*, March 2010.

[2] O.M. Teyeb, V.V. Phan, B. Raaf and S. Redana, *Dynamic Relaying in 3GPP LTE-Advanced Networks*, EURASIP Journal on Wireless Communications and Networking, Volumen 2009.

[3] C. Coletti, P. Mogesen and R. Irmer, *Performance Analysis of Relays in LTE for a Realistic Suburban Deployment Scenario*, Vehicular Technology Conference (VTC Spring), 2011 IEEE 73rd, pp 1-5.

[4] T. Beniero, S. Redana, J. Hämäläinen and B. Raaf, *Effect of Relaying on Coverage in 3GPP LTE-Advanced*, Vehicular Technology Conference (VTC Spring), 2009. IEEE 69th, pp 1-5.

[5] Y. Okumura, E. Ohmori, T. Kawano and K. Fukuda. *Field Strength and its Variability in VHF and UHF Land-Mobile Radio Service*, Review of the Electrical Communication Laboratory, 16, 1968.

[6] C.Q. Hien, J.M. Conrat and J.C. Cousin, *Propagation Path loss Models for LTE-Advanced Urban Relaying Systems*, IEEE International Symposium on Antennas and Propagation (APSURSI), July 2011, pp 2797-2800.

[7] C.Q. Hien, J.M. Conrat and J.C. Cousin, *On the impact of receive antenna height in a LTE-Advanced relaying scenario*, European Wireless Technology Conference (EuWIT) 2010, pp 129-132.

[8] 3GPP, *TS 25.215 V9.2.0, Physical layer, Measurements (Release 9)*, March 2010.

[9] A. Mihaiuti, A. Ignea, *The influence of the mobile communications receiver antenna height in the urban propagation scenario*, Doctor ETc 2009, pp 67-70.

[10] K. Hiltunen, *Comparison of Different Network Densification Alternatives from the LTE Downlink Performance Point of View*, NomadicLab, Ericsson Research, 2011.

Appendix E

Indoor WiFi and Femto Deployment Study

Realistic Indoor Wi-Fi and Femto Deployment Study as the Offloading Solution to LTE Macro Networks

Liang Hu*, Claudio Coletti*, Nguyen Huan*, István Z. Kovács †, Benny Vejlgaard†,
Ralf Irmer‡, Neil Scully‡

* Aalborg University, Aalborg, Denmark
† Nokia Siemens Networks, Aalborg, Denmark
‡Vodafone Group R&D, Newbury, United Kingdom

Abstract— **This paper investigates the downlink performance of indoor deployed Wi-Fi and Femto as the offloading solution to the LTE macro cellular networks in a realistic large-scale dense-urban scenario. With an assumed broadband traffic volume growth of 50x compared to today's levels, it is evaluated that a dual-carrier LTE macro network will not be able to provide sufficient service coverage with a 1 Mbps minimum data rate and, indoor coverage is identified as the major bottleneck.. We evaluate the performance of indoor Wi-Fi and Femto cell deployment to offload the congested LTE macro network. We show that, in a dual-carrier LTE macro case with a total of 30 MHz spectrum, Wi-Fi access point density of 230/km2 is required to meet the set target of 90% coverage with a minimum user data rate of 1 Mbps. For the same scenario it was found that an out-band Femto access point density of 1200/km2 is required. Furthermore, we show that in-band Femto cell cannot meet the set network requirement even at a very high access point density. We also show that Wi-Fi and Femto cell can offload the same amount of traffic when they are deployed at the same access point density.**

I. Introduction

Mobile data traffic is growing explosively with the popularity of various mobile devices that offer ubiquitous mobile internet and diverse multimedia authoring and playback capabilities. For instance, Vodafone has seen its data traffic grow from a trickle to a point where it almost exceeds voice traffic already in 2008; AT&T has seen a data growth of over 5000% from 2008-2010; Cisco [1] predicts that overall mobile data traffic is expected to grow to 6.3 exabytes per month by 2015, a 26-fold increase over 2010, where mobile video traffic accounts for 66.4% of the total traffic.

Despite the tremendous data traffic growth, operators are facing the big challenge that the revenue per user is decoupled from the data traffic generated per user, e.g. under the current mostly adopted 'flat-rate' pricing: whereas the data traffic grows exponentially, the revenue growth is rather slow, e.g. mobile data traffic increase by 100% annually, while the revenues only increase by 16% annually [2]. To alleviate this challenge, operators have to consider a cost-effective way to evolve their mobile networks to accommodate explosive traffic as well as keeping high revenue.

Wi-Fi is recognized by key mobile operators as a promising solution for cost-effectively adding mobile network capacity by leveraging low-cost access points and free unlicensed spectrum. Wi-Fi is a mature and widely adopted technology in most mobile devices. Millions of existing user deployed residential access points potentially already offload a lot of mobile data traffic. Thus, Wi-Fi can offer 'time-to-capacity' advantage over other network evolution options e.g. by adding more Macro/Micro Base Stations or upgrading 3G Base Stations to 4G LTE (Long Term Evolution) Base Stations. As another mobile data offloading solution, Femto cell is a kind of low-power base station which is usually installed by end-users in the residential and enterprise places. It aims at improving network coverage and capacity by site densification and increasing the spectrum spatial reuse. Similar to Wi-Fi, Femto cell utilizes the end-users' fixed DSL line as the backhaul network and is free of site acquisition fee, which also makes Femto cell a cost-effective solution.

There are very few quantitative studies on realistic Wi-Fi offloading potential and especially the comparison with Femto cell offloading, in particular in large-scale real deployment scenarios. A recent paper [3] has studied Wi-Fi offloading by using the measured user mobility traces as a basis to evaluate the offloading potential of existing residential Wi-Fi networks. Along another line[4][5], there are also a few studies on the performance of Femto offloading based on 3GPP regular network assumptions. In contrast, we provide a comprehensive quantitative study on Wi-Fi and Femto cell offloading in a large-scale real dense-urban deployment scenario. Outdoor Pico cells can also handle increasing traffic, however this paper focuses on Wi-Fi and Femto cell offloading.

II. Network Modeling Framework

A. Cellular Network Layout and Real Building Database

This study has been carried out in a dense urban scenario- a LTE macro cellular deployment in a European city. The size of the investigated area is approximately 1.27 km^2, containing 4 three-sector macro sites with optimized antenna down-tilt and average inter-site distance of 340 m. Furthermore, interfering cells from base stations located outside the investigated area are considered to remove border effects. Each sector is assumed to be equipped with 2 carriers, operating at 800 MHz and 2600 MHz bands. Furthermore, the studied area is divided into pixels with 10 x 10 m resolution. The offered traffic load is defined as the number of simultaneously connected users with a minimum data rate of 1 Mbps average during the peak hours. In 2010, the measured 3G data traffic load is on average 11.6 users over the investigated area and it is predicted to increase by a factor of 50x to 558 users for the purpose of this study.

The offered traffic load is fixed throughout our study. For accurate indoor modeling, real 3D building database of the investigated area is employed as shown in Fig.1. There are 916 buildings with 5 floors on average per building. It accounts for 36% of the total area. The building height is also considered: 1) when estimating the path loss between macro cells and outdoor locations; 2) floor penetrations in indoor propagation 3D Propagation Model.

To accurately estimate link budgets, a 3D ray-tracing tool is used to evaluate path loss and antenna pattern effects with regard to the radio link between macro cells and outdoor users. Such a tool models the radio propagation at street level by considering realistic positions and heights of the buildings that are imported from the previously mentioned 3D building map, as shown in Fig 1. Given the outdoor path loss predictions from ray-tracing tool, the indoor penetration loss within the building is calculated through an additional loss (in dB) equal to $0.6 \cdot d_i + L_{extwall}$, where d_i is the distance (in meters) from the indoor location to the external wall observing the highest received signal strength, and $L_{extwall}$ defines the penetration through the external wall that is set at 20 dB. Furthermore, for the outdoor-indoor path loss calculation, the floor height gain is modeled such that users located at higher floors have a received signal strength gain of 3.4 dB/floor.

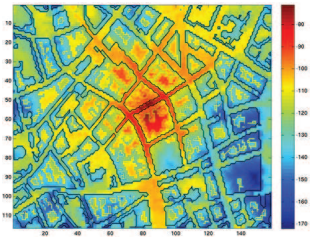

Figure 1. Path Loss (dB) Prediction from a specific Macro cell including 3D-Building information and real antenna radiation pattern.

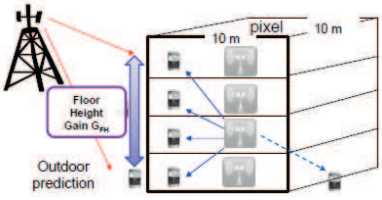

Figure 2. Outdoor -Indoor Floor Height Gain and 3D user distribution

When considering indoor small cells (WiFi/Femto), a statistical model based on [6] is considered, and it is defined as follows:

$$PL_{ind}(dB) = 38.46 + 20\log_{10}R + 0.6 \cdot d_{2D,indoor} + \sum_i L_{ow,i} \quad (1)$$

where R is the distance between the small cell and a generic user (indoor or outdoor), $d_{2D,indoor}$ is the distance covered inside the buildings and L_{ow} is a penetration loss of 20 dB due to each penetrated external wall. In terms of fading effects, fast fading effect is not modeled since users are static in our study; slow fading effect is captured by ray-tracing tool for outdoor base stations and is not modeled for indoor base stations to improve the simulation speed.

B. Spatial Traffic Modeling

The network traffic load is simulated in terms of number of simultaneous active users, randomly placed in the map according to a spatial user density map. Essentially, the user density map is defined as a probability of placing a user in a pixel of the map. There are 4 steps to generated spatial user density map: 1) the spatial user density map was firstly derived from cell-level packet-switched (Release 99 + HSDPA) traffic measurements averaged for busy hour traffic conditions. By assuming each user generates the same amount of traffic, traffic density by the number of simultaneous active users per cell is equivalent to the traffic density by the carried traffic per cell; 2) on top of cell-level measurement, we also differentiate indoor and outdoor traffic; Typically, in each cell coverage area, we force 70% of the traffic to be generated from indoor area and 30% from outdoor area; 3) To obtain even finer granularity of the traffic density map, on top of the above, traffic hotspot is artificially generated by overlaying a log-normal distribution with a standard deviation of 4 dB and a correlation distance of 50m; 4) To model the user distribution on 3D multi-floor buildings, the traffic density of each pixel is further divided among various floors of that pixel as shown in Fig 2; Here we assume the ground floor accounts for 50% of the total traffic density of that pixel and the remaining 50% are equally divided into higher floors; In practice, the ground floors are usually shops or conference rooms which generate more traffic than higher floors.

C. Macro LTE Network Modeling

The user association has two phases: 1) user is associated to the base station that gives the best experienced Signal Interference Noise Ratio (SINR) across all carriers; 2) When the macro sectors have multiple carriers, user association is balanced among multiple carriers by being preferably allocated to the carrier with larger product of experienced user SINR and available radio resource of that carrier, i.e., user are prioritized to high SINR and high bandwidth carrier. The carrier aggregation is not modeled i.e., users only connect to one carrier.

When users connect to Macro or Femto cells, the peak physical layer user data rate is a function of the average received SINR at the user location and is approximated by using the SINR to spectrum efficiency (SE) mapping method in [7] similar to the studies in [8]. Radio resources are shared with the purpose of minimizing the number of *users in outage*, i.e., the users who are experiencing a data rate lower than a required minimum data rate. Given the fixed amount of radio resources available per cell, the resource sharing algorithm sorts the connected users in descending order according to their experienced SINR. Then, the resources are allocated to the sorted list of users so that whenever possible each user achieves the minimum required data rate. Finally, when applicable, the remaining cell resources are allocated equally to all the served users in a round robin way.

D. Network Key Performance Indicator（KPI）

The selected network KPI is the network outage level at a given minimum data rate, defined as the probability:

$$P = \Pr[R_i < r_{\min}] \quad (1)$$

where $r_{\min}$ [Mbps] is the minimum user data rate required for achieving acceptable user experience, R_i [Mbps] is the user data rate experienced on average by the *i*-th user. It means that there is a threshold $r_{\min}$ [Mbps] below which the user experience becomes unacceptable. The uplink (UL) and downlink (DL) data rate requirements are defined as $r_{\min}^{UL}$ $r_{\min}^{DL}$ respectively. In our study, the network KPI is particularly defined as 90% network coverage (maximum 10% network outage) with minimum data rate of 1 Mbps in DL and 0.25 Mbps in UL. Our Wi-Fi and Femto cell deployment are driven by meeting the DL KPI, as DL is often the bottleneck of the network performance.

III. Wi-Fi Performance Modeling

In this study, we mainly look into the performance of 802.11g Wi-Fi as the Macro offloading solution, as it is the most popular installed 802.11 interface for the time being and available in most smartphones and netbooks. As 802.11n is getting more and more popular, we also plan to study 802.11n in future work.

A. Physical layer performance mapping curve

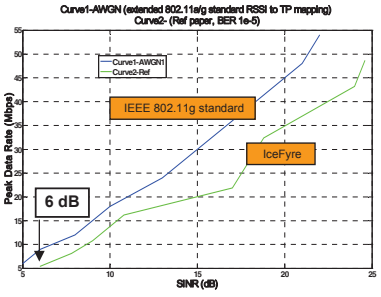

Figure 3. Wi-Fi 11g SINR to PHY Peak Data Rate Mapping

We firstly model IEEE 802.11g physical layer performance using SINR to physical peak data rate mapping curves, as shown in Fig 3. In the mapping curve, we assume that the frame size is fixed to 1500 Bytes and that the packet error rate is 10%. In Fig 3, there are two mapping curves: the blue one is the mapping curve from IEEE 802.11g standard under Additive White Gaussian Noise (AWGN) channel condition, whereas the green curve is from a real 802.11g Wi-Fi product (IceFyre Semiconductor [9]) where a fading channel condition is assumed. In this paper, we assume a fading channel condition and use IceFyre curve as the physical layer performance basis of 802.11g. It means that users need to have at least 6 dB SINR value to be able to connect to Wi-Fi access point.

B. Wi-Fi radio resource sharing model

In contrast to centralized scheduling in cellular wireless system, Wi-Fi uses distributed CSMA/CA (Carrier Sensing Multiple Access / Collision Avoidance) as the MAC (Medium Access Protocol) protocol for radio resource sharing. Due to protocol overhead e.g. DIFS, exponential back-off, the radio resource usage can be quite low e.g. 55% for a single 802.11g user operating on 54 Mbps data rate mode. Besides, collisions can happen from time to time, which further reduces the radio resource usage. To model radio resource usage, we employ the well-known Bichani's model [10]. The radio media usage efficiency is defined as *P,* which is a function of the number of users in the Wi-Fi cell and their experienced instantaneous SINR (Signal to Interference and Noise ratio). Due to limited space of the paper, mathematical derivation of *P* can be found in [10].

Having the radio resource usage *P,* the long-term average user throughput can be modeled as follows: we assume that each user generates both downlink (DL) and uplink (UL) traffic (being a DL and UL user at the same time), and there are N DL users and thus also N UL users in the Wi-Fi cell. To model the asymmetry load of DL and UL, a full-buffered traffic model is applied in DL whereas finite-buffered model is applied in UL, i.e., access point always has DL frames to transmit, whereas users have UL frames to transmit with probability β. Define the physical layer peak data rate of user i as PHY_i, which is obtained from the mapping curve in section III A. The DL and UL throughput for user i is computed as follows:

$$Throughput_i^{DL} = \frac{\beta}{\beta \bullet \sum_{i=1..N} \frac{1}{PHY_i} + \frac{1}{N}\left(\sum_{j=1..N} \frac{1}{PHY_j}\right)} \bullet P \quad (2)$$

$$Throughput_i^{UL} \frac{\frac{1}{N}\left(\sum_{j=1..N} \frac{1}{PHY_j}\right)}{\beta \bullet \sum_{i=1..N} \frac{1}{PHY_i} + \frac{1}{N}\left(\sum_{j=1..N} \frac{1}{PHY_j}\right)} \bullet P \quad (3)$$

The equations (2) (3) are derived by using a key property of 802.11 Wi-Fi networks [11] under full-buffered traffic model - Throughput Fairness: 1) set of DL users of the same Wi-Fi cell have the same average throughput in the long term, independent of their SINR; 2) set of UL users of the same Wi-Fi cell have the same average throughput in the long term, independent of their SINR. To make UL/DL throughput ratio fulfill the ratio $r_{\min}^{UL} / r_{\min}^{DL}$ define in section II, β is set as:

$$\beta = \frac{r_{\min}^{UL}}{r_{\min}^{DL}} \bullet \frac{1}{N} \quad (4)$$

Due to the limited space of the paper, the mathematical derivation of the model is not presented here.

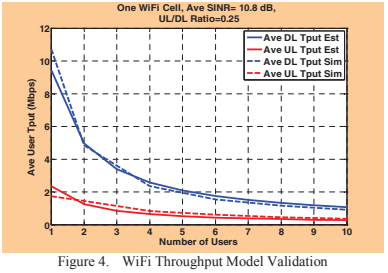

Figure 4. WiFi Throughput Model Validation

The analytical Wi-Fi throuhgput model is validated via a dynamic system-level 802.11g simulator. Asume one Wi-Fi cell and every user has SINR of 10.8 dB, the user throughput is evaluated againt number of users in the cell. As shown in Fig.4, the model matches perfectly with the system-level simulation results, especially when the number of users is large.

IV. SIMULATION ASSUMPTIONS & CASES DESCRIPTION

The Wi-Fi and Femto offloading potential have been evaluated by a MATLAB-based network planning and static simulation tool. Four simulation cases (see 0) are considered: as a reference scenario, the LTE 2-carrier macro network layout is based on existing live 3G macro network layout which is then upgraded to LTE. Second case presents indoor Wi-Fi deployment on top of the macro reference layer, for various access point densities. The last two consider out-band and in-band Femto cell deployment respectively to complement the macro network. In-band Femto means Femto cell operates on the same carrier as Macro cell, whereas out-band Femto operates on a different carrier than the carrier of Macro cell. Both Wi-Fi and Femto cells transmit at 20 dBm and they are equipped with omni directional antennas. 558 active users are generated in the full network area of 1.27/km2 with 916 buildings (accounts for 36% of the total area). The average number of floors per Building is 5**.** The target KPI is a minimum data rate of 1 Mbps at 90% network coverage. This KPI is chosen to reflect the requirement that as many users as possible have a good user experience, rather than a smaller proportion of users having a very high data rate. With the above assumptions, from the network simulation, the reference macro-only network is only able to reach a network outage of 46 % compared to a target value of 10% and average user throughput of 600 kbps. To improve macro network performance so as to meet the KPI, indoor offloading solutions-Wi-Fi and Femto cells are required.

TABLE 1. SIMULATION CASES AND SPECTRUM ALLOCATION OVERVIEW

Simulation Cases	**Spectrum Allocation**		
	800 MHz (1st) (FDD, 10 MHz)	***2600 MHz (2nd) (FDD, 20 MHz)***	***2400 MHz (20 MHz)***
Macro-only Reference case	Macro (Tx. Power 43 dBm)	Macro (Tx. Power 43 dBm)	-
Macro & Wi-Fi	Macro	Macro	Wi-Fi (Tx. Power 20 dBm)
Macro & Out-band Femto	Macro	Femto (Tx Power 20 dBm)	-
Macro & In-band Femto	Macro	Macro Femto (Tx Power 20 dBm)	-

V. SIMULATION RESULTS

In this section, we demonstrate Wi-Fi and Femto cell offloading gain by extensive simulation results. In subsection A, we provide the fixed simulation parameters. In subsection B, we study the Wi-Fi offloading gain under various access point densities and compare it against LTE Femto cell offloading.

The fixed simulation parameters of Wi-Fi are shown in Table 2. Multi-radio technologies-LTE and Wi-Fi 802.11g are simulated simultaneously. We assume that all user terminals are equipped with both LTE and 802.11g radio interfaces. We assume traffic steering policy between Wi-Fi and LTE Macro as follows: whenever the user detects a Wi-Fi access points, it will always firstly connect to Wi-Fi on the condition that it has at least SINR of 6 dB and can get the minimum data rate (1 Mbps) if connected to Wi-Fi,; Otherwise, it connects to LTE macro network.

A. Simulation Parameters

Table 2. Fixed Simulation parameters of Wi-Fi

Parameter	**Setting**
Radio standard	Wi-Fi 802.11g
Frame size	1500 Bytes
Carrier frequency	2400 MHz
Wi-Fi channel deployment	In-band deployed, 20 MHz band
Traffic Steering Policy	Always connect to Wi-Fi before Macro
Deployment option	Indoor Traffic-driven deployment
Building model	916 3D buildings, 36% of the total area 5 floors on average
Minimum ISD of APs AP to Macro site	20 m 50 m
UE admission mode	Open Subscriber Group
Traffic model	Full buffered
Indoor/Outdoor traffic ratio	70% / 30%
Spatial traffic modeling	See section II C

Table 3 Fixed Simulation parameters of LTE Femto cell

Parameter	**Setting**
Radio standard	LTE
Carrier frequency	2600 MHz, 20 MHz band
Traffic Steering Policy	In-band Femto: Best server SINR Out-band Femto: with Range Extension Best server SINR with 3 dB bias towards Femto cell

We assume that all Wi-Fi APs operate on the same channel of 20 MHz bandwidth, which corresponds to the worst case scenario. Assigning different non-overlapped channels to APs can further optimize the performance. Yet, in practice, this further gain can be cancelled out by considering external Wi-Fi APs interferences at 2.4GHz band. We assume a fixed MAC frame size of 1500 Bytes. Wi-Fi indoor traffic-driven deployment is considered, where APs are placed in indoor traffic hotpot area. The minimum inter-site distance (ISD) of access points is set to 20 m which corresponds to the indoor Wi-Fi coverage diameter. We assume Open Subscriber Group (OSG) model where users can be admitted to any of the Wi-Fi access points.

The fixed simulation parameters of Femto cell is listed in Table 3. In both out-band and in-band case, Femto cell is always deployed at 2600 MHz band. Macro network is deployed at both 800 MHz and 2600 MHz band for in-band Femto case and at 800 MHz for out-band Femto case. In terms of traffic steering for in-band Femto cell, a pure best server SINR detection method is assumed i.e., users always connect to the base station (either Femto or macro site) with the highest SINR over all carriers. No Range Extension (RE) feature is assumed for in-band Femto case, since it may result in radio link failure during user mobility. No cross-tier interference mitigation scheme is modeled. In contrast, in the out-band Femto case, RE is applied in the form of 3dB SINR bias towards Femto cell in the best server SINR detection, i.e., users gain 3 dB SINR bias towards Femto cell in the best server detection among all base stations. Other parameters are the same as Wi-Fi such as indoor traffic-driven deployment, OSG, macro site and AP minimum ISD, and traffic modeling.

B. Wi-Fi and Femto offloading gain VS Access Point Density

We firstly study the Wi-Fi and Femto cell offloading gain in terms of network outage at minimum data rate of 1 Mbps. All our network evolution studies are driven by the required node deployment density to meet the KPI - 10% network outage at minimum data rate of 1 Mbps. As shown in Fig 5, the reference dual-carrier LTE macro network has the network outage of 45% at minimum data rate 1 Mbps. Wi-Fi access point (AP) density of 300/km2 improve network outage dramatically by 38 percentage points i.e., network outage from 45**%** to **7%**, by using traffic-centric ground-floor only (GF-Only) indoor deployment. In particular, the APs are deployed in indoor traffic hotspot and at ground-floor of the building. This means 230 AP/km2 is more than sufficient to reach the network KPI - 10% network outage. From Fig 5, it is also observed that indoor Wi-Fi deployment can efficiently improve network outages both from indoor and outdoor network areas, e.g. with Wi-Fi at 230 AP/km2, the indoor outage improves from 32% to 2%, while the outdoor network outage improves from 14% to 5%. Indoor Wi-Fi deployment offloads the heavy load of macro network so as to improve overall network performance. Lastly, simulation results show that all outage users are from macro network while Wi-Fi cell has zero users in outage.

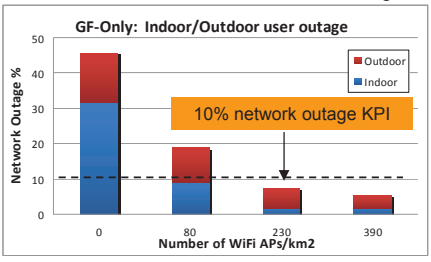

Figure 5. Wi-Fi deployment: Indoor / Outdoor network outage

Fig 6 and 7 show the out-band and in-band LTE Femto cell offloading gain in terms of network outage at minimum data rate of 1 Mbps for both indoor and outdoor area. In the out-band case, Femto cell is deployed at 2600 MHz band with 20 MHz bandwidth whereas macro network is deployed at 800 MHz band with 10 MHz bandwidth. Range extension of 3 dB SINR bias is applied to improve the percentage of users connected to Femto cells. Fig 6 shows that 1200 Femto cell APs/km2 are needed to meet the network KPI 10% network outage at 1 Mbps. Compared to the Wi-Fi case, the macro network has only a single carrier at 800 MHz with 10 MHz band, thus 4 times higher Femto AP density than Wi-Fi is needed to reach the KPI. Simulation results also show that all network outage is from macro network while Femto cell has zero outage users. In the in-band Femto case, the situation is even worse in Fig 7. Even 1200 Femto cell APs/km2 is not sufficient to reach the network KPI 10% network outage at 1 Mbps. This is mainly due to the fact that Femto APs create strong in-band interference to macro network at 2600 MHz as shown in Fig 8. Femto cell has very good SINR with on average 14.7 dB, however macro carrier at 2600 MHz only has average SINR of 0.7 dB. In this case, Range Extension combined with interference mitigation schemes such as eICIC can be expected to improve in-band Femto cell offloading performance.

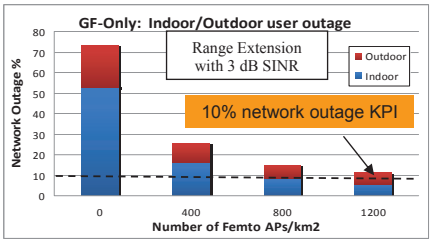

Figure 6. Out-band Femto: Indoor / Outdoor network outage

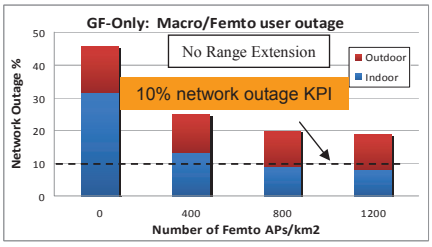

Figure 7. In-band Femto deployment: Indoor / Outdoor network outage

Secondly, the percentage of users offloaded to Wi-Fi and Femto cell are studied. Fig 8 shows 24% to 53% mobile users can be offloaded to indoor Wi-Fi network when the AP densities range from 80 APs/km2 to 390APs/km2. In the case of out-band Femto, with 400 Femto/km2, 51% mobile users can be offloaded to Femto cell, almost the same as Wi-Fi offloading. However, since there is only single-carrier at macro network (compared to 2-carriers macro in Wi-Fi case), 51% mobile users offloaded to Femto still results in 24% network outage shown in Fig 6. Therefore higher AP density of 1200 APs/km2 is required to offload more users (69%) so as to meet the network KPI, as shown in Fig 6. The in-band Femto case is not shown, since anyway it cannot meet the network KPI even at a very high node density as shown in Fig.7.

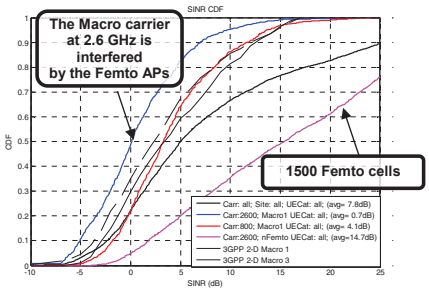

Figure 8. SINR Distribution for in-band Femto cell + Macro network

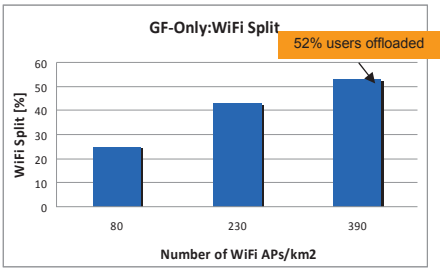

Figure 9. Wi-Fi deployment: % offloaded users vs.AP Density

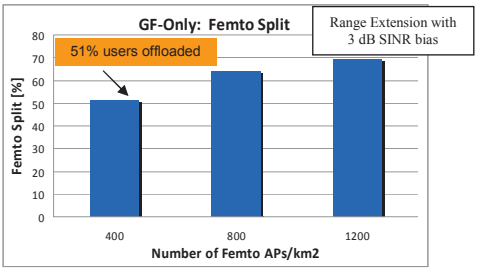

Figure 10. Out-band Femto: Percentage of offloaded users vs. AP Density

VI. Conclusion

We have studied the performance of indoor Wi-Fi and Femto cell deployment as the offloading solutions to a LTE macro network in a realistic dense urban area under the assumption of 50x growth of mobile broadband traffic growth. To evaluate the offloading potential, we have used a 3-D radio propagation model based on Ray-tracing with real building database and spatial traffic distribution from live 3G network. In the case of indoor Wi-Fi deployment, we showed that an access point (AP) density of 230 AP/km2 can already meet the target network Key Performance Indicator (KPI) of 90% network coverage with a minimum data rate of 1 Mbps. In the case of out-band LTE Femto cell deployment, even with range extension, much higher AP density of 1200 AP/km2 is required to meet the KPI. The least favorable scenario is the deployment of in-band Femto cells, where Femto cells share one carrier with the macro layer. A high-density and uncoordinated Femto cell deployment creates a strong in-band interference coupling to the Marco layer which results in high overall network outage and even with 1200 Femto AP/km2 the target network KPI cannot be achieved. We have also shown that for the same access point density Wi-Fi APs and out-band Femto cells can offload similar amount of users. Finally, the performance of in-band femto could potentially be improved with interference mitigation, which is left for future study.

References

[1] Cisco VNI Forecast, "Cisco Visual Networking Index: Global Mobile data Traffic Forecast Update 2010-2015," February , 2012.

[2] Gartner Forecast, "Mobile Data Traffic and Revenue, Worldwide, 2010-2015", July 4 2011

[3] K. Lee, "Mobile Data Offloading: How Much Can Wi-Fi Deliver?", ACM CoNext 2010

[4] J Gora , T.E Kolding,. "Deployment Aspects of 3G Femtocells", IEEE PIMRC 2009, Tokyo

[5] D Calin, H Claussen "On femto deployment architectures and macrocell offloading benefits in joint macro-femto deployments", IEEE Communication Magzine, Volume: 48 , Issue: 1 , 2010

[6] 3GPP TR 36.814, "Further Advancements for E-UTRA, Physical Layer Aspects," version 9.0.0, December 2009

[7] P. Mogensen, "LTE Capacity compared to the ShannonBound," Proc. IEEE 65th VTC, May 2007

[8] J. Elling, "Mobile Broadband Network Evolution Towards 2015 – A Copenhagne Area Case Study," Telektronikk, January 2010

[9] J. Yee and H. Pezeshki-Esfahani, "Understanding Wireless LAN Performance Tradeoffs," http://www.commsdesign.com, Nov 2002

[10] G. Bianchi, "Performance Analysis of the IEEE 802.11 Distributed Coordination Function," IEEE JSAC Communications, March 2000

[11] A. Duda. "Understanding the Performance of 802.11 Networks". In Proceedings of PIMRC'08, Cannes, France, 15-18 September 2008

List of Acronyms

2G Second Generation

3G Third Generation

4G Fourth Generation

3GPP Third Generation Partnership Project

AF Amplify-and-Forward

AMC Adaptive Modulation and Coding

CAGR Compound Annual Growth Rate

CAPEX Capital Expenditures

CDF Cumulative Distribution Function

CSG Closed Subscriber Group

DAS Distributed Antenna System

DF Decode-and-Forward

DSL Digital Subscriber Line

FD Full-Duplex

FDD Frequency Division Duplexing

GPS Global Positioning System

GSM Global System for Mobile communication

HARQ Hybrid Automatic Repeat Request

HeNB Home enhanced eNodeB

HSDPA High Speed Downlink Packet Access

HSPA High Speed Packet Access

ICIC Inter-Cell Interference Cancellation

IMPEX Implementation Expenditures

IMT-A International Mobile Telecommunications-Advanced

IRC Interference Rejection Combining

ISD Inter-site Distance

ITU International Telecommunications Union

KPI Key Performance Indicator

LOS Line of Sight

LTE Long Term Evolution

MIMO Multiple Input Multiple Output

NLOS Non-Line of Sight

OFDM Orthogonal Frequency Division Multiplexing

OPEX Operational Expenditures

OSG Open Subscriber Group

QAM Quadrature Amplitude Modulation

RAT Radio Access Technology

RF Radio Frequency

RRH Remote Radio Head

SINR Signal to Interference plus Noise Ratio

TCO Total Cost of Ownership

TDD Time Division Duplexing

UTM Universal Transverse Mercator

WGS-84 World Geodetic System-84

Bibliography

[1] Rysavy Research/4G Americas, "Mobile Broadband Explosion: 3GPP Broadband Evolution to IMT-Advanced," *White Paper*, September,2011.

[2] H. Holma and A. Toskala, *WCDMA for UMTS: HSPA Evolution and LTE*. New York, NY, USA: John Wiley & Sons, Inc., 2007.

[3] E. Dahlman, S. Parkvall, J. Skold, and P. Beming, *3G Evolution, Second Edition: HSPA and LTE for Mobile Broadband*. Academic Press, 2 ed., 2008.

[4] Ericsson, "Mobile Data Traffic Surpasses Voice," *Press Release*, September, 2011.

[5] D. Astely, E. Dahlman, A. Furuskar, Y. Jading, M. Lindstrom, and S. Parkvall, "Lte: the evolution of mobile broadband," *Communications Magazine, IEEE*, vol. 47, pp. 44 –51, april 2009.

[6] S. Sesia, I. Toufik, and M. Baker, *LTE, The UMTS Long Term Evolution: From Theory to Practice*. Wiley Publishing, 2009.

[7] P. Mogensen, T. Koivisto, K. Pedersen, I. Kovacs, B. Raaf, K. Pajukoski, and M. Rinne, "Lte-advanced: The path towards gigabit/s in wireless mobile communications," in *Wireless Communication, Vehicular Technology, Information Theory and Aerospace Electronic Systems Technology, 2009. Wireless VITAE 2009. 1st International Conference on*, pp. 147 –151, may 2009.

[8] S. Parkvall, E. Englund, A. Furuskär, E. Dahlman, T. Jösson, and A. Paravati, "Lte evolution towards imt-advanced and commercial network performance," in *Communication Systems (ICCS), 2010 IEEE International Conference on*, pp. 151 –155, nov. 2010.

[9] ITU-R, "Requirements related to technical performance for IMT-Advanced radio interface(s)," *Recommendation M.2134*, Nov. 2008.

[10] Cisco, "Cisco Visual Networking Index: Global Mobile Data Traffic Forecast Update, 2011–2016," *Cisco VNI Forecast, White Paper*, February 14, 2012.

[11] comScore, Inc., "Digital Omnivores: How Tablets, Smartphones and Connected Devices are Changing U.S. Digital Media Consumption Habits ," *comScore Whitepaper*, October 10, 2011.

[12] T. Giles, J. Markendahl, J. Zander, P. Zetterberg, P. Karlsson, G. Malmgren, and J. Nilsson, "Cost drivers and deployment scenarios for future broadband wireless networks - key research problems and directions for research," in *Vehicular Technology Conference, 2004. VTC 2004-Spring. 2004 IEEE 59th*, vol. 4, pp. 2042 – 2046 Vol.4, may 2004.

[13] K. Johansson, J. Zander, and A. Furuskar, "Modelling the cost of heterogeneous wireless access networks," *Int. J. Mob. Netw. Des. Innov.*, vol. 2, pp. 58–66, May 2007.

[14] Greger Blennerud, "Mobile Broadband – Busting the scissor effect myth," *Ericsson, Strategy mobile broadband*, February, 2010.

[15] G. Micallef, "Methods for reducing the energy consumption of mobile broadband networks," *Telektronik, Final Issue*, vol. 106, no. 1, pp. 121 –128, 2010.

[16] C. Mehlfuhrer, S. Caban, and M. Rupp, "Cellular system physical layer throughput: How far off are we from the shannon bound?," *Wireless Communications, IEEE*, vol. 18, pp. 54 –63, december 2011.

[17] M. Dohler, R. Heath, A. Lozano, C. Papadias, and R. Valenzuela, "Is the phy layer dead?," *Communications Magazine, IEEE*, vol. 49, pp. 159 –165, april 2011.

[18] Z. Shen, A. Papasakellariou, J. Montojo, D. Gerstenberger, and F. Xu, "Overview of 3gpp lte-advanced carrier aggregation for 4g wireless communications," *Communications Magazine, IEEE*, vol. 50, pp. 122 –130, february 2012.

[19] A. Damnjanovic, J. Montojo, Y. Wei, T. Ji, T. Luo, M. Vajapeyam, T. Yoo, O. Song, and D. Malladi, "A survey on 3gpp heterogeneous networks," *Wireless Communications, IEEE*, vol. 18, pp. 10 –21, june 2011.

[20] K. Lee, J. Lee, Y. Yi, I. Rhee, and S. Chong, "Mobile data offloading: how much can wifi deliver?," in *Proceedings of the ACM SIGCOMM 2010 conference*, SIGCOMM '10, (New York, NY, USA), pp. 425–426, ACM, 2010.

[21] K. Johansson, C. Bergljung, C. Cedervall, and P. Karlsson, "Capacity expansion for non-uniform spatial traffic distributions," in *Personal, Indoor*

and Mobile Radio Communications, 2007. PIMRC 2007. IEEE 18th International Symposium on, pp. 1 –5, sept. 2007.

[22] Zheng, Y., "How to Operate - Boosting WiMax indoor coverage," *Huawei Communicate*, pp. 31–32, April, 2009.

[23] Tzvika Naveh, "Mobile Backhaul: Fiber vs. Microwave - Case Study Analyzing Various Backhaul Technology Strategies," *Ceragon White Paper*, October, 2009.

[24] P. Tian, H. Tian, J. Zhu, L. Chen, and X. She, "An adaptive bias configuration strategy for range extension in lte-advanced heterogeneous networks," in *Communication Technology and Application (ICCTA 2011), IET International Conference on*, pp. 336 –340, oct. 2011.

[25] N. Jorgensen, D. Laselva, and J. Wigard, "On the potentials of traffic steering techniques between hsdpa and lte," in *Vehicular Technology Conference (VTC Spring), 2011 IEEE 73rd*, pp. 1 –5, may 2011.

[26] S. Barbera, P. Michaelsen, M. Saily, and K. Pedersen, "Mobility performance of lte co-channel deployment of macro and pico cells," in *Wireless Communications and Networking Conference (WCNC), 2012 IEEE*, pp. 2863 –2868, april 2012.

[27] D. Lopez-Perez, I. Guvenc, G. de la Roche, M. Kountouris, T. Quek, and J. Zhang, "Enhanced intercell interference coordination challenges in heterogeneous networks," *Wireless Communications, IEEE*, vol. 18, pp. 22 –30, june 2011.

[28] L. Gabriel, M. Grech, F. Kontothanasi, A. Mukhopadhyay, M. Nicoloau, and A. Sharma, "Economic benefits of son features in lte networks," in *Sarnoff Symposium, 2011 34th IEEE*, pp. 1 –5, may 2011.

[29] Ericsson, "It All Comes Back to Backhaul," *White Paper*, February, 2012.

[30] S. Chia, M. Gasparroni, and P. Brick, "The next challenge for cellular networks: backhaul," *Microwave Magazine, IEEE*, vol. 10, pp. 54 –66, august 2009.

[31] K. Johansson, *Cost Effective Deployment Strategies for Heterogeneous Wireless Networks*. PhD thesis, KTH Royal Institute of Technology, 2007.

[32] H. Claussen, L. Ho, and L. Samuel, "Financial analysis of a pico-cellular home network deployment," in *Communications, 2007. ICC '07. IEEE International Conference on*, pp. 5604 –5609, june 2007.

[33] H. Claussen, L. Ho, and F. Pivit, "Effects of joint macrocell and residential picocell deployment on the network energy efficiency," in *Personal, Indoor and Mobile Radio Communications, 2008. PIMRC 2008. IEEE 19th International Symposium on*, pp. 1 –6, sept. 2008.

[34] S. Strzyz, K. Pedersen, J. Lachowski, and F. Frederiksen, "Performance optimization of pico node deployment in lte macro cells," in *Future Network Mobile Summit (FutureNetw), 2011*, pp. 1 –9, june 2011.

[35] Y. Wang and K. I. Pedersen, "Performance analysis of enhanced inter-cell interference coordination in lte-advanced heterogeneous networks," in *Vehicular Technology Conference (VTC Spring), 2012 IEEE 75th*, pp. 1 –5, may 2012.

[36] J. Elling, M. Sorensen, P. Mogensen, E. Lang, Y. Wang, and O. Teyeb, "Mobile broadband network evolution towards 2015 – a copenhagen area case study," *Telktronik, Final Issue*, vol. 106, no. 1, pp. 138 –148, 2010.

[37] R. Pabst, B. Walke, D. Schultz, P. Herhold, H. Yanikomeroglu, S. Mukherjee, H. Viswanathan, M. Lott, W. Zirwas, M. Dohler, H. Aghvami, D. Falconer, and G. Fettweis, "Relay-based deployment concepts for wireless and mobile broadband radio," *Communications Magazine, IEEE*, vol. 42, pp. 80 – 89, sept. 2004.

[38] D. Soldani and S. Dixit, "Wireless relays for broadband access [radio communications series]," *Communications Magazine, IEEE*, vol. 46, pp. 58 –66, march 2008.

[39] Redana, S. et al., "Final assessment of relaying concepts for all CGs scenarios under consideration of related WINNER L1 and L2 protocol functions," *IST-4-027756 WINNER II - Deliverable 3.5.3 v1.0*, Sep, 2007.

[40] C. Hoymann, W. Chen, J. Montojo, A. Golitschek, C. Koutsimanis, and X. Shen, "Relaying operation in 3gpp lte: challenges and solutions," *Communications Magazine, IEEE*, vol. 50, pp. 156 –162, february 2012.

[41] A. Bou Saleh, S. Redana, B. Raaf, T. Riihonen, J. Hamalainen, and R. Wichman, "Performance of amplify-and-forward and decode-and-forward relays in lte-advanced," in *Vehicular Technology Conference Fall (VTC 2009-Fall), 2009 IEEE 70th*, pp. 1 –5, sept. 2009.

[42] O. Bulakci, S. Redana, B. Raaf, and J. Hämäläinen, "Performance enhancement in lte-advanced relay networks via relay site planning," in *Vehicular Technology Conference (VTC 2010-Spring), 2010 IEEE 71st*, pp. 1 –5, may 2010.

[43] A. B. Saleh, S. Redana, J. Hämäläinen, and B. Raaf, "On the coverage extension and capacity enhancement of inband relay deployments in lte-advanced networks," *JECE*, vol. 2010, pp. 4:1–4:10, Jan. 2010.

[44] T. Beniero, S. Redana, J. Hamalainen, and B. Raaf, "Effect of relaying on coverage in 3gpp lte-advanced," in *Vehicular Technology Conference, 2009. VTC Spring 2009. IEEE 69th*, pp. 1 –5, april 2009.

[45] P. Moberg, P. Skillermark, N. Johansson, and A. Furuskar, "Performance and cost evaluation of fixed relay nodes in future wide area cellular networks," in *Personal, Indoor and Mobile Radio Communications, 2007. PIMRC 2007. IEEE 18th International Symposium on*, pp. 1 –5, sept. 2007.

[46] K. Doppler, C. Wijting, and K. Valkealahti, "On the benefits of relays in a metropolitan area network," in *Vehicular Technology Conference, 2008. VTC Spring 2008. IEEE*, pp. 2301 –2305, may 2008.

[47] E. Lang, S. Redana, and B. Raaf, "Business impact of relay deployment for coverage extension in 3gpp lte-advanced," in *Communications Workshops, 2009. ICC Workshops 2009. IEEE International Conference on*, pp. 1 –5, june 2009.

[48] B. Timus, *Studies on the Viability of Cellular Multihop Networks with Fixed Relays*. PhD thesis, KTH, Communication Systems, CoS, 2009. QC 20100812.

[49] R. Irmer and F. Diehm, "On coverage and capacity of relaying in lte-advanced in example deployments," in *Personal, Indoor and Mobile Radio Communications, 2008. PIMRC 2008. IEEE 19th International Symposium on*, pp. 1 –5, sept. 2008.

[50] R. Schoenen, W. Zirwas, and B. Walke, "Capacity and coverage analysis of a 3gpp-lte multihop deployment scenario," in *Communications Workshops, 2008. ICC Workshops '08. IEEE International Conference on*, pp. 31 –36, may 2008.

[51] A. Bou Saleh, S. Redana, B. Raaf, and J. Hamalainen, "Comparison of relay and pico enb deployments in lte-advanced," in *Vehicular Technology Conference Fall (VTC 2009-Fall), 2009 IEEE 70th*, pp. 1 –5, sept. 2009.

[52] V. Chandrasekhar, J. Andrews, and A. Gatherer, "Femtocell networks: a survey," *Communications Magazine, IEEE*, vol. 46, pp. 59 –67, september 2008.

[53] D. Calin, H. Claussen, and H. Uzunalioglu, "On femto deployment architectures and macrocell offloading benefits in joint macro-femto deployments," *Communications Magazine, IEEE*, vol. 48, pp. 26 –32, january 2010.

[54] Informa, "Small cell market status - Informa," *Small cell Forum - White Paper*, June, 2012.

[55] J. Markendahl and O. Mandkitalo, "A comparative study of deployment options, capacity and cost structure for macrocellular and femtocell networks," in *Personal, Indoor and Mobile Radio Communications Workshops (PIMRC Workshops), 2010 IEEE 21st International Symposium on*, pp. 145 –150, sept. 2010.

[56] J.-B. Vezin, L. Giupponi, A. Tyrrell, E. Mino, and B. Miroslaw, "A femtocell business model: The befemto view," in *Future Network Mobile Summit (FutureNetw), 2011*, pp. 1 –8, june 2011.

[57] G. de la Roche, A. Valcarce, D. Lopez-Perez, and J. Zhang, "Access control mechanisms for femtocells," *Communications Magazine, IEEE*, vol. 48, pp. 33 –39, january 2010.

[58] T. Kolding, P. Ochal, P. Czerepinski, and K. Pedersen, "Impact of carrier configuration and allocation scheme on 3g femtocell offload effect," in *Vehicular Technology Conference (VTC Spring), 2011 IEEE 73rd*, pp. 1 –5, may 2011.

[59] J. Gora and T. Kolding, "Deployment aspects of 3g femtocells," in *Personal, Indoor and Mobile Radio Communications, 2009 IEEE 20th International Symposium on*, pp. 1507 –1511, sept. 2009.

[60] Y. Wang and K. Pedersen, "Time and power domain interference management for lte networks with macro-cells and henbs," in *Vehicular Technology Conference (VTC Fall), 2011 IEEE*, pp. 1 –6, sept. 2011.

[61] A. Szufarska, K. Safjan, S. Strzyz, K. Pedersen, and F. Frederiksen, "Interference mitigation methods for lte-advanced networks with macro and henb deployments," in *Vehicular Technology Conference (VTC Fall), 2011 IEEE*, pp. 1 –5, sept. 2011.

[62] 3GPP, "Evolved universal terrestrial radio access (e-utra);further advancements for e-utra physical layer aspects (release 9)," *Tech. Spec. 36.814 V9.0.0*, Mar 2010.

[63] J. Andrews, R. Ganti, M. Haenggi, N. Jindal, and S. Weber, "A primer on spatial modeling and analysis in wireless networks," *Communications Magazine, IEEE*, vol. 48, pp. 156 –163, november 2010.

[64] Northstream, "LTE and the 1800 MHz opportunity," *White Paper*, March, 2012.

[65] T. Taleb and A. Kunz, "Machine type communications in 3gpp networks: potential, challenges, and solutions," *Communications Magazine, IEEE*, vol. 50, pp. 178 –184, march 2012.

[66] ABI Research, "The Emergence of Compact Base Stations in the New RAN Architecture Paradigm," *White Paper*, 2010.

[67] Nokia Siemens Networks, "Single RAN made simple managing site and frequency evolution to tomorrow's mobile broadband world," *White Paper*, 2009.

[68] R. Vieira, R. Paiva, J. Hulkkonen, R. Jarvela, R. Iida, M. Saily, F. Tavares, and K. Niemela, "Gsm evolution importance in re-farming 900 mhz band," in *Vehicular Technology Conference Fall (VTC 2010-Fall), 2010 IEEE 72nd*, pp. 1 –5, sept. 2010.

[69] B. Modlic, G. Sisul, and M. Cvitkovic, "Digital dividend – opportunities for new mobile services," in *ELMAR, 2009. ELMAR '09. International Symposium*, pp. 1 –8, sept. 2009.

[70] H. Karimi and G. Lapierre, "On the impact of adjacent-channel interference from tdd terminal stations to fdd terminal stations in the 2500-2690 mhz band," in *Global Mobile Congress 2009*, pp. 1 –6, oct. 2009.

[71] K. Pedersen, F. Frederiksen, C. Rosa, H. Nguyen, L. Garcia, and Y. Wang, "Carrier aggregation for lte-advanced: functionality and performance aspects," *Communications Magazine, IEEE*, vol. 49, pp. 89 –95, june 2011.

[72] S. Kumar, I. Kovacs, G. Monghal, K. Pedersen, and P. Mogensen, "Performance evaluation of 6-sector-site deployment for downlink utran long term evolution," in *Vehicular Technology Conference, 2008. VTC 2008-Fall. IEEE 68th*, pp. 1 –5, sept. 2008.

[73] B. Hagerman, D. Imbeni, J. Barta, A. Pollard, R. Wohlmuth, and P. Cosimini, "Wcdma 6-sector deployment - case study of a real installed umts-fdd network," in *Vehicular Technology Conference, 2006. VTC 2006-Spring. IEEE 63rd*, vol. 2, pp. 703 –707, may 2006.

[74] F. Gunnarsson, M. Johansson, A. Furuskar, M. Lundevall, A. Simonsson, C. Tidestav, and M. Blomgren, "Downtilted base station antennas - a simulation model proposal and impact on hspa and lte performance," in *Vehicular Technology Conference, 2008. VTC 2008-Fall. IEEE 68th*, pp. 1 –5, sept. 2008.

[75] J. Niemela, T. Isotalo, and J. Lempiainen, "Optimum antenna downtilt angles for macrocellular wcdma network," *EURASIP Journal on Wireless Communications and Networking*, vol. 2005, no. 5, p. 610942, 2005.

[76] M. Caretti, M. Crozzoli, G. Dell'Aera, and A. Orlando, "Cell splitting based on active antennas: Performance assessment for lte system," in *Wireless and Microwave Technology Conference (WAMICON), 2012 IEEE 13th Annual*, pp. 1 –5, april 2012.

[77] Nokia Siemens Networks, "Active Antenna Systems, a step-change in base station site performance," *White Paper*, 2012.

[78] L. Liu, R. Chen, S. Geirhofer, K. Sayana, Z. Shi, and Y. Zhou, "Downlink mimo in lte-advanced: Su-mimo vs. mu-mimo," *Communications Magazine, IEEE*, vol. 50, pp. 140 –147, february 2012.

[79] M. Baker, "From lte-advanced to the future," *Communications Magazine, IEEE*, vol. 50, pp. 116 –120, february 2012.

[80] D. Lee, H. Seo, B. Clerckx, E. Hardouin, D. Mazzarese, S. Nagata, and K. Sayana, "Coordinated multipoint transmission and reception in lte-advanced: deployment scenarios and operational challenges," *Communications Magazine, IEEE*, vol. 50, pp. 148 –155, february 2012.

[81] ABI Research, "Small Cells: Outdoor Pico and Micro Markets," *Research Report*, 2012.

[82] L. Gabriel, M. Grech, F. Kontothanasi, A. Mukhopadhyay, M. Nicoloau, and A. Sharma, "Economic benefits of son features in lte networks," in *Sarnoff Symposium, 2011 34th IEEE*, pp. 1 –5, may 2011.

[83] Z. Ghebretensaee and, J. Harmatos, and K. Gustafsson, "Mobile broadband backhaul network migration from tdm to carrier ethernet," *Communications Magazine, IEEE*, vol. 48, pp. 102 –109, october 2010.

[84] P. Briggs, R. Chundury, and J. Olsson, "Carrier ethernet for mobile backhaul," *Communications Magazine, IEEE*, vol. 48, pp. 94 –100, october 2010.

[85] ABI Research, "Small Cells: Outdoor Pico and Micro Markets," *Research Report*, 2012.

[86] S. Chia, M. Gasparroni, and P. Brick, "The next challenge for cellular networks: backhaul," *Microwave Magazine, IEEE*, vol. 10, pp. 54 –66, august 2009.

[87] I. Czajkowski, "High-speed copper access: a tutorial overview," *Electronics Communication Engineering Journal*, vol. 11, pp. 125 –148, jun 1999.

[88] P. Cota and T. Pavicic, "New technologies for improvement of characteristics in dsl access networks," in *MIPRO, 2011 Proceedings of the 34th International Convention*, pp. 511 –516, may 2011.

[89] Ericsson, "Microwave capacity evolution," *Ericsson Review*, 2011.

[90] S. Elayoubi and M. Francisco, "Comparing backhauling solutions in wifi networks," in *Vehicular Technology Conference Fall (VTC 2010-Fall), 2010 IEEE 72nd*, pp. 1 –5, sept. 2010.

[91] 3GPP, "Evolved universal terrestrial radio access (e-utra);physical layer for relaying operation (release 10)," *Tech. Spec. 36.216 V10.3.1*, Sept 2011.

[92] Small cell Forum , "Enterprise Femtocell Deployment Guidelines," *White Paper*, February, 2012.

[93] Small cell Forum , "Case Study - AT&T," *White Paper*, February, 2012.

[94] Y. Wang, K. I. Pedersen, and F. Frederiksen, "Detection and protection of macro-users in dominant area of co-channel csg cells," in *Vehicular Technology Conference (VTC Spring), 2012 IEEE 75th*, pp. 1 –5, may 2012.

[95] 3GPP, "Evolved universal terrestrial radio access (e-utra);overall description; stage 2 (release 10)," *Tech. Spec. 36.300 V10.8.0*, June 2012.

[96] A. Saleh, A. Rustako, and R. Roman, "Distributed antennas for indoor radio communications," *Communications, IEEE Transactions on*, vol. 35, pp. 1245 –1251, december 1987.

[97] Z. Liu, T. Sorensen, J. Wigard, and P. Mogensen, "Das, uncoordinated femto and joint scheduling systems for in-building wireless solutions," in *Vehicular Technology Conference (VTC Spring), 2011 IEEE 73rd*, pp. 1 –5, may 2011.

[98] Ruckus Wireless, "Dealing with Density: The Move to Small-Cell Architectures," *White Paper*, February, 2012.

[99] Yankee Group, "The Changing Face of Wi-Fi Mobile Data Offload," *Report*, December, 2011.

[100] R. Van Nee, "Breaking the gigabit-per-second barrier with 802.11ac," *Wireless Communications, IEEE*, vol. 18, p. 4, april 2011.

[101] K. Johansson, A. Furuskar, P. Karlsson, and J. Zander, "Relation between base station characteristics and cost structure in cellular systems," in *Personal, Indoor and Mobile Radio Communications, 2004. PIMRC 2004. 15th IEEE International Symposium on*, vol. 4, pp. 2627 – 2631 Vol.4, sept. 2004.

[102] M. Nawrocki, H. Aghvami, and M. Dohler, *Understanding UMTS Radio Network Modelling, Planning and Automated Optimisation: Theory and Practice*. John Wiley & Sons, 2006.

[103] J. Laiho, A. Wacker, and T. Novosad, *Radio Network Planning and Optimisation for UMTS*. John Wiley & Sons, 2006.

[104] 3GPP, "Evolved universal terrestrial radio access (e-utra);lte physical layer; general description (release 10)," *Tech. Spec. 36.211 V9.1.0*, Dec 2010.

[105] J. Oszmianski, K. Safjan, M. Dottling, and A. Bohdanowicz, "Impact of traffic modeling and scheduling on delay and spectral efficiency of the winner system," in *Vehicular Technology Conference, 2008. VTC Spring 2008. IEEE*, pp. 2661 –2665, may 2008.

[106] M. Hata, "Empirical formula for propagation loss in land mobile radio services," *Vehicular Technology, IEEE Transactions on*, vol. 29, pp. 317 – 325, aug 1980.

[107] T. S. Rappaport, *Wireless communications principles and practice, second edition*. Prentice Hall, 2001.

[108] J. D. Parsons, *The Mobile Radio Propagation Channel*. John Wiley & Sons, Ltd, 2001.

[109] K. Johansson, C. Bergljung, C. Cedervall, and P. Karlsson, "Capacity expansion for non-uniform spatial traffic distributions," in *Personal, Indoor and Mobile Radio Communications, 2007. PIMRC 2007. IEEE 18th International Symposium on*, pp. 1 –5, sept. 2007.

[110] S. Almeida, J. Queijo, and L. Correia, "Spatial and temporal traffic distribution models for gsm," in *Vehicular Technology Conference, 1999. VTC 1999 - Fall. IEEE VTS 50th*, vol. 1, pp. 131 –135 vol.1, 1999.

[111] U. Gotzner and R. Rathgeber, "Spatial traffic distribution in cellular networks," in *Vehicular Technology Conference, 1998. VTC 98. 48th IEEE*, vol. 3, pp. 1994 –1998 vol.3, may 1998.

[112] A. Furuskar, M. Almgren, and K. Johansson, "An infrastructure cost evaluation of single- and multi-access networks with heterogeneous traffic density," in *Vehicular Technology Conference, 2005. VTC 2005-Spring. 2005 IEEE 61st*, vol. 5, pp. 3166 – 3170 Vol. 5, may-1 june 2005.

[113] B. Ahn, H. Yoon, and J.-W. Cho, "Joint deployment of macrocells and microcells over urban areas with spatially non-uniform traffic distributions," in *Vehicular Technology Conference, 2000. IEEE VTS-Fall VTC 2000. 52nd*, vol. 6, pp. 2634 –2641 vol.6, 2000.

[114] J. Caffery and G. Stuber, "Overview of radiolocation in cdma cellular systems," *Communications Magazine, IEEE*, vol. 36, pp. 38 –45, apr 1998.

[115] K. Petrova and B. Wang, "Location-based services deployment and demand: a roadmap model," *Electronic Commerce Research*, vol. 11, pp. 5–29, 2011. 10.1007/s10660-010-9068-7.

[116] K. Pedersen, G. Monghal, I. Kovacs, T. Kolding, A. Pokhariyal, F. Frederiksen, and P. Mogensen, "Frequency domain scheduling for ofdma with limited and noisy channel feedback," in *Vehicular Technology Conference, 2007. VTC-2007 Fall. 2007 IEEE 66th*, pp. 1792 –1796, 30 2007-oct. 3 2007.

[117] A. Pokhariyal, G. Monghal, K. Pedersen, P. Mogensen, I. Kovacs, C. Rosa, and T. Kolding, "Frequency domain packet scheduling under fractional load for the utran lte downlink," in *Vehicular Technology Conference, 2007. VTC2007-Spring. IEEE 65th*, pp. 699 –703, april 2007.

[118] A. Pokhariyal, *Downlink Frequency-Domain Adaptation and Scheduling - A Case Study Based on the UTRA Long Term Evolution*. Institut for Elektroniske Systemer, Aalborg Universitet, 2007.

[119] Z. Shen, A. Papasakellariou, J. Montojo, D. Gerstenberger, and F. Xu, "Overview of 3gpp lte-advanced carrier aggregation for 4g wireless communications," *Communications Magazine, IEEE*, vol. 50, pp. 122 –130, february 2012.

[120] H. Wang, C. Rosa, and K. Pedersen, "Performance analysis of downlink inter-band carrier aggregation in lte-advanced," in *Vehicular Technology Conference (VTC Fall), 2011 IEEE*, pp. 1 –5, sept. 2011.

[121] D. de Andrade, A. Klein, H. Holma, I. Viering, and G. Liebl, "Performance evaluation on dual-cell hsdpa operation," in *Vehicular Technology Conference Fall (VTC 2009-Fall), 2009 IEEE 70th*, pp. 1 –5, sept. 2009.

[122] J. Nielsen, G. Pedersen, K. Olesen, and I. Kovacs, "Statistics of measured body loss for mobile phones," *Antennas and Propagation, IEEE Transactions on*, vol. 49, pp. 1351 –1353, sep 2001.

[123] N. Wei, A. Pokhariyal, C. Rom, B. Priyanto, F. Frederiksen, C. Rosa, T. Sorensen, T. Kolding, and P. Mogensen, "Baseline e-utra downlink spectral efficiency evaluation," in *Vehicular Technology Conference, 2006. VTC-2006 Fall. 2006 IEEE 64th*, pp. 1 –5, sept. 2006.

[124] G. Berardinelli, *Air Interface for Next Generation Mobile Communication Networks: Physical Layer Design.* Department of Electronic Systems, Aalborg University, 2010.

[125] J. G. Proakis, *Digital Communications.* McGraw-Hill, 4 ed., Aug. 2001.

[126] P. Mogensen, W. Na, I. Kovacs, F. Frederiksen, A. Pokhariyal, K. Pedersen, T. Kolding, K. Hugl, and M. Kuusela, "Lte capacity compared to the shannon bound," in *Vehicular Technology Conference, 2007. VTC2007-Spring. IEEE 65th*, pp. 1234 –1238, april 2007.

[127] D. de Melo Carvalho Filho and M. de Alencar, "Base station deployment based on artificial immune systems," in *Communication Systems, 2008. ICCS 2008. 11th IEEE Singapore International Conference on*, pp. 1591 –1596, nov. 2008.

[128] H. yu Wei, S. Ganguly, and R. Izmailov, "Ad hoc relay network planning for improving cellular data coverage," in *Personal, Indoor and Mobile Radio Communications, 2004. PIMRC 2004. 15th IEEE International Symposium on*, vol. 2, pp. 769 – 773 Vol.2, sept. 2004.

[129] K. Tutschku, "Demand-based radio network planning of cellular mobile communication systems," in *INFOCOM '98. Seventeenth Annual Joint Conference of the IEEE Computer and Communications Societies. Proceedings. IEEE*, vol. 3, pp. 1054 –1061 vol.3, mar-2 apr 1998.

[130] N. Scully, J. Turk, R. Litjens, U. Turke, M. Amirijoo, T. Jansen, and L. Schmelz, "Socrates d2.6 review of use cases and framework," *INFSO-ICT-216284 SOCRATES*, vol. II, pp. 1–28, 2009.

[131] A. Lobinger, S. Stefanski, T. Jansen, and I. Balan, "Load balancing in downlink lte self-optimizing networks," in *Vehicular Technology Conference (VTC 2010-Spring), 2010 IEEE 71st*, pp. 1 –5, may 2010.

[132] F. Report, "Digital mobile radio towards future generation systems cost 231 final report," *European Commission*, no. EUR 18957, 1999.

[133] T.-S. Chu and L. Greenstein, "A quantification of link budget differences between the cellular and pcs bands," *Vehicular Technology, IEEE Transactions on*, vol. 48, pp. 60 –65, jan 1999.

[134] 3GPP, "Selection procedures for the choice of radio transmission technologies of the umts," *Tech. Spec. 30.03 V9.0.0*, Apr 1998.

[135] Regulator Bundesnetzagentur, "German spectrum assignment." http://www.bundesnetzagentur.de/frequenzversteigerung2010/, May 2010.

[136] Nokia Siemens Networks, "Nokia Siemens Networks Flexi Multiradio BTS - all-purpose Flexi BTS featuring 3 technologies in 1." www.nokiasiemensnetworks.com/sites/default/files/document/nokia_siemens_networks_flexi_multiradio_base_station_data_sheet.pdf, 2009. Datasheet.

[137] X. Wang, X. Yang, and Z. Li, "Co-existence analysis of lte micro cell and lte out-band backhaul," in *Vehicular Technology Conference Fall (VTC 2010-Fall), 2010 IEEE 72nd*, pp. 1 –5, sept. 2010.

[138] Ayvazian, B., "LTE TDD & FDD Network Convergence in Europe," *Heavy Reading White Paper*, June 2012.

[139] J. Winters, "Optimum combining in digital mobile radio with cochannel interference," *Selected Areas in Communications, IEEE Journal on*, vol. 2, pp. 528 –539, july 1984.

[140] Y. Ohwatari, N. Miki, T. Asai, T. Abe, and H. Taoka, "Performance of advanced receiver employing interference rejection combining to suppress inter-cell interference in lte-advanced downlink," in *Vehicular Technology Conference (VTC Fall), 2011 IEEE*, pp. 1 –7, sept. 2011.

[141] Nokia Siemens Networks, "On advanced ue mmse receiver modeling in system simulation," *3GPP T-doc R1-111031*, Feb 2011.

[142] NTT DOCOMO, "Influence of channel estimation error on mmse-irc receiver," *3GPP T-doc R1-111639*, May 2009.

[143] F. Frederiksen, P. Mogensen, and J.-E. Berg, "Prediction of path loss in environments with high-raised buildings," in *Vehicular Technology Conference, 2000. IEEE VTS-Fall VTC 2000. 52nd*, vol. 2, pp. 898 –903 vol.2, 2000.

[144] J. Medbo, J. Furuskog, M. Riback, and J.-E. Berg, "Multi-frequency path loss in an outdoor to indoor macrocellular scenario," in *Antennas and Propagation, 2009. EuCAP 2009. 3rd European Conference on*, pp. 3601 –3605, march 2009.

[145] J.-E. Berg, "Building penetration loss at 1700 mhz along line of sight street microcells," in *Personal, Indoor and Mobile Radio Communications, 1992. Proceedings, PIMRC '92., Third IEEE International Symposium on*, pp. 86 –87, oct 1992.

[146] Ericsson, "Heterogeneous networks - meeting mobile broadband expectations with maximum efficiency," *Ericsson White Paper*, February 2012.

[147] L. Hu, I. Kovacs, P. Mogensen, O. Klein, and W. Stormer, "Optimal new site deployment algorithm for heterogeneous cellular networks," in *Vehicular Technology Conference (VTC Fall), 2011 IEEE*, pp. 1 –5, sept. 2011.

[148] I. Kovacs, P. Mogensen, B. Christensen, and R. Jarvela, "Mobile broadband traffic forecast modeling for network evolution studies," in *Vehicular Technology Conference (VTC Fall), 2011 IEEE*, pp. 1 –5, sept. 2011.

[149] Cisco, "Cisco Visual Networking Index: Global Mobile Data Traffic Forecast Update, 2010–2015," *Cisco VNI Forecast, White Paper*, February 1, 2011.

[150] B. Gompertz, "On the nature of the function expressive of the law of human mortality, and on a new mode of determining the value of life contingencies," *Philosophical Transactions of the Royal Society of London*, vol. 115, pp. pp. 513–583, 1825.

[151] Ofcom, "Assessment of future mobile competition and proposals for the award of 800 MHz and 2.6 GHz spectrum and related issues," *Published Consultation*, March 22,2011.

[152] T. Yang and L. Zhang, "Approaches to enhancing autonomous power control at femto under co-channel deployment of macrocell and femtocell," in *Personal Indoor and Mobile Radio Communications (PIMRC), 2011 IEEE 22nd International Symposium on*, pp. 71 –75, sept. 2011.

[153] 3GPP, "Evolved universal terrestrial radio access (e-utra);mobility enhancements in heterogeneous networks (release 11)," *Tech. Spec. 36.839 V11.1.0*, Dec 2012.

[154] 3GPP, "Evolved universal terrestrial radio access (e-utra);physical layer; measurements (release 11)," *Tech. Spec. 36.214 V11.0.0*, September 2012.

[155] G. Monghal, *Downlink Radio Resource Management for QoS Provisioning in OFDMA Systems*. Department of Electronic Systems, Aalborg University, 2009.

[156] S. M. Ross, *Simulation, Fourth Edition*. Orlando, FL, USA: Academic Press, Inc., 2006.

[157] R. A. Brealey and S. C. Myers, *Principles of Corporate Finance with Cdrom*. McGraw-Hill Higher Education, 6th ed., 2000.